

i

1

AMS/MAA | THE CARUS MATHEMATICAL
MONOGRAPHS

Oscillations: swings and vibrations from a mathematical viewpoint

**Henk Broer, Marcello Seri and Floris
Takens**

The same equations have the same solutions.

Richard P. Feynman

Contents

Preface	vii
Preamble: oscillations and mathematics	xi
Chapter 1 It oscillates forever	1
1.1 The pendulum, the spring and some other examples	2
1.2 The pendulum as a spring: linearization	9
1.3 The phase plane and the line element field	11
1.4 Energy	21
1.5 Period of oscillation	27
1.6 Exercises	32
Chapter 2 It oscillates in resonance	39
2.1 Friction	40
2.2 Loss of energy due to friction	43
2.3 The damped harmonic oscillator with periodic forcing, resonance	50
2.4 Resonance in non-harmonic oscillators with periodic forcing	55
2.5 The stabilization of oscillations	61
2.6 Exercises	64
Chapter 3 Oscillations in daily life	69
3.1 Two further examples of oscillators	72
3.2 Coupling finitely many oscillations	74
3.3 Vibrations of continuous media	87
3.4 Other vibrational phenomena	105
3.5 An exercise on Hooke's n -body problem	113

Preface to the appendices	115
Appendix A Johann Bernoulli's brachistochrone	117
A.1 Geometric optics	118
A.2 The brachistochrone as a light ray	124
A.3 Scholium	126
Appendix B Small oscillations revisited	127
B.1 Intermezzo on linear algebra	129
B.2 Beats revisited	138
B.3 Scholium	139
B.4 Selected exercises	143
Appendix C The Foucault problem	147
C.1 The Foucault pendulum	148
C.2 Scholium	154
Appendix D Chaos in periodically forced oscillators	157
D.1 The Hénon attractor	159
D.2 The stroboscopic map	165
D.3 Scholium	169
Appendix E More on resonance	177
E.1 Huygens' clocks	180
E.2 Arnold resonance tongues and fractal geometry	180
E.3 A theoretical digression into circle maps	182
E.4 Parametric resonance: Mathieu's equation and the like	191
E.5 Scholium	194
Appendix F Solutions of selected exercises	207
F.1 Exercises from Section 1.6	208
F.2 Exercises from Section 2.6	217
F.3 Exercise from Chapter 3: On Hooke's n -body problem	223
F.4 Exercise from Appendix B: One more Hookian problem	225
F.5 Exercise from Appendix E: On Kepler's third law	226
Bibliography	229

Preface

The idea for this book comes from the syllabus of a course for high school teachers held in Groningen in the 1980s. At the time differential equations were included in the school curriculum and a mathematical treatment of *oscillations* was well in reach of the audience. Since then, the syllabus evolved and has been used both by master's and graduate students at the University of Groningen and, a few times, for didactical projects at secondary schools.

In writing this book, we aimed the main body of text at bachelor and master science students, as well as at high school teachers and their teacher trainers. As in the original syllabus, in the book we will explore oscillations guided by the works of Christiaan Huygens on the pendulum clock and on resonance phenomena.

Throughout the main text we assume a high school background, including some knowledge of basic trigonometry and of elementary differential and integral calculus.

In the present version, we revised the material with fresh eyes and we added a number of appendices for the interested reader.

The first appendix deals with Johann Bernoulli's brachistochrone, that happens to be the same cycloid that we shall meet in the main text and that Huygens made such extensive use of. We included this since the authors affiliation in Groningen and since Bernoulli also lived and worked in Groningen between 1695 and 1705.

Another appendix deals with small oscillations and Lissajous figures, extending material from the main text. An intermezzo of linear algebra, allows us to reframe our considerations in the main text in terms of spectral theory. This helps us to get a deeper understanding of the subject.

In a next appendix we discuss the Foucault experiment, designed to illustrate the rotation of the earth. Here Lissajous figures again show up. We will also discuss spherical precession, a phenomenon that complicates the Foucault experiment, and briefly mention the role played on this by the later Nobel Prize laureate Kamerlingh Onnes during his doctoral studies in Groningen.

For inspiration of the more advanced and curious reader we further included appendices on chaos and resonances, subjects that have

developed greatly since the 1980s. Among other things, we discussed celestial resonances and gave a brief excursion into quantum physics. These appendices need a broader mathematical background for which we lean on the rich bibliography at the end of the book. In fact these appendices may well be seen as an invitation to this bibliography.

The latter two appendices touch on ongoing research in the broad area of dynamical systems, in which the Groningen school has quite a lot of impact. Since Floris Takens's profound influence on the original contents, and since he played a major role in the later developments, we found it appropriate to add him posthumously as a co-author.

We hope that high school teachers, as well as their teacher trainers, and university professors can find material in the book for all kinds of projects, seminars, presentations, etc.

We thank Jan Epema and the late Max Kuipers for their help in preparing the original syllabus. We also thank Hans Beijers, Aernout van Enter, George Huitema, Francesco Paparelli, Alef Sterk, Ferdinand Verhulst and the anonymous referees for their meticulous reading and for many useful comments. And thanks go to Bernd Krauskopf for his help with Appendix D and to Dzemilia Sero for her help in refining the presentation in some parts of the manuscript.

Henk Broer and Marcello Seri
Groningen, Autumn 2024

Preamble: oscillations and mathematics

At the time of the ancient Greeks, geometry, arithmetic, and algebra were already playing a leading role in mathematics and astronomy [149, 172]. We have to wait until the 16th and 17th centuries for infinitesimal considerations to seriously enter the picture, in the end leading to the differential and integral calculus as we know it today. The development of these *new methods* went hand in hand with gaining astonishing new insights in mechanics and optics. These advances led to what we nowadays call classical mechanics and geometric optics, and marked the beginning of the *scientific revolution*.

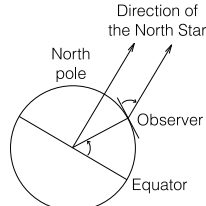
Classical mechanics studies phenomena of motion, e.g., all kinds of vibrations and oscillations. Two particular examples are the rotating and oscillatory motions of the planets and moons of our solar system, the study of which is central in celestial mechanics. Both examples are governed by the same principles.

Proper celestial observations started alongside the introduction of telescopes, with the effect of bridging optics and mechanics. Although these subjects seem far apart, we must realize that precise celestial observations also need precise clocks and such clocks require oscillating devices to function, like a regularly moving pendulum or a vibrating balance spring.

Navigation on the open sea

Travel across deserts and seas has been a prime motivation for these developments. Indeed, from early on, some knowledge of celestial phenomena and the corresponding timetables have been indispensable for determining the travelers' position on earth and the direction to travel in. And when ships no longer stayed close to the coast, navigation became an increasingly difficult problem. Indeed, how to determine one's position on the open sea? Nowadays with the Global Positioning System (GPS) this seems a piece of cake, but at those times it surely was a big issue.

Determining the latitude on the Northern Hemisphere is relatively easy. The North Star, or Polaris, is an almost fixed point in the sky very close to the northern celestial pole. With



the help of a sextant one can, at least in principle, determine the angle between the North Star and the horizon: this angle is exactly the northern latitude of your position, see the figure on the side.

The determination of the longitude, however, is a quite different matter [158]. For this, one needs a clock that keeps track of a reference time, say, e.g., the Greenwich time. Sailors on board, then, can determine noon local time by “shooting the sun”. If the time difference with Greenwich is T hours, then the longitude equals

$$T \times \frac{360}{24} = 15T \text{ degrees.}$$

So the real problem is to have a good clock on board that is synchronous with Greenwich. The development of such a clock touches on one of the themes of this book, also compare with [37].

Huygens and some other names

A few of the names that were important for the era at hand are Galileo Galilei (1564-1642), Johannes Kepler (1571-1630), René Descartes (1596-1650), Christiaan Huygens (1629-1695), Isaac Newton (1643-1727), Gottfried Wilhelm Leibniz (1646-1716) and Johann Bernoulli (1667-1748).

Next to the classical mathematics as inherited from the ancient Greeks, a *new method* was being developed where infinitesimal considerations began to play a serious role. Newton, Leibniz, and Bernoulli were setting the foundations that eventually led to the differential and integral calculus as this is known to us now. Among other things, this led to a full mathematical understanding of Kepler’s work on the solar system.

Galileo laid the mathematical foundation of this development, by refining the telescope and by deducing the first kinetic theory of celestial bodies based on a principle of relativity and heliocentrism. This took place half a century before calculus was born.

Remark 1. The art of lens grinding had already been practiced for a couple of centuries and, in order to construct and improve on their telescopes, both Galileo and Huygens also took part in this.

The torch was carried further by Huygens in his groundbreaking *Horologium Oscillatorium* [102, 1] on the pendulum clock, that forms a major inspiration for the present book. He used intricate infinitesimal considerations with amazing results, but only at the end of his life, at the instigation of Leibniz, he developed plans to learn 'real' calculus.

Huygens's lifetime fell in the Dutch Golden Age that roughly runs from 1588 to 1672. For general background see Israel [103]. This was a period of great wealth for the Republic of the United Netherlands. The *Dutch East-India Company* (VOC, Vereenigde Oost-Indische Compagnie) caused trade to expand quickly, attracting immigrants and stimulating the growth of the main cities and ports. In this age the Dutch trade, industry, science, and art as well as the military were among the most acclaimed in the world.

Christiaan Huygens was born as the son of Constantijn Huygens (1596-1687), a well-known poet, composer, and diplomat in which capacity he was secretary to the Princes of Orange Frederik Hendrik and Willem II. Christiaan as a young man already was outstanding in his ability to solve problems in mathematics and mechanics. In 1644 he took up studies in mathematics and law, at first at Leiden University, and later in Breda. Under the influence of the Princes of Orange Maurits and especially under the more enlightened Frederik Hendrik, these cities had an excellent capacity for teaching and, thanks to intellectual freedom, also for science. Many scientists and philosophers from abroad fled, looking for shelter in the Netherlands, which contributed to a highly stimulating and intellectual atmosphere.

Christiaan Huygens was both a scientist and an engineer, compare with [2, 3, 28, 65, 160, 170, 181]. His more theoretical work ranges from mechanics and optics to astronomy; we already mentioned his *Horologium Oscillatorium*. In particular, he also wrote about Saturn's rings. Concerning his practical work, he invented and improved various instruments like lenses, microscopes, telescopes, and clocks. Huygens had a great international reputation: from 1663 on he was a Fellow of the Royal Society in London and between 1666 and 1683 he was appointed Directeur de Récherche at the Académie des Sciences

in Paris by King Louis XIV, being the first scientist in this prestigious position.

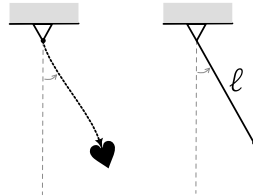
Remark 2. René Descartes was an influential French philosopher, scientist, and mathematician. He spent much of his working life in the Dutch Republic. He is credited as the father of analytic geometry, used in the discovery of the infinitesimal calculus. Descartes was also one of the key figures in the scientific revolution.

A few problems of Huygens

Galileo had already observed that the period of oscillation of a pendulum is independent of its mass and that, for small deflections, this period is approximately independent of the amplitude. These discoveries inspired a closer investigation of the pendulum motion. So Huygens, both for their practical applications and for a deeper understanding of these phenomena, posed the following problems.

- (1) What is generally understood as a pendulum is a mathematical ideal of a 'real' pendulum. For instance, in the mathematical pendulum, we assume that all mass is concentrated in one point. What should be the length ℓ of an ideal pendulum to ensure that it moves exactly as the 'real' one?
- (2) It was already known that the period of oscillation of a pendulum is not constant but increases with the amplitude. But what is the exact period of oscillation of a pendulum as a function of its length and especially of the amplitude of oscillation?
- (3) The motion of a pendulum mass can be thought of as that of a bead that slides without friction along a circular wire under the influence of constant gravity. One may well ask then whether there exists a wire profile along which the period of oscillation is independent of the amplitude?

The profile Huygens was looking for now is known as the *isochronous curve*.



The first and third of these problems were rather nasty in Huygens' time and contributed to motivating the further development of calculus. Since then they have become rather simple exercises, as we will see in Section 1.6. Indeed, from our approach it directly follows that the isochronous curve, that is actually called cycloid, is also the *tautochronous* curve along which the downtime of the bead is the same from whatever height it drops. Due to Johann Bernoulli we know that the curve is also *brachistochrone*: along this curve it takes the shortest time for the bead to descend. In Appendix A we shall see how intimately intertwined mathematics, mechanics and optics are in Bernoulli's solution. The second problem turned out to be surprisingly more difficult.

Later developments

Since then, research on oscillations has continued steadily and expanded. One direction of interest was the study of sound and light as vibrational phenomena. A milestone in this development came in the 19th century with the electromagnetic oscillations ensuing from the theory of James Clerk Maxwell (1831-1879). All kinds of new questions surfaced in the 20th century with the subsequent development of electronics, a period often referred to as *radio time*. One of the pioneers in this direction was the Dutch physicist Balthasar van der Pol (1889-1959), a long-time member of the Philips Research Laboratories in the city of Eindhoven.

The discipline of dynamical systems, that includes the study of oscillators in networks of other dynamical agents, thrived on the continuous stream of new challenges and has kept growing in complexity over the last century. New phenomena that showed up were *multior quasiperiodicity* and *chaos*. The advent of numerical methods and electronic computer further stimulated its development and the opportunities for mathematical exploration. We touch on a few of these newer aspects in Appendices D and E.

Outline of what follows

We conclude this preamble with an outline of what follows. In Chapter 1, *It oscillates forever*, we are led by the second and third problems

of Huygens. We present the pendulum as an example of an oscillator without friction and damping and deal with such oscillations in a geometric fashion. In Chapter 2, *It oscillates in resonance*, external forces due to friction, damping, and forcing come into play. By means of a number of mechanical and electronic examples, we encounter the phenomenon of *resonance*. Chapter 3, *Oscillations in daily life*, gives several examples, for instance on coupled oscillations, where we meet Lissajous figures. Another example is concerned with oscillations as they occur in a string, in sound, water, etc. These phenomena have a more complex nature, since apart from motion in time spatial configurations like *waves* become important.

All chapters are closed by a number of exercises, whose solutions are sketched in Appendix F.

The book closes with a choice of appendices that may be of interest to the reader. Appendix A is devoted to Johann Bernoulli's *brachistochrone problem*, where mathematics, mechanics, and optics are nicely intertwined. Appendix B, *Small oscillations revisited*, extends Chapter 3 and deals with the theory of small oscillations and Lissajous figures as these occur in linearizations of coupled oscillators. This appendix is introduced by an intermezzo on linear algebra. The next appendix is entitled *The Foucault problem*; As a 19th century application of the theory of small oscillations, we describe the Foucault experiment, designed to demonstrate the rotation of the earth, and also reveal the phenomenon of spherical precession that complicates this setup.

Appendix D, *Chaos in periodically forced oscillators*, treats aspects of the more recent chaos theory as this occurs in the present context. Here we shall meet the partly experimental *Benedicks-Carleson Ansatz* that forms a structuring element. Appendix E, *More on resonance*, extends Chapter 2 in various ways and discusses another problem of Huygens concerning synchronization of weakly coupled pendulum clocks as a leading example. The appendix concludes with an excursion into mathematically related aspects of *quantum physics* and a discussion of (part of) the extremely rich subject of *celestial*

resonances. It turns out that in both appendices *fractal sets* form an intrinsic component of the theory.

The book ends with the aforementioned Appendix F, *Solutions of selected exercises.*

Remark 3. The appendices all close with a *scholium*. Here we went somewhat deeper, often referring to technical literature for the details. These are meant as an inspiration for more advanced students and curious readers. We hope they will regard such a scholium as an invitation to this literature.

Chapter 1

It oscillates forever

In this chapter, we study the oscillatory motion of certain simple physical systems. For now, we only consider motions without friction or damping. As we shall see, this means that the energy remains preserved during the motion and that it just keeps oscillating. We shall not delve too deep into the physical derivation of the mathematical descriptions but instead provide some useful references for the interested reader.

1.1 The pendulum, the spring and some other examples

1.1.1 The pendulum

The pendulum consists of a weight of mass m attached to a rigid rod of length ℓ which is suspended from a pivot. For simplicity, we assume that the weight is a point mass (or material point) and that the rod is massless.

We assume that the motion occurs in a vertical plane, under the influence of a constant gravitational acceleration g . As we know from elementary mechanics, the gravitational force acting on the material point then is mg pointing in the downward direction. This force can be decomposed into two components,

one parallel to the rod and one orthogonal to it, see Figure 1.1. The rigidity of the rod keeps the point mass at a fixed distance from the pivot, effectively cancelling the motion parallel to this. The remaining orthogonal component is the force acting in the angular direction. An exercise in planar geometry shows this component is given by $-mg \sin x$, where x denotes the angle between the rod and its vertical equilibrium position, increasing from left to right.

The effect of this orthogonal component then is to pull the point mass toward this vertical position.

So the point mass is constrained to move on a circular arc. If the angle x is expressed in radians, the distance between the material

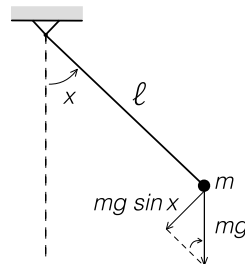


Fig. 1.1. Pendulum

point and its equilibrium position along the circle is given by the arclength ℓx .

It is our aim to describe the motion of the pendulum. Therefore we need to find out how the angle x changes with respect to the time t . In other words, the motion is going to be a function $t \mapsto x(t)$. The relation between the force acting on a system and its motion is provided by Newton's well-known law

$$F = m a, \quad (1.1)$$

where F denotes the force, m the mass of the material point, and a its acceleration [132]. As said before, no motion takes place in the radial direction, and therefore Newton's law will only effect the angle x . By definition, the acceleration is the rate of variation of the velocity, which in turn is the rate of variation of the position. This mathematically translates to

$$a = \frac{d^2(\ell x)}{dt^2} = \ell \frac{d^2x}{dt^2},$$

where $\frac{d^2x}{dt^2}$ denotes the second derivative of the function $t \mapsto x(t)$.

Replacing F and a in Newton's law we obtain

$$-mg \sin x = m\ell \frac{d^2x}{dt^2}$$

or, more concisely,

$$\frac{d^2x}{dt^2} = -\frac{g}{\ell} \sin x. \quad (1.2)$$

Remark 4. (1) Note that we already tacitly used Newton's law when we said that the gravitational force equals mg , where g is the constant gravitational acceleration.

(2) Observe that in equation (1.2), which completely determines the motion of the pendulum, the mass m plays no role. As mentioned in the Preamble, the independence of the motion of the pendulum from its mass m was already established experimentally by Galileo.

Newton himself used the notation \dot{x} and \ddot{x} for differentiation. So

$$\dot{x} = \frac{dx}{dt} \quad \text{and} \quad \ddot{x} = \frac{d^2x}{dt^2}. \quad (1.3)$$

Many authors have adopted this dot notation, and from now on we will also do this.

1.1.2 The spring

A point mass with weight m is attached to a wall by a spring. We assume that the point can **only** move on the horizontal plane, without friction; in this way, its motion is not affected by gravity. Compare Figure 1.2. Furthermore, we denote by x the distance of the point mass from the equilibrium position: the position in which the spring is neither compressed nor extended. As before, if we know x as a function of time t , we can describe completely the motion of the point mass.

The force acting on the point mass in this new setting is the restoring force of the spring, in the opposite direction of the deviation from the equilibrium. According to *Hooke's law*, this force is proportional to the deviation

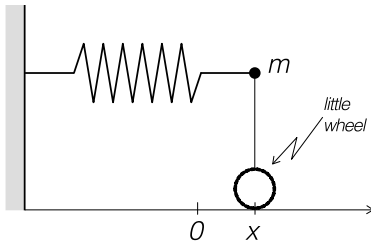


Fig. 1.2. Spring

where the positive proportionality constant k , called the *spring constant*, is a property of the spring in question. Newton's law (1.1) again provides the connection between force and motion:

$$-kx = m\ddot{x},$$

or

$$\ddot{x} = -\frac{k}{m}x. \quad (1.4)$$

Remark 5. Here we kept gravity out of the game by assuming that the motion was horizontal. In Exercise 1.6.1 we shall discuss what happens when the spring is mounted vertically so that gravitation also plays a role.

Equation (1.4) can be explicitly solved by

$$x(t) = A \cos(\omega t) + B \sin(\omega t) \quad \text{where} \quad \omega = \sqrt{\frac{k}{m}}. \quad (1.5)$$

Here A and B are arbitrary. We can just consider them as generic constants and check that all the functions of the form (1.5) satisfy the equation (1.4). The actual choice of A and B depends on the position and velocity of the system at time $t = 0$, or at any other fixed time for that matter. For convenience one normally uses $t = 0$. Computing the velocity out of (1.5)

$$\dot{x}(t) = -A\omega \sin(\omega t) + B\omega \cos(\omega t), \quad (1.6)$$

then using (1.5) and (1.6) we conclude

$$A = x(0) \quad \text{and} \quad B = \frac{1}{\omega} \dot{x}(0).$$

When taking, for instance, $x(0)$ and $\dot{x}(0) = \left. \frac{dx}{dt} \right|_{t=0}$ both equal to 0, the system remains at rest. Indeed, this implies $A = B = 0$ and by (1.5) we find that $x(t) = 0$ for all t .

It can be convenient to rewrite (1.5) in the more compact form

$$x(t) = R \cos(\phi - \omega t), \quad (1.7)$$

where R and ϕ have taken the role of A and B . Indeed, we can mimic the previous computation of $x(0)$ and $\dot{x}(0)$ as

$$x(0) = R \cos \phi \quad \text{and} \quad \dot{x}(0) = R\omega \sin \phi.$$

To see where this is coming from, we can use the trigonometric formula

$$\cos(\alpha + \beta) = \cos(\alpha) \cos(\beta) - \sin(\alpha) \sin(\beta)$$

and rewrite (1.7) as

$$R \cos(\phi - \omega t) = R \cos(\phi) \cos(\omega t) + R \sin(\phi) \sin(\omega t),$$

which recovers equation (1.5) by taking $A = R \cos(\phi)$ and $B = R \sin(\phi)$. Taking the square of A and B and adding them up, we can see that $R = \sqrt{A^2 + B^2}$.

Figure 1.3 shows the graph of the function (1.7). The maximal extension R is called the *amplitude* of the vibration or oscillation. As one can also see from the picture, the *vibration time* or the *period of oscillation* is $2\pi/\omega$ and thus its *frequency*, i.e., the number of

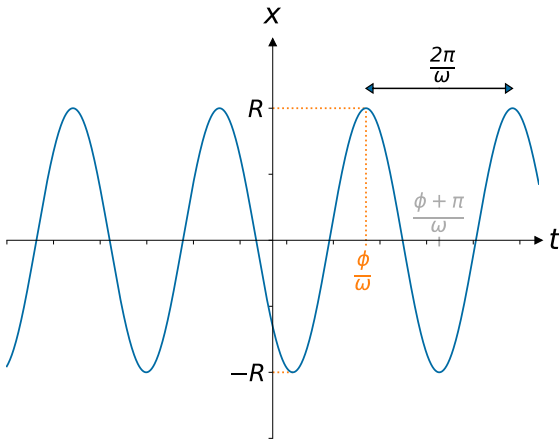


Figure 1.3. Vibration (1.7) of the spring

oscillations per second, is $\omega/2\pi$. We call ω the circular or angular frequency.

Remark 6. (1) The definition $\omega = \sqrt{k/m}$ implies that ω is larger if the mass is smaller and the spring stiffer: loose springs with large masses are slower than stiff springs with small masses. Does that reflect your experience?

(2) The frequency of the oscillations is $\omega/2\pi$ and therefore independent of R .

1.1.3 The U-pipe

In this example, we consider a U-shaped pipe of constant section containing some liquid, see Figure 1.4. The top of the pipe is open, allowing the fluid to move freely. By the principle of communicating vessels, when the liquid is at rest, it will be at the same height on both sides of the pipe.

Denote by x the height of displacement of the liquid from its equilibrium position as depicted in Figure 1.4. Also in this case we

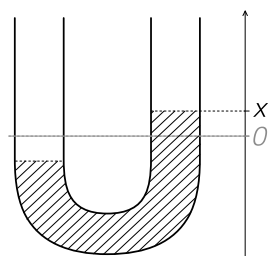


Fig. 1.4. U-pipe

aim to apply Newton's law (compare with [132, Book II, Sec. VIII, Proposition XLIV and Theorem XXXV]) and describe the motion of the liquid's level.

While this model is a standard exercise in university physics courses, the precise derivation of its equation of motion is out of the scope of this book and we will only broadly sketch its main elements.

Let ρ be the specific weight of the liquid and O the surface area of the horizontal cross-section of the pipe legs. Then, the restoring force is given by the extra weight of the liquid in the column. If M denotes the total mass of the liquid, then

$$M \frac{d^2x}{dt^2} = -2 O \rho g x .$$

We end up with an equation that is of the same type as (1.4) which we just derived for the spring! Therefore, the motion is again of the form (1.7) where the period is now given by

$$\omega^2 = 2 \frac{O \rho g}{M} .$$

1.1.4 The L-C circuit

This final example comes from electricity theory. Suppose you have a circuit with a capacitor of capacitance C and an inductor coil with inductance L .

Don't worry if you don't know the physical terminology in this derivation, you can get an idea of the parts involved using a classical analogy of this system as a closed pipe with some liquid. The voltage is something that makes the liquid flow, that is, induces a current, the capacitor is a little bucket that gets filled before letting the water flow through it and the inductance is something that resists changes in the flow (whatever this may mean). For the general physical background we refer to [152].

A current with intensity I flows through the circuit, and we would like to compute the function $t \mapsto I(t)$, describing how the intensity changes over time, compare with Figure 1.5.

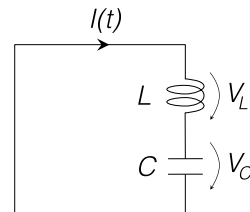


Fig. 1.5. L-C circuit

Let V_L denote the voltage across the inductor and V_C the voltage across the capacitor. By *Kirchoff's law*, the sum of the voltages across the elements in the circuit vanishes:

$$V_C + V_L = 0. \quad (1.8)$$

Moreover, the constitutive relations for the circuit elements provide the following additional equations:

$$I = C \frac{dV_C}{dt} \quad \text{and} \quad V_L = L \frac{dI}{dt}. \quad (1.9)$$

Differentiating (1.8) gives

$$\frac{dV_C}{dt} + \frac{dV_L}{dt} = 0, \quad (1.10)$$

which, by (1.9), can be rewritten as

$$\frac{I}{C} + L \frac{d^2 I}{dt^2} = 0,$$

or, again adopting the dot-notation (1.3),

$$\ddot{I} = -\frac{1}{CL} I. \quad (1.11)$$

And again this equation is of the same type as equation (1.4), so the motion is of the form (1.7) with $\omega^2 = 1/LC$.

Remark 7. A solution of (1.11), due to the way we derived its equation of motion, immediately solves (1.10) but it is not necessarily satisfying Krikhoff's Law (1.8).

This is not a problem here, since $I = C dV_C/dt$ implies that V_C is only determined up to an additive constant. Therefore it is always possible to ensure that (1.8) holds true by adding an appropriate constant.

1.1.5 On modeling

In the four examples of this section, we obtained equations of motion under assumptions that do not hold for real systems. To begin with, in all the examples we neglected frictional forces: air resistance, friction at the suspension points, electrical resistance, surface friction in the pipes, etc. We will return to this in the next chapter, in particular, we will see how friction will cause all oscillations to die out.

Another problem in our hypotheses is the following. The pivot of most pendulums cannot constrain them to only vertical oscillations. Small perturbations can make the motion considerably more complicated than the one described by equation (1.2). The same applies when reducing material bodies with a physical dimension to point masses.

However, all this does not diminish the usefulness of our considerations. In general, one should understand this in the following way. Our equations of motion describe idealized *models* of the physical reality. They only describe reality up to a certain extent: by approximation or by the representation of only certain aspects.

1.2 The pendulum as a spring: linearization

In Section 1.1.1, we derived the equation of motion for the ideal pendulum (1.2) in a form that, to some extent, resembles the equation of motion of the spring (1.4):

$$\begin{aligned}\ddot{x} &= -\omega^2 \sin x, & \omega = \sqrt{g/\ell} & \quad (\text{pendulum}), \\ \ddot{x} &= -\omega^2 x, & \omega = \sqrt{k/m} & \quad (\text{spring}).\end{aligned}$$

However, while the latter admits solutions in closed form as (1.5) or (1.7), this is not so straightforward for the former.

We now introduce an approximation of the pendulum equation as follows. Observe that the line $y = x$ at $(x, y) = (0, 0)$ is tangent to the curve $y = \sin x$, a statement also expressed by the famous limit

$$\lim_{x \rightarrow 0} \frac{\sin x}{x} = 1.$$

Therefore, in a small neighborhood of the origin, the function $x \mapsto \sin x$ is well approximated by $x \mapsto x$. For x small, we can approximate the equation of motion of the pendulum (1.2) by

$$\ddot{x} = -\frac{g}{\ell} x.$$

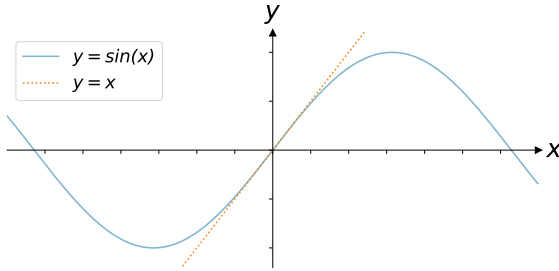


Figure 1.6. $\sin x \approx x$ near $x = 0$.

Since this has the same form as the spring equation (1.4), its solutions are given by (1.7):

$$x(t) = R \cos(\phi - \omega t) \quad \text{where} \quad \omega = \sqrt{\frac{g}{\ell}}.$$

In other words, in the *small oscillations approximation*, the pendulum oscillates like a spring with stiffness $k = g/\ell$ and mass $m = 1$.

Remark 8. As already observed for the spring, we see that in the small oscillations approximation all the solutions have the same frequency

$$\frac{1}{2\pi} \sqrt{\frac{g}{\ell}},$$

independent of the amplitude of the oscillation.

This again corresponds to an experimental fact already known to Galileo, as mentioned in the Preamble: the oscillation time of a pendulum with small oscillations is *approximately* independent of their amplitudes.

The technique presented in this section is called *linearization*: we replaced the curve $y = \sin x$ by the straight line $y = x$. Such an approach is widely applied in practice to attack a large variety of problems. We will get back to this in Chapter 3 and in Appendix B.

1.3 The phase plane and the line element field

Until now we focused on two types of differential equations, namely

$$\ddot{x} = -x \quad \text{and} \quad \ddot{x} = -\sin x, \quad (1.12)$$

where, for simplicity, all the constants have been normalized to 1. For the first type, we could easily compute all the solutions in dependence of the time t , but for the second one we are not so lucky. This motivated the development of other means to say something about the behavior of the solutions, even without having an explicit formula for them. As we will see, these means have a strong geometric character.

1.3.1 The phase plane

Instead of considering a differential equation involving a second derivative, we can reformulate the equations of motion as a system of differential equations in which only first derivatives occur.

This is done by giving to \dot{x} its own name, say y , and considering it as a new unknown function of the time t . We can then try to solve for the two unknown functions x and y of t , where $x(t)$ denotes the *position* of the point particle at time t and $y(t)$ its *velocity* at that time. In the case of our examples in (1.12) we get

$$\begin{cases} \dot{x} = y \\ \dot{y} = -x \end{cases} \quad \text{and} \quad \begin{cases} \dot{x} = y \\ \dot{y} = -\sin x \end{cases} \quad (1.13)$$

recalling the dot-notation (1.3). The top equation is always the same, it is just the definition of velocity.

We can further reduce these systems to a single differential equation by eliminating time and taking y as a function of x . This can be done with the help of the chain rule

$$\frac{dy}{dt} = \frac{dy}{dx} \frac{dx}{dt} \quad \text{or, in other words,} \quad \frac{dy}{dx} = \frac{\frac{dy}{dt}}{\frac{dx}{dt}}.$$

This reduces the systems in (1.13) to

$$\frac{dy}{dx} = -\frac{x}{y} \quad \text{and} \quad \frac{dy}{dx} = -\frac{\sin x}{y}. \quad (1.14)$$

Both of these equations can be solved explicitly in terms of integrals, something that in the literature is often referred to as *solution by quadrature*. To see this, it is convenient to think of $\frac{dy}{dx} = \lim \frac{\Delta y}{\Delta x}$ as the limit of the ratio of ‘infinitely small’ increments, here denoted Δx and Δy . Then (1.14) can be rewritten as

$$y \Delta y = -x \Delta x \quad \text{and} \quad y \Delta y = -\sin x \Delta x,$$

the limit form of which is

$$y dy = -x dx \quad \text{and} \quad y dy = -\sin x dx,$$

Summing both sides over the increments and taking the limit just amounts to taking the usual integral. For the former this leads to

$$\frac{1}{2}y^2 = -\frac{1}{2}x^2 + \text{const.}$$

where const is an integration constant. Equivalently we write

$$x^2 + y^2 = C, \tag{1.15}$$

where $C \geq 0$ is an arbitrary constant. For the latter we similarly get

$$y^2 = 2 \cos x + C, \tag{1.16}$$

where $C \geq -2$ is also arbitrary.

The (x, y) -plane that contains the solution curves of a system of differential equations like (1.13), is called the *phase plane*. Below, we shall see that we are developing a method to describe situations that are far more general than the pendulum or the spring.

Remark 9. (1) The small increments often are called *infinitesimals* and the somewhat heuristic handling of these has lasted for several centuries since the pioneering work of Newton and Leibniz. We note that differential and integral calculus also is named *infinitesimal calculus*. A proper, modern way to deal with expressions as dx and dy as *differential forms* is dealt with in courses on advanced (and multivariate) calculus [159].

(2) Be that as it may, but here we have to mention that most people keep thinking in terms of infinitesimals when doing concrete computations. For examples also see below, in particular see some of the exercises.

- (3) There also exists a formal way to deal with infinitely small and with infinitely large numbers, as was developed by Robinson [145].

Determinism. The phase plane is an extremely important tool in the study of physical phenomena such as oscillations. In general, the solution curve $(x(t), y(t))$ for systems like the one in (1.13) is uniquely determined by the state $(x(0), y(0))$ at $t = 0$. In more mundane terms, if for a system like the spring or the pendulum both the position *and* the velocity at any given moment is known, then position and velocity are determined for the entire future of the system. This is a consequence of Newton's law, which says that to describe the motion of a system we only need to look at its acceleration

$$a = \ddot{x} = \dot{y},$$

and that higher derivatives of x with respect to t are not needed. The mathematical background of this is the Theorem of Existence and Uniqueness of solutions of *first order* differential equations [100]: this theorem guarantees that once the initial positions and velocities are given, the equation of motion provided by Newton's law has a unique solution, which completely determines the future of the system.

Remark 10. (1) You can check for yourself that such determinism of the future does not apply if you only look at the position $x(0)$: $x(t)$ for $t > 0$ can *not* be determined by the mere position $x(0)$ alone.

- (2) In general we call systems of the form (1.13) *deterministic*: the state at one moment determines the entire evolution. Here it is important that the system is autonomous, i.e., that the right-hand side does not explicitly depend on t . In Appendix D we shall come back to this.

Motion in the phase plane. In the remainder of this section we study the motion of systems in the phase plane. Here we have to bear in mind, that the actual (physical) motion that we observe is only the first component $x(t)$, i.e., the position. To visualize also the velocity component $y(t)$, we would need the help of a more technical tool such as, for instance, the tachometer of a car.

The motion in the phase plane is propagated by the *velocity vector*

$$\begin{pmatrix} \dot{x} \\ \dot{y} \end{pmatrix} = \begin{pmatrix} \frac{dx}{dt} \\ \frac{dy}{dt} \end{pmatrix}$$

as a function of t . One of its components is the *velocity* of the motion

$$\dot{x} = y,$$

while the other is the *acceleration* of the same motion

$$\dot{y} = \ddot{x}.$$

In the equations in (1.14) we have eliminated the time t . The advantage of this is that we could easily determine the *integral curves* (or *solution curves*, or *trajectories*) of those systems in the phase plane, particularly in the cases (1.15) and (1.16). We have to realize that this came with a cost: by eliminating time we have lost the time parametrization of the integral curves.

In the next section, we will relate our observations with the *conservation of energy*. However, before moving on we look at our examples one more time.

1.3.1.1 The spring

We start recalling the relevant equations:

$$\ddot{x} = -x \quad \text{or} \quad \begin{cases} \dot{x} = y \\ \dot{y} = -x, \end{cases}$$

with integral curves $x^2 + y^2 = C$, $C \geq 0$, see (1.15). This is a family of circles centered at the origin $(x, y) = (0, 0)$ and parametrized by C (i.e., with radius \sqrt{C}). What can we learn from this?

To begin with, each solution $t \mapsto (x(t), y(t))$, of the system of differential equations moves in the (x, y) -plane along one of these circles. Position and velocity at a particular moment, say at $t = 0$, uniquely identify this circle: after all, only one circle in the family of circles passes through the point $(x(0), y(0))$. But there is more.

We can also reconstruct *how* the point $(x(t), y(t))$ moves along the circle as a function of t , despite the fact that we have apparently eliminated time from our problem. The answer lies in the fact that

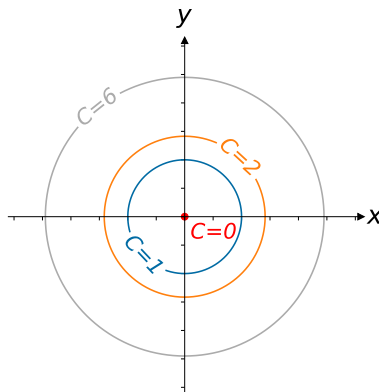


Figure 1.7. Integral curves of the spring

$y = \dot{x} = \frac{dx}{dt}$, so $y(t)$ is the x -component (i.e., the horizontal component) of the velocity vector

$$\begin{pmatrix} \dot{x} \\ \dot{y} \end{pmatrix} = \begin{pmatrix} \frac{dx}{dt} \\ \frac{dy}{dt} \end{pmatrix}$$

at time t , and that the velocity vector has to be tangent to the circle, thereby completely fixing this velocity vector.

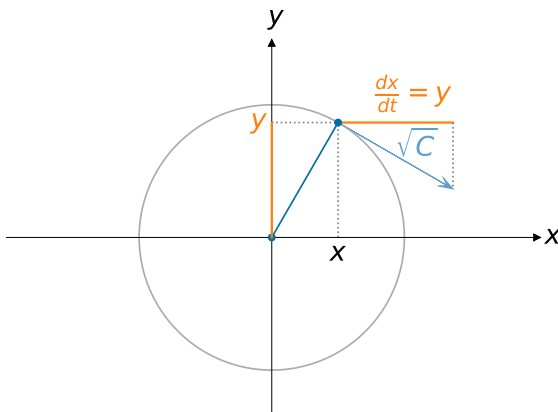


Figure 1.8. Reconstructed velocity vector of the spring

To illustrate this, in Figure 1.8 we have fixed an arbitrary point (x, y) on a circle $x^2 + y^2 = C$. The velocity vector points along the tangent to the circle at the point (x, y) , and its x -component is equal to y . We now see two congruent triangles rotated over 90° with respect to each other. Therefore, the *length* of the velocity vector has to be equal to the circle radius, which in this case is \sqrt{C} . This means that the point $(x(t), y(t))$ moves clockwise with uniform velocity \sqrt{C} along the circle $x^2 + y^2 = C$ (you could also say that it moves with uniform angular velocity -1).

When comparing these observations with the explicit solutions (1.7) for this case

$$\begin{aligned} x(t) &= R \cos(\phi - t) \\ y(t) &= \dot{x}(t) = R \sin(\phi - t) \end{aligned}$$

we see also that the point $(x(t), y(t))$ moves clockwise at uniform velocity R along the circle $x^2 + y^2 = R^2$. As you can see, both descriptions match exactly if we take $R = \sqrt{C}$.

Remark 11. (1) There is a special integral curve $x^2 + y^2 = C$ with $C = 0$. What motion of a spring or a (linearized) pendulum does this correspond to?

(2) We call the oscillations $x = x(t)$ of the spring with equation $\ddot{x} = -x$ *harmonic* as they are the projection of *uniform* circular motions. This terminology goes back to the ancient Greeks.

In Exercise 1.6.4 you can see that we can similarly interpret the oscillations of the more general equation $\ddot{x} = -\omega^2 x$.

In general, we shall call any mechanical, electronic, or other system described by such an equation of motion a *harmonic oscillator*. In Figure 1.9 we show how the above picture and the graph of the trajectory $x = x(t)$ are related to each other.

1.3.1.2 The pendulum

Next, consider the pendulum equation

$$\ddot{x} = -\sin x \quad \text{or its system form} \quad \begin{cases} \dot{x} = y \\ \dot{y} = -\sin x, \end{cases}$$

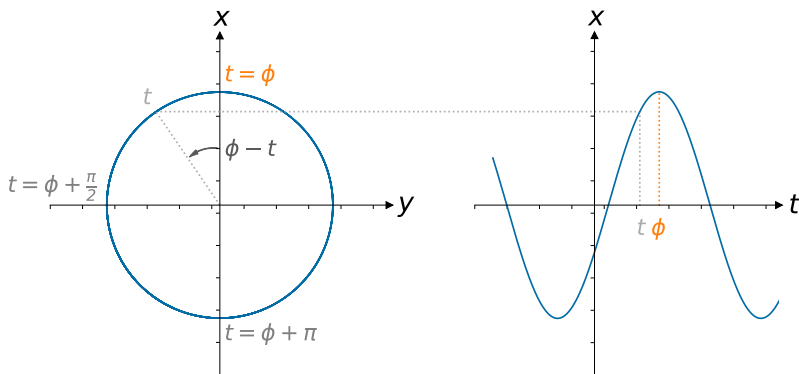


Figure 1.9. Oscillation related to circular motion in the phase plane

with integral curves $y^2 = 2 \cos x + C$, $C \geq -2$, see (1.16). By plotting the integral curves $y = \pm\sqrt{2 \cos x + C}$ for various values of C , we find Figure 1.10.

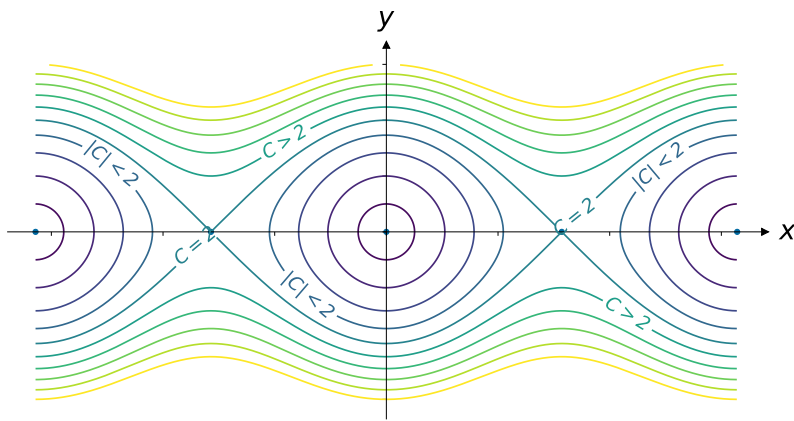


Figure 1.10. Integral curves of the pendulum

- (1) For $C = -2$ only the points $(x, y) = (2k\pi, 0)$ with integer k , satisfy the equation. Each such point represents a “motion” of the pendulum where constantly $x(t) = 2k\pi$ and, also constantly,

$y(t) = \dot{x}(t) = 0$: the pendulum is at rest in its lowest position. These *singular points* therefore correspond to the *stable equilibrium position* of the pendulum.

- (2) For $-2 < C < 2$, the domain of the functions $\pm\sqrt{2\cos x + C}$ is constrained by $\cos x \geq -\frac{C}{2}$. At the boundary points the tangent lines are vertical. Together the two graphs describe a closed oval curve centered around the points $(x, y) = (2k\pi, 0)$. Such curves correspond to “ordinary” oscillations of the pendulum around its stable equilibrium point.

You can check that the point $(x(t), y(t))$ traverses the curve in finite time, the *period of oscillation*, also see Section 1.5, after which the pendulum returns to the original position and velocity: the motion is periodic. You can see also that the amplitude always remains smaller than π .

- (3) For $C > 2$, the functions $\pm\sqrt{2\cos x + C}$ are defined for all real values of x . Their graph corresponds to rotational motions: here the pendulum does full swings, which means that it is turning over. In the equation with the plus sign, $\dot{x} = y > 0$: $x(t)$ is increasing as a function of t and therefore the pendulum moves counterclockwise. Similarly, for the minus sign the motion goes clockwise. As you can see in Figure 1.10, the velocity of the pendulum is maximal at its lowest position $x = 2k\pi$, and minimal at $x = (2k+1)\pi$, when it passes through its upside down position.
- (4) For $C = 2$ the curves are at the boundary between the regions of ordinary oscillations and of the rotational motions of the pendulum. The points $x(t) = ((2k+1)\pi, 0)$ are special here: they are also *singular* but correspond to the *unstable equilibrium* in which the pendulum is at rest in its upside-down position.

Moreover, there are two possible motions of the pendulum, both starting and ending in this unstable equilibrium: one going clockwise and the other counterclockwise. A further difference between these motions and the previous ones, is that they last *infinitely long*: the velocity vector $(\dot{x}, \dot{y}) = (y, -\sin x)$ decreases to 0 as it approaches the singular points $((2k+1)\pi, 0)$.

We conclude that the formula $y = \pm\sqrt{2\cos x + C}$, together with the above figure, contains a great deal of information on the motion of the pendulum. We repeat that this is especially important since, as opposed to the harmonic oscillator, for the pendulum there is no explicit time-parametrized solution like (1.5) or (1.7).

Remark 12. (1) In the case 2 of “ordinary” oscillations, again consider the velocity vector

$$\begin{pmatrix} \dot{x} \\ \dot{y} \end{pmatrix} = \begin{pmatrix} y \\ -\sin x \end{pmatrix}.$$

A direct computation shows that its length is always greater than or equal to $\sqrt{1 - C^2/4}$:

$$\begin{aligned} \dot{x}^2 + \dot{y}^2 &= 2\cos x + C + \sin^2 x \\ &= C + 2 - (1 - \cos x)^2 \\ &\geq C + 2 - \left(1 + \frac{C}{2}\right)^2 = 1 - \frac{C^2}{4}. \end{aligned}$$

This immediately implies that the oval curves are traversed in finite time.

(2) The *geometric* reconstruction of the velocity vector

$$\begin{pmatrix} \dot{x} \\ \dot{y} \end{pmatrix}$$

from the integral curves $y^2 = 2\cos x + C$, $C \geq -2$, runs exactly as for the spring in Section 1.3.1.1: indeed, this reconstruction only relies on the fact that $\dot{x} = y$ and that the velocity vector is always tangent to the integral curve.

Pictures like Figures 1.7 and 1.10 are generally called *phase portraits*. These phase portraits depict characteristic integral curves of the systems of differential equations (1.13), with an arrow indicating the direction in which the point $(x(t), y(t))$ moves along the curve.

1.3.2 Line element fields

Let us return to the differential equations (1.14), now written as

$$x \, dx + y \, dy = 0 \quad \text{and} \quad \sin x \, dx + y \, dy = 0.$$

Reasoning in terms of small increments, as we did before at the beginning of Section 1.3.1, these equations define *line element-* or *direction fields* in the (x, y) -plane. The direction is given at each point (x, y) by the respective velocity vectors,

$$\begin{pmatrix} y \\ x \end{pmatrix} \quad \text{or} \quad \begin{pmatrix} y \\ -\sin x \end{pmatrix} :$$

the corresponding ratios $-x/y$ and $-\sin x/y$ are precisely the *slopes* of the corresponding integral curve $y = y(x)$ at the point x . See Figure 1.11 below for the case of the spring.

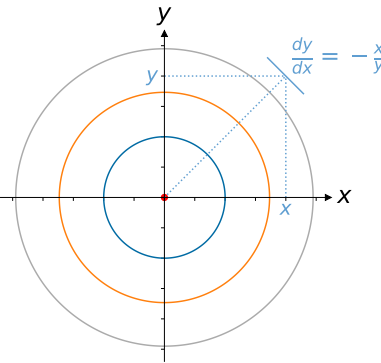


Figure 1.11. Line element at the point (x, y) related to the spring

This idea can be extended to any differential equation of the form

$$\ddot{x} = F(x), \tag{1.17}$$

where $F(x)$ can be interpreted as the force that “sustains” the motion. Using the familiar formulæ $\dot{x} = \frac{dx}{dt} = y$ and $\dot{y} = \frac{dy}{dt} = F(x)$, we arrive at the line element field

$$-F(x) dx + y dy = 0.$$

How can we perform the geometric reconstruction of the velocity vector from the line element in this general case?

In the next section, we develop a general method to describe the integral curves belonging to a differential equation of the form (1.17) or, in other words, to describe its phase portrait.

1.4 Energy

For both the pendulum and the spring almost all motions are periodic: the system returns to a previous state and the motion repeats itself. This suggests that no *energy* is lost throughout the evolution of the system. In what follows we will investigate this conjecture in detail.

1.4.1 Kinetic and potential energy

Let us consider an oscillating system with sustaining force $F = F(x)$. We saw at the end of the last section that its equation of motion is given by (1.17)

$$\ddot{x} = F(x).$$

For simplicity, we assume that for the point mass we always have $m = 1$. In the phase plane we get the system of equations

$$\begin{cases} \dot{x} = y \\ \dot{y} = F(x). \end{cases}$$

Because we assumed $m = 1$, the *kinetic energy* T of the state (x, y) with velocity $y = \dot{x}$ is given by $T = \frac{1}{2}y^2$: this is a well-known formula from early mechanics courses, think of “ $T = \frac{1}{2}mv^2$ ”.

Next, let us look at the *potential energy* V of the system. To this end we generally define

$$V(x) = - \int_0^x F(s) \, ds. \quad (1.18)$$

The integral is the total amount of *work* done (or the energy that has to be delivered) to bring the system from the position 0 to the position x . Physically it is important that the variable x (and therefore also s) describes a *real distance* and not an angle, as for example in the pendulum, compare Exercise 1.6.11. To fix thoughts let us first consider a few examples.

- (1) Considering free fall motion of a mass $m = 1$ in a constant gravitational field with acceleration g , the force is $F(s) = -g$ for any height s . The corresponding potential energy $V(x)$ of the point mass at height x then is

$$V(x) = - \int_0^x F(s) \, ds = gx.$$

Again, a well-known formula: think of “ mgh ”.

- (2) One way to obtain the “good” potential energy for the pendulum is to consider it as a special case of the above item 1. In that case, the height can be computed as $\ell(1 - \cos x)$, see Figure 1.12. Therefore

$$V(x) = g\ell(1 - \cos x).$$

See also Section 1.6.11.

- (3) In the case of the spring, only the sustaining force $F(s) = -ks$ plays a role. Using the definition (1.18), we obtain

$$V(x) = - \int_0^x F(s) \, ds = \frac{1}{2} kx^2.$$

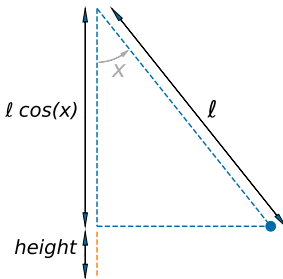


Figure 1.12. The height of the point mass of the pendulum

The lower limit 0 in the integral defining the potential (1.18) is not really important, you can just as well take another constant. This is due to the fact that only *differences* in potential energy play a role in the equations of motion. You can immediately see this from the formulas. Indeed, from the definition it immediately follows that

$$F(x) = -\frac{dV}{dx}(x),$$

therefore an additive constant in $V(x)$ will not affect the equation of motion $\ddot{x} = F(x)$.

1.4.2 Conservation of energy

In our case where the mass $m = 1$, the total energy of the system in the state (x, y) is given by

$$H(x, y) = \frac{1}{2}y^2 + V(x). \quad (1.19)$$

The title of this section seems to imply that energy is conserved, but what does that mean?

Suppose that, at some moment $t = t_0$, the system is in the state $(x, y) = (x(t_0), y(t_0))$ with energy $H(x, y) = E$. Then H should have the same value E for all t , i.e.,

$$H(x(t), y(t)) = E \quad \text{for all } t.$$

Note that in an oscillating system like the spring, in general both x and $y = \frac{dx}{dt}$ keep changing all the time, and therefore also both the kinetic energy $\frac{1}{2}y^2$ and the potential energy $V(x)$. The fact that the total energy H is conserved means that there is a continuous conversion of the kinetic energy into potential energy and vice versa. We now mathematically show that energy conservation indeed does apply.

Theorem 1. *The curve determined by the equation $H(x, y) = E$ is an integral curve of the line element field $y dy - F(x)dx = 0$.*

Proof. We take the equation $H(x, y) = E$ and (1.19) and solve for y :

$$y = \pm\sqrt{2(E - V(x))}.$$

For such a graph we find

$$\frac{dy}{dx} = \pm \frac{\frac{dV}{dx}(x)}{\sqrt{2(E - V(x))}} = \frac{F(x)}{y},$$

which exactly means that it solves the equation $y dy = F(x)dx$. \square

Without giving a proof, we state that there is at most one integral curve of $y dy - F(x)dx = 0$ passing through each point of the (x, y) -plane. Theorem 1 then tells us exactly what these integral curves are: they are formed by all the possible curves with equation $H(x, y) = E$. A curve $H(x, y) = E$ is called the *energy level* with energy E .

But why is the entire plane filled with energy levels? In the above proof we have been a bit sloppy with the case $y = 0$. See the Exercises 1.6.3 and 1.6.4. We will come back to this in Section 2.2.2.

At this point, some of you may have looked at Figure 1.10 and wondered how we can reconcile the Existence and Uniqueness Theorem with the fact that curves seem to cross each other at certain points, giving the impression that more than one integral curve passes through those points.

In the corresponding description of the dynamics in Section 1.3.1.2, you will notice that those points are the unstable equilibria, where the pendulum stands upside down. The points themselves form singular curves, and the integral curves approaching them do so in an asymptotic sense: they approach (going forward or backward in time depending on which part of the curve we consider). Since the velocities in the unstable equilibria vanish, the time to reach them is infinite.

1.4.3 Energy conservation and the phase portrait

We can now use Theorem 1 to determine the phase portrait of our system.

For the spring with spring constant $k = 1$ we have $F(x) = -x$. We can take as potential $V(x) = \frac{1}{2}x^2$, to get total energy $H(x, y) = \frac{1}{2}y^2 + \frac{1}{2}x^2$. The energy level with energy E is therefore the curve

$$\frac{1}{2}y^2 + \frac{1}{2}x^2 = E.$$

And again we find the circles that we already met in Section 1.3.1.

In exactly the same way we can find the integral curves of the pendulum. For simplicity, we take m, ℓ and g all equal to 1. Now $F(x) = -\sin x$ and we can choose $V(x) = 1 - \cos x$, obtaining $H(x, y) = \frac{1}{2}y^2 + 1 - \cos x$. The energy level $H(x, y) = E$ is then described by

$$y = \pm\sqrt{2(E + \cos x - 1)},$$

as we already saw in Section 1.3.1.

1.4.3.1 The general case

Returning to the general case, from the relation $y = \pm\sqrt{2(E - V(x))}$ we can graphically determine the integral curves for any given potential energy V .

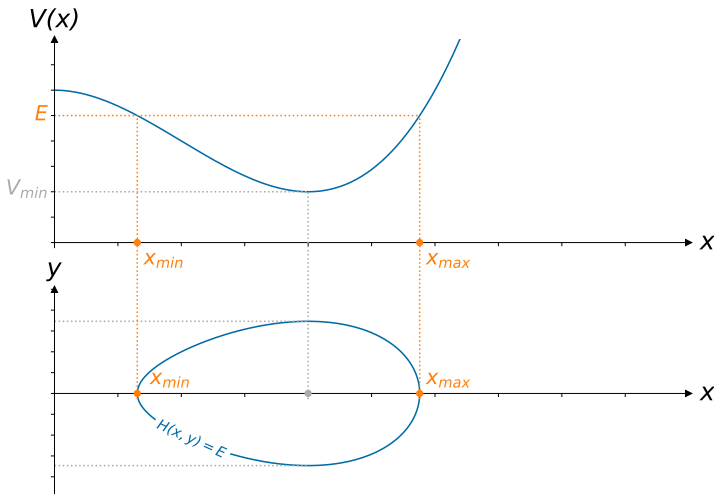


Figure 1.13. Potential V with a minimum and a corresponding integral curve. From the formula $E = \frac{1}{2}y^2 + V(x)$, we see that for $y = 0$ the energy value E on the $V(x)$ -axis are exactly values of the potential energy $E = V(x)$; from the graph of this function we then find the corresponding values $x = x_{\min}$ and x_{\max} , as described in the text.

Suppose the function V , around some minimum, is given by the graph in Figure 1.13. Fix some value for E . The function V attains this value for $x = x_{\min}$ and $x = x_{\max}$, i.e., at those points $V(x) = E$. Since $\frac{1}{2}y^2 \geq 0$ for any value of y , we know that the motion with energy E must be confined to the interval $x_{\min} \leq x \leq x_{\max}$: after all we must always have $V(x) \leq E$. Moreover, the formula also implies that at x_{\min} and x_{\max} we have $y = 0$ and at the minimum V_{\min} we have $y = \pm\sqrt{2(E - V_{\min})}$.

In Figure 1.13 we present a schematic sketch of the integral curve. In Exercise 1.6.6, you can experiment with a number of potential energy functions (also known as *potentials*) and with the corresponding phase portraits. In the same exercise you are also asked to derive a number of general properties of the phase portrait that only depend on the shape of the graph of V .

Let us briefly return to the idea of the bead that slides frictionless along a wire (or the marble rolling in a gutter); also compare one of Huygens' problems mentioned in the Preamble.

There is a very pictorial way to imagine motion of a system with potential function $V = V(x)$, as the one outlined in Figure 1.14 and energy E .

You can think of this as the motion of a bead that slides back and forth along a wire shaped as the graph of the function $x \mapsto V(x)$. You can then imagine that the bead is released at some height E , falls down – thereby gaining velocity and therefore kinetic energy – and then climbs up the wire, slowing down until the height E is reached again.

However nice this thought may be, we have to keep in mind that this is only approximately correct: unless you use the arclength parameter along the wire instead of the variable x , the shape of the wire and that of the graph of the function $x \mapsto V(x)$ do not exactly match.

For instance, for the pendulum the shape of the wire is circular, but $V(x) = 1 - \cos x$. In Exercise 1.6.8 we will return to this, as well as to the problem of designing a wire the potential energy of which is exactly equal to $V(x) = \frac{1}{2}\omega^2x^2$, i.e., of the harmonic oscillator. This will be the way to solve Huygens' problem of finding an isochronous curve posed in the Preamble. See also the comments in Remark 8.

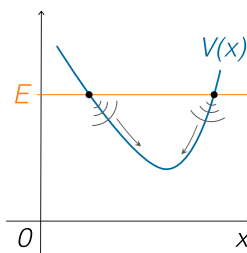


Fig. 1.14. Sliding or rolling in a potential well

1.4.3.2 Two examples

We conclude this section with two examples of a given graph $V = V(x)$, where we sketch the corresponding phase portraits. See the Figures 1.15 and 1.16. Note that the scales on the x -axis and y -axis are not equal.

Let us explain Figure 1.15 a bit further. As in Figure 1.13, the energy values E_1, \dots, E_5 , correspond to values x via the graph of the function V , so that the point $(x, 0)$ in the phase plane lies on the corresponding energy level. Figure 1.16 goes completely similar.

1.5 Period of oscillation

Although we can compute at any point (x, y) of the phase plane the velocity vector $(y, F(x))$, we have effectively lost the ability to determine the global behavior of the system as a function of time. However, when studying oscillatory motion it is useful to have an expression in terms of the potential V for the *period of oscillation*. This is a classical issue, compare Huygens' problems mentioned in the Preamble, and the time has come for us to address it.

1.5.1 A general expression for the period of oscillation

Let us assume that the oscillatory motion occurs in the energy level E with $x_{\min} \leq x \leq x_{\max}$, see Figure 1.17. Using the fact that $y = \frac{dx}{dt}$ and equation (1.19), we get that

$$\frac{dx}{dt} = \pm \sqrt{E - V(x)}.$$

Let $t_{\min} < t_{\max}$ be consecutive times such that $x(t_{\min}) = x_{\min}$ and $x(t_{\max}) = x_{\max}$, that is two consecutive times in between which the upper arc of the trajectory in Figure 1.17 is traversed. We first rewrite the above expression in an infinitesimal form

$$dt = \frac{\pm 1}{\sqrt{E - V(x)}} dx.$$

Next, integrating both sides of this equation with respect to t from t_{\min} to t_{\max} , choosing the plus-sign since we move along the upper

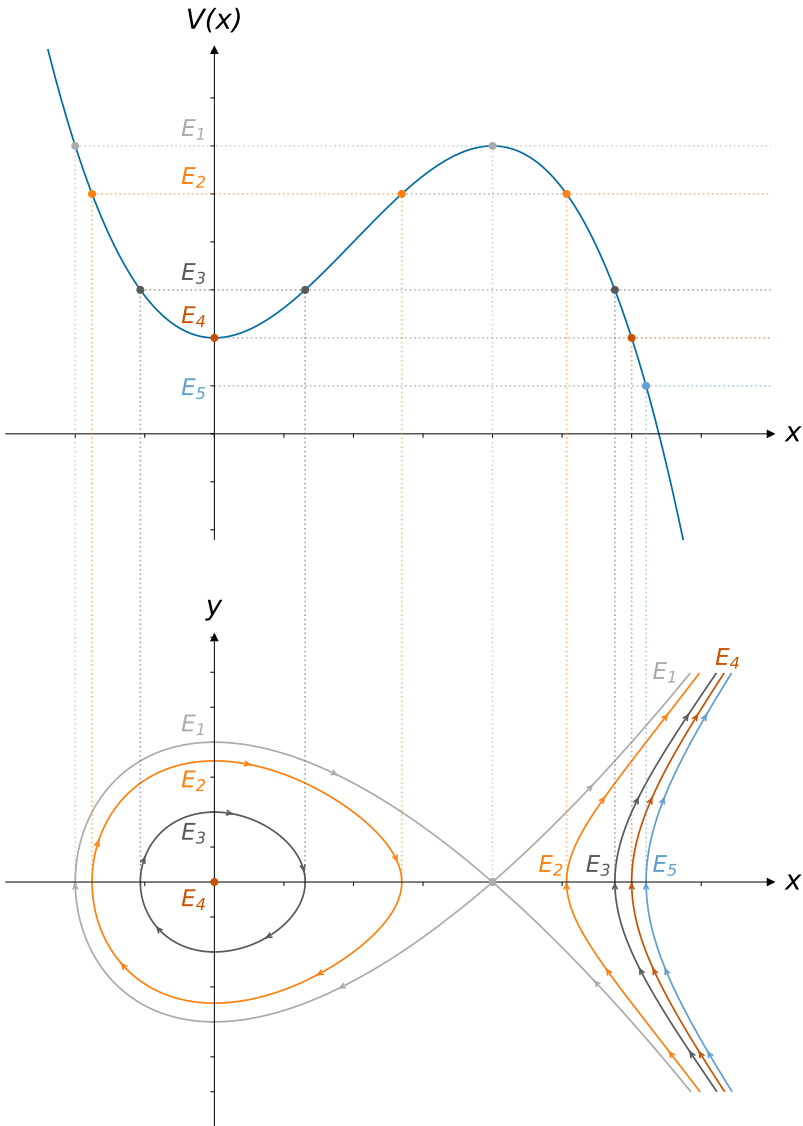


Figure 1.15. Phase portrait of a potential V with a minimum and a maximum, the corresponding equilibria are called *center* and *saddle point*. Can you imagine what the term “saddle point” refers to?

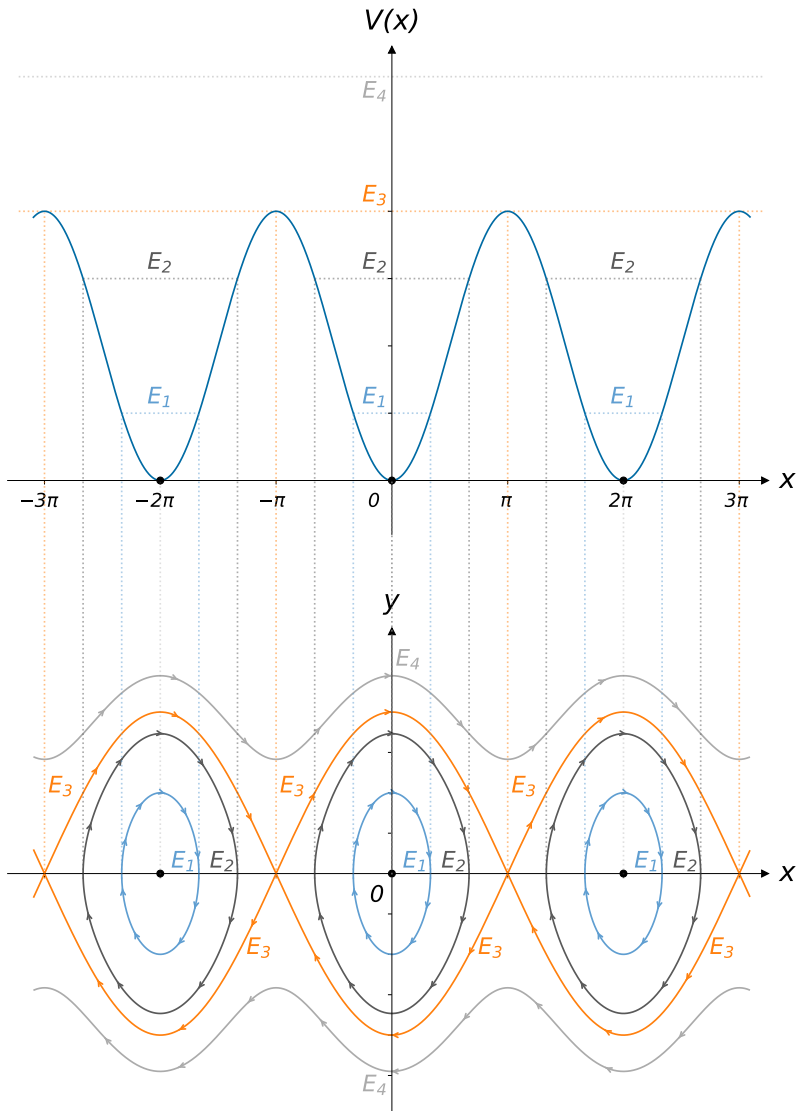


Figure 1.16. Phase portrait of the pendulum with potential $V(x) = 1 - \cos x$

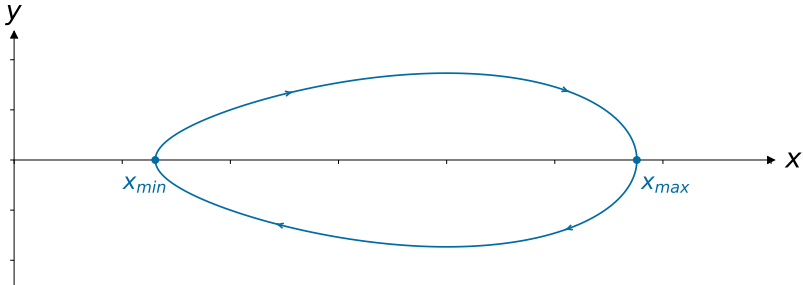


Figure 1.17. A single oscillatory motion

branch, for the *half period* of the motion we get

$$\frac{1}{2}P(E) = t_{\max} - t_{\min} = \int_{x_{\min}}^{x_{\max}} \frac{dx}{\sqrt{2(E - V(x))}}.$$

The fact that the integral is half of the period follows from a symmetry consideration: indeed, the motion is symmetric under reflection in the x -axis, compare Exercise 1.6.2.

1.5.2 Spring and pendulum

Again first consider the example of the spring

$$\ddot{x} = -x,$$

where we choose $V(x) = \frac{1}{2}x^2$. Then for $E > 0$ we find

$$x_{\min} = -\sqrt{2E} \quad \text{and} \quad x_{\max} = +\sqrt{2E},$$

which implies

$$P(E) = 2 \int_{-\sqrt{2E}}^{\sqrt{2E}} \frac{dx}{\sqrt{2E - x^2}}.$$

This integral can be explicitly computed with some knowledge of elementary calculus, from which we recall that

$$\frac{d}{dx} \arcsin x = \frac{1}{\sqrt{1 - x^2}}.$$

This directly gives

$$P(E) = 2\pi,$$

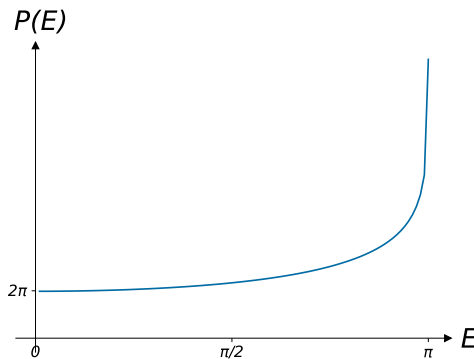


Figure 1.18. Numerical approximation of the period $P(E)$ (1.20) of the pendulum as a function of the amplitude x_{\max}

which is independent of the energy E . This *isochrony* is not new: we already observed this in Remark 2.

Together with Huygens, we find the case of the pendulum

$$\ddot{x} = -\sin x,$$

far more interesting. In this case, given the energy E , we have

$$P(E) = 2 \int_{x_{\min}}^{x_{\max}} \frac{dx}{\sqrt{2 \cos x + 2E - 2}}. \quad (1.20)$$

This integral turns out to be very difficult to compute. It has even been *proven* that the integral cannot be expressed in terms of “elementary” functions. It turns out that similar integrals occur in the computation of the arclength of an ellipse, the reason why one speaks of *elliptic integrals*, see Exercise 1.6.10. Such integrals also emerge when one tries to find a general solution for the pendulum in terms of time parametrization.

Remark 13. (1) Be that as it may, but having a closed expression (1.20) at our possession is convenient. Indeed, it enables us to approximate the period of oscillation, for instance by numerical means. Compare Figure 1.18.

- (2) Elliptic integrals have kept mathematicians busy throughout the centuries, and even today they remain a subject of active research – in particular their algebraic and geometric properties.

We conclude this section with a comment on the period of the pendulum which follows without any calculation. Choosing again the potential energy $V(x) = 1 - \cos x$, the oscillating motions take place in energy levels E for $0 < E < 2$, see Section 1.3.1. The closer E is to 2, the closer the corresponding integral curve passes to the unstable equilibrium of the upside-down pendulum. This equilibrium indeed occurs exactly at the energy level $E = 2$.

Since the velocity vector $(y, -\sin x)$ near the equilibrium gets smaller, the motion of the point $(x(t), y(t))$ on the integral curve gets slower. As a result, the period of oscillation $P(E)$ increases as E approaches 2. In fact, one can show that

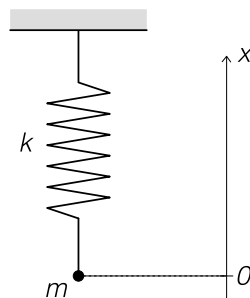
$$\lim_{E \nearrow 2} P(E) = \infty,$$

again compare Figure 1.18. One immediate consequence of this is that the period of oscillation of the pendulum varies with the energy (and therefore the amplitude) of the oscillation, and is not constant as with the spring. We express this by saying that the pendulum is an *anisochronous* oscillator.

1.6 Exercises

1.6.1 The vertical spring

Consider a point particle with mass m that is mounted at the end of a vertically suspended spring that moves in the vertical direction only (and cannot swing). We indicate its position by x : the x -axis therefore is vertical. The point $x = 0$ corresponds to the position at which the spring is at rest: the spring is stretched to compensate the gravity $-mg$ acting on the mass. We assume that, according to Hooke's law, the spring



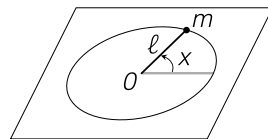
exerts a force that is proportional to deviation:

$$F(x) = -kx.$$

- (1) At what height is the point mass at rest?
- (2) Find the equation of motion for $x(t)$.
- (3) Determine the solutions of the equation of motion.

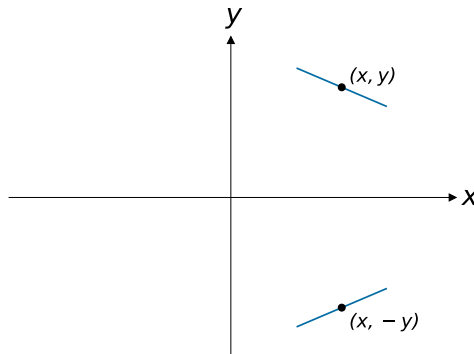
1.6.2 The horizontal pendulum

Consider a pendulum with length ℓ and mass m in the horizontal plane. The pendulum rotates without friction around a fixed point O . If x denotes the displacement angle with respect to a given axis, give the equation of motion for $x(t)$ and determine all its solutions. Sketch a phase portrait. In what way can this pendulum be interpreted as a limit of the usual vertical pendulum?



1.6.3 Symmetries of the line elements field

Show that the line elements field $y \, dy - F(x) \, dx = 0$ is symmetric with respect to reflections in the x -axis. I.e., if the direction of the field at a point (x, y) is (ξ, η) , its direction at the point $(x, -y)$ is given by $(\xi, -\eta)$. What does this imply for the directions at points of the x -axis? What does this imply for the integral curves?



1.6.4 Ellipses and time rescalings on the spring

Consider a point particle of mass $m = 1$ attached to a spring with stiffness k . The potential (or potential energy) of the spring is $V(x) = \frac{1}{2}kx^2$.

- (1) Determine the equation of the energy level E in the phase plane, give a sketch.
- (2) Show that the energy level becomes a circle if you replace y with $z = y/\sqrt{k}$.
- (3) Check that by rescaling the time with $\tau = t\sqrt{k}$, the equation of motion becomes $\ddot{x} = -x$. How is this related to the previous point?

1.6.5 Amplitudes and energies

Consider a spring with potential $V(x) = \frac{1}{2}kx^2$ and a pendulum with potential $V(x) = -\frac{g}{l} \cos x$. In both cases, compute the amplitude of the oscillation in terms of the energy. (The amplitude is half of the difference between the maximum and minimum value that the x coordinate assumes throughout the periodic motion.)

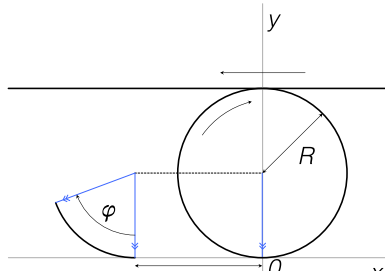
1.6.6 Phase portraits

A number of potential functions are outlined in Figure 1.19. Sketch the corresponding phase portraits and discuss the effect of (local) maxima and minima and of horizontal asymptotes on how the level curves fill up the phase plane.

1.6.7 The cycloid

If one rolls a bicycle wheel on the ground, ensuring that it always moves in the same vertical plane, then its valve describes a curve that is called *cycloid*. Here we will study the case of a bicycle wheel rolling along the ceiling.

You can see the latter depicted on the right: R denotes the radius of the wheel and φ the angular displacement of the valve



from the vertical direction. The position of the valve on the circle is indicated by a double arrow.

Remark 14. We are assuming the tire to be infinitely thin. Otherwise, the valve would lie on the inner side of the tire and never reach the floor, thereby tracing a different curve called *trochoid*.

- (1) Use the figure to show that the following is a parametrization of the cycloid

$$\begin{cases} x(\varphi) = -R(\varphi + \sin \varphi) \\ y(\varphi) = R(1 - \cos \varphi). \end{cases}$$

In the sequel, we shall refer to R as the *radius* of the cycloid and to φ as its *rolling angle*, see Appendix A.

- (2) Sketch the cycloid in the (x, y) plane for $-\pi \leq \varphi \leq \pi$. Does this curve have any symmetries? Where does it have a horizontal tangent? And where a vertical one?
- (3) Let $s(\varphi)$ be the arclength of the cycloid, measured from $\varphi = 0$. Show that $s(\varphi) = R\sqrt{2(1 - \cos \varphi)} = 4R \sin(\frac{1}{2}\varphi)$.
- (4) Finally, show that

$$y(\varphi) = \frac{1}{8R}s^2(\varphi).$$

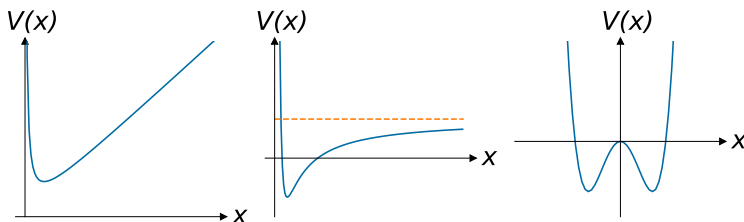
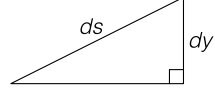


Figure 1.19. Potential energy profiles. From left to right: $V(x) = x + \frac{1}{x}$, $V(x) = \frac{4}{x^2} - \frac{8}{x} + 2$ and $V(x) = x^4 - 2x^2$

Hint for 2: in general, one can use the Pythagorean Theorem to compute the length of an infinitesimal piece of curve parametrized by some parameter ϕ .

Referring to the figure on the right we get

$$ds = \sqrt{\left(\frac{dx}{d\varphi}\right)^2 + \left(\frac{dy}{d\varphi}\right)^2} d\varphi.$$


If we now fill in the values for x and y from the first item of the exercise, we get

$$ds = R\sqrt{2(1 + \cos \varphi)} d\varphi = 2R \cos\left(\frac{1}{2}\varphi\right) d\varphi.$$

It then follows that $s(\varphi) = 4R \sin\left(\frac{1}{2}\varphi\right)$. Note that this is an arclength 'with sign' which can serve as a real coordinate with $\varphi = 0$ as the origin.

1.6.8 Huygens' isochronous and tautochronous curve

In the text, we have seen that a bead that slides along a circular wire (or a marble that rolls into a circular gutter) corresponds to a potential $V(x) = 1 - \cos x$. Which potential corresponds to a bead that slides along a wire, bent according to a cycloid as in the previous exercise?

- (1) Show that the cycloid is an isochronous curve.
- (2) A *tautochronous* curve is defined by the fact that, from whatever height the bead is dropped, the downtime is always the same.
Show that the cycloid is also tautochronous.

1.6.9 Period and area

Consider an oscillator with potential $V(x)$ as depicted in Figure 1.20. Let $A(E)$ be the area in the phase plane that is enclosed by the energy level $H(x, y) = E$ (shaded in the figure). Let $P(E)$ be the period of the oscillation with energy E . Show that the following holds

$$P(E) = \frac{dA(E)}{dE}.$$

Hint: in the figure, we indicated the energy level $H(x, y) = E$ alongside with $H(x, y) = E + dE$. Try to prove that the shaded area

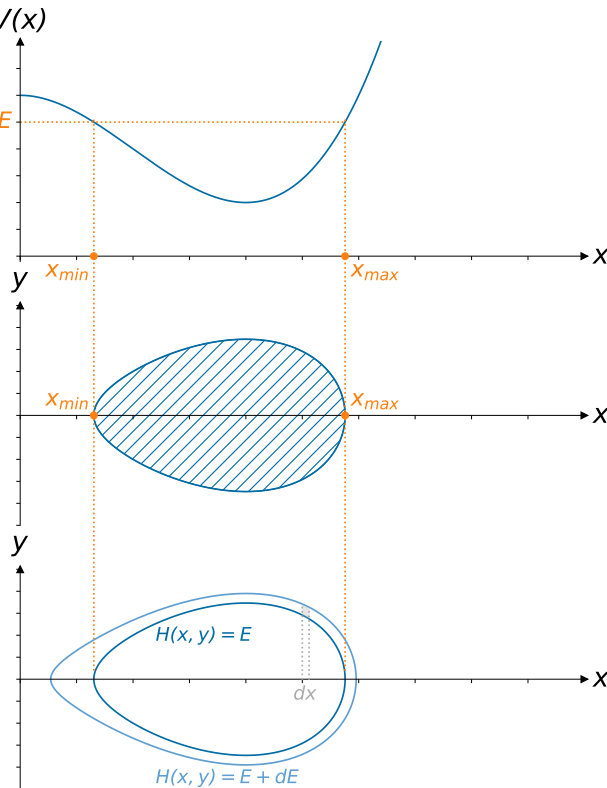


Figure 1.20. Phase portrait of an oscillator

is equal to dE multiplied by the time that the oscillator needs to move from x_0 to $x_0 + dx$.

1.6.10 Elliptic integrals

When studying the period of oscillation of the pendulum we encountered elliptic integrals. By definition, an elliptic integral is any expression of the form

$$\int R \left(x, \sqrt{P(x)} \right) dx$$

where $P(x)$ is a polynomial of degree 4 and where $R(x, y)$ is a rational function of x and y . I.e., $P(x)$ is a polynomial of the form $P(x) = \alpha + \beta x + \gamma x^2 + \delta x^3 + \epsilon x^4$ and $R(x, y)$ is the quotient of two polynomials in x and y , e.g.,

$$R(x, y) = \frac{x^2 - xy - y^3}{1 - x^2 + y^2}.$$

Show that the expression

$$\int \frac{dx}{\sqrt{2 \cos x + C}},$$

used in Section 1.5.2 to describe the period of the pendulum, can be transformed into an elliptic integral by a substitution.

Show that calculating the arclength of a piece of ellipse (also) gives rise to an elliptic integral.

Hint: An ellipse is a curve that can be described by the equation

$$\frac{x^2}{a^2} + \frac{y^2}{b^2} = 1.$$

1.6.11 The potential energy of the pendulum

Derive the potential energy of the pendulum with length ℓ by using a variable u which, unlike the angle x , corresponds to a real distance and then applying

$$V(x) = - \int_0^x F(s) ds.$$

What happens if you directly compute the potential energy out of the equation of motion

$$\ddot{x} = -\frac{g}{\ell} \sin x,$$

so neglecting the fact that x is not a real distance?

Chapter 2

It oscillates in resonance

If you look around, you will notice that almost nothing vibrates “forever” in the sense of the previous chapter. That is because, in reality, energy is always lost to frictional or damping forces. Damping by air resistance, friction at suspension points, electrical resistance: all possible causes for energy loss. However, according to a thermodynamic principle, energy is always preserved and the “lost” mechanical or electric energy is just transferred into thermal energy, or heat.

If we do not exert any external forces on such a system with friction to keep the oscillation going, it will eventually “die out” and end up remaining in an equilibrium position. To prevent this, a pendulum clock is forced by gravity – via the “weights” – or by a wound coil spring.

Without entering into the details of the physics describing the principles above, we will successively involve these two new effects into our story by introducing *friction*, *damping* and *external forcing*, where our main interest lies in the mathematical study of *periodically forced oscillators* with or without friction and damping.

2.1 Friction

2.1.1 A friction directly proportional to the velocity

How do we fit the frictional force into our mathematical description? From our experience we know that in general, friction increases with the velocity, just think of air resistance. The easiest way to express this is to assume that the strength of the frictional force is directly proportional to the velocity, i.e.,

$$W = -c\dot{x}, \quad c > 0. \tag{2.1}$$

This type of friction is known as *linear friction*. The minus sign here is to indicate the “opposing” character of W . With the help of Newton’s law we get the equation of motion

$$\ddot{x} = F(x) - c\dot{x}, \tag{2.2}$$

recalling that $\dot{x} = \frac{dx}{dt}$ and $\ddot{x} = \frac{d^2x}{dt^2}$. Here $F = F(x)$ is the usual sustaining force from the previous chapter. For the *pendulum* and the

harmonic oscillator (e.g., the spring) this gives the following equations of motion

$$\ddot{x} = -\omega^2 \sin x - c\dot{x}, \quad \text{and} \quad (2.3)$$

$$\ddot{x} = -\omega^2 x - c\dot{x}. \quad (2.4)$$

Recall from Chapter 1 that for a pendulum of length ℓ in the constant gravitational field with acceleration g we have $\omega^2 = g/\ell$ and for a spring with mass m and stiffness k we have $\omega^2 = k/m$.

Of course there are more ways than (2.1) to translate into mathematics an increase in frictional force with velocity. From the physical point of view, (2.1) is not always a good choice: for instance, air resistance increases much faster at high velocities than in direct proportionality to the velocity.

To give you an example, a very different type of friction, is the so-called *Coulomb-* or *dry friction*. Mathematically, it looks like this

$$W = \begin{cases} a & \text{if } \dot{x} < 0 \\ -a & \text{if } \dot{x} > 0 \end{cases}.$$

Dry friction is briefly discussed in Chapter 3, see also Exercise 2.6.3.

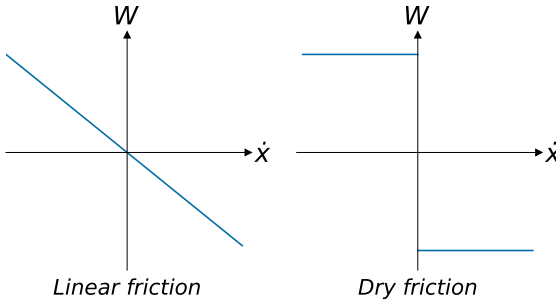


Figure 2.1. Linear versus dry friction

There are two reasons behind our choice to focus on (2.1): firstly, it is not a bad description in many *practical* situations, and secondly, it is mathematically relatively easy to use.

Remark 15. (1) Friction typically occurs when contact with a solid body takes place, for instance friction at the suspension point of a pendulum or friction when moving a body over a surface.

- (2) Damping is caused by the motion of an object through air. The linear form (2.1) can be used to model this and in this case goes under the name of *Rayleigh damping*.
- (3) A moving car experiences air resistance, say Rayleigh damping. At the same time its tires on the road experience friction, say linear friction. In practice, often a mix of damping and friction will occur.

By the way, when the tires are too deflated there is too much friction, however, if there is no friction at all the car cannot move.

2.1.2 The R-L-C circuit

This is another example from electronics. As we will see, in this case the “choice” (2.1) naturally follows from Ohm’s law. In the L-C circuit from Chapter 1 we neglected the resistance of the wires. Instead of ignoring it, we will now assume that the circuit contains a resistor with resistance R , which may also include separate additional resistors. While the physics of the electrical circuit is not really important for our purposes, we can continue using the analogy from Section 1.1.4 with a closed pipe filled with liquid and think of a resistor as a clogged section of the pipe that slows down the flow passing through it. As before, we refer to [152] for the physical background.

According to Ohm’s law, the voltage difference V_R across the resistor is given by

$$V_R = I R$$

where, as before, I is the current. Kirchhoff’s law then requires that

$$V_R + V_L + V_C = 0,$$

which, by a similar calculation as in Section 1.1.4, implies that

$$R \frac{dI}{dt} + L \frac{d^2I}{dt^2} + \frac{I}{C} = 0,$$

or

$$L \frac{d^2I}{dt^2} = -R \frac{dI}{dt} - \frac{1}{C} I.$$

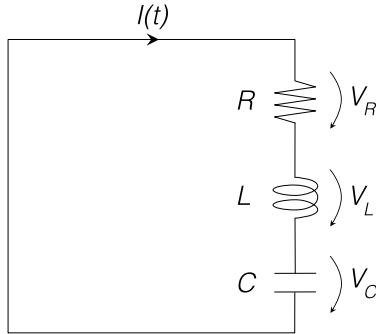


Figure 2.2. R-L-C circuit

Due to Ohm's law, the friction or damping term now is

$$W = -R \frac{dI}{dt},$$

which is of the form (2.1). The equation of motion thus becomes of type (2.2).

- Remark 16.* (1) In the present context friction takes on a different shape only in special physical conditions, such as with very high intensity of the current I or with *superconductivity*.
- (2) In the sequel we shall often neglect the subtle differences in the terminology and generally speak of *damped oscillations*, letting alone the exact physical causes.

2.2 Loss of energy due to friction

We have already mentioned the experimental fact that damping causes the motions to die out into equilibrium states. In what follows we will study a mathematical description of damping and give phase pictures of the damped harmonic oscillator and of the damped pendulum.

In the previous section, we met the general equation

$$\ddot{x} = F(x) - c\dot{x}, \quad c > 0.$$

For a damped oscillator, special cases are (2.3) and (2.4) from Section 2.1.1: the pendulum and the harmonic oscillator, both with damping.

Again we first consider the phase plane. The equations of motion take the form

$$\begin{cases} \dot{x} = y \\ \dot{y} = F(x) - cy. \end{cases} \quad (2.5)$$

In analogy to Chapter 1, we set $F(x) = -\frac{dV}{dx}(x)$. Then, the total energy is $H(x, y) = \frac{1}{2}y^2 + V(x)$. Eliminating time t from (2.5) as before, we end up with the line element field

$$\frac{dy}{dx} = \frac{F(x)}{y} - c,$$

or

$$(cy - F(x)) dx + y dy = 0.$$

Mathematically, we can translate that energy is lost during the motion into saying that for a solution $(x(t), y(t))$ of (2.5), the function $H(x(t), y(t))$ decreases with t . We will show that this is indeed the case (except at the equilibrium points) by looking at the line element field. Recall that the integral curves of the line element field correspond precisely to the integral curves $(x(t), y(t))$ of (2.5), see Section 1.3.

2.2.1 When the undamped motion oscillates

For an oscillating motion of the *undamped* system we know that the energy is conserved. Indeed, such a motion sits in a level curve $H(x, y) = E$ for a certain value of E . For instance think of a situation where E is slightly above a local minimum in the potential function V . We now show that adding damping will result in a motion for which the energy decreases.

The line element at a point (x, y) on the energy level with energy E is determined by the velocity vector $\begin{pmatrix} y \\ F(x) - cy \end{pmatrix}$. Now observe that

$$\begin{pmatrix} y \\ F(x) - cy \end{pmatrix} = \begin{pmatrix} y \\ F(x) \end{pmatrix} + \begin{pmatrix} 0 \\ -cy \end{pmatrix}.$$

Here $(y, F(x))$ is the velocity vector of the undamped system and therefore it is tangent to the curve $H(x, y) = E$; see Section 1.4. The vector $(0, -cy)$ is vertical and points towards the x -axis (unless $y = 0$). This means that their sum points towards the inner area of the curve $H(x, y) = E$, see Figure 2.3, i.e., to the area in the phase

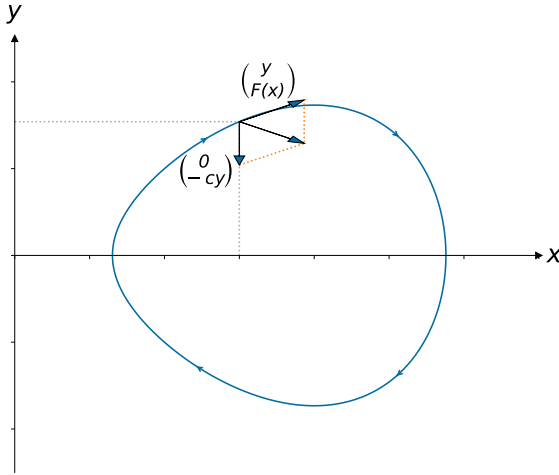


Figure 2.3. Integral curve of an oscillation

plane with *lower* energy. In turn, this means that H decreases during the evolution of the system. So in the case where the undamped motion oscillates, we are done.

Before we consider the general case, let us consider the damped harmonic oscillator with $\omega = 1$

$$\ddot{x} = -x - c\dot{x}.$$

In the (x, y) -plane, this takes the form

$$\begin{cases} \dot{x} = y \\ \dot{y} = -x - cy. \end{cases}$$

Unless $x = y = 0$, the undamped motion always oscillates and our previous remarks apply. Since now $H(x, y) = \frac{1}{2}(x^2 + y^2)$, the energy levels are concentric circles around $(x, y) = (0, 0)$, see Section 1.4.

This means that the integral curves of the damped system are *spirals*, see Figure 2.4. (What is the direction on the x -axis? And on the y -axis?)

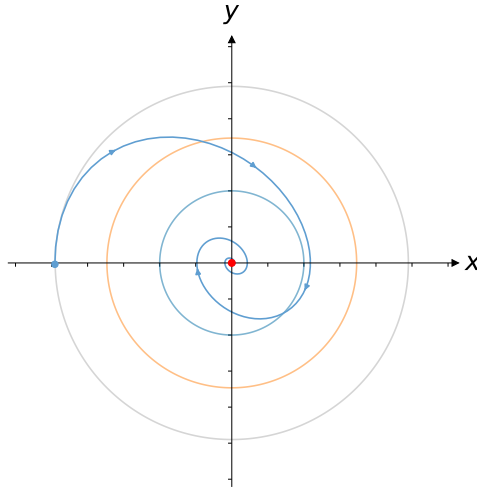


Figure 2.4. A typical damped oscillation in the phase plane

In this simple case the solution $x(t)$ can be written explicitly as

$$\begin{aligned} x(t) &= e^{-\frac{c}{2}t}(A \cos(\nu t) + B \sin(\nu t)) \\ &= e^{-\frac{c}{2}t} R \cos(\phi - \nu t), \quad \text{where} \\ \nu^2 &= 1 - \frac{c^2}{4}. \end{aligned}$$

Compare with formulæ (1.5) and (1.7) from Chapter 1. You can verify that the formula above provides a solution just by substitution into the differential equation. Direct calculations can also confirm that the integral curves $(x(t), y(t))$ in the phase plane do have a spiraling shape. For $c = \frac{1}{2}$ we give numerical evidence for this in Figure 2.5. It is also useful to plot $x(t)$ and see how it changes as c gets larger, see Figure 2.6 and Figure 2.7. The oscillation dampens very quickly for large values of c .

Remark 17. In this example we fixed $\omega = 1$. For a generic value of ω we have $\nu^2 = \omega^2 \left(1 - \frac{c^2}{4\omega^2}\right)$, compare this with Exercise 1.6.4. Note that in all cases $\nu \leq \omega$.

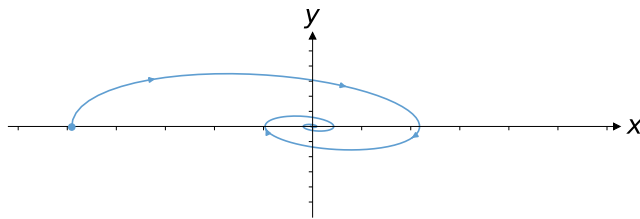


Figure 2.5. Damped oscillation in the phase plane with $\omega = 1$ and $c = \frac{1}{2}$

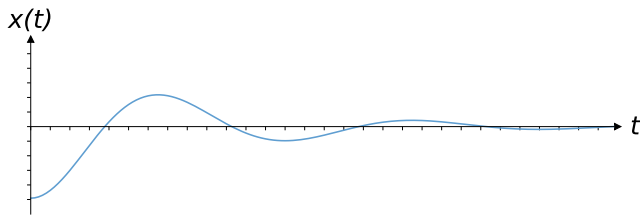


Figure 2.6. Plot of $x(t)$ with $c = \frac{1}{2}$

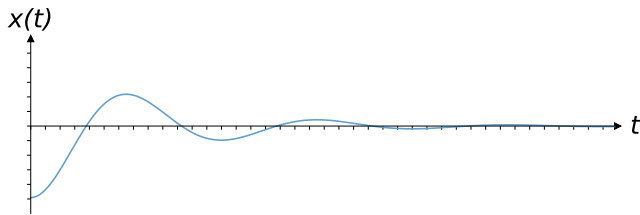


Figure 2.7. Plot of $x(t)$ with $c = 1$

2.2.2 The general case

We shall see that the considerations for the general case do not differ much from the previous ones. Due to the form of the energy function $H(x, y) = \frac{1}{2}y^2 + V(x)$, the vector $(\begin{smallmatrix} 0 \\ -cy \end{smallmatrix})$ always points in the direction of lower energy. Indeed, since the vector $(\begin{smallmatrix} y \\ F(x) \end{smallmatrix})$ is always tangent to the energy level, the sum $F(x) - cy$ is necessarily always pointing in the direction of lower energy.

Remark 18. We have included the following calculation for those who know a bit about partial derivatives and the Chain Rule. Starting out from the formulæ

$$H(x, y) = \frac{1}{2}y^2 + V(x) \quad (\text{energy}),$$

$$F(x) = -\frac{dV}{dx}(x) \quad (\text{relationship between force and potential}),$$

$$\begin{cases} \dot{x} = y \\ \dot{y} = F(x) - cy \end{cases} \quad (\text{damped equations of motion}),$$

we aim to investigate the change of H along an integral curve $(x(t), y(t))$ of these equations of motion. In fact we shall prove that

$$\frac{d}{dt} H(x(t), y(t)) = -cy^2(t)$$

which indeed means that the energy H decreases. (*Why?*)

Proof. The proof consists of a direct computation:

$$\begin{aligned} \frac{d}{dt} H(x(t), y(t)) &= \frac{\partial H}{\partial x}(x(t), y(t)) \frac{dx}{dt}(t) + \frac{\partial H}{\partial y}(x(t), y(t)) \frac{dy}{dt}(t) \\ &= \frac{dV}{dx}(x(t)) \cdot \frac{dx}{dt}(t) + y(t) \cdot \frac{dy}{dt}(t) \\ &= -F(x(t))y(t) + y(t)(F(x(t)) - cy(t)) \\ &= -F(x(t))y(t) + F(x(t))y(t) - cy^2(t) \\ &= -cy^2(t), \end{aligned}$$

as was to be proven. □

Note that this formula, applied with $c = 0$, proves the proposition in Section 1.4.3, namely that in the *undamped* case the energy is a conserved quantity.

Let us explain our considerations in the case of the damped pendulum, for simplicity taking $g/\ell = 1$:

$$\ddot{x} = -\sin x - c\dot{x},$$

which in the phase plane takes the form

$$\begin{cases} \dot{x} = y \\ \dot{y} = -\sin x - cy \end{cases}. \tag{2.6}$$

As before, we choose as potential energy $V(x) = 1 - \cos x$. Then the

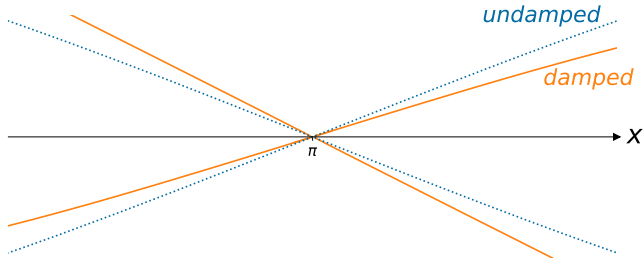


Figure 2.8. The saddle point $(x, y) = (\pi, 0)$ of the undamped and the damped pendulum (note that these coincide) and a small neighbourhood of this. Introducing the damping makes the convergence to the point faster and the escape slower, thereby increasing the slope of the incoming integral curve (top left and bottom right) and reducing the slope of the outgoing ones (bottom left and top right). Compare with the equilibrium point on the left or right hand side of Figure 2.9

following holds.

- (1) It is easily seen that the equilibrium points (singularities $\dot{x} = 0 = \dot{y}$) are the same as in the undamped case: $(x, y) = (k\pi, 0)$ for any integer number k .
- (2) For $0 < E < 1$ the undamped motion is an ordinary oscillation. In that area of the phase plane we can apply the reasoning of Section 2.2.1: the integral curves spiral towards the equilibrium points $(x, y) = (2k\pi, 0)$, for integers k .
- (3) Without proof we mention that the equilibrium points $(x, y) = ((2k + 1)\pi, 0)$, k integer, remain “of the same type” as in the undamped case: these are again called *saddle points*. Compare with Exercise 1.6.6 and its solution in Section F.1.6; also see Section 1.4.3, in particular Figure 1.15

To explain this further we observe the following. These saddle-points have two *incoming* and two *outgoing* integral curves, which

have pairwise the same tangent line at the saddle point itself. The difference with the undamped situation is that these curves are shifted: upwards to the left of the saddle point and downwards to the right. See Figure 2.8.

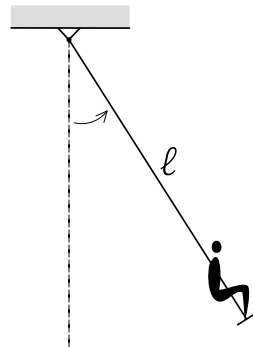
This is exactly the effect of the damping ($-\frac{0}{cy}$) which is added to the velocity vector at each point (x, y) of the phase plane.

The consequences of the above considerations are sketched qualitatively in Figure 2.9. This should also clarify how the other integral curves move in between.

It is not difficult to see that all solutions are moving towards an equilibrium point. Almost all of them go to $(x, y) = (2k\pi, 0)$ for integer k , corresponding to the stable equilibrium. Apart from periodicity in the x direction, there are *exactly two* integral curves ending up in the unstable equilibrium with the pendulum upside down. Compare with Figure 2.10.

2.3 The damped harmonic oscillator with periodic forcing, resonance

In this section we include in the game external forces that vary periodically in time. Just think of a swing that gets pushed periodically, or rather forced by a person that stands or sits on it while performing periodic motions. You can also think of a pendulum whose suspension point moves periodically up and down, or of an R-L-C circuit powered by an alternating current generator. In this section we will restrict ourselves to the linearized situation where the undamped and non-forced oscillator is harmonic.



2.3.1 “The” solution in the harmonic case

We start by considering the harmonic or linear case

$$\ddot{x} = -\omega^2 x - c\dot{x} + A \sin(\Omega t). \quad (2.7)$$

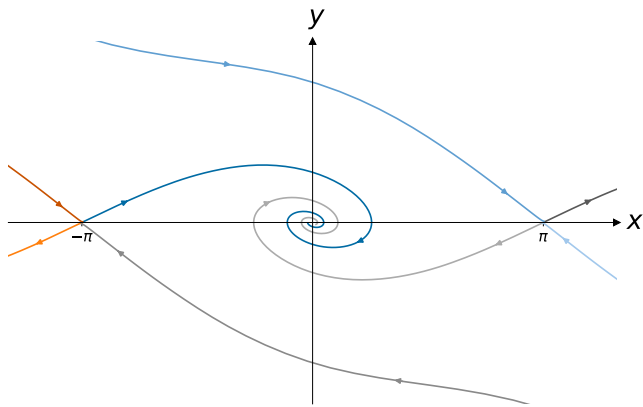


Figure 2.9. Sketch of phase portrait of the damped pendulum

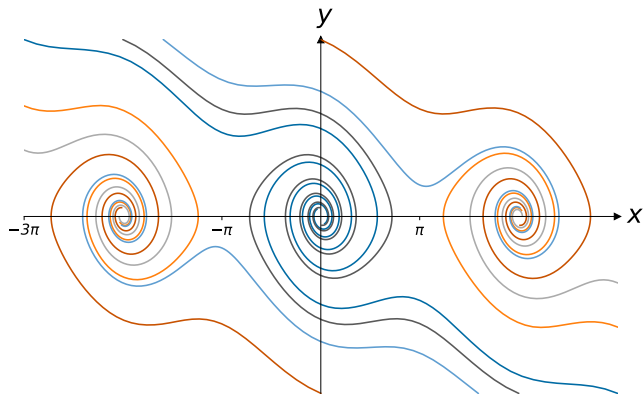


Figure 2.10. Numerical phase portrait of the damped pendulum (2.6) for $c = 0.3$, where we omitted the integral curves tending to the saddle point as these were already shown in Figure 2.9.

Here the novelty is the external forcing $A \sin(\Omega t)$, a time-periodic function with frequency $\frac{\Omega}{2\pi}$. In this simple case we can solve explicitly the equation of motion (2.7) and it turns out that it has a periodic solution, which for $\omega \neq \Omega$ reads

$$x(t) = B \sin(\Omega t + \Phi), \quad (2.8)$$

where B and Φ are given by

$$\begin{aligned} B &= \frac{A}{\sqrt{(\Omega^2 - \omega^2)^2 + c^2\Omega^2}} \quad \text{and} \\ \tan \Phi &= \frac{c\Omega}{\Omega^2 - \omega^2}, \quad -\pi < \Phi < 0. \end{aligned} \quad (2.9)$$

You can check this immediately by substituting this solution in (2.7), also see Exercise 2.6.4. Without proof we mention that this periodic solution, apart from *transient phenomena* (see below), is the only solution to the equation of motion (2.7). In Figure 2.11 we depict the

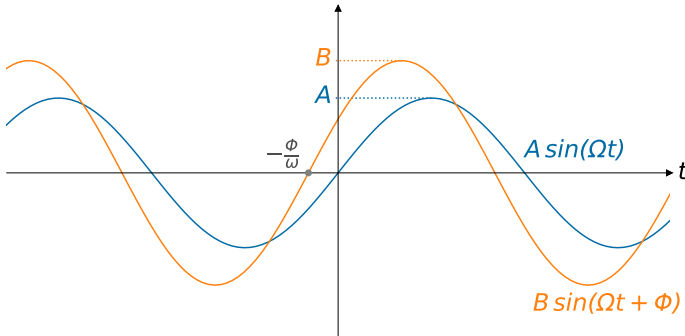


Figure 2.11. Sketch of the periodic solution $B \sin(\Omega t + \Phi)$, see (2.8), together with the external forcing $A \sin(\Omega t)$, see (2.7)

graphs of the functions $t \mapsto A \sin(\Omega t)$ and $t \mapsto B \sin(\Omega t + \Phi)$. The periodic solution $x(t) = B \sin(\Omega t + \Phi)$ has the same period $\frac{2\pi}{\Omega}$ as the driving force $U(t) = A \sin(\Omega t)$, it is only shifted somewhat in time: the solution lags behind the forcing by $\frac{\Phi}{\Omega}$ units of time. We call Φ the *phase difference* between the two.

But what did we mean by ‘transient phenomena’? First observe that (2.8) does not cover all possible solutions of (2.7). Indeed, if we add to it a solution of the *homogeneous* equation, that is equation (2.7) where we set $A = 0$, then you can check with a direct computation that we have found another solution. In fact, an arbitrary solution of (2.7) has the form

$$x(t) = \tilde{B}e^{-\frac{\zeta}{2}t} \cos(\tilde{\omega}t + \tilde{\phi}) + B \sin(\Omega t + \Phi), \quad \tilde{\omega} = \sqrt{k - \frac{c^2}{4}},$$

where Φ , \tilde{B} and $\tilde{\phi}$ depend on the initial conditions. Observe that the additional term in general does not vanish, but that it decays exponentially. Therefore, when enough time has passed it has become negligible compared to the main oscillatory term. It is quite remarkable to think that different initial conditions only affects the transient phenomena and the phase shift, but not the “main” amplitude and frequency of the oscillations.

Next, let us return to the example of the R-L-C circuit, see Section 2.1.2. Suppose that we include in the circuit an Alternating

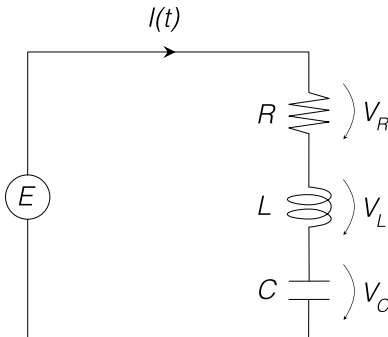


Figure 2.12. RLC circuit with an AC source E

Current (AC) source supplying the voltage

$$E(t) = A \cos(\Omega t).$$

Reasoning as before, Kirchhoff’s law gives

$$V_R + V_L + V_C + A \cos(\Omega t) = 0,$$

which in turn leads to

$$L\ddot{I} = -\frac{1}{C}I - R\dot{I} + A\Omega \sin(\Omega t).$$

This is an equation of type (2.7); therefore all the above results apply.

2.3.2 Resonance in harmonic oscillators with periodic forcing

When looking at (2.9), we see that the amplitude B of the periodically forced equation (2.8) blows up for $c = 0$ and $\omega = \Omega$. This implies that B becomes large when the damping c is small and Ω is close to ω , see (2.9). Recall that $\frac{\omega}{2\pi}$ exactly is the frequency of the oscillator without damping and forcing, the so-called *natural frequency*. In other words, when the frequency of the forcing is close to the natural frequency and the damping is small, the amplitude of the generated oscillation may become large. This whole scenario is called *resonance*. In Appendix E we shall also encounter other examples of resonance.

Let's philosophize a bit about the present resonance. Consider the above example concerning the forced R-L-C circuit. Imagine that the AC voltage source gives a “signal” E that combines various frequencies. Then signals with frequencies that are close to the natural frequency $\frac{1}{2\pi}\frac{1}{\sqrt{LC}}$ of the circuit will be *amplified!* Surely this will be the case when the resistance R is small. When tuning a radio this phenomenon is being used to select the signal of the station that one wants to hear.

There are also lots of cases where it is important to avoid the occurrence of resonance. One that you may have experienced yourself is when walking while holding a cup of coffee or tea in your hand. When the oscillation of the body matches with the natural oscillation frequency of the fluid in the cup, resonance occurs which may well make you spill the contents all over the place [123] It is even more important to avoid resonances on a bridge! A bridge has all kinds of parts that can vibrate. Assuming for a moment that these consist of harmonic vibrations, then there is a natural frequency for each of those. If a periodic force now is exerted on the bridge with a frequency close to such a natural frequency, oscillations (deflections)

of the material can become very large, possibly with disastrous consequences. Such periodic forces can for instance be supplied by a passing train or by the wind, or simply groups of people passing by – as notoriously occurred on June 10, 2000, during the inauguration of the Millennium Bridge in London. This could also happen when a column of soldiers is marching over the bridge, in which case the “out of step” command will be given.

We conclude this section with some numerical plots. In Figure 2.13 we depict solutions of the equation of motion

$$\ddot{x} = -x - c\dot{x} + \sin(\Omega t), \quad (2.10)$$

for different values of c and for $\Omega = 1.2$, together with the plot of the forcing $\sin(\Omega t)$. In Figure 2.14 you can find the corresponding

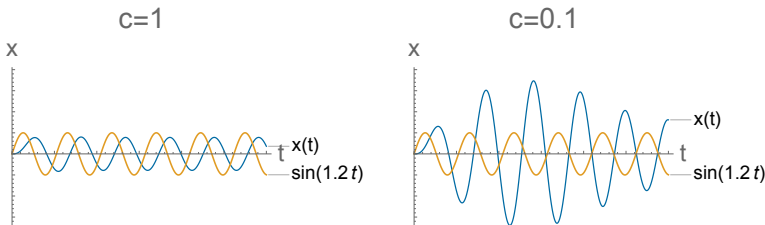


Figure 2.13. Solutions of (2.10) for $\Omega = 1.2$ and $c \in \{1, 0.1\}$ together with the periodic forcing term

integral curves in the phase plane. Why can the curves intersect in this case?

Finally, Figure 2.15 shows the amplitude B in equation (2.9) of the solution of (2.10) with $c = 0.1$ as a function of Ω . Here we see a clear example of a *resonance peak*. If in the radio receiver the peak is narrow and high, it is possible to tune sharply to the corresponding frequency. If the peak is wide and low, sharp tuning is impossible.

2.4 Resonance in non-harmonic oscillators with periodic forcing

Harmonic or linear oscillators, with or without damping, already form an incredible source of mathematical insights. They also play a

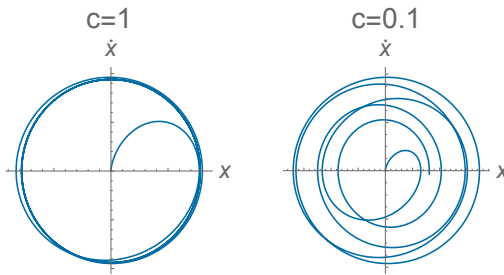


Figure 2.14. Phase curves of equation (2.10) for $\Omega = 1.2$ and $c \in \{1, 0.1\}$

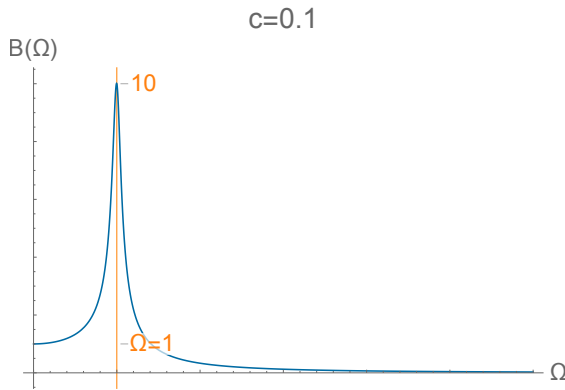


Figure 2.15. Resonance peak: amplitude B (2.9) as function of Ω for equation (2.10) with $c = 0.1$

tremendous role in all kinds of physical or engineering applications. If we let go of the harmonic character, as with the pendulum, things become far more difficult; this is especially true for resonance phenomena. Active mathematical research is still being carried out on this, for more information see Appendix E. Below we give two examples, both based on the pendulum, and give an impression of the kind of motions you can expect.

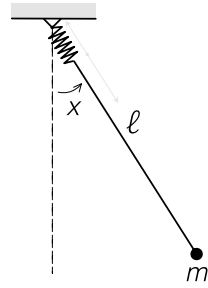
2.4.1 Parametric resonance

In the introduction to Section 2.3 we already mentioned the example of an undamped pendulum whose suspension point moves up and down periodically.

Here we consider a similar system that is slightly simpler to model: if we assume that the rod terminates with an oscillating spring and the total length of the rod and the spring at rest is ℓ , then we can model this system with the following equation of motion

$$\ddot{x} = -\omega^2(1 + A \cos(\Omega t)) \sin x, \quad \omega^2 = \frac{g}{\ell}, \quad (2.11)$$

where the spring oscillates with frequency $\frac{\Omega}{2\pi}$ and amplitude A .



For $A = 0$, that is, when the rod is of a fixed length, we have already seen in Chapter 1 that the pendulum generally oscillates around the lower, stable equilibrium. If we linearize the oscillation, applying the small oscillation approximation described in Section 1.2, we replace $\sin x$ by x , obtaining the *Mathieu equation*

$$\ddot{x} = -\omega^2(1 + A \cos(\Omega t))x$$

to which we shall return in Appendix E.

We state the following without proof. When A is small and Ω is close to an integer multiple of $\omega/2$, the oscillations are no longer confined around the equilibrium point $(x, \dot{x}) = (0, 0)$: the equilibrium loses stability. The shaded regions in Figure 2.16, commonly called *resonance tongues*, provide a schematic representation of the regions of instability in the (Ω, A) -plane. It turns out that in these shaded regions the upside-down equilibrium point $(x, \dot{x}) = (\pi, 0)$ of (2.11) can become stable. Refer to Appendix E for a more detailed explanation of this phenomenon.

Here we speak of *parametric resonance*. We give two examples of how this resonance manifests itself in real life. These concern specifically the resonance originating from $\Omega = \frac{1}{2}\omega$. The destabilizing effects of this resonance cause ships that go on an increasing wind astern to start rolling and even capsize. The stabilizing property seems to be

used by circus artists to get more stability when performing balancing tricks, compare with Arnold [5, Section 25].

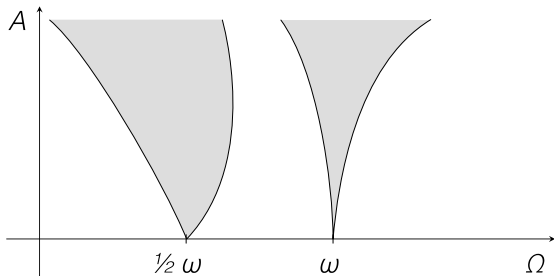


Figure 2.16. Sketch of resonance tongues for the Mathieu equation, inside the tongues the lower equilibrium is unstable; for a more realistic picture see Appendix E.

2.4.2 Non-linear modeling

In the previous cases, the types of motion that occurred were quite clear. Let us review them for a moment:

- (1) The system is stationary, there is no motion;
- (2) The system is in a periodic motion, it oscillates;
- (3) After some transient phenomena the system ends up in either of the two above situations.

However, when considering the pendulum with both damping and forcing

$$\ddot{x} = -\omega^2 \sin x - c\dot{x} + A \cos(\Omega t), \quad (2.12)$$

we witnessed different types of dynamics.

Indeed, to fix thoughts let us set $\omega^2 = 6.4$, $c = 0.6$ and $A = 3.8$, and let Ω vary. With numerical means and a computer you can easily generate images of the evolution $t \mapsto x(t)$ for different values of Ω , as shown in Figure 2.17. For $\Omega \in \{1.6, 1.7, 1.8\}$ one can see that the motion is not of the types listed above. More or less oscillating behavior is alternated abruptly by behavior in which the

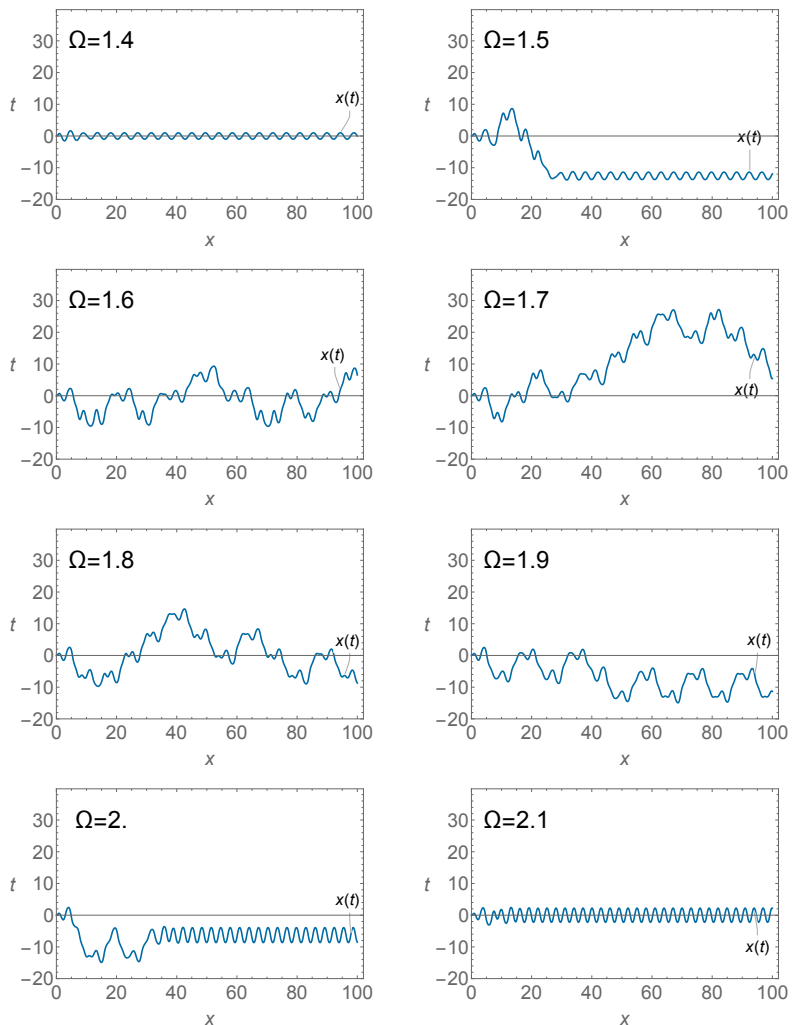


Figure 2.17. Motions of the forced damped pendulum (2.12) for various values of Ω

pendulum does a full swing once or several times. Moreover, these are no transient phenomena that eventually disappear and make way for “calmer” motions. Such motions that get increasingly unpredictable in the longer run, are called *chaotic*.

Example 1 (Quasi-periodicity). One type of motion not mentioned yet is called *multi-* or *quasi-periodic*. This, albeit looking unpredictable, is still one of the “calm” and predictable types. To explain this concept we introduce the two functions

$$\begin{aligned}f(t) &= \sin(2t) + \sin(3t) \\g(t) &= \sin(2t) + \sin(\sqrt{2}t)\end{aligned}$$

and ask ourselves what is the difference between the two.

The function f turns out to be periodic. Indeed by using the trigonometric formula

$$\sin \alpha + \sin \beta = 2 \sin\left(\frac{1}{2}(\alpha + \beta)\right) \cdot \cos\left(\frac{1}{2}(\alpha - \beta)\right),$$

we see that

$$f(t) = 2 \sin \frac{5}{2}t \cdot \cos \frac{1}{2}t.$$

The first factor of f has period $\frac{4}{5}\pi$ and the second 4π , from which we see that the product f has period $\frac{4}{5}\pi$. So the function f is still periodic.

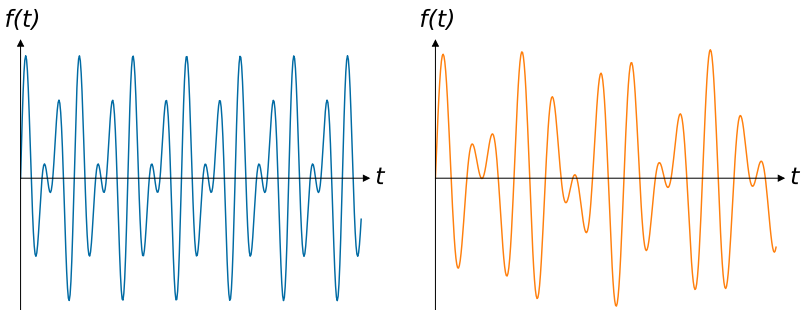


Figure 2.18. Plot of the periodic function $f(t)$ and the quasi-periodic function $g(t)$ from Example 1.

However, whatever you try to do to the function g , you won't find a period: it is not periodic. The thing is that g has *two* periods: $2\sqrt{2}\pi$ and 4π . Since from Euclid [72, Book X] it is already known that $\sqrt{2}$ cannot be written as a fraction of integer numbers (i.e., $\sqrt{2}$ is not rational), the two periods cannot be “reconciled”. We call g multi- or quasi-periodic. In Appendices D and E we meet quasi-periodicity again.

Equations like (2.11) and (2.12) are often used to model physically far more complicated systems, mainly for behavioral reasons: the dynamical behavior somehow resembles that of the more complicated system.

Remark 19. The Josephson junction that plays a role in superconductivity is an example of a system where (2.12) is being used as a non-linear model; compare with [112].

For more information about the new types of dynamics we refer to the Appendices D and E.

2.5 The stabilization of oscillations

How does a child on a swing slow down the rocking motion?

Almost everyone knows from experience that this is being done by moving one's body in an “appropriate” way. Phenomenologically we may speak of *stabilization*: the “behavior” of the swinger brings the swing into its equilibrium position. It is not that easy to translate this specific behavior into mathematical terms.

Let us thus discuss the following, highly simplified situation. Consider the harmonic oscillator $\ddot{x} = -x$ (think of the swing), on which a force F can be applied (think of the person on the swing). The equation of motion describing the total system (swing with swinger) is quite familiar now:

$$\ddot{x} = -x + F.$$

We are left with the following question. Can we determine a force F such that motions are being stabilized? In other words, if the swing is out of its equilibrium state $(x, \dot{x}) = (0, 0)$, how can we send it back

there by the force F . Moreover, this force should be determined by the state of the system itself. This set-up is called *feedback*. To be precise, such an F is a *feedback control*.

2.5.1 First attempt

First, let us try to achieve our objective by simplifying as far as possible the system under consideration, ignoring any friction and letting F be a suitable function of the deviation x alone. For each choice of $F = F(x)$ we get as “total” equation of motion

$$\ddot{x} = -x + F(x).$$

However, this equation is of the kind we already studied in Chapter 1. Namely, by defining

$$V(x) = \int_0^x (\xi - F(\xi)) d\xi,$$

we can rewrite the equation of motion as

$$\ddot{x} = -\frac{dV}{dx}.$$

For these equations, we saw that the energy $E = \frac{1}{2} \left(\frac{dx}{dt} \right)^2 + V(x)$ is a conserved quantity. This means that you can only end up at an equilibrium point if you were already there in the first place. So, unfortunately, this first attempt was unsuccessful.

2.5.2 Second attempt

Let us try to take $F = -\frac{dx}{dt}$. In this case we are done: the equation of motion is

$$\ddot{x} = -x - \dot{x}$$

and it only has motions that lose energy and evolve towards $(x, \dot{x}) = (0, 0)$. This is exactly what we want: after the transient phenomena, we are in equilibrium and the motion has stabilized; see Section 2.2.

The practical drawback of this method is that the instantaneous velocity $\dot{x}(t)$ cannot be measured so easily: while this was not a point of concern for our previous analysis, since this is a control problem and thus suddenly it matters since it implies that the control is less feasible. See also comments in Section 1.3.1 with respect to the phase plane.

2.5.3 Third attempt

Finally, let us try to choose a force F that even though it depends on the position x , it does not depend on the position of the swing at the time where F is exerted. Instead, let F depend on the position the swing had some fixed time earlier, say δ . To be more precise we take F of the form

$$F(t) = Ax(t - \delta),$$

where A is some constant. In this case, the “total” equation of motion reads

$$\ddot{x} = -x + Ax(t - \delta). \quad (2.13)$$

For small δ we can use the approximation

$$x(t - \delta) = x(t) - \delta\dot{x}(t),$$

and for $A > 0$ we get roughly the equation of a damped harmonic oscillator: all solutions lose energy and evolve towards $(x, \dot{x}) = (0, 0)$, again see Section 2.2.

Also in this case we have obtained stabilization although we did not obtain it via a rigorous computation and, instead, we reasoned via an approximation. That is why it is a good idea to double-check the result by numerical means once again, see Figure 2.19. Feedback con-

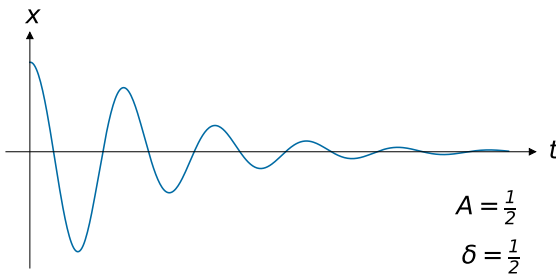


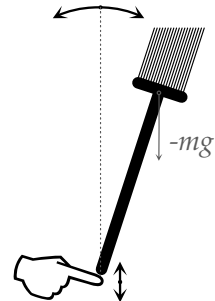
Figure 2.19. Plot of the harmonic oscillator with feedback control (2.13)

trols like the one presented in this chapter play an important role in automatic control systems such as automatic pilots, chemical process controllers, etc.

2.5.4 Stabilizing the inverted pendulum

In Arnold [5, Section 25E] the stabilization is discussed of an inverted pendulum when the point of suspension oscillates in the vertical direction. We recall that the pendulum mass is mounted on a stiff rod.

This effect can be “demonstrated” on a broomstick balancing on your finger. Indeed, when the broomstick slightly leans, say, to the left, then you lower your finger so that the stick becomes vertical again. Then you push up until the stick threatens to fall to the right, and the process repeats. In this way both the pendulum mass and the point of suspension can perform an approximate harmonic motion. Can you see that the finger has to move up and down twice as fast as the broom moves from left to right and back?



In Appendix E we come back to this subject, when dealing with the 1:2-resonance. Indeed, for small amplitudes of the vertical oscillation of the suspension point, the motion of the inverted pendulum is well-approximated by the Mathieu equation and allows for a similar stability analysis. See Appendix E.5.1 and also Figure 2.16.

2.6 Exercises

2.6.1 Negative damping

In electronics there are many oscillators with negative damping. Show that a positive-damping oscillator changes into a negative-damping oscillator with the transformation $\tau = -t$ (i.e., by reversing the direction of time). What does this say about the energy and the phase portrait of negative damping oscillators?

2.6.2 Tossing a fair coin

Consider a point particle moving under the influence of the following potential

$$V(x) = x^4 - 2x^2,$$

compare Exercise 1.6.6. Introducing a (small) damping, the equation of motion changes into

$$\ddot{x} = -\frac{dV}{dx}(x) - c\dot{x}, \quad c > 0 \text{ small.}$$

Describe the phase portrait of this system and find out what is the connection with “tossing a fair coin”.

2.6.3 A “controlled” oscillator

Consider a harmonic oscillator whose center is moving with respect to the velocity as described by the following equation of motion

$$\ddot{x} = -x - a \operatorname{sgn}(\dot{x}),$$

where $a > 0$ and $\operatorname{sgn}(x) = x/|x|$ if $x \neq 0$ and 0 otherwise. Discuss the phase portrait of the system and describe the connection to the “dry friction” introduced in Section 2.1.1.

2.6.4 A damped oscillator with forcing

A harmonic oscillator with damping is driven by an external force. If the external force is $F(t) = A \sin(\Omega t)$, the motion of the oscillator is given by $x(t) = B \sin(\Omega t + \phi)$, after the extinction of the transient phenomenon. Here A, B and Ω are three positive constants. See formula (2.8).

- (1) How large is the energy supplied to the oscillator by the external force per period?
- (2) Let the equation of motion of the damped oscillator be given by

$$\ddot{x} = -x - c\dot{x} + F(t), \quad c > 0.$$

For the motion $x(t) = B \sin(\Omega t + \phi)$ as mentioned above, how much energy per period is lost by the oscillator due to the damping?

- (3) Using the results from the points above, show that $\sin \phi$ is negative.
- (4) At a time in which $x(t)$ is maximal, that is, when $\Omega t + \phi = (2k + \frac{1}{2})\pi$, the velocity of the point mass is zero and its acceleration is $-B\Omega^2$. At that time there is no acting damping force: only the

driving force $-B$ of the oscillator and the external force $F(t)$ are affecting its motion. Use this information to show that

$$B(1 - \Omega^2) = A \cos \phi.$$

- (5) Use the above results to show that

$$\tan \phi = -\frac{c\Omega}{1 - \Omega^2} \quad \text{and} \quad B = \frac{A}{\sqrt{c\Omega^2 + (1 - \Omega^2)^2}}$$

2.6.5 The Van der Pol–Liénard differential equation

In a few steps we will arrive at the phase portrait of the following equation of motion,

$$\epsilon \ddot{x} = -x + \dot{x} - \dot{x}^3,$$

which describes the evolution of an oscillator with non-linear damping. In particular, we will focus on the case where ϵ is a small positive number.

Give, in the following order, the phase portraits of

- (1) $\dot{x} = -x, \quad \epsilon \dot{y} = -y;$
- (2) $\dot{x} = -x, \quad \epsilon \dot{y} = -(x + y);$
- (3) $\dot{x} = y, \quad \epsilon \dot{y} = -(x + y);$
- (4) $\dot{x} = y, \quad \epsilon \dot{y} = -(x + y + y^3);$
- (5) $\dot{x} = y, \quad \epsilon \dot{y} = -(x - y + y^3);$

Hint: The idea is to make a clear distinction between the so-called slow motion and the fast motion. We here assume that ϵ is very small.

In case 1. we then get the following situation. In the first, very short phase, the x coordinate will hardly change and the y coordinate will become almost equal to zero: one could say that the equation $\epsilon \dot{y} = -y$ is dominant. In the second phase, the motion will take place at or near the “curve of slow motion” Σ , obtained by setting the right-hand side of the second equation equal to zero: in case 1. this is the x -axis. On Σ , the motion is given by the first equation. So we get a picture like in Figure 2.20.

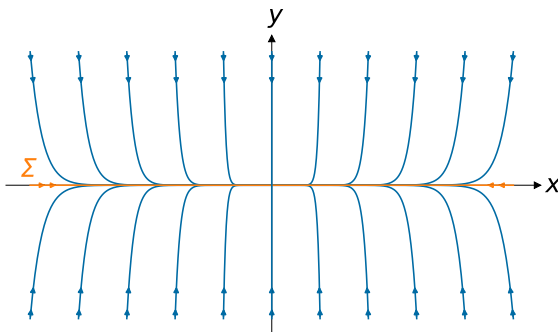


Figure 2.20. Phase portrait of the first case in Exercise 2.6.5

Finally, describe what happens when we “continuously deform” the equations from case 4. to case 5. You can do this by making the equation dependent on a parameter $\mu \in [-1, 1]$:

$$\dot{x} = y, \quad \epsilon \dot{y} = -(x + \mu y + y^3).$$

For what value of μ does the phase picture change most drastically? Describe this change.

Chapter 3

Oscillations in daily life

Oscillations that we encounter in our daily lives, for instance in nature or at the core of our hi-tech devices, are generally of a far more complicated nature than we have seen so far. However, the concepts introduced earlier such as energy, friction and damping, external forces, resonance and the like continue to play an important role. It is also often possible to describe physically complicated phenomena in a simplified manner using examples as we saw in the previous chapters. It is important to ensure that simplifications do not throw away the child with the bath water: it remains necessary to trace back enough of the original problem to achieve meaningful conclusions.

In general, every mathematical description of reality will, almost necessarily, lead to some losses. It is therefore important to find *an as good as possible description*. The development of such descriptions is called *modeling*. In this context, we would like to point at a simplification that is often tacit, namely *linearization*, see also Section 1.2. In order not to lose too much in that process, deviations from equilibrium states should not become too large. Please, keep these thoughts in mind while reading the present chapter, of which we are now going to outline the contents.

Real life examples. In Section 3.1 we present a few real-life examples of oscillations, where some further terminology from physics will be needed. These examples are meant as illustrations of the range of phenomena that can be described with the ideas presented in the text, where we have to emphasize the importance of the above remark on simplifications.

Coupled oscillators. In Section 3.2 we discuss oscillatory phenomena that can be understood as composed of a *finite* number of oscillations in the sense of the previous chapters. This section has a more mathematical nature with a focus on Lissajous figures, where *two* coupled oscillations in the sense of Chapter 1 play a role. As a further example, we will consider a pendulum whose motions are not confined to one vertical plane, but where the point mass is allowed to perform spatial motions; we speak of a *spherical pendulum*. Note that the point mass then is allowed to move over a sphere, which explains the name of the pendulum. The dynamics of such a system

again turns out to be a combination of two “ordinary” oscillations. In Appendix B we shall deal more generally with coupled oscillators and also encounter the spherical pendulum in the context of the Foucault experiment.

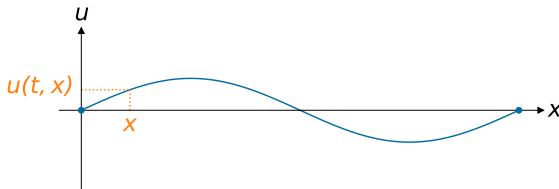


Figure 3.1. Vibrating string

Vibrations in continuous media. Next, in Section 3.3 we shall discuss vibrations of *continuous* media. This kind of vibration can be thought of as composed of an *infinite* number of “ordinary” oscillations. Our leading example will be the sound vibration in an *organ pipe*.

To fix thoughts we first briefly start discussing a vibrating string. In Figure 3.1 we depict such a string that can move in the (x, u) -plane. We assume that the end points of the string are firmly fixed at the points $(x, u) = (0, 0)$ and $(x, u) = (1, 0)$. In addition, we assume that each point of the string can only move in the vertical direction, i.e. the u -direction.

In the idle state, the string coincides with the interval $[0, 1]$ on the x -axis. At a given time t we indicate the (vertical) deviation at a point x with $u(t, x)$. For fixed t , the shape (or configuration) of the string is then given by the graph of the function $x \mapsto u(t, x)$. The question then is how this function changes over time.

Roughly speaking we can say that for every point $x \in [0, 1]$ we consider the evolution of $t \mapsto u(t, x)$, so that its motion is an oscillation in the spirit of Chapter 1. In that sense we have an infinite number of “ordinary” oscillations. Note that these oscillations are far from independent: indeed, due to the elastic properties of the string, the oscillations are strongly coupled.

Remark 20. As already noted, the mathematical treatment of string oscillations, or sound vibrations in an organ pipe, is far more complicated than what we saw earlier. This is because we are now dealing with both the spatial variable x and the time t . The equation of motion of the function $x \mapsto u(t, x)$ thereby becomes a so-called *partial differential equation*, a subject that we shall only briefly touch upon. For an introductory text we refer to Olver [136].

In Section 3.3 will investigate how such a system of “infinitely many oscillators” can be approximated by (linear) systems consisting of a finite number of point masses, interconnected by massless strings. This is called *discretization* of the continuous system. This discretization is further elaborated in the case of an *organ pipe*: the *longitudinal* air vibrations in the pipe are somewhat easier to deal with than the *transverse* vibrations of the string. At the end of the chapter, we briefly discuss a few other vibration and wave phenomena, including those related to *sound* and *light*.

3.1 Two further examples of oscillators

In this section we briefly deal with two miscellaneous real-life examples of oscillations in the sense of Chapter 1. In both cases, less emphasis will be given to precise mathematical statements in favour of more phenomenological discussions; also some physical principles will be used without further comments.

3.1.1 A plank bridge

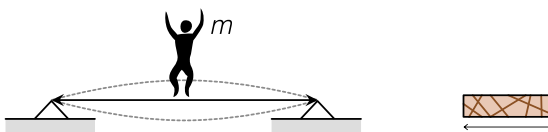


Figure 3.2. Plank bridge over a ditch

A person with mass m stands in the middle of a massless plank lying over a ditch. Due to gravity, the plank bends a little. According

to the *linear* theory, this sag is equal to $u = mg/k$, where g is the acceleration of gravity and k is the stiffness of the plank, *interpreted as a spring*. See also Exercise 1.6.1. This approach “works” as long as the sag is small.

By performing knee bends in a constant rhythm, someone can check that the plank *resonates* at a frequency $f = \frac{1}{2\pi} \sqrt{\frac{k}{m}}$, compare with Section 2.3. The person is acting here as a *drive* or *forcing*. Therefore $f = \frac{1}{2\pi} \sqrt{\frac{g}{u}}$, so the larger u , the lower the *natural frequency* f . Does that correspond to your own intuition?

Remark 21. You can also observe such resonance phenomena with a piano, where the dampers are off the strings, or with a guitar. An external sound can cause a certain string to resound, or resonate.

3.1.2 Rolling of a ship

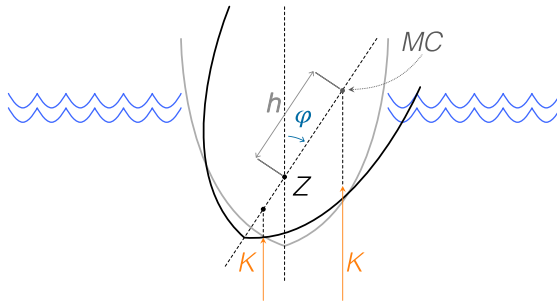


Figure 3.3. Boat rolling about its longitudinal axis

In this example, we consider the *rolling* of a ship, that is, the tilting of the ship about its longitudinal axis, see Figure 3.3. Also within rolling oscillations resonance phenomena can occur. In a small boat, we can become aware of this by wiggling it transversally with the correct rhythm or when the boat responds to waves coming in from the side.

In this case, for the natural frequency, we need to replace the formula $\omega^2 = k/m$ from Section 2.3 by $\omega^2 = c/I$: here c represents the revolving torque per unit of angular displacement exerted by the

upward force K due to buoyancy and I is the moment of inertia with respect to the longitudinal axis. Again see Figure 3.3. For background, refer to [93, 152].

How does c show up in this game? Well, when the angle $\varphi = 0$ then the force K acts exactly in a plane of symmetry. Assuming that the center of gravity Z also lies in this plane, we see that K does not exert a torque on Z . If the ship now tilts over angle ϕ , e.g., clockwise as in the figure, then the right part of the ship dives a little deeper into the water, while the left part rises a little. The upward pressure (or buoyancy) increases slightly on the right and decreases on the left. The resulting upward force K consequently moves to the right. For small angles φ , the working line of K will intersect the axis of symmetry at a fixed point MC , the so-called *metacentre*. The distance h from Z to MC is called the *metacentric height*. Now it holds true that $c = Kh$ (can you see why?). From this it follows that the higher MC , the larger the natural frequency.

We note that h is partly determined by the shape of the ship. For example, a round biscuit tin where Z and MC practically coincide has little to no *shape stability* (the ability of a vessel to stay upright due to its shape). How about a submarine? And a manned rowing boat with a fairly high center of gravity? Keep this in mind if you ever try to stand up in a small rowing boat.

Remark 22. The history of buoyancy and shape stability studies goes back at least to Archimedes of Syracuse (287-212 BC). His famous law, part of his two volumes on hydrostatics entitled *On floating bodies*, marked a turning point in the understanding of floating stability. Archimedes' law states that the buoyancy force on a floating body is an upward force with magnitude equal to the weight of the fluid displaced by the body. This law lies at the core of the above discussion. For general background information again compare with [93, 152].

3.2 Coupling finitely many oscillations

All the examples that we have seen so far involved only one position variable, in a more fancy language: the *configuration* space is always one-dimensional. Another way of saying the same, is that these are

systems with one *degree of freedom*. In engineering these cases are referred to as *1-mass-spring systems*, where tacitly the model is assumed linear.

We now turn to oscillatory phenomena the description of which requires a finite number of position variables, the so-called number of *degrees of freedom* of the system in question.

The considerations to follow require a bit more mathematics and a more thorough treatment is postponed to Appendix B.

3.2.1 Lissajous figures

Both in the Preamble and in Section 1.4.3 we encountered the idea of conceiving an oscillator as a bead sliding along a wire or as a marble in a gutter (disregarding friction and the rolling motion). Now, to formalize the current ideas, we replace the gutter by a bowl. Each point on the bowl is a possible position of the marble. The bowl is considered as a two-dimensional surface and hence the number of degrees of freedom of such a system equals two. The problem in this section is what kind of figures can be described by the marble on this surface. This can be even more interesting when the bowl is not exactly rotationally symmetrical, but say, oblong.

In part III of Minnaert's *The Nature of Light and Colour in the Open Air* [125] there is a discussion of a tree branch swaying in the wind. This system generally has a different stiffness in the vertical and the horizontal direction, and the end of the branch will describe figures similar to the ones of the marble in an oblong bowl. If you would tie a flashlight to the branch at dark, you could observe what these figures look like.

The *linear* theory of this type of motion is mathematically well known under the name of *small oscillations*, see Section 1.2 and Appendix B. With the aid of linear algebra (vector geometry), we can show the following. With an *appropriate choice* of position variables y_1 and y_2 , the system will look like a set of two *uncoupled* (i.e., independent) harmonic oscillators

$$\begin{cases} \ddot{y}_1 = -\omega_1^2 y_1 \\ \ddot{y}_2 = -\omega_2^2 y_2 \end{cases}$$

In the example of the marble in the oblong bowl, the variables y_1 and y_2 could respectively describe the direction of the length and the width of the bowl. In that case, we would have $\omega_1 < \omega_2$. (Why?) Oscillations of the system occurring along the line $y_2 = 0$, so only in the y_1 variable, are called *characteristic*. As known from Chapter 1 all oscillations have the same frequency $\omega_1/2\pi$, which is a *characteristic frequency*. The same can be said of oscillations along the line $y_1 = 0$, which have characteristic frequency $\omega_2/2\pi$. We can now easily present all possible solutions using (1.7) from Section 1.1:

$$\begin{pmatrix} y_1(t) \\ y_2(t) \end{pmatrix} = \begin{pmatrix} R_1 \cos(\phi_1 - \omega_1 t) \\ R_2 \cos(\phi_2 - \omega_2 t) \end{pmatrix}$$

where the constants R_1, R_2, ϕ_1, ϕ_2 are determined by the *state* of the system at any given time, say at $t = 0$. The curves in the (y_1, y_2) -plane described by such solutions are called *Lissajous figures*. Their shape is largely determined by the ratio ω_1/ω_2 of the characteristic frequencies. We give some examples in Figure 3.4.

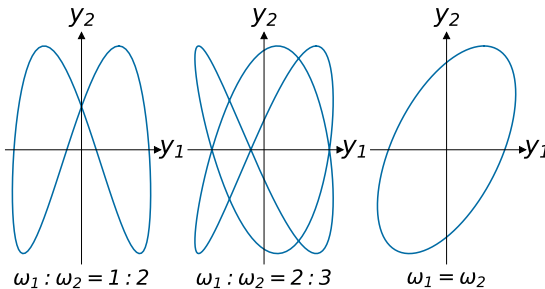


Figure 3.4. Lissajous figures

Remark 23. When $\omega_1 = \omega_2$, such as in the case of a rotationally symmetrical bowl or for the spherical pendulum mentioned before, the Lissajous figures are ellipses (or degenerates ellipses in the form of straight-line segments). For details on small oscillations of the spherical pendulum we refer to Appendix B.

- (1) The *non-linear* theory of problems of two (or more) degrees of freedom is also particularly rich. In connection with the spherical

pendulum, we mention the phenomenon of *spherical precession*. The motion of the pendulum in this case is not an ellipse, but a *rosette*. You can think of it as (almost) an ellipse that slightly rotates during each swing, again see Appendix B.

- (2) The spherical pendulum is still pretty tame. In more general examples, the motions can become so complicated that one speaks of *chaos*, see Section 2.4. In such cases, the mathematical theory is still quite unexplored. For certain impressions see Appendix D.

Conclusive comments and questions. As said before the shape of the Lissajous figure is “largely” determined by the ratio ω_1/ω_2 . It can be shown that degeneration into straight-line segments is *always* possible by choosing R_1, R_2, ϕ_1, ϕ_2 appropriately. Do you have any idea what happens when the ratio ω_1/ω_2 is irrational (e.g., if $\omega_1/\omega_2 = 1/\sqrt{2}$)?

In Section 1.3.1 we encountered the phase plane. It is important to stress that the (y_1, y_2) -plane occurring here should not be confused with this. What are the differences?

If in this context we perform the construction of Section 1.3, we obtain a four-dimensional *phase space* or *state space* with similar properties as the phase plane. The most important of these again is *determinism*: the future of the evolution of the system is fully determined once we know the state of the system at any given time, that is, at which point of the phase space the system is located.

Note that such a point in the phase space is composed of the *positions* y_1 and y_2 and the *velocities* $\dot{y}_1 = \frac{dy_1}{dt}$ and $\dot{y}_2 = \frac{dy_2}{dt}$ (compare (1.3)): these four coordinates $(y_1, y_2, \dot{y}_1, \dot{y}_2)$ exactly describe the state of the system.

3.2.2 Beats

Beats as we know them. We probably all know the phenomenon of *beat tones*: it happens when we hear the sound of two tones that are close to each other in frequency, the result is a sound that pulses continuously, decreasing and increasing.

Besides in the context of musical instruments, you can hear it in the sound of a twin-engine aircraft. A primitive way to explain this

phenomenon is the following: two sound waves reach the eardrum of our ear and deflect the membrane by quantities proportional to $\sin((\omega - \delta)t)$ and $\sin((\omega + \delta)t)$. Here we assume that δ is small and,

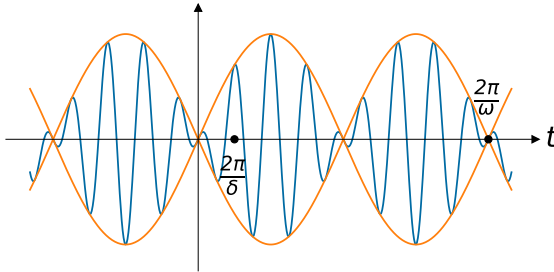


Figure 3.5. A (schematic) beat tone

for the sake of convenience, we also assume that the amplitude is the same in both cases, say 1. According to the sum-to-product formulas from trigonometry,

$$\sin(\alpha) + \sin(\beta) = 2 \sin\left(\frac{\alpha + \beta}{2}\right) \cos\left(\frac{\alpha - \beta}{2}\right),$$

thus the *superposition* of both deflections yields,

$$\sin((\omega - \delta)t) + \sin((\omega + \delta)t) = 2 \cos(\delta t) \sin(\omega t).$$

We hear the pitch corresponding to the frequency $\frac{\omega}{2\pi}$; while the process of mutually reinforcing and quenching of the wave has frequency $\frac{\delta}{2\pi}$. What happens when the amplitudes of the two signals are not equal?

3.2.2.1 Beats in coupled oscillators

We next discuss a problem that shows a certain similarity with the above: also here beats occur. As we shall see this occurrence has to do with an *exchange of energy*. Let us come to the point at once.

Two identical pendulums are linked by a spring as shown in Figure 3.6. All motions take place in one vertical plane. For simplicity we fix the masses, the lengths of the pendulums, and the acceleration of gravity, all equal to 1. Furthermore, the length of the unloaded

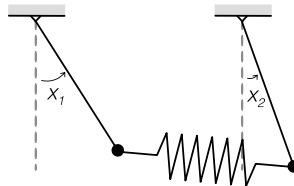


Figure 3.6. Two pendulums coupled by a spring

spring is equal to the distance between the suspension points. We will denote by k the spring constant. In the course of the story that unfolds now, we will choose k small (in a sense to be explained below), which is why one speaks of *weak coupling*.

Here we recognize a system with 2 degrees of freedom: the configuration of the system is determined by the angular positions x_1 and x_2 . In what follows, we are going to investigate the behavior of the system in the vicinity of the equilibrium solution $x_1 = x_2 = 0$.

First, let's describe the type of behavior that is of interest to us. If we let one of the pendulums, say the left one, be at rest in the lower equilibrium and let the other, the right one, perform small oscillations, the following happens. After a while, the right pendulum will come to rest in its lower equilibrium while the left one “takes over” the motion. Now left and right switch roles: after about the same time, the left pendulum is at rest and the right one is moving. This process is repeated forever, the kinetic energy is continuously transferred from one pendulum to the other and vice versa. This can be demonstrated in a test setup, although the “everlasting” character cannot exist in reality due to the ever-present damping . . .

Remark 24. Let us for a while consider the left pendulum on its own. In a somewhat one-sided view of the case, you could say that it is forced by the right pendulum in a rather complicated way. Somehow, the motion of the left pendulum is very reminiscent of the vibration of the eardrum in the example of sound beats as discussed earlier. This is one reason to speak of beats in this case as well.

In the above we used the term “small oscillations”. This means that for a proper mathematical description, we first switch to a linear model: as in Section 1.2, we approximate $\sin x_1 \approx x_1$ and $\sin x_2 \approx x_2$. We now show that the resulting linear system completely falls within the theory of small oscillations. Indeed, when modelling the coupled system by

$$\begin{aligned}\ddot{x}_1 &= -x_1 - \kappa(x_1 - x_2) \\ \ddot{x}_2 &= -x_2 - \kappa(x_2 - x_1),\end{aligned}\tag{3.1}$$

where $\kappa > 0$ is the spring constant of the connection. As said earlier, the main point of this theory is that for a suitable choice of position variables the system completely decouples. It should be clear at this point that these variables cannot be x_1 and x_2 : the entire description above with the energy transfer indicates that these are strongly coupled. However we do have

Proposition 1 (Decoupling the coupled system). *The change of position variables given by*

$$z_1 = x_1 + x_2 \quad \text{and} \quad z_2 = x_1 - x_2$$

transforms the coupled system (3.1) into the uncoupled system

$$\begin{aligned}\ddot{z}_1 &= -\omega_1 z_1 \\ \ddot{z}_2 &= -\omega_2 z_2,\end{aligned}\tag{3.2}$$

with frequencies $\omega_1 = 1$ and $\omega_2 = \sqrt{1 + 2\kappa}$.

Proof. Our proof is just a small calculation:

$$\ddot{z}_1 = \ddot{x}_1 + \ddot{x}_2 = -x_1 - x_2 - \kappa(x_1 - x_2 + x_2 - x_1) = -z_1,$$

and similarly

$$\ddot{z}_2 = \ddot{x}_1 - \ddot{x}_2 = -x_1 + x_2 - \kappa(x_1 - x_2 - x_2 + x_1) = -(1 + 2\kappa)z_2.$$

□

Remark 25. For reasons that will be explained in Appendix B we like to work with the new variables

$$y_1 = \frac{1}{\sqrt{2}}z_1 \quad \text{and} \quad y_2 = \frac{1}{\sqrt{2}}z_2,$$

which take the system (3.2) to the completely similar form

$$\ddot{y}_1 = -y_1$$

$$\ddot{y}_2 = -(1 + 2\kappa)y_2,$$

as you can check by a direct computation.

From the above, we can directly obtain the sketch in Figure 3.7. Why does the spring constant k play no role in the value of ω_1 and

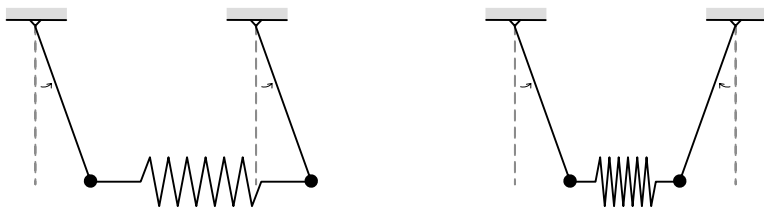


Figure 3.7. Characteristic oscillations of the coupled pendulum system (3.1). Left: $y_2 = z_2 = 0$, leading to characteristic oscillations of the y_1 -variable with frequency $\omega_1 = 1$. This means that $x_2 = x_1$ and that the pendulums move *in phase*. Right: $y_1 = z_1 = 0$, giving characteristic oscillations of the y_2 -variable with frequency $\omega_2 = \sqrt{1 + 2\kappa}$. This means that $x_1 = -x_2$ and that the pendulums move *in anti-phase*.

how can one see that $\omega_1 < \omega_2$ without explicit computation?

Remark 26. Our choice of the y - and z -variables in Proposition 1 may seem a bit ad hoc, although guided by intuition and well justified by Figure 3.7. In Appendix B we shall revisit the decoupling problem from a far more general point of view opening a wide range of applications. To make this possible we need some *linear algebra*, to be introduced in Section B.1.

Here comes another analogy to the sound beats: we are apparently dealing with two uncoupled oscillators with frequencies that, for small κ , are close to each other. The *tones* in the sound example here correspond to *characteristic oscillations*.

Let us first try to understand the beat phenomenon without calculations. It is an important property of the linear theory that any motion of both pendulums can be written as a *superposition* (addition) of the characteristic oscillations just described. This is schematically depicted in Figure 3.8. During the first few periods, the motion is largely

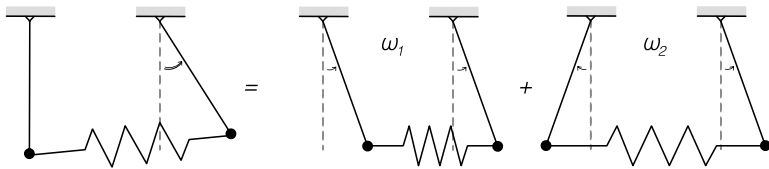


Figure 3.8. The superposition principle

restricted to the right pendulum, the left one remains approximately at rest. This happens because ω_1 and ω_2 are almost equal. However, ω_2 is *slightly* larger than ω_1 , so the oscillation with ω_2 is *slightly* faster than that with ω_1 . Therefore, if we wait long enough, the ω_2 -motion has a “phase” that becomes 180° ahead of the ω_1 -motion. The superposition of both these oscillations, sketched in Figure 3.9, shows that now the right pendulum has become stationary, while the left one is swinging with the initial amplitude. And so on. Therefore this reasoning gives a solid qualitative description of the motion.

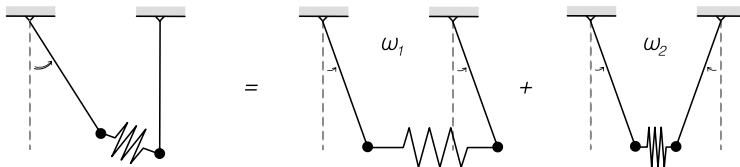


Figure 3.9. The superposition principle continued

Now let us compute a few things. To this end, we first write out the characteristic oscillations in the x_1 and x_2 variables. From the above definitions of the z - and the y -variables one can simply verify

that vice versa we have

$$x_1 = \frac{1}{\sqrt{2}}(y_1 + y_2) \quad \text{and} \quad x_2 = \frac{1}{\sqrt{2}}(y_1 - y_2).$$

As we saw in Section 3.2.1, the formulas for the characteristic oscillations in the y variables are

$$\begin{aligned} y_1(t) &= R_1 \cos(\phi_1 - \omega_1 t), & y_2(t) &= 0 \quad \text{and} \\ y_1(t) &= 0, & y_2(t) &= R_2 \cos(\phi_2 - \omega_2 t), \end{aligned}$$

where $\omega_1 = 1$ and $\omega_2 = \sqrt{1 + 2k}$. In the x variables these correspond to

$$\begin{aligned} x_1(t) &= x_2(t) = \frac{1}{\sqrt{2}}R_1 \cos(\phi_1 - \omega_1 t) \quad \text{and} \\ x_1(t) &= -x_2(t) = \frac{1}{\sqrt{2}}R_2 \cos(\phi_2 - \omega_2 t). \end{aligned}$$

As said before, in the linear theory you can interpret all motions as the sum of characteristic oscillations. It follows that we now have the general solutions

$$\begin{pmatrix} x_1(t) \\ x_2(t) \end{pmatrix} = \frac{1}{\sqrt{2}} \begin{pmatrix} R_1 \cos(\phi_1 - \omega_1 t) + R_2 \cos(\phi_2 - \omega_2 t) \\ R_1 \cos(\phi_1 - \omega_1 t) - R_2 \cos(\phi_2 - \omega_2 t) \end{pmatrix}$$

where R_1, R_2, ϕ_1, ϕ_2 depend on the state of the system at any fixed time, say at $t = 0$.

The kind of motion of interest to us now, so where the beats (should) occur, has the property that $R_1 = R_2$ and $\phi_2 = \pi - \phi_1$. Substituting these values, after possibly applying a translation in the t variable, we can safely assume that $\phi_1 = 0$. This means that we are left with

$$x_1(t) = \frac{1}{\sqrt{2}}R(\cos(\omega_1 t) - \cos(\omega_2 t)), \quad x_2(t) = \frac{1}{\sqrt{2}}R(\cos(\omega_1 t) + \cos(\omega_2 t)),$$

where $R = R_1 = R_2$. Again applying some trigonometry we obtain

$$\begin{aligned} x_1(t) &= -R\sqrt{2} \sin\left(\frac{1}{2}(\omega_1 + \omega_2)t\right) \sin\left(\frac{1}{2}(\omega_1 - \omega_2)t\right) \\ x_2(t) &= R\sqrt{2} \cos\left(\frac{1}{2}(\omega_1 + \omega_2)t\right) \cos\left(\frac{1}{2}(\omega_1 - \omega_2)t\right). \end{aligned}$$

Next we use that $\omega_1 = 1$ and $\omega_2 = \sqrt{1 + 2k}$. Recalling the fact that k is small, we have that *approximately* $\omega_2 \approx 1 + k$. Can you see why

this is true? (Hint: we found it helpful to remember that for small $k > 0$ one has $k^2 \ll k$.) The motion then gets the form

$$\begin{aligned}x_1(t) &= R\sqrt{2} \sin((1 + \frac{1}{2}k)t) \sin(\frac{1}{2}kt) \quad \text{and} \\x_2(t) &= R\sqrt{2} \cos((1 + \frac{1}{2}k)t) \cos(\frac{1}{2}kt),\end{aligned}\tag{3.3}$$

depicted in Figure 3.10. This computation confirms what we saw

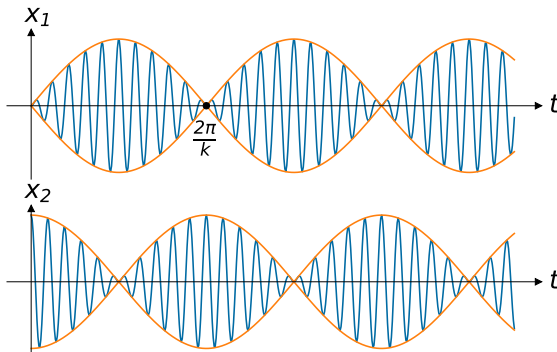


Figure 3.10. Beats of the weakly coupled oscillators

before; evidently we now get more detailed information, such as the frequencies of oscillation and beating, the maximum amplitudes, and so on. It is good to think a bit about the similarities and differences between this example of the weakly coupled pendulums and that of the sound beats.

To complete the story, in Figure 3.11 we give the Lissajous figure that belongs to the motion described by formula (3.3). Try to find a practical difference between this Lissajous figure and those in Section 3.2.1, particularly paying attention to the observability.

That is all concerning the weakly coupled pendulums. This kind of beat may occur in many variations, think of two identical springs, weakly coupled by a third, or the so-called Wilberforce pendulum, briefly discussed below. It is also quite easy to devise test set-ups to try out for yourself. However, it is more difficult to find these beat phenomena in everyday life.

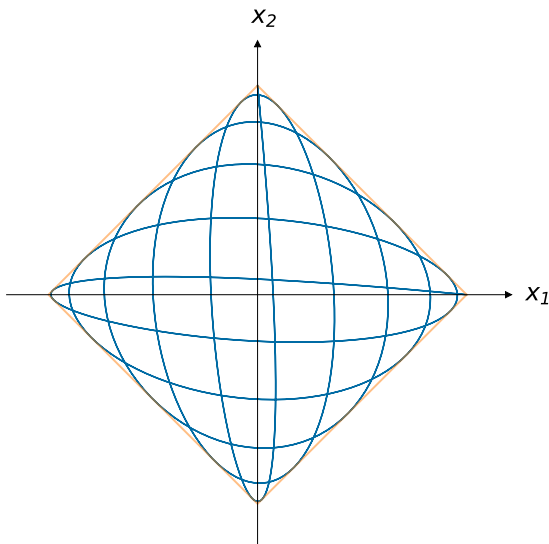
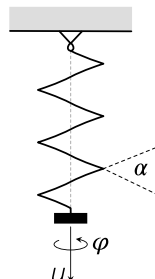


Figure 3.11. Lissajous figure of the weakly coupled oscillators

Nevertheless, we suggest the following experiment. The main ingredient for this is a well-tuned piano. Detach the dampers from the strings and find a tone where the string is doubled once. As in Section 1.6.1, we view these two strings as 1-mass-spring systems with the same spring constant (pitch). The string suspension, the soundboard, and the air create a weak coupling between the two. Now excite one of the strings with your hand, leaving the other at rest. What do you expect to hear and what do you hear? Note that this setup is different from one where you would aim to demonstrate sound beats.

Wilberforce. To conclude the discussion on beats consider the Wilberforce spring: a system consisting of a rather long vertical coil spring attached to a rigid cylindrical-shaped body at the bottom, compare with the figure to the right.



In a first approximation, we observe two types of oscillation: vertical motions (in the u direction) and rotations about the vertical axis (in the φ direction), also called torsional oscillations.

After linearization around the equilibrium state where the system is at rest, we can speak about the frequencies of these two oscillators. These depend on the elastic properties of the spring, the mass and the moment of inertia of the cylinder about the vertical axis. We here assume that these two frequencies are equal.

On closer inspection, both oscillators turn out to be weakly coupled. Indeed, since we are dealing here with a coil spring (spiral), a weak torsional force occurs when moving in the vertical direction; the spring will tend to slightly coil or uncoil itself depending on the compression or extension. In this case, the pitch angle α of the spiral spring plays a role. Based on the above, we would expect beats in which energy in the vertical oscillator is exchanged with energy in the torsion pendulum. And, indeed, you can observe these beats in the physical realizations of this pendulum. You can find plenty of examples on the internet.

3.2.3 More than two degrees of freedom

Whether or not we are dealing with two or more degrees of freedom is not very important for the linear theory. Mutatis mutandis, the above story concerning small oscillations can now be told again. The important point is that with a suitable choice of position variables such a system reduces to a finite number of *decoupled* systems of one degree of 1-degree-of-freedom oscillators, compare Appendix B.

Regarding the non-linear theory, we only want to add the following to what has already been said at the end of Section 3.2.1: the complexity of the systems increases somewhat if we consider three or more degrees of freedom instead of only two.

We conclude this section with an example of the motions of a *tugboat* (that we conceive of as a rigid body). In Section 3.1 we already met with the *rolling motion* of a boat. Similar considerations also apply to so-called *yawing*, a rotational motion about the transverse axis, see Figure 3.12.

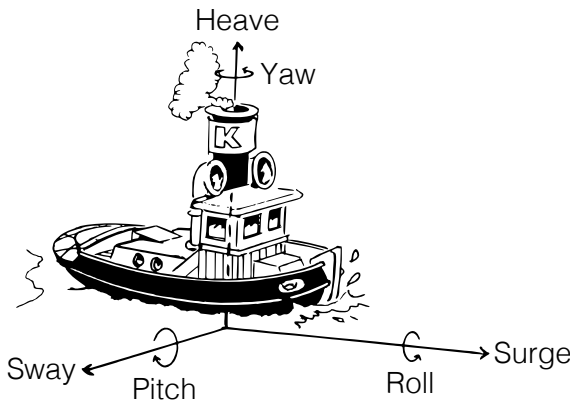


Figure 3.12. Superposition of oscillations in a boat; the tugboat is called *De Kraak* [168]

The metacentric heights for both motions will generally not be the same. A third oscillation that a ship can perform is called *heaving*: it concerns the vertical motions of the ship.

In general, a *rigid body* can perform six motions, three translations and three rotations: the system has six degrees of freedom. This also applies to a boat, as long as we consider it as a rigid body. We have added the nautical names relating to these motions in Figure 3.12. If we restrict ourselves to the oscillatory motion that the ship can perform in more or less calm water, that is, rolling, pitching and yawing, then we have a system of three degrees of freedom.

3.3 Vibrations of continuous media

In the introduction to this chapter we already met the vibrating string. Further examples of systems that involve a continuum of oscillations are membranes, beams, air, water, ... We already mentioned the partial differential equations that here act as equations of motion. In general, these equations lend themselves badly to the kind of mathematical analysis we have seen so far. In part because the required theory has not *yet* been developed. In many practical problems people *rely instead on* numerical analysis, which often provides sufficiently useful answers.

3.3.1 Discretizing the continuum

The discretization of the vibrating medium is one approach that can be used for a numerical treatment of vibrating continua, but also for deriving partial differential equations to model them. As said before, the organ pipe is going to be our leading example.

3.3.1.1 The organ pipe

We consider an organ pipe modeled as a cylindrically shaped tube. Our objective is study the oscillatory motion of the air particles in the pipe. For simplicity, we assume that the pipe is closed at both openings, see Figure 3.13. Note that a real organ pipe is always open, at least at the one end where the air is blown in.

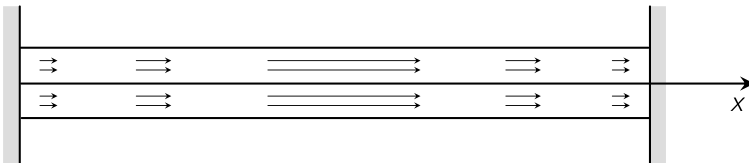


Figure 3.13. Schematic organ pipe

We also make the following assumptions:

- (1) Gravity does not affect the motion of the air particles;
- (2) The air particles can only move in the longitudinal direction, parallel to the pipe. By our choice of coordinates this will be the x -direction;
- (3) We neglect any friction at the pipe wall.

An air particle that at rest has x -coordinate x_0 now moves in the x -direction that we denote by

$$t \mapsto x_0 + u(t, x_0).$$

So here $u(t, x_0)$ corresponds to the x -displacement of the particle at time t . Finally, since both ends $x_0 = 0$ and $x_0 = L$ of the pipe are closed, for all t we have $u(t, 0) \equiv 0 \equiv u(t, L)$; compare this with our comments on the vibrating string at the beginning of this chapter.

Remark 27. The length L of the organ pipe is important for the pitch. For the moment we simply take $L = 1$, but later we will come back to this.

In a discrete approach, we replace the above description by a model that considers the air particles as a system of n equal point masses, joined by identical massless springs, see Figure 3.14. Again all motion occurs in the x -direction. Since the evolution of the system is independent of the vertical position, one can think of these point masses as representing vertical slices of the air in the pipe.

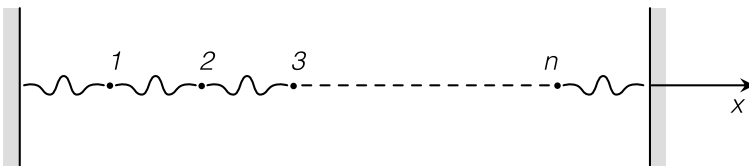


Figure 3.14. Discretized organ pipe

The idea is that as n gets ever larger, this system will become an increasingly better approximation of the air in the organ pipe. Let us clarify this somewhat vague statement. First of all, we must determine the size m of the masses and the spring constants. Since the springs are massless, we distribute the total air mass M equally over the point masses, that is, we could choose $m = \frac{M}{n}$. If we do this, however, we penalize unevenly the extrema of the n -pipe relative to the center. This problem is avoided if we always take $m = \frac{M}{n+1}$. The “residual” mass m then is distributed in two halves over the two extrema. For the rest of the story, we stick to this last choice.

Next, we consider the spring constant k . We start by noting the following *physical fact*: If a spring with stiffness k is cut into two equal pieces, each of the two halves will have stiffness $2k$. Check that out for yourself, if you have a small spring laying around, try to cut it in half and check how each half responds to being stretched or compressed.

Now suppose that K is the return force of the air column in the pipe which is (adiabatically) “pressed” or “stretched”. Recalling that

the length of the pipe equals $L = 1$, the pressure difference thus occurring is multiplied by the area of the cross-section of the pipe. So it turns out to be natural to give each of the $n + 1$ springs the stiffness constant $k = (n + 1)K$.

In what sense can we now speak of a good approximation? At this point it should be clarified that an organ pipe can produce more than one tone. It is a well known fact in acoustics, that has fascinated scientists since the middle ages: while Newton and Huygens already provided some preliminary explanations [169], the first complete mathematical derivation is due to Helmholtz in 1860 [91].

The lowest of such tones is the so-called *fundamental (tone)*: Helmholtz original computation showed that all air particles oscillate with the frequency $f_0 = \frac{1}{2} \sqrt{\frac{K}{M}}$. This is remarkably accurate, albeit not exact, as was confirmed almost a century later. See [114], where the first accurate physical explanation of the phenomenon was provided. The fundamental tone is achieved when the air in the pipe oscillates over the whole length of the pipe, as shown in Figure 3.13. If we believe that this resembles the oscillation of a spring, then we can expect that the frequency of the fundamental tone is proportional to $\sqrt{\frac{K}{M}}$, compare to Section 1.1.2. In addition to the fundamental, there are the so-called *harmonics* consisting of *overtones*.

The first overtone is produced by the configuration in Figure 3.15, where the air in the center of the pipe is at rest. Here, all air particles oscillate with the frequency $f_1 = 2f_0 = \sqrt{\frac{K}{M}}$, this overtone sounds an *octave* higher than the fundamental. Similarly, you also have second, third, etc. overtones: the frequency of the ℓ^{th} overtone is $f_\ell = (\ell + 1)f_0$. What you hear in practice is always a combination

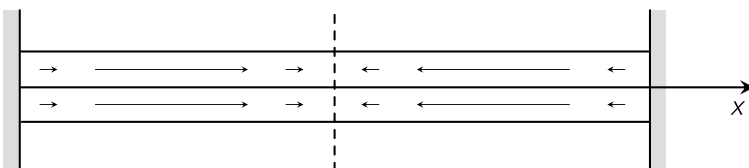


Figure 3.15. The first overtone

(superposition) of fundamental and overtones. In our approximate model, fundamental and harmonics correspond to *characteristic oscillations*. Recall from Section 3.2 that all possible motions are (linear) combinations of characteristic oscillations, also see Appendix B. In the first approximation $n = 1$ we have only one characteristic os-

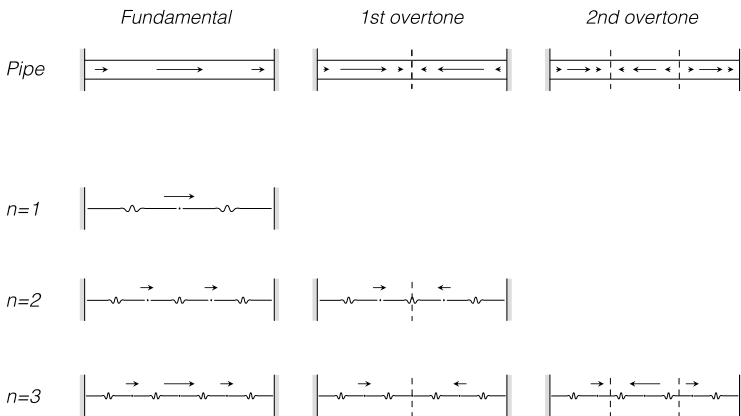


Figure 3.16. The fundamental and other harmonics as n increases

cillation and therefore the pipe can only produce the analog of the fundamental. For $n = 2$ there are two characteristic oscillations that we already know from Section 3.2.2. They correspond to the fundamental and the first overtone, etc.

Below we will compute the characteristic frequencies for $n = 1, 2$ and 3 and see that these differ from the frequencies of the corresponding overtones. However, these differences become smaller as n gets larger, we aim to show this in more detail in the case of the fundamental. It is in this sense that we can speak of an increasingly better approximation of the organ pipe.

Computation of the characteristic frequencies. Now follows the computation of the characteristic frequencies for $n = 1, 2$ and 3.

Case $n = 1$: Let u denote the deviation of the mass from the equilibrium state. Then one of the springs is extended by the amount

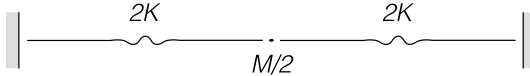


Figure 3.17. Case $n = 1$

$|u|$, while the other is compressed by $|u|$. Therefore, the equation of motion is given by

$$\frac{M}{2}\ddot{u} = -2K(u + u)$$

or

$$M\ddot{u} = -8Ku.$$

From Chapter 1 we know that solutions are oscillating with $\omega = 2\sqrt{2}\sqrt{\frac{K}{M}}$ and the corresponding frequency of oscillation is

$$\frac{\omega}{2\pi} = \frac{\sqrt{2}}{\pi}\sqrt{\frac{K}{M}} \approx 0.450\sqrt{\frac{K}{M}}.$$

Comparing this to the fundamental frequency $f_0 = 0.5\sqrt{\frac{K}{M}}$, we see a rather crude though not unreasonable approximation.

Case $n = 2$: As said before, we already met this system in Section 3.2.2, also compare Appendix B. In complete analogy to



Figure 3.18. Case $n = 2$

the case where $n = 1$, if u_1 and u_2 denote the deviations of the left and right air masses from equilibrium respectively, then we get the equations of motion

$$\begin{cases} \frac{M}{3}\ddot{u}_1 = -3K(2u_1 - u_2), \\ \frac{M}{3}\ddot{u}_2 = -3K(2u_2 - u_1). \end{cases}$$

From these, we immediately get the characteristic oscillations (also see Figure 3.16) and their corresponding frequencies

$$(1) \quad u_1 = u_2:$$

$$M\ddot{u}_1 = -9Ku_1 \Rightarrow \frac{\omega_1}{2\pi} = \frac{3}{2\pi}\sqrt{\frac{K}{M}} \approx 0.477\sqrt{\frac{K}{M}};$$

$$(2) \quad u_1 = -u_2:$$

$$M\ddot{u}_1 = -27Ku_1 \Rightarrow \frac{\omega_2}{2\pi} = \frac{3\sqrt{3}}{2\pi}\sqrt{\frac{K}{M}} \approx 0.827\sqrt{\frac{K}{M}}.$$

Comparing $\frac{\omega_1}{2\pi}$ with $f_0 = 0.5\sqrt{\frac{K}{M}}$, we see that the approximation has improved. We also recover the next harmonic, even though the distance between $\frac{\omega_2}{2\pi}$ and $f_1 = 1.0\sqrt{\frac{K}{M}}$ is still quite large.

Case $n = 3$: This is our first serious encounter with a system of 3 degrees of freedom. We follow the same strategy as before. If

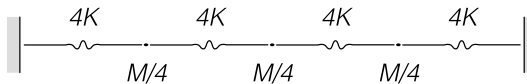


Figure 3.19. Case $n = 3$

u_1 , u_2 and u_3 are the deviations from the equilibrium of the left, middle and right masses, respectively, then the equations of motion are

$$\begin{cases} \frac{M}{4}\ddot{u}_1 = -4K(2u_1 - u_2), \\ \frac{M}{4}\ddot{u}_2 = -4K(2u_2 - u_1 - u_3), \\ \frac{M}{4}\ddot{u}_3 = -4K(2u_3 - u_2). \end{cases}$$

Also here, we can compute the characteristic oscillations (also see Figure 3.16) and their frequencies:

$$(1) \quad u_1 = u_3, u_2 = \sqrt{2}u_1:$$

$$M\ddot{u}_1 = -16(2-\sqrt{2})Ku_1 \Rightarrow \frac{\omega_1}{2\pi} = \frac{2\sqrt{2-\sqrt{2}}}{\pi}\sqrt{\frac{K}{M}} \approx 0.487\sqrt{\frac{K}{M}};$$

$$(2) \quad u_1 = -u_3, u_2 = 0:$$

$$M\ddot{u}_1 = -32Ku_1 \Rightarrow \frac{\omega_2}{2\pi} = \frac{2\sqrt{2}}{\pi}\sqrt{\frac{K}{M}} \approx 0.900\sqrt{\frac{K}{M}};$$

$$(3) \quad u_1 = u_3, u_2 = -\sqrt{2}u_1:$$

$$M\ddot{u}_1 = -16(2+\sqrt{2})Ku_1 \Rightarrow \frac{\omega_3}{2\pi} = \frac{2\sqrt{2+\sqrt{2}}}{\pi} \sqrt{\frac{K}{M}} \approx 1.176 \sqrt{\frac{K}{M}}.$$

Let us compare these with the fundamental and the first harmonics. Both $\frac{\omega_1}{2\pi}$ and $\frac{\omega_2}{2\pi}$ respectively provide better approximations of $f_0 = 0.5\sqrt{\frac{K}{M}}$ and $f_1 = 1.0\sqrt{\frac{K}{M}}$ with respect to the case $n = 2$. We also recover the harmonic $f_2 = 1.5\sqrt{\frac{K}{M}}$ even though $\frac{\omega_3}{2\pi} = 1.176\sqrt{\frac{K}{M}}$ is still a rather poor approximation.

On the length L of the organ pipe. We now come to the discussion of the length L of the organ pipe as announced in Remark 27, noting that L is not explicitly showing in the expression $\frac{K}{M}$. To solve this problem we first introduce some new constants.

So, if L is the length of the pipe, we further introduce σ as the area of its cross-section, ρ as the density (specific weight) of the air in the pipe and κ the “stiffness constant” of a pipe of unit length and unit cross-section area.

Then the mass of the air in the pipe is given by the volume of the pipe, so area of the cross-section times the length, multiplied by the air density: $M = \sigma L \rho$. Physical considerations also show that $K = \frac{\sigma \kappa}{L}$. While this is harder to justify without additional knowledge, we can understand this as follows: we already said that the stiffness constant K is the return force of the air column in the pipe while being “pressed” or “stretched”. Then the pressure difference will depend on the “stiffness” of the gas times the area of the cross-section of the pipe which determines how much air can be “pressed” or “stretched”, but is inversely proportional to the length of the pipe, which provides the available space for the air to be “pressed” or “stretched”.

The first identity is quite obvious and the second follows by a similar reasoning as the one used above when determining the spring constant of the springs in the approximation with n masses and $n+1$ springs. It then follows that $\frac{K}{M} = \frac{1}{L^2} \frac{\kappa}{\rho}$, so that, for example, the fundamental becomes

$$f_0 = \frac{1}{2L} \sqrt{\frac{\kappa}{\rho}}. \tag{3.4}$$

Note that σ does not appear in (3.4). Moreover, the role of L may now become clear: doubling it gives a halving of the fundamental frequency and thus a reduction of the fundamental by 1 octave. Hence the classical custom of dividing organ registers into 2-foot, 4-foot, 8-foot, 16-foot, and 32-foot registers. Here, the number of feet stands for the length of the longest pipe in that register. Here the fundamental is always one octave lower than in the previous register.

3.3.1.2 Towards a partial differential equation

Let us further speculate for a while about our approach to the organ pipe by an n degrees of freedom system. As before, let u_1, u_2, \dots, u_n

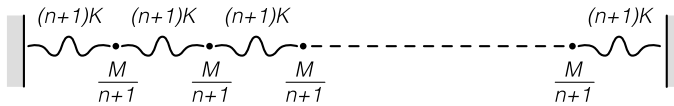


Figure 3.20. Case of arbitrary n

denote the deviation of the n masses from their equilibrium. The usual reasoning, completely analog to the case $n = 3$, leads to the equations of motion

$$\begin{cases} \frac{M}{n+1} \ddot{u}_1 = -(n+1)K(2u_1 - u_2), \\ \frac{M}{n+1} \ddot{u}_j = -(n+1)K(2u_j - u_{j-1} - u_{j+1}), \quad 2 \leq j \leq n-1, \\ \frac{M}{n+1} \ddot{u}_n = -(n+1)K(2u_n - u_{n-1}), \end{cases}$$

compare the above case $n = 3$. We are no longer concerned with computing the characteristic frequencies $\omega_1 < \omega_2 < \dots < \omega_n$, but instead, we want to arrive at the equation of motion of the continuous system through an infinitesimal consideration. Let $x = \frac{jL}{n+1}$ and



Figure 3.21. Infinitesimal consideration

$\Delta x = \frac{L}{n+1}$. Then, for $2 \leq j \leq n-1$, the j^{th} mass has position x and

is surrounded by the $(j-1)^{\text{th}}$ and $(j+1)^{\text{th}}$ masses respectively at the positions $x - \Delta x$ and $x + \Delta x$. Then the equation of motion of the j^{th} mass reads as

$$\begin{aligned} M\ddot{u}_j &= -(n+1)^2 K(2u_j - u_{j-1} - u_{j+1}) \\ &= (n+1)^2 K[(u_{j+1} - u_j) - (u_j - u_{j-1})]. \end{aligned} \quad (3.5)$$

With a slight abuse of notation, we write:

$$u(x) = u_j, \quad u(x - \Delta x) = u_{j-1}, \quad \text{and} \quad u(x + \Delta x) = u_{j+1}$$

and observe that $L = (n+1)\Delta x$. The right hand side of equation (3.5) then can be rewritten as

$$\begin{aligned} &(n+1)^2 K[(u_{j+1} - u_j) - (u_j - u_{j-1})] \\ &= \frac{L^2 K}{(\Delta x)^2} [(u(x + \Delta x) - u(x)) - (u(x) - u(x - \Delta x))] \\ &= \frac{L^2 K}{\Delta x} \left[\frac{u(x + \Delta x) - u(x)}{\Delta x} - \frac{u(x) - u(x - \Delta x)}{\Delta x} \right] \\ &\approx \frac{L^2 K}{\Delta x} \left[\frac{du}{dx} \left(x + \frac{\Delta x}{2} \right) - \frac{du}{dx} \left(x - \frac{\Delta x}{2} \right) \right] \\ &\approx L^2 K \frac{d^2 u}{dx^2}(x). \end{aligned}$$

In the transitions \approx we approximate the expression by a differential quotient:

$$\frac{du}{dx}(x) = \lim_{\Delta x \rightarrow 0} \frac{u(x + \Delta x) - u(x)}{\Delta x},$$

so as Δx becomes smaller, the fraction on the right hand side becomes closer to the derivative of u at points in the small interval $[x, x + \Delta x]$. For convenience we use it to approximate the middle point $x + \frac{\Delta x}{2}$. The second approximation is then justified in a similar way by observing that the second derivative of u is the derivative of its derivative, and thus

$$\frac{d^2 u}{dx^2}(x) = \lim_{\Delta x \rightarrow 0} \frac{\frac{du}{dx} \left(x + \frac{\Delta x}{2} \right) - \frac{du}{dx} \left(x - \frac{\Delta x}{2} \right)}{\Delta x}.$$

Compare with the infinitesimal considerations of Section 1.3.1. Since the intervals of air mass get smaller as n increases, this approximation becomes more precise as n gets larger. Gradually u has become a

function of x , while at the same time, u is also still a function of the time t . As in the introductory treatment of the vibrating string we write $u = u(t, x)$. Now, we change slightly the notation, writing

$$\frac{\partial^2 u}{\partial x^2} \text{ instead of } \frac{d^2 u}{dx^2} (= u'') \quad \text{and} \quad \frac{\partial^2 u}{\partial t^2} \text{ instead of } \frac{d^2 u}{dt^2} (= \ddot{u}),$$

and speak about *partial derivatives* of u with respect to t and x . In summary, we have arrived at the equation of motion

$$M \frac{\partial^2 u}{\partial t^2} = L^2 K \frac{\partial^2 u}{\partial x^2},$$

or, using the constants introduced earlier,

$$\frac{\partial^2 u}{\partial t^2} = \frac{\kappa}{\rho} \frac{\partial^2 u}{\partial x^2}. \quad (3.6)$$

This is a so-called *partial differential equation*. The fact that the pipe is closed at both ends is expressed by the *boundary conditions*

$$u(t, 0) \equiv 0, \quad u(t, L) \equiv 0.$$

Equation (3.6) is known as the *wave equation*. The reason for this is that for a suitably chosen positive number v , all solutions have the form

$$u(t, x) = g(x + vt) \quad \text{and} \quad u(t, x) = g(x - vt).$$

Here g is a (rather) arbitrary function, which has to be chosen in agreement with the boundary conditions, which are generally different from problem to problem. See below for more details. A solution of the above form is called a *traveling wave*. Why would one have chosen this name? The number v is called the (*wave*) *propagation speed* or *phase speed*. Justify this (first) name as well. In our case, $v = \sqrt{\frac{\kappa}{\rho}}$ and v is exactly the speed of sound. Let us examine the above in more detail.

First, we discuss the fact that necessarily $v = \sqrt{\frac{\kappa}{\rho}}$. This can be seen by substituting the traveling wave $u(t, x) = g(x \pm vt)$ in the wave equation. By the chain rule

$$\frac{\partial^2 u}{\partial t^2} = v^2 g'' \quad \text{and} \quad \frac{\partial^2 u}{\partial x^2} = g'',$$

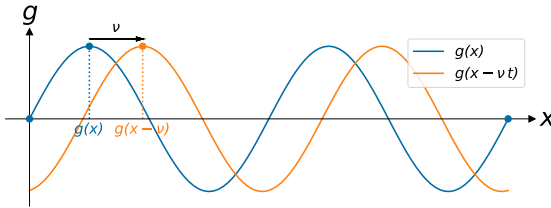


Figure 3.22. Each curve represents a snapshot of a traveling wave $g(x - vt)$ at a fixed time, respectively $t = 0$ and $t = 1$, showing how the wave moves to the right with speed v .

which reduces the wave equation to

$$v^2 g'' = \frac{\kappa}{\rho} g''.$$

The latter equation, with the unknown function g , then is soluble exactly when $v^2 = \frac{\kappa}{\rho}$.

It may now be clear that traveling waves with propagation speed $v = \sqrt{\frac{\kappa}{\rho}}$ are indeed solutions of the wave equation. Our second observation is that sums (superpositions) of such traveling wave solutions are again solutions of the wave equation themselves. (This has to do with the linearity of the differential equation, also see the analogous comments in Section 3.2). So we find that for (rather) arbitrary functions g_1 and g_2

$$u(t, x) = g_1(x - vt) + g_2(x + vt) \quad (3.7)$$

satisfies the wave equation. The word “rather”, which has been used already twice, refers to the differentiability conditions that the relevant functions (g or g_1 and g_2) must satisfy. It can be shown that, apart from this issue, equation (3.7) represents the most general solution of the wave equation. For further background see [136]. For an elegant derivation of the wave equation for a vibrating string from first principles, see [173].

Back to the organ pipe. In the above discussion, we disregarded the boundary. Now let us consider solutions of the above general type

(3.7) that also satisfy the boundary conditions $u(t, 0) \equiv 0 \equiv u(t, L)$. For this purpose, we first take the solutions

$$g_1(x) = \frac{1}{2} \cos\left(\frac{k\pi}{L}x\right), \quad g_2 = -g_1, \quad k = 1, 2, 3, \dots$$

then we obtain

$$\begin{aligned} u_k(t, x) &= \frac{1}{2} \cos\left(\frac{k\pi}{L}(x - vt)\right) - \frac{1}{2} \cos\left(\frac{k\pi}{L}(x + vt)\right) \\ &= \frac{1}{2} \cos\left(\frac{k\pi}{L}x\right) \cos\left(\frac{k\pi}{L}(-vt)\right) - \frac{1}{2} \sin\left(\frac{k\pi}{L}x\right) \sin\left(\frac{k\pi}{L}(-vt)\right) \\ &\quad - \frac{1}{2} \cos\left(\frac{k\pi}{L}x\right) \cos\left(\frac{k\pi}{L}vt\right) + \frac{1}{2} \sin\left(\frac{k\pi}{L}x\right) \sin\left(\frac{k\pi}{L}vt\right) \\ &= \sin\left(\frac{k\pi}{L}x\right) \sin\left(\frac{k\pi}{L}vt\right), \quad k = 1, 2, 3, \dots \end{aligned}$$

If, on the other hand, we choose

$$g_1(x) = \frac{1}{2} \sin\left(\frac{k\pi}{L}x\right), \quad g_2 = g_1, \quad k = 1, 2, 3, \dots,$$

and by a computation similar to the one above, we obtain

$$u_k(t, x) = \sin\left(\frac{k\pi}{L}x\right) \cos\left(\frac{k\pi}{L}vt\right), \quad k = 1, 2, 3, \dots.$$

You can check that the boundary conditions are satisfied for both of these choices of u_k . Such a solution u_k is often called k^{th} harmonic; To understand the reasons for such a name, also see the remarks in Section 1.3.1. The first harmonics form the fundamental of the pipe, while for $k \geq 2$ the k^{th} harmonic forms the $(k-1)^{\text{th}}$ overtone. To elaborate a bit more on this, we define

$$\lambda_k = \frac{2L}{k} \quad \text{and} \quad \omega_k = \frac{k\pi}{L}v, \quad k = 1, 2, 3, \dots,$$

and obtain

$$u_k(t, x) = \begin{cases} \sin\left(\frac{2\pi}{\lambda_k}x\right) \sin(\omega_k t) \\ \sin\left(\frac{2\pi}{\lambda_k}x\right) \cos(\omega_k t) \end{cases} \quad k = 1, 2, 3, \dots.$$

Now observe that $f_{k-1} = \omega_k / 2\pi$ is the frequency of the air particles in the solutions u_k . The constant λ_k is called the *wavelength* of the solution: the larger k , the shorter the wavelength and the higher the frequency (pitch) of the corresponding tone. Intuitively, sound waves all travel at about the same speed, the speed of sound, and the wavelength measures the distance between the consecutive 'maxima' of the wave: in the same time interval, waves with shorter wavelength will reach your ear more often than the ones with longer wavelength, thereby leading to a higher pitch.

Before starting to discretize the organ pipe, we observed that the tone you hear is a combination of the fundamental and the overtones. Mathematically we can express this by writing

$$u(t, x) = \sum_{k=1}^{\infty} \sin\left(\frac{2\pi}{\lambda_k}x\right) (a_k \sin \omega_k t + b_k \cos \omega_k t) \quad (3.8)$$

as an infinite series, a so-called *Fourier series*. Here the numbers $a_1, b_1, a_2, b_2, \dots$ are called *amplitudes*. They determine the *timbre* of the tone. Note that also here we abundantly use the superposition principle.

The corresponding theory was founded by Jean-Baptiste Joseph Fourier (1768-1830) while working on his treatise *Théorie analytique de la chaleur* (The Analytical Theory of Heat) in 1822. For the moment we treat the infinite series in (3.8) as a formal object, which means that we operate only term by term without worrying about issues of convergence. For some further information see the remarks below.

Remark 28. (1) Earlier we said that organ pipes have to be open at least at one end; this is where air is blown up while the other end is "covered". In that case we use the same equation (3.6) in the form

$$\frac{\partial^2 u}{\partial t^2} = v^2 \frac{\partial^2 u}{\partial x^2},$$

but now imposing the *boundary conditions*

$$u(t, 0) \equiv 0 \quad \text{and} \quad \frac{\partial u}{\partial x}(t, L) \equiv 0.$$

It is a worthwhile exercise to try and adapt the foregoing theory to this case.

- (2) The above derivation of the Fourier series (3.8) rests on the traveling wave solution (3.7). In Asmar [13, §3.3] you can find a similar result for the initial value problem

$$\frac{\partial^2 u}{\partial t^2} = v^2 \frac{\partial^2 u}{\partial x^2}$$

with boundary conditions $u(t, 0) \equiv 0 \equiv u(t, L)$, and with initial values

$$u(0, x) = f(x) \quad \text{and} \quad \frac{\partial u}{\partial t}(0, x) = g(x),$$

leading to the same Fourier series. In this case the amplitudes are determined by

$$a_k = \frac{2}{vk\pi} \int_0^L g(x) \sin \frac{k\pi}{L} x \quad \text{and} \quad b_k = \frac{2}{L} \int_0^L f(x) \sin \frac{k\pi}{L} x,$$

and, as before,

$$\omega_k = \frac{k\pi}{L} v, \quad k = 1, 2, 3, \dots$$

For other linear partial differential equations that allow for a similar treatment we refer to [13].

- (3) A more serious problem is how to deal with the infinite series (3.8) and whether our termwise reasoning carries over to the entire series. Two fundamental questions are, firstly, when the series indeed converges to the function u and, secondly, whether differentiation of the sum coincides with the sum of the differentiated terms. Without going into the details, we can say that everything runs well when the functions g_1 and g_2 in (3.7) are sufficiently often differentiable.

The same holds for the functions f and g in item (2) above. In that case the transformation

$$(f, g) \mapsto (a_1, b_1, a_2, b_2, \dots)$$

is called a *Fourier transform*. Many variations of this operation exist [13, 136].

The study of partial differential equations as presented here, is dealt with in *functional analysis*, a branch of mathematics in the world of infinite dimensional linear algebra [136]. This is a subject that extends the concepts in Section B.1 to vector spaces that have infinite dimension: as in the above example, the elements may well consist of functions or of infinite sequences. The analysis and generalization of Fourier transforms has nowadays evolved into a separate branch of mathematics, called *harmonic analysis*. But this is beyond the scope of our book and requires a deeper background in mathematics.

Now that we have derived the wave equation as a partial differential equation and therefore as a continuous description for the dynamics of strings, organ pipes and the like, we may well wonder what this equation in return can tell us about the phenomena.

We have already seen that this equation allows for standing waves and traveling wave solutions, that the superposition principle works with which we can generate any solution, compare with the Fourier series. This leads to many interesting phenomena, like the doppler effect and the dispersion of water waves in ponds for example, which we will briefly discuss in Section 3.4, below.

A detailed analysis of the wave equation and a proper discussion of its properties requires a background in functional analysis and a great deal of advanced mathematics, and again exceeds the scope of our book. Instead we refer to Weinberger [173] and Olver [136]. In Appendix B we briefly touch upon *spectral theory*, a powerful theory in the study of partial differential equations. Elements of spectral theory also return in Appendix E.

3.3.2 Strings, beams, etc.

The organ pipe is an illustrative example of all kinds of vibrations, e.g., longitudinal vibrations of an elastic rod, but also of transverse string vibrations and even, albeit as a rough approximation, transverse ship vibrations, where the idea that a ship is a rigid body has to be abandoned; compare with the Sections 3.1.2 and 3.2.3.

First we return to the string, also see the introduction to this chapter. In the discretization, we replace the string by a finite number

of points of equal mass, connected by identical, massless springs. The difference with the organ pipe is that now the masses may only move transversely, i.e., perpendicular to the line connecting them when they are at rest, see Figure 3.23.

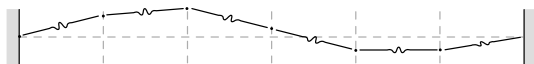


Figure 3.23. A discretized string

We can literally repeat the story about fundamental, overtones and characteristic oscillations that we developed for the organ pipe and summarize the result in Figure 3.24. Although the computations of

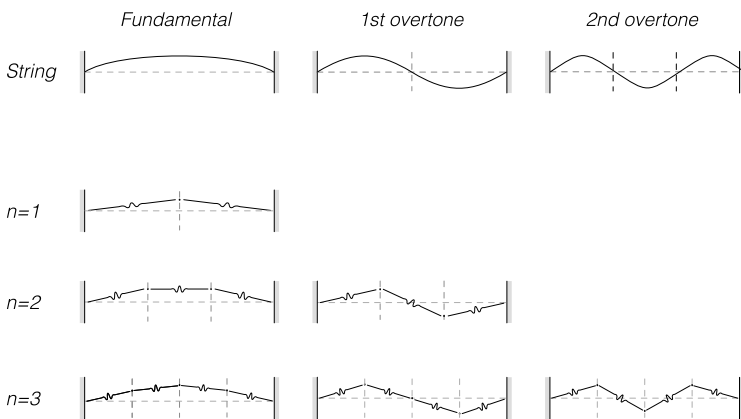


Figure 3.24. Characteristic oscillations of a discretized string for different values of n

these characteristic oscillations are somewhat more involved than for the organ pipe, there is no mathematical difference between the two situations.

If for an arbitrary time t , the deviation of the string is given by the function $x \mapsto u(t, x)$ as indicated in the introduction, then the

equation of motion is again the wave equation

$$\frac{\partial^2 u}{\partial t^2} = v^2 \frac{\partial^2 u}{\partial x^2},$$

where now $v^2 = s/\rho$. Here s is the tension of the string and ρ the mass density. If the string has length L (in the introduction we took $L = 1$), then the boundary conditions are $u(t, 0) = 0 = u(t, L)$. Compare this with our treatment of the organ pipe: both ends of the string are fixed. We can now repeat the computations from Section 3.3.1.1. Graphs of the functions $x \mapsto u_n(t, x)$, for t fixed and $n = 1, 2$ and 3 are depicted in Figure 3.24. What are frequency f_0 and wavelength λ_1 of the fundamental? Note that, in principle, the waves in the string propagate at a speed different from the sound waves in air.

Next we turn to the oscillations of a boat. The analysis is, at least

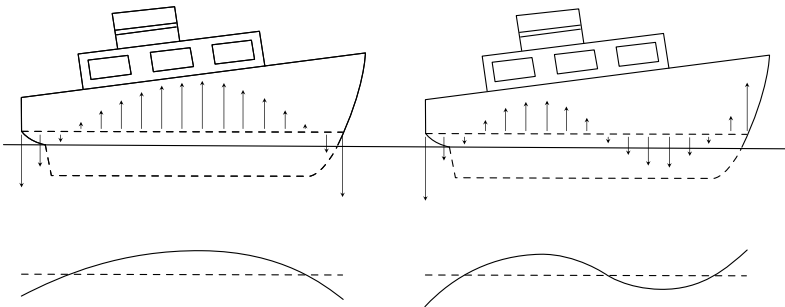


Figure 3.25. Oscillations of a boat

in principle, no different to the string. See Figure 3.25.

Bars or beams containing longitudinal or transverse vibrations can also be treated entirely according to the above recipe. The assumption is always that there is only one space variable at stake. Two-dimensional continua such as plates and shells like the floor of a bridge or the wings and body of an airplane, follow an analogous albeit somewhat more complicated theory. Discretizations always play an important role in both practical computations and more theoretical considerations.

Remark 29. In *practice*, it is often not enough to rely solely on computations, however accurate. This is because we are always working within a model, in which all kinds of more or less essential matters are not included; compare remarks made earlier in Section 1.1.5 and in the introduction to the present chapter. These often *cannot* be included in the model for mainly two reasons: Firstly, because certain effects are not known well enough, e.g., precise effects of energy losses due to something like friction. Secondly, because otherwise the model becomes unmanageably complicated, e.g., due to certain nonlinear effects.

In many cases one has to resort to experimental data. In some cases such data can be obtained using scaled models in, for example, a wind tunnel or gutter. Often, however, such data only become available when the construction in question (e.g. a ship) has already been completely built. In the latter case, constructive retrospective changes, the desirability of which is determined based on measurements, can not always be realized or only at very high costs.

3.4 Other vibrational phenomena

Finally, in this brief section we discuss several different oscillatory phenomena that everyone has likely experienced in real life. We only sketch the overarching ideas and the keywords for further investigation of the interested reader. We also use a less rigorous mathematical style and recommend you to consult additional physics books, e.g., the Feynman Lecture Notes [77] or Minnaert [125].

3.4.1 Sound and light

We already encountered sound as an air vibration extensively in Section 3.3.1 concerning the organ pipe. There we only dealt with one spatial variable but in general, there is a three-dimensional spatial continuum to deal with. Each of us is probably familiar with phenomena associated with the wave character of sound: we only mention *interference* and the *Doppler effect*.

Interference and the Doppler effect. Interference phenomena arise from the *superposition* of two or more waves: we have already

encountered sound beats in Section 3.2.2. The superposition leads to mutual extinction or amplification of the waves. Spectacular examples of amplification can be met in the well-known whisper galleries, etc. Moreover, blind spots in concert halls can be understood in terms of destructive interference.

Doppler phenomena arise from frequency changes due to *relative motions* of the sound source relative to the observer. Think of the bell of the level crossing, which rings higher for the railway passenger when the train approaches the crossing and lower when the train moves away from it. Or think of the change in pitch of the siren of a police car that passes by when you are standing on a sidewalk.

Remark 30. (1) It is less evident that light also has a wave character.

In this context, there is a famous historical controversy in which already Huygens and Newton were involved. Roughly speaking, the former proposed a *wave theory* and the latter a *particle theory*. Only in the 19th century, Maxwell came up with a theory in which light is understood as an electromagnetic wave phenomenon, thereby providing a physical justification of Huygens's idea. In the 20th century, quantum mechanics has finally settled the dispute by showing that light has a dual nature exhibiting both wave and particle aspects.

(2) A problem with all this is the following. If light is a wave phenomenon, then what is it that exactly vibrates? For a long time, physicists have thought that there is a medium in space, called *ether*, in which the light waves move. Nowadays we live in an etherless era and probably this will remain so.

Interestingly, in connection with radio and television waves, other special cases of Maxwell's electromagnetism, people still speak of the ether in their colloquial language. However, whether or not such a thing as this ether exists, leaves mathematics indifferent. The only important thing is that in Maxwell's theory the components of the electromagnetic field satisfy the equation

$$\frac{\partial^2 u}{\partial t^2} = c^2 \left(\frac{\partial^2 u}{\partial x^2} + \frac{\partial^2 u}{\partial y^2} + \frac{\partial^2 u}{\partial z^2} \right),$$

in which a careful reader will immediately recognize the *wave equation*. Here x , y , and z are the space variables and c is the speed of light.

The wave character of electromagnetism for instance can be observed in *fading*, a phenomenon in which the strength and quality of a radio signal fluctuate over time and distance. Since the fluctuation is quite irregular it is often modeled in a stochastic way.

A large number of the examples given below could have not been discovered until the 19th century.

Miscellaneous comments. We conclude this section with a few comments on daily life phenomena that can be explained in terms of the above.

- (1) *Interference* of light waves may explain well the changing color patterns in oil stains on water. Also the so-called *fading* in short-wave receivers can be understood as an interference phenomenon: radio waves of the same wavelength reach the observer along paths of different length. What one hears is the alteration of extinction and amplification of the sound coming from the radio, just as in the case of beats.
- (2) The *Doppler effect* can also serve to explain the so-called *red-shift* observed in the radiation that reaches us from the distant, *expanding* universe.
- (3) In wave theory, *dispersion* means dependence of the propagation speed on the wavelength.

The refraction of white light through a prism and the associated decomposition in all colors is a well-known phenomenon that can be explained in terms of dispersion. Replacing the prism with a water droplet similarly explains the phenomenon of a *rainbow*. Compare with Arnold [9, Chapter 9]. For dispersion in water waves, see below.

- (4) In the world of radio and television, the concept of *resonance* is also extremely important, compare with Chapter 2: the incoming electromagnetic radiation forms the external *drive* of the electric

circuit constructed inside a receiver. The resonance peaks then make it possible to select a certain wavelength range upon reception: this is exactly what one does if one *tunes* the receiver to a particular station.

- (5) Finally, we also mention the *polarization phenomenon* that is being used in sunglasses and LCD screens. This has to do with the so-called *transversality* of the light waves. When waves pass through a material with a certain “crystalline” structure, the vibrations are extinguished in all directions except one, thus obtaining *polarized* light.

3.4.2 Water waves

On water surface waves we will be brief and just refer to Minnaert’s *The Nature of Light and Colour in the Open Air* [125]. It should be noted that this treatment is more involved than with air vibrations, due to the so-called *surface tension*. It is also worth mentioning that in [125] all known wave phenomena mentioned above are beautifully illustrated by means of water waves; this includes the phenomenon of *radiation pressure*. The latter has been used in 2010 by the JAXA IKAROS mission for a new type of solar propulsion in space travel: the solar sail. A large, thin sail that is propelled by the radiation pressure of sunlight.

Dispersion in the rippling of water waves occurs when a stone is dropped in a shallow pond or puddle. The stone will give rise to a “wavepacket” consisting of waves with different wavelengths, with the longer waves propagating faster than the shorter ones. Here we also see the phenomenon of interference: the peak of the packet appears where the waves interact with each other constructively. Moreover, the waves attenuate at different rates depending on the wavelengths. This means that waves that started “bundled” together, will spread out over time, giving rise to the familiar dancing pattern of circular ripples as illustrated in Figure 3.26.

Remark 31. Curiously the phenomenon of dispersion does not occur in odd dimensions, where the waves will always propagate at the same speed. You can hear this in the sound, e.g. of a firecracker, where

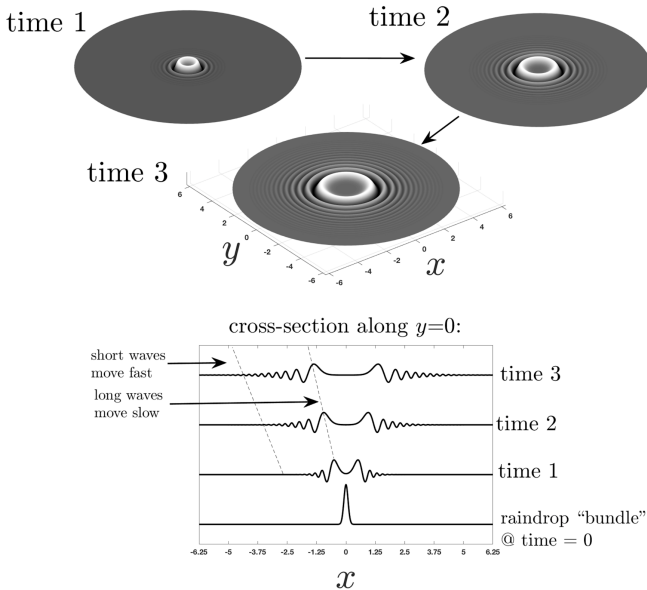


Figure 3.26. A model of waves in a dispersive puddle, after a raindrop hits. The top three figures show what happens after a drop hits the puddle, with arrows indicating the passage of time. The bottom figure shows the cross-sectional view through the puddle, highlighting that the initial wave bundle caused by the raindrop splits into waves of different sizes. Large waves in the center move more slowly than small waves at the perimeter. Figure and caption by Nate Barlow [20].

the sound you perceive is the same independently of where you are standing. Similarly, there is no dispersion for electromagnetic waves in space, this is crucial for example in telecommunications. For the mathematical details, we refer to Olver [136, Chapter 8.5].

3.4.3 Relaxation oscillations

This chapter is concluded by briefly describing *relaxation oscillations*, a group of oscillation phenomena that you may encounter often in everyday life. Here think of the sound of a fiddled violin string, of a

chamois that “squeaks” over a glass pane or a “singing” wine glass, or a piece of chalk that “crunches” on a blackboard, but also creaking doors and vibrations of propeller shafts in ships. The physics of such oscillations is quite involved and is still the subject of active research. Considerations about energy and forces are central in their mathematical understanding, and dry friction plays a major role, compare with Section 2.1.

Mathematically speaking, relaxation oscillations can be characterized by saying that deviations as a function of time should alternate periods of *slow* and *fast* variation. Figure 3.27 presents two cases: we

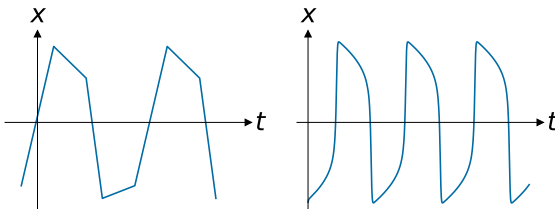
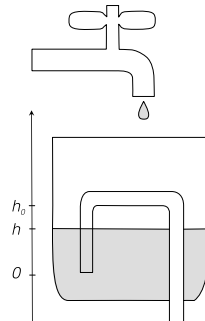


Figure 3.27. Relaxation oscillations

consider a variable x as a function of time t . Where does $x = x(t)$ vary slowly and where fast? A proper mathematical description of relaxation oscillations and their analysis is beyond the scope of this book but we will try to give you some intuition by some concrete examples.

The Tantalus cup. The *Tantalus cup* or *Pythagorean cup* consists of a vessel to which water is continuously added from a tap. A tube that can act as a *siphon* passes through the bottom of the vessel as indicated in the figure on the right. Let h denote the height of the water level in the vessel, then h periodically varies between two extreme values. The lowest value of h is slightly below $h = 0$, see the figure. From this state, h slowly increases as a function of time t : i.e. the vessel is *slowly* filled with tap water.



Once the water level increases slightly above the height $h = h_0$, the pipe is completely filled with water and starts acting as a siphon. The vessel now empties *quickly* to slightly below $h = 0$; with some goodwill, you could call this phase of motion “relaxing”: the system gives up quite suddenly its surplus of potential energy. Then h slowly increases again, etc.

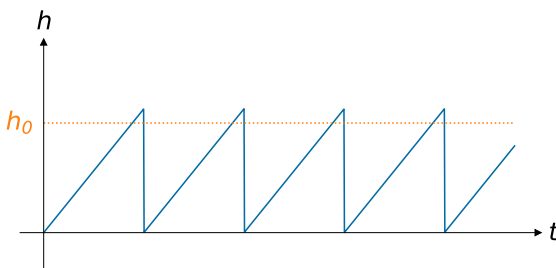


Figure 3.28. Relaxation oscillations of the Tantalus cup

In Figure 3.28 you see h as a function of the time t . (We note however that the dynamics of h above the level h_0 is more complicated than shown here.) Similar *sawtooth* graphs are common in electronic devices, such as television sets or mobile phones. In such systems, the underlying physics is clear, at least in principle. However, this is not the case at all in the following example.

Heart beat. Consider the motion of a *muscle fiber* in the human heart. The underlying physiology is particularly complex, but here we are looking for a “simple” mathematical model with the same *qualitative* properties as that of the motion of the muscle fiber. The properties that we have in mind are:

- (1) The existence of a more or less *stable equilibrium*, a state corresponding to the so-called *diastole*, in which the heart muscle is relaxed;
- (2) For some electrochemical variable x , there exist a threshold value $x = x_1$, such that once $x > x_1$ an action is triggered: the heart muscle contracts, this is the so-called *systole*. The excitation of the muscle fiber caused by an electromagnetic pulse emitted by a *pacemaker*, forces it to exceed the threshold value $x = x_1$;

- (3) There is a jump back to the equilibrium state, the heart muscle relaxes again.

If y denotes the length of our muscle fiber, Figure 3.29 schematically shows what the above properties mean. Here x_0 and y_0 are the values of x and y in the diastolic state. The contraction and relaxation are fast motions of y , which are alternated with slow motions in diastole and systole. The dynamics depicted in Figure 3.29 can be

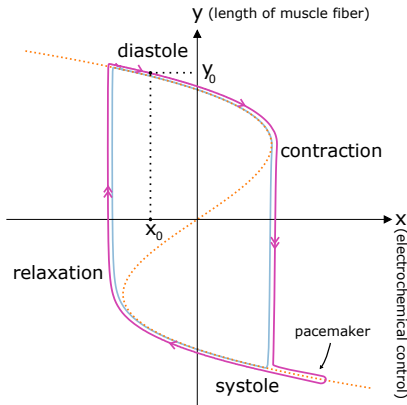


Figure 3.29. Relaxation oscillations for the muscle fiber of the heart

described rather explicitly using the Van der Pol–Liénard differential equations

$$\begin{cases} \dot{x} = y - y_0 \\ \epsilon \dot{y} = -(x - y + y^3) \end{cases} .$$

Here, $y_0 < \frac{1}{\sqrt{3}}$ and $\epsilon > 0$ is a small constant. Give a (rough) sketch of y as a function of the time t . Compare this with Exercise 2.6.5 and the discussion in the solutions in Appendix F.2.5.

Remark 32. The latter example stems from E.C. Zeeman's *Catastrophe Theory* [182, Chapter 3]. Zeeman also shows that the above differential equations to some extent form the simplest mathematical model having the properties 1, 2, and 3 mentioned above. This theory has been developed from the 1970s on, also compare with [143, 7].

The latter of these references presents more recent developments, including the more general *singularity theory*. We recommend the interested reader to consult these references in order to know more.

The pacemaker of the heartbeat is part of the autonomous nervous system. There exists a more general theory of neuronal activity where increases in voltage can produce cascades of spikes. The leading Hodgkin-Huxley model [97] also lies at the basis of Zeeman analysis [182, Chapter 3].

3.5 An exercise on Hooke's n -body problem

Lissajous figures appear in many different problems. As an interesting example we report here two problems by Bottema, namely problem 673 [29] and problem 683 [30].

Part 1. A particle P of unit mass moves in the plane of a given triangle $A_1A_2A_3$. The force F_i on P is directed towards A_i and is equal to $k\overline{PA}_i$ for $i = 1, 2, 3$, where k is a positive constant and \overline{PA}_i denotes the distance between P and A_i . Prove that there is a motion of P the path of which coincides with the Steiner ellipse S of $A_1A_2A_3$ (the ellipse S that passes through the vertices and whose tangent at any vertex is parallel to the opposite side). Show moreover that P covers the three arcs A_1A_2 , A_2A_3 , and A_3A_1 of S in equal time.

Let us look now at what happens if we allow n points to move under the influence of a similar mutual attraction. In other words, let us investigate the motion under universal Hookian gravitation.

Part 2. The particles A_i with masses m_i ($i = 1, 2, \dots, n$) move in three-dimensional space. Any two distinct particles A_i, A_j attract each other by the force $F = k^2 m_i m_j d_{i,j}$, where $k > 0$ and $d_{i,j}$ denotes the distance $\overline{A_iA_j}$. We suppose that the motions of A_i and A_j are not disturbed if they pass simultaneously through the same point. Determine the general motion of the particles.

Preface to the appendices

As said before, we included a choice of appendices that may be of interest to the reader. The first three appendices [A, Johann Bernoulli's brachistochrone](#), [B, Small oscillations revisited](#) and [C, The Foucault problem](#) remain quite close to the material of the main text. In the second appendix some helpful linear algebra is included for generalizing the analysis of Section [3.2.2.1](#). The last Appendix [F](#) has the self-explanatory title *Solutions of selected problems*. The style of these appendices generally remains close to that of the main text.

The remaining appendices are aimed at somewhat more advanced readers. Although their contents are related to material in the main text, they also touch on developments in ongoing research. Therefore these appendices require a broader background in mathematics that we have covered by referencing to the extensive bibliography. We hope that the curious reader will enjoy taking notice of all this and lets him- or herself be inspired by the ideas that are exposed.

A similar remark holds for some of the *Scholia* that finish the chapters of the main text.

One of the amazing discoveries of the second half of the 20th century is that evolutions of nonlinear systems, although being deterministic, in the longer run can become unpredictable in the sense that tiny variations of initial data eventually result in dramatic differences in the evolution. Examples vary from the planetary system, to population dynamics and climate science. This property was coined *chaos* by James E. Yorke (1941-) [[115](#)]. We met this term for the first time in Section [2.4.2](#), when considering resonance in nonlinear oscillators with periodic forcing. In Appendix [D, Chaos in periodically forced oscillators](#) we come back to this and show in what sense

chaotic behaviour is related to randomness. Chaos also appears in Appendix E.

Throughout the book the examples are mostly chosen from the more conceivable classical physics. However, complex wave functions that harbor a probability density, such as the ones that occur in quantum physics, are not so very conceivable. Nevertheless, the mathematics developed in the book often turns out to be useful in quantum physical contexts. For instance, considerations on the Mathieu equation in Chapter 2 are useful in Schrödinger's wave theory as will be demonstrated in Appendix E, *More on resonance*. And the mathematics of the organ pipe of Chapter 3 happens to coincide with that of a quantum particle in a box.

The authors

Appendix A

Johann Bernoulli's brachistochrone

In the Preamble we mentioned several problems put forward by Huygens, among which to find the isochronous and the tautochronous curve. We already claimed that nowadays the verification that the cycloid solves both problems has become quite elementary, compare Exercises 1.6.7 and 1.6.8. We also mentioned the brachistochrone problem put forward by Johann Bernoulli, that is, to find the curve of swiftest decent, i.e., with the shortest “down time”. Surprisingly, here the cycloid showed up again. Since this is a slightly more difficult exercise, we here include its solution as an appendix. Although the problem was formulated in the mechanical terms of sliding beads (or rolling marbles), Bernoulli added optics to the picture using the Fermat Principle and Snell's Law, thereby obtaining the desired curve as a light ray!

Johann Bernoulli was born in Basel (Switzerland) in 1667 and moved to Groningen in 1695 and back to Basel in 1705, where he died in 1748. Among others, Christiaan Huygens recommended Bernoulli's appointment in Groningen and, like Huygens, he had a great international reputation. From 1699 on he was Associé Étranger of the Académie des Sciences in Paris and from 1712 on he was Fellow of the Royal Society in London. He became also a member of the Academies in Bologna, Berlin, and Saint Petersburg. His most well-known students are his son Daniel (1700-1782) and Leonhard Euler (1707-1783). For an extensive historical account, we refer to Van Maanen [117].

The brachistochrone problem goes as follows. Given two points A and B in a vertical plane, with A higher than B , what is the wire profile along which a bead slides from A to B in the shortest time? The motion takes place under a constant vertical gravitation and there is no friction. The present story largely follows [37, Section 4.3.2] and is mimicking Bernoulli's solution [24].

A.1 Geometric optics

In analogy with Chapter 3, we are going to discretize the continuum, first dividing it in two layers, and later on in an increasing number of equally thick layers.

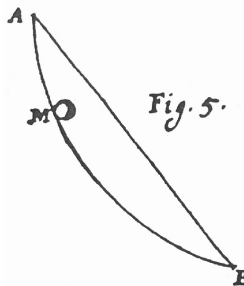


Figure A.1. The brachistochrone problem: for which profile does the bead M slide in the shortest possible time from A to B ? From *Opera Johannis Bernoullii, 1742* [24]

Throughout our considerations we restrict to a so-called *flat earth atmosphere*, that is a model in which the refraction index of the air only depends on the height, where we moreover constrain the motion to one vertical plane. The horizontal coordinate is denoted x and the vertical coordinate y . The velocity of light is denoted v , depending on the position. We assume that $v = v(y)$ only depends on the vertical coordinate y . The *refraction index* is defined as

$$n(y) := \frac{c}{v(y)},$$

where c is the velocity of light in vacuo. For simplicity we take $c = 1$.

Definition 1 (Fermat Principle). Given two points A and B then a *light ray* between A and B is the path that takes the shortest time.

This definition asks for minimality of the traveling time, but often we only ask this time to be extremal and speak of the *weak Fermat Principle*. One of the prime examples is the case where A and B are the focal points of an ellipse, where the light ray reflects in the elliptic curve. In that case, the time needed is constant.

A.1.1 Fermat implies Snell

We divide the atmosphere into two horizontal layers numbered 1 and 2, separated by the common boundary $y = 0$, see Figure A.2. The angles with the normal to the boundary are denoted by α_1 for $y \geq 0$ and α_2 for $y \leq 0$. The refraction indices are n_1 for $y > 0$ and n_2 for $y < 0$, with corresponding propagation velocities v_1 and v_2 .

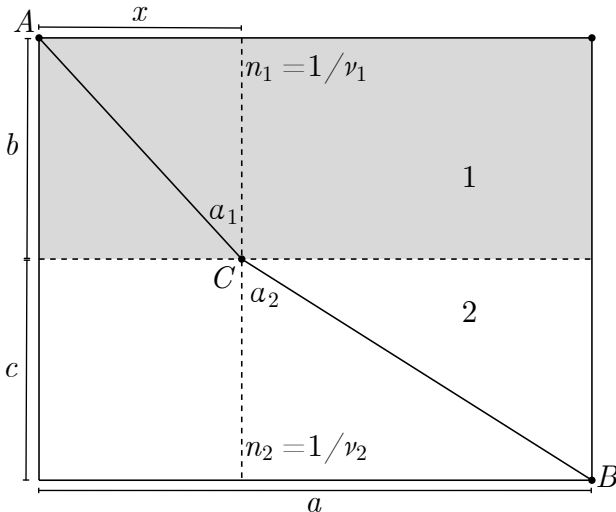


Figure A.2. Snell's law follows from the Fermat Principle

We now formulate

Theorem 2 (Snell's Law). *Under the above circumstances assume that A lies in the upper half plane $y > 0$, C on the boundary $y = 0$ and B in the lower half plane $y < 0$. Then the broken straight line ACB is a light ray according to the weak Fermat Principle if and only if*

$$n_1 \sin \alpha_1 = n_2 \sin \alpha_2 .$$

Proof. Let $x = x_C$ indicate the position of C on the line $y = 0$ that separates both layers. Let t_{AC} denote the time for the light ray

needed to travel from A to C and t_{CB} the time needed to travel from C to B . We then have to find an extremum of $t_{AC} + t_{CB}$. The facts that $|A - C| = t_{AC} \cdot v_1$ and that $v_1 = 1/n_1$ yield that

$$t_{AC} = n_1 |A - C|.$$

By the Pythagorean Theorem we know that

$$|A - C| = \sqrt{x^2 + b^2} \quad \text{so} \quad t_{AC} = n_1 \sqrt{x^2 + b^2}.$$

Differentiation with respect to x then gives

$$\frac{d}{dx} t_{AC}(x) = \frac{n_1 x}{\sqrt{x^2 + b^2}} = n_1 \sin \alpha_1.$$

Analogously we find

$$\frac{d}{dx} t_{CB}(x) = -\frac{n_2 (a - x)}{\sqrt{(a - x)^2 + c^2}} = n_2 \sin \alpha_2,$$

again see Figure A.2. We may conclude that

$$\frac{d}{dx} (t_{AC}(x) + t_{BC}(x)) = 0$$

if and only if

$$n_1 \sin \alpha_1 = n_2 \sin \alpha_2,$$

as was to be proven. □

Remark 33. (1) Reflections in the boundary layer are easily incorporated in this story [37], but since we only consider motions that are monotonic in terms of $y \mapsto x(y)$, for simplicity we exclude reflections.

- (2) In this case the extremum also is a minimum as you can verify by inspecting the second derivative.
- (3) Leibniz [111] already essentially gave this proof in 1684.

A.1.2 A conservation law

In this subsection instead of two layers, we take many of them in an increasing number, so discretizing the continuum, see Figure A.3. In fact, as boundaries we take equidistant horizontal lines separating the layers $1, 2, 3, \dots, N$ where in each layer the speed of light is constant. In layer number j the refraction index is n_j and the angles at the lower

boundary of layer j with the vertical direction are α_j from above and α'_j from below ($1 \leq j \leq N$).

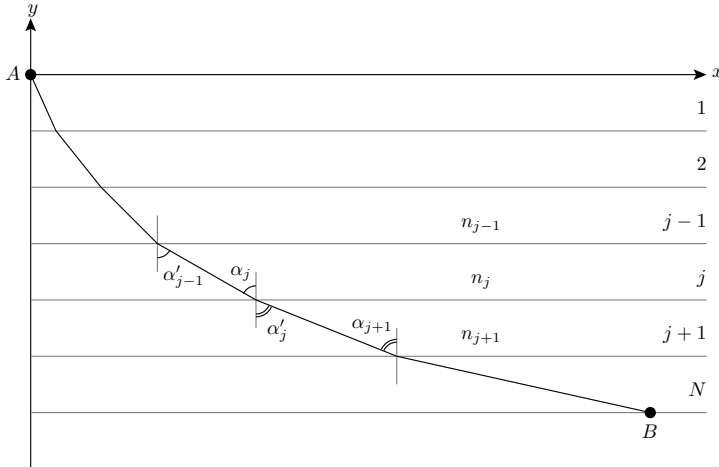


Figure A.3. Bernoulli's optical set-up: the continuous medium is discretized into layers of constant propagation velocity.

As a direct consequence of Theorem 2 we have

Corollary 1 (Conservation Law). *Under the above circumstances a broken straight line from A to B is a light ray according to the weak Fermat Principle if and only if*

$$n_j \sin \alpha_j = n_{j+1} \sin \alpha_{j+1} \quad (1 \leq j \leq N-1).$$

Proof. According to Theorem 2 always

$$n_j \sin \alpha_j = n_{j+1} \sin \alpha'_{j+1},$$

while from Euclidean geometry it is known that always

$$\alpha'_j = \alpha_{j+1}.$$

The assertion follows directly from this. \square

We may consider α_j as a parameter along the light ray, which in the continuous limit for $N \rightarrow \infty$ is just called $\alpha = \alpha(y)$: the *inclination*

of the ray. We have thus obtained a quantity that is conserved during the propagation of the light:

$$S = n \sin \alpha. \quad (\text{A.1})$$

Remark 34. (1) As said earlier we exclude reflections, otherwise $\alpha(y)$ would be multivalued. The light ray is pointing down, therefore the map $y \mapsto x(y)$ is monotonically decreasing and we have

$$\frac{dx}{dy} = -\tan \alpha$$

- (2) Note that the form of the light ray is completely determined by the value of S . The propagation along the ray is governed by the refraction index $n = 1/v$.
- (3) The conservation of S is related to the invariance of the problem under horizontal translations. In fact, roughly speaking, any continuous symmetry of a variational problem is associated to a conserved quantity. This deep result, which is of a sparkling elegance and which forms a cornerstone of modern physics, is known as *Noether's Theorem* [5, 134]. Emmy Noether (1882–1935), who proved this in 1918, was one of the most important mathematicians of the past century, often overlooked in history books [146, 147]. Her contributions, which span a large range of mathematical domains, include the development of algebraic geometry, laying the foundation of modern algebra.
- (4) Snell's law itself is still showing up in modern research, for example, it was recently generalized to non-euclidean spaces in order to describe certain problems in celestial mechanics related to central mass galaxies [60, 61].

A.2 The brachistochrone as a light ray

Theorem 3 (The brachistochrone). *Under the above circumstances, the brachistochrone curve has the cycloidal form*

$$\begin{aligned}x(\alpha) &= \frac{1}{4S^2g} (2\alpha - \sin(2\alpha)) \\y(\alpha) &= \frac{1}{4S^2g} (-1 + \cos(2\alpha)),\end{aligned}$$

passing through $A = (0, 0)$ for $\alpha = 0$ and where the constant S determines the scale of the curve such that it passes through B .

Before giving a proof, we have some comments.

- (1) Referring back to Exercise 1.6.7, in this case the cycloid has rolling angle $\varphi = 2\alpha - \pi$ and radius $R = 1/(4S^2g)$.
- (2) There are two conserved quantities. Apart from S , we have the energy H of the motion in a constant gravitational field

$$H = \tfrac{1}{2}mv^2(y) + mgy.$$

The refraction index $n(y) = 1/v(y)$ can now be determined as follows. Since we assume that the bead starts at a height $y = y_0$ at rest, $v(y_0) = 0$. It then follows that during the entire motion we have $H = mgy_0$ and, in particular, $H = 0$ when taking $y_0 = 0$. The corresponding falling speed therefore equals $v(y) = \sqrt{-2gy}$, where $y \leq 0$. The refraction index then is

$$n(y) = \frac{1}{\sqrt{-2gy}} \quad \text{where } y \leq 0.$$

We now are ready to prove Theorem 3, more or less following Bernoulli [24].

Proof. Since the motion is downward, we have $dx/dy = -\tan \alpha$. In this proof we use both the conserved quantities

$$S = n(y) \sin \alpha \quad \text{and} \quad H = \tfrac{1}{2}mv^2(y) + mgy.$$

The desired profile will be of the form

$$(x(\alpha), y(\alpha)). \tag{A.2}$$

where α is the inclination with respect to the y -direction. Since H is constant, differentiating the latter of the two above formulæ we get for all y

$$v'(y) = -\frac{g}{v(y)}. \quad (\text{A.3})$$

Rewriting the former formula as $\sin \alpha = Sv(y)$ and differentiating with respect to α gives

$$\cos \alpha = Sv'(y) \frac{dy}{d\alpha}. \quad (\text{A.4})$$

With help of the formulæ (A.3) and (A.4) we can determine the derivatives $dy/d\alpha$ and $dx/d\alpha$ for the parametrized profile (A.2). First we consider $dy/d\alpha$:

$$\begin{aligned} \frac{dy}{d\alpha} &\stackrel{(\text{A.4})}{=} \frac{\cos \alpha}{Sv'(y)} \\ &\stackrel{(\text{A.3})}{=} -\frac{v(y)}{Sg} \cos \alpha \\ &\stackrel{(\text{A.1})}{=} -\frac{1}{2S^2g} \sin(2\alpha). \end{aligned} \quad (\text{A.5})$$

We can then use this expression and some trigonometric gymnastics to determine the other derivative:

$$\begin{aligned} \frac{dx}{d\alpha} &= -\tan \alpha \frac{dy}{d\alpha} \\ &\stackrel{(\text{A.5})}{=} \frac{v(y)}{Sg} \sin \alpha \\ &\stackrel{(\text{A.1})}{=} -\frac{1}{2S^2g} (1 - \cos(2\alpha)). \end{aligned}$$

Integration then gives

$$\begin{aligned} y(\alpha) &= C_y + \frac{1}{4S^2g} \cos(2\alpha) \\ x(\alpha) &= C_x + \frac{1}{4S^2g} (2\alpha - \sin(2\alpha)), \end{aligned}$$

where we choose the constants of integration C_y and C_x in such a way that $x(0) = 0 = y(0)$, leading to $C_y = -1/(4S^2g)$ and $C_x = 0$.

So we end up with

$$x(\alpha) = \frac{1}{4S^2g} (2\alpha - \sin(2\alpha))$$

$$y(\alpha) = \frac{1}{4S^2g} (-1 + \cos(2\alpha))$$

as was to be proven. □

A.3 Scholium

The cycloid has been a subject of general interest in the 17th century, not just in relation to Huygens' or Bernoulli's problems, compare [1, 3, 35, 36, 37, 89, 140, 176, 181]; in [120] the ‘much talked of’ curve is even compared to Helen of Troy.

As we mentioned, Johann Bernoulli put forth his brachistochrone problem in 1696 in a contest published in the journal *Acta Eruditorum* [24]. One year later he published his solution in the same journal. A number of his contemporaries quickly responded, Newton and Leibniz being two of them. In fact, Newton's solution was sent under a pseudonym but Bernoulli recognized the “lion by his paw” (ex ungue leonem). For the mathematical details see Goldstine [85].

The brachistochrone problem and its solutions mark the birth of the long and broad development of the Variational Principle, nowadays a cornerstone of many scientific disciplines. Publication of this problem and a lot of related work has made Johann Bernoulli one of the founding fathers of this development.

However, we note that in a modern *Variational Calculus* class the brachistochrone problem is no more than an exercise, see e.g. [108, Exercise 8.20]. For additional discussions see [84, 107, 157, 164].

Appendix B

Small oscillations revisited

We encountered small oscillations already several times, for instance when linearizing the pendulum in Section 1.2, or when studying beats in Section 3.2.2. In this appendix we study the small oscillations and the Lissajous figures of Section 3.2 in a more general setting, namely in coupled oscillators of the form

$$\begin{aligned}\ddot{x}_1 &= -\frac{\partial U}{\partial x_1} \\ \ddot{x}_2 &= -\frac{\partial U}{\partial x_2},\end{aligned}\tag{B.1}$$

where $U = U(x_1, x_2)$ is a potential function with a minimum at the origin $(x_1, x_2) = (0, 0)$, that is,

$$\frac{\partial U}{\partial x_j} = 0 \quad \text{for } j = 1, 2.$$

This set-up is a direct extension of the theory as presented in Section 1.4 and in particular of Proposition 1.

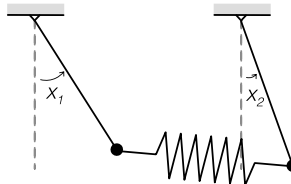


Figure B.1. Two coupled pendulums, compare Figure 3.6

We let the example of beats in Section 3.2.2 be a running gag, in particular illustrating how the background mathematics looks there. We recall the equations of motion (3.1)

$$\begin{aligned}\ddot{x}_1 &= -x_1 - \kappa(x_1 - x_2) \\ \ddot{x}_2 &= -x_2 - \kappa(x_2 - x_1),\end{aligned}$$

where κ is the spring constant of the connection. A direct computation shows that this model fits with the general set-up of (B.1) when choosing

$$U(x_1, x_2) = \frac{1}{2} \left((x_1^2 + x_2^2) + \kappa(x_1 - x_2)^2 \right).$$

To illustrate this further recall the decoupling change of variables

$$y_1 = \frac{1}{\sqrt{2}}(x_1 + x_2) \quad \text{and} \quad y_2 = \frac{1}{\sqrt{2}}(x_1 - x_2), \quad (\text{B.2})$$

that fit with the characteristic motions of Figure 3.7, as these occur for $y_1 = 0$ and $y_2 = 0$. This and other changes of variables are *linear* and for a better understanding we need to dive a bit into linear algebra. Below we present the main ideas relevant for our discussion, for general background referring to [5, 98].

In the next Appendix we shall again encounter small oscillations and Lissajous figures, but then in the context of the Foucault pendulum.

B.1 Intermezzo on linear algebra

In this section we discuss the linear algebra needed to develop a general theory of small oscillations. For convenience we develop the theory for the plane \mathbb{R}^2 , staying close to its geometry, but remark at once that the whole theory can be generalized to higher dimensions and to more abstract spaces. This intermezzo leads us through a discussion of linear maps and their matrix representations, composition of linear maps and the corresponding matrix multiplication, determinants, eigenvalues and eigenvectors, quadratic forms and basis transformations.

B.1.1 Linear maps

On the space \mathbb{R}^2 , let us distinguish the (column-) vectors

$$\mathbf{e}_1 = \begin{pmatrix} 1 \\ 0 \end{pmatrix} \quad \text{and} \quad \mathbf{e}_2 = \begin{pmatrix} 0 \\ 1 \end{pmatrix}.$$

Any vector

$$\mathbf{x} = \begin{pmatrix} x_1 \\ x_2 \end{pmatrix}$$

can then be expressed as

$$\mathbf{x} = x_1 \mathbf{e}_1 + x_2 \mathbf{e}_2.$$

We call the \mathbf{e}_1 and \mathbf{e}_2 a *basis* of \mathbb{R}^2 , seen as a vector space. This basis is called the *standard basis*.

We consider \mathbf{x} as the arrow connecting the origin 0 with the point with coordinates x_1 and x_2 and in this case sometimes speak of position vector. In this case next to \mathbf{x} also consider the horizontal and vertical vectors

$$\begin{pmatrix} x_1 \\ 0 \end{pmatrix} \quad \text{and} \quad \begin{pmatrix} 0 \\ x_2 \end{pmatrix}$$

then using Pythagoras's theorem we can compute the *length* of \mathbf{x} as

$$|\mathbf{x}| = \sqrt{x_1^2 + x_2^2}. \quad (\text{B.3})$$

Definition 2 (Linear map). A map $A : \mathbb{R}^2 \rightarrow \mathbb{R}^2$ is said to be *linear* if for all vectors \mathbf{x} and \mathbf{y} and all real numbers λ and μ we have

$$A(\lambda\mathbf{x} + \mu\mathbf{y}) = \lambda A(\mathbf{x}) + \mu A(\mathbf{y}). \quad (\text{B.4})$$

We now investigate how to express A in coordinates, using the above standard basis. If we define

$$A(\mathbf{e}_1) = \begin{pmatrix} a_{11} \\ a_{21} \end{pmatrix} \quad \text{and} \quad A(\mathbf{e}_2) = \begin{pmatrix} a_{12} \\ a_{22} \end{pmatrix},$$

then, by formula (B.4), we have for any \mathbf{x}

$$\begin{aligned} A(\mathbf{x}) &= x_1 A(\mathbf{e}_1) + x_2 A(\mathbf{e}_2) \\ &= x_1 \begin{pmatrix} a_{11} \\ a_{12} \end{pmatrix} + x_2 \begin{pmatrix} a_{21} \\ a_{22} \end{pmatrix} = \begin{pmatrix} a_{11}x_1 + a_{12}x_2 \\ a_{21}x_1 + a_{22}x_2 \end{pmatrix}. \end{aligned}$$

The latter formula is our first example of *matrix multiplication*, namely of the matrix

$$\begin{pmatrix} a_{11} & a_{12} \\ a_{21} & a_{22} \end{pmatrix} \quad \text{and the vector} \quad \begin{pmatrix} x_1 \\ x_2 \end{pmatrix}.$$

In general, we specify this as follows

$$A(\mathbf{x}) = \begin{pmatrix} a_{11} & a_{12} \\ a_{21} & a_{22} \end{pmatrix} \begin{pmatrix} x_1 \\ x_2 \end{pmatrix} = \begin{pmatrix} a_{11}x_1 + a_{12}x_2 \\ a_{21}x_1 + a_{22}x_2 \end{pmatrix}. \quad (\text{B.5})$$

So the linear map A written out with the standard basis just coincides with the matrix, which is why we simply write

$$A = \begin{pmatrix} a_{11} & a_{12} \\ a_{21} & a_{22} \end{pmatrix}.$$

Can you see what matrix is associated to the identity map $\text{Id}(\mathbf{x}) = \mathbf{x}$?

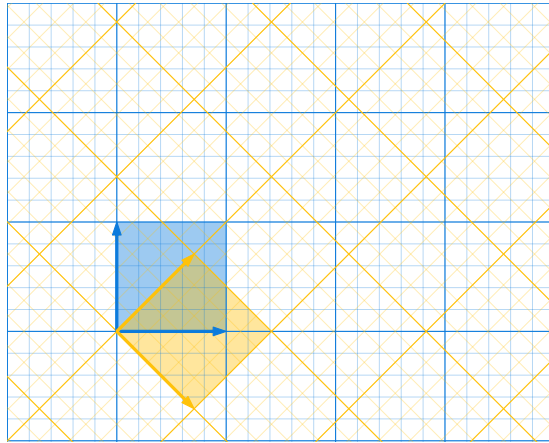


Figure B.2. Transformation of the coordinates by the matrix C). The straight lines correspond to the standard Euclidean coordinates \mathbf{x} , and the skew lines to the new coordinates $\mathbf{y} = C\mathbf{x}$.

Example 2 (Rotating the standard basis). Returning to the context of beats, we consider the change of variables (B.2)

$$y_1 = \frac{1}{\sqrt{2}}(x_1 + x_2) \quad \text{and} \quad y_2 = \frac{1}{\sqrt{2}}(x_1 - x_2),$$

which we now can rephrase in terms of a linear map C . See Figure B.2.

As before we have

$$\mathbf{y} = \begin{pmatrix} y_1 \\ y_2 \end{pmatrix}$$

and by (B.5) we get

$$\mathbf{y} = \begin{pmatrix} y_1 \\ y_2 \end{pmatrix} = \frac{1}{\sqrt{2}} \begin{pmatrix} x_1 + x_2 \\ x_1 - x_2 \end{pmatrix} = \frac{1}{\sqrt{2}} \begin{pmatrix} 1 & 1 \\ 1 & -1 \end{pmatrix} \begin{pmatrix} x_1 \\ x_2 \end{pmatrix} = C(\mathbf{x}).$$

Indeed, taking

$$C(\mathbf{e}_1) = \frac{1}{\sqrt{2}} \begin{pmatrix} 1 \\ 1 \end{pmatrix} \quad \text{and} \quad C(\mathbf{e}_2) = \frac{1}{\sqrt{2}} \begin{pmatrix} 1 \\ -1 \end{pmatrix}, \quad (\text{B.6})$$

we see that

$$C = \frac{1}{\sqrt{2}} \begin{pmatrix} 1 & 1 \\ 1 & -1 \end{pmatrix}.$$

Note that the images of the basis are again *orthogonal* (or perpendicular) and the factor $1/\sqrt{2}$ was only used to give the images of \mathbf{e}_1 and \mathbf{e}_2 unit length, see equation (B.3). In fact, as we shall explore later on, we can use (B.6) as a new basis of \mathbb{R}^2 .

B.1.2 Composing and inverting linear maps

Now suppose we have two linear maps

$$A = \begin{pmatrix} a_{11} & a_{12} \\ a_{21} & a_{22} \end{pmatrix} \quad \text{and} \quad B = \begin{pmatrix} b_{11} & b_{12} \\ b_{21} & b_{22} \end{pmatrix}$$

defined by their matrices and consider the *composition* of the two maps

$$\mathbb{R}^2 \xrightarrow{B} \mathbb{R}^2 \xrightarrow{A} \mathbb{R}^2$$

In the same spirit as before, we compute $B(A(\mathbf{x}))$ as

$$\begin{aligned} B(A(\mathbf{x})) &= B \begin{pmatrix} a_{11}x_1 + a_{12}x_2 \\ a_{21}x_1 + a_{22}x_2 \end{pmatrix} \\ &= \begin{pmatrix} b_{11}(a_{11}x_1 + a_{12}x_2) + b_{12}(a_{21}x_1 + a_{22}x_2) \\ b_{21}(a_{11}x_1 + a_{12}x_2) + b_{22}(a_{21}x_1 + a_{22}x_2) \end{pmatrix} \\ &= \begin{pmatrix} b_{11}a_{11} + b_{12}a_{21} & b_{11}a_{12} + b_{12}a_{22} \\ b_{21}a_{11} + b_{22}a_{21} & b_{21}a_{12} + b_{22}a_{22} \end{pmatrix} \begin{pmatrix} x_1 \\ x_2 \end{pmatrix}, \end{aligned}$$

where the terms had to be rearranged a bit. Here we meet the second example of matrix multiplication, namely of the matrices A and B :

$$BA = \begin{pmatrix} b_{11}a_{11} + b_{12}a_{21} & b_{11}a_{12} + b_{12}a_{22} \\ b_{21}a_{11} + b_{22}a_{21} & b_{21}a_{12} + b_{22}a_{22} \end{pmatrix}. \quad (\text{B.7})$$

Remark 35. When computing the element with index ij in the product BA you can take row i in the matrix B and column j in A and compute the matrix product

$$(b_{i1}b_{i2}) \begin{pmatrix} a_{1j} \\ a_{2j} \end{pmatrix} = b_{i1}a_{1j} + b_{i2}a_{2j}.$$

This fact can be helpful when applying formula (B.7).

The *inverse* A^{-1} of the linear map A , if it exists, is the map such that $A^{-1}A = AA^{-1} = \text{Id}$. We claim that

$$A^{-1} = \frac{1}{a_{11}a_{22} - a_{12}a_{21}} \begin{pmatrix} a_{22} & -a_{12} \\ -a_{21} & a_{11} \end{pmatrix}, \quad (\text{B.8})$$

which only exists for $a_{11}a_{22} - a_{12}a_{21} \neq 0$. You can check this by using formula (B.7).

B.1.3 Determinants

We abbreviate the denominator in the above formula by

$$\det A = a_{11}a_{22} - a_{12}a_{21}.$$

This is called the *determinant* of A . The determinant has a geometric meaning.

Proposition 2 (Properties of the determinant). *For two vectors $\mathbf{a}_1 = \begin{pmatrix} a_{11} \\ a_{12} \end{pmatrix}$ and $\mathbf{a}_2 = \begin{pmatrix} a_{21} \\ a_{22} \end{pmatrix}$, denote by $(\mathbf{a}_1, \mathbf{a}_2) = \begin{pmatrix} a_{11} & a_{12} \\ a_{21} & a_{22} \end{pmatrix}$ the matrix that has these two vectors as its columns. Then we have*

- (1) $\det(\mathbf{a}_1, \mathbf{a}_2) = -\det(\mathbf{a}_2, \mathbf{a}_1)$,
- (2) $\det(\mathbf{a}_1, \mathbf{a}_2 + \lambda \mathbf{a}_1) = \det(\mathbf{a}_1, \mathbf{a}_2)$, for all real numbers λ ,
- (3) $\det(AB) = \det A \cdot \det B$,
- (4) $\det(\mathbf{a}_1, \mathbf{a}_2)$ equals the oriented area of the parallelogram generated by the vectors \mathbf{a}_1 and \mathbf{a}_2 (see Figure B.3).

Proof. The first three properties can be checked by direct computation. A proof of the last property is postponed to Exercise B.4.1. \square

B.1.4 Eigenvalues and eigenvectors

Given a linear map A , a number λ is called an *eigenvalue* of A if there exists a vector $\mathbf{v} \neq \mathbf{0}$ such that

$$A(\mathbf{v}) = \lambda \mathbf{v}, \quad (\text{B.9})$$

and such a vector \mathbf{v} is a corresponding *eigenvector*. Note that when \mathbf{v} is an eigenvector, then so are all scalar multiples of \mathbf{v} (with the same eigenvalue λ).

Proposition 3 (Characteristic polynomial). *The eigenvalues of A are the roots of the characteristic polynomial*

$$\det(A - \lambda \text{Id}) .$$

Proof. First observe that for any linear map B , the fact that $B(\mathbf{v}) = 0$ for some $\mathbf{v} \neq \mathbf{0}$ implies that B is non-invertible. Indeed, in such case $B(\mathbf{0}) = \mathbf{0}$ and $B(\mathbf{v}) = \mathbf{0}$, and it is not possible to properly define an inverse of B at the value $\mathbf{0}$. Moreover, by (B.8), non-invertibility of B is equivalent to $\det B = 0$.

Next observe that equation (B.9) can be reformulated as

$$(A - \lambda \text{Id}) \mathbf{v} = 0 \quad \text{for some } \mathbf{v} \neq 0 .$$

By the first observation this is equivalent to saying that the map $A - \lambda \text{Id}$ is non-invertible, which in turn is equivalent to

$$\det(A - \lambda \text{Id}) = 0 .$$

□

In the present case of 2×2 -matrices, finding the eigenvalues just amounts to solving quadratic equations. After that, finding eigenvectors \mathbf{v} from (B.9), is just a matter of solving linear equations.

Remark 36. (1) If D is a diagonal matrix

$$D = \begin{pmatrix} d_1 & 0 \\ 0 & d_2 \end{pmatrix} ,$$

then the eigenvalues of D are d_1 and d_2 .

(2) The linear map

$$A = \begin{pmatrix} 0 & 1 \\ -1 & 0 \end{pmatrix}$$

has the characteristic polynomial $\lambda^2 + 1$, which has no real roots. In this case the eigenvalues are the complex numbers $\pm i$. Can you see how A transforms the plane?

B.1.5 The inner product and quadratic forms

On \mathbb{R}^2 there exists a special operation, called *inner product*, that assigns to any two vectors real number. This number will turn out to be very helpful for computing lengths and angles and it is defined as follows. For two vectors

$$\mathbf{x} = \begin{pmatrix} x_1 \\ x_2 \end{pmatrix} \quad \text{and} \quad \mathbf{y} = \begin{pmatrix} y_1 \\ y_2 \end{pmatrix},$$

we define

$$\langle \mathbf{x}, \mathbf{y} \rangle = x_1 y_1 + x_2 y_2.$$

The inner product again is a very geometrical object as we shall see now. First of all, for any vector \mathbf{x} we have that $\langle \mathbf{x}, \mathbf{x} \rangle = x_1^2 + x_2^2 = |\mathbf{x}|^2$, where $|\cdot|$ denotes the length (B.3) of the vectors. Furthermore, it has the following properties.

Proposition 4 (Properties of the inner product). (1) *For any two vectors \mathbf{x} and \mathbf{y} we have*

$$\langle \mathbf{x}, \mathbf{y} \rangle = |\mathbf{x}| |\mathbf{y}| \cos \theta,$$

where θ is the angle between \mathbf{x} and \mathbf{y} .

(2) *For any \mathbf{x} and \mathbf{y}*

$$\langle \mathbf{x}, \mathbf{y} \rangle = 0 \quad \text{if and only if} \quad \mathbf{x} \perp \mathbf{y},$$

that is, when \mathbf{x} and \mathbf{y} are perpendicular.

Proof. Let $\theta = \beta - \alpha$, see Figure B.3. Then

$$\mathbf{x} = \begin{pmatrix} |\mathbf{x}| \cos \alpha \\ |\mathbf{x}| \sin \alpha \end{pmatrix} \quad \text{and} \quad \mathbf{y} = \begin{pmatrix} |\mathbf{y}| \cos \beta \\ |\mathbf{y}| \sin \beta \end{pmatrix},$$

and therefore

$$\langle \mathbf{x}, \mathbf{y} \rangle = |\mathbf{x}| |\mathbf{y}| (\cos \alpha \cos \beta + \sin \alpha \sin \beta) = |\mathbf{x}| |\mathbf{y}| \cos(\beta - \alpha).$$

The latter property then immediately follows. \square

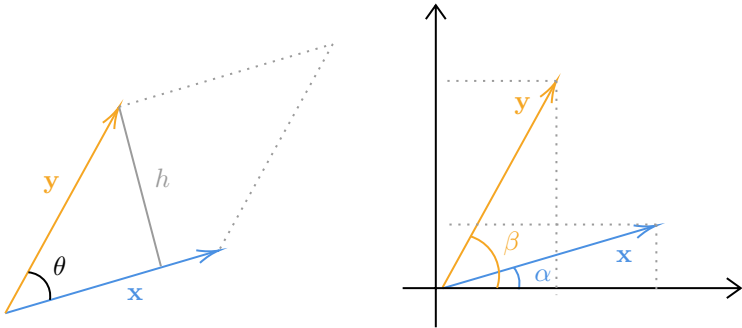


Figure B.3. Parallelogram useful for the proofs of Propositions 2 and 4.

B.1.6 Quadratic forms

Any function $F : \mathbb{R}^2 \times \mathbb{R}^2 \rightarrow \mathbb{R}$ that is linear in both variables is called a *bilinear form*: that is, for any $\mathbf{x}, \mathbf{y}, \mathbf{z} \in \mathbb{R}^2$ and any $\lambda \in \mathbb{R}$ we have

$$F(\mathbf{x} + \lambda \mathbf{z}, \mathbf{y}) = F(\mathbf{x}, \mathbf{y}) + \lambda F(\mathbf{z}, \mathbf{y})$$

and

$$F(\mathbf{x}, \mathbf{y} + \lambda \mathbf{z}) = F(\mathbf{x}, \mathbf{y}) + \lambda F(\mathbf{x}, \mathbf{z}).$$

For any linear map B we can define the following bilinear form

$$(\mathbf{x}, \mathbf{y}) \mapsto \langle B\mathbf{x}, \mathbf{y} \rangle,$$

and check with a direct computation that for any $\mathbf{x}, \mathbf{y} \in \mathbb{R}^2$ the following holds:

$$\langle B\mathbf{x}, \mathbf{y} \rangle = \langle \mathbf{x}, B^T \mathbf{y} \rangle,$$

where B^T is the *transposed* of B . This means the following: if

$$B = \begin{pmatrix} b_{11} & b_{12} \\ b_{21} & b_{22} \end{pmatrix} \quad \text{then} \quad B^T = \begin{pmatrix} b_{11} & b_{21} \\ b_{12} & b_{22} \end{pmatrix},$$

so the off-diagonal elements are switched.

Note that when $B = \text{Id}$, the identity map, the quadratic form is just the inner product.

In the sequel we shall assume that the matrix B is *symmetric*, i.e., such that $B^T = B$, and call the corresponding bilinear form a *quadratic form*. This is the case of small oscillations. In fact this

symmetry holds for all systems of the form (B.1). The reason is that mixed second derivatives commute:

$$\frac{\partial^2 U}{\partial x_1 \partial x_2} = \frac{\partial^2 U}{\partial x_2 \partial x_1},$$

The latter holds true for all functions $U(x_1, x_2)$ that are sufficiently often differentiable.

B.1.7 Basis transformations

We conclude this part by going back to Figure B.2 and discussing *basis transformations*. Suppose a linear map $B : \mathbb{R}^2 \rightarrow \mathbb{R}^2$ is given and we would like to transform this to another basis with help of the invertible linear map C , as sketched in the diagram below:

$$\begin{array}{ccc} \mathbb{R}^2 & \xrightarrow{B} & \mathbb{R}^2 \\ C \downarrow & & \downarrow C \\ \mathbb{R}^2 & \xrightarrow{D} & \mathbb{R}^2 \end{array}$$

We say that the diagram commutes whenever $DC = CB$, just follow the arrows. In that case we have

$$D = CBC^{-1}. \quad (\text{B.10})$$

Proposition 5 (Isometry). *The basis transformation C is an isometry, in the sense that for all \mathbf{x} and \mathbf{y}*

$$\langle C\mathbf{x}, C\mathbf{y} \rangle = \langle \mathbf{x}, \mathbf{y} \rangle,$$

if and only if $C^{-1} = C^T$.

Proof.

$$\langle C\mathbf{x}, C\mathbf{y} \rangle = \langle C^T C \mathbf{x}, \mathbf{y} \rangle = \langle C^{-1} C \mathbf{x}, \mathbf{y} \rangle = \langle \text{Id } \mathbf{x}, \mathbf{y} \rangle = \langle \mathbf{x}, \mathbf{y} \rangle$$

□

Instead of C being an isometry one usually says that C is an *orthogonal* matrix.

Remark 37. (1) The fact that C is orthogonal implies that it transforms orthonormal bases to orthonormal bases.

- (2) Any symmetric linear map B has real eigenvalues. You can see this by examining the discriminant of its characteristic polynomial.

B.2 Beats revisited

We now are ready to fit the contents of Section 3.2.2, in particular, Proposition 1, into the above context. Recall from (3.1) that we specified the equations of motion as

$$\begin{aligned}\ddot{x}_1 &= -x_1 - \kappa(x_1 - x_2) \\ \ddot{x}_2 &= -x_2 - \kappa(x_2 - x_1),\end{aligned}$$

where κ is the spring constant of the connection. As we saw this model fits with the general set-up of (B.1) when choosing

$$U(x_1, x_2) = \frac{1}{2} ((x_1^2 + x_2^2) + \kappa(x_1 - x_2)^2).$$

It then turns out that we can express the potential energy U as a quadratic form $U(\mathbf{x}) = \frac{1}{2}\langle B\mathbf{x}, \mathbf{x} \rangle$, where B has the symmetric form

$$B = \begin{pmatrix} 1 + \kappa & -\kappa \\ -\kappa & 1 + \kappa \end{pmatrix}.$$

You can check this for yourself by writing down explicitly all the terms.

By Proposition 3, the eigenvalues of B can be directly computed from the quadratic equation $\det(B - \lambda \text{Id}) = 0$. The answer is

$$\lambda_1 = 1 \quad \text{and} \quad \lambda_2 = 1 + 2\kappa. \tag{B.11}$$

Now we look for the basis transformation C such that

$$D = CBC^{-1} = \begin{pmatrix} \lambda_1 & 0 \\ 0 & \lambda_2 \end{pmatrix},$$

where the λ 's are as in (B.11). We have already found the linear map C before by inspecting Figure B.2: the mutually perpendicular eigenvectors (of unit length) for the eigenvalues (B.11) are given by

$$C(\mathbf{e}_1) = \frac{1}{\sqrt{2}} \begin{pmatrix} 1 \\ 1 \end{pmatrix} \quad \text{and} \quad C(\mathbf{e}_2) = \frac{1}{\sqrt{2}} \begin{pmatrix} 1 \\ -1 \end{pmatrix},$$

which are exactly the columns of C :

$$C = \frac{1}{\sqrt{2}} \begin{pmatrix} 1 & 1 \\ 1 & -1 \end{pmatrix}.$$

How can you see that C is an orthogonal matrix?

In summary, when considering the diagram just above formula (B.10), in the upper row we use the coordinates x_1 and x_2 , while in the lower row we use y_1 and y_2 . Note that all of this confirms Proposition 1. This solution may still look somewhat like the rabbit pulled out of the hat, but we now have set the stage for a more profound solution.

B.3 Scholium

We continue the discussion on small oscillations at a deeper level, referring to Arnold [5, Section 23] for details. After that we point out how things generalize to higher dimensions.

B.3.1 Sylvester's Inertial Theorem

There is a famous result due to the English mathematician James Joseph Sylvester (1814-1897), named the *Inertial Theorem*, nowadays known as the *Spectral Theorem* [98, Theorem 2.5.6]. We refer to [161] for an interesting historical account.

The spectral theorem asserts the following.

Any symmetric linear map B has an orthonormal basis of eigenvectors and there exists an orthogonal basis transformation C putting B on this new basis according to equation (B.10). In other words, B is diagonalizable by an orthogonal transformation.

Indeed, we saw above that D gets the diagonal form

$$D = \begin{pmatrix} \lambda_1 & 0 \\ 0 & \lambda_2 \end{pmatrix},$$

where λ_1 and λ_2 are its eigenvalues. In fact, the theorem provides an algorithm to find the basis transformation C .

For a slightly more general treatment of small oscillations, we observe that also the kinetic energy

$$T = \frac{1}{2}(\dot{x}_1^2 + \dot{x}_2^2)$$

can be expressed as a quadratic form

$$T = \frac{1}{2}\langle A\dot{\mathbf{x}}, \dot{\mathbf{x}} \rangle,$$

where here $A = \text{Id}$ simply is the identity map (corresponding to the standard inner product). In fact, in the theory A may be any symmetric linear map with positive eigenvalues, which then serves to define a new inner product. One can then define the *Lagrangian* function

$$L = T - U$$

which leads to the celebrated *Euler-Lagrange* equations, of which the general theory of small oscillations studies the linearization. This is too advanced to be treated here, but equation (B.1) is the present remnant of this theory.

B.3.2 Further generalizations

In the above we restricted our attention to linear maps $\mathbb{R}^2 \rightarrow \mathbb{R}^2$. The entire theory directly generalizes to the case of $\mathbb{R}^n \rightarrow \mathbb{R}^n$ for arbitrary n without extra complications. In fact, in Exercise B.4.6 below, the theory of Sylvester has to be applied in \mathbb{R}^3 . Moreover, also linear maps $\mathbb{R}^n \rightarrow \mathbb{R}^m$, for arbitrary n and m , are widely studied and applied.

Here we have chosen to present the theory in a more concrete way, but as we hinted above, linear algebra is a vast and deep subject with a wide range of applications, including very tangible ones like quantum mechanics, signal processing and machine learning. In mathematical curricula, the topic is usually approached more abstractly, starting with an axiomatic definition of vector space, both finite and infinite dimensional, and developing the rest of the theory from there. For a more comprehensive treatment we refer the reader to the open-access book [17] or any other textbook on the subject.

As announced in Chapter 3, in particular in Remark 28, we like to point at a powerful tool in the study of partial differential equations, namely at *spectral theory*, that we will briefly illustrate on the wave equation. To this end we consider the following mapping, called operator,

$$u \mapsto W(u) = \frac{\partial^2 u}{\partial t^2} - \frac{\partial^2 u}{\partial x^2},$$

that runs from a space of functions to itself. This space is chosen so that u is sufficiently often differentiable and satisfies appropriate constraints at the boundary of the system. Sweeping under the rug a number of important technical subtleties, one can try to mimic the finite dimensional case and define the number λ to be an eigenvalue of W whenever there exists a function u , not equal to the zero function, such that

$$W(u) = \lambda u.$$

The set of all such eigenvalues and their accumulation points is called the *spectrum* of W and the corresponding functions u are called eigenfunctions. In general, the spectrum of such operators is far more complicated than the spectrum of a matrix: it can be continuous, it can be unbounded and it can exhibit fractal geometry. We will see examples of this in Appendix E.5.1, in particular concerning certain Schrödinger operators.

Nevertheless, one can completely characterize an operator by its spectrum and, moreover, the eigenfunctions often form a basis of the space of solutions of W , in analogy to the eigenvectors of a matrix. This has pushed mathematicians to develop a very rich theory to study and approximate the spectrum of operators, and characterize their properties. A Spectral Theorem similar to the one we saw before holds for the kind of operators in this chapter: these so-called self-adjoint operators have a certain symmetry property that makes them somewhat similar to symmetric matrices.

In our presentation we have mostly focused on the directly descriptive aspects of the theory of oscillations, where given the description of a system we have enquired about its behavior. It is also possible to take the opposite approach, whereby one starts from measured data, for example, the sound of a musical instrument, and tries to

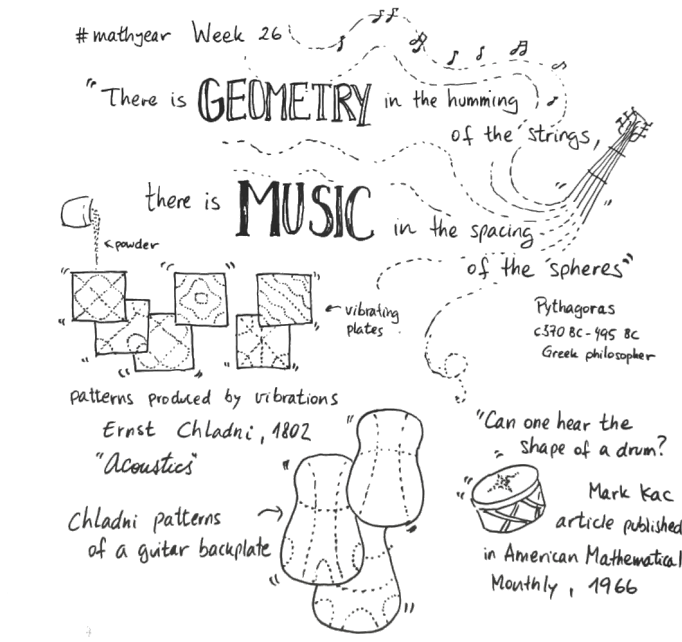


Figure B.4. Spectral theory links mathematics and music, courtesy of Constanza Rojas-Molina. If you feel creative, consider contributing to the #mathyear challenge.

infer the underlying physical model, in this case, the specific musical instrument that produced it.

In 1966 the mathematician Mark Kac famously asked the question “Can one hear the shape of a drum?” in a paper in the American Mathematical Monthly [104], giving new life to this (older) problem and inspiring a vast literature on the subject. It was already known since the 19th century, that the knowledge of the full spectrum of the Laplace operator on a domain, think of a drum, carries a lot of information about the structure of the domain. H. Lorentz had already conjectured this in 1910 in his “Old and new problems in physics” lectures at Göttingen [116], and the first mathematical proofs started appearing the year later, culminating in an important work of H. Weyl in 1911, showing in great generality that the growth of the spectrum

of the Laplace operator is proportional to the volume of the drum. See the introduction to [59] for a comprehensive historical account. Counterexamples to Kac's question were only found in 1992 [87], but the problem is far from being solved: indeed, it is possible to hear the shape of a drum by adding some additional minor restrictions to the allowed shapes [183], and this question remains a very active field of research.

For a rigorous introduction to the spectral theory of linear operators, including all aspects mentioned above, we refer to [27]. For some fascinating connections between mathematics and music, with an eye towards spectral theory, we refer to [88].

B.4 Selected exercises

B.4.1 Determinant and surface area

For two vectors

$$\mathbf{x} = \begin{pmatrix} x_1 \\ x_2 \end{pmatrix} \quad \text{and} \quad \mathbf{y} = \begin{pmatrix} y_1 \\ y_2 \end{pmatrix},$$

denote

$$\det(\mathbf{x}, \mathbf{y}) = \det \begin{pmatrix} x_1 & y_1 \\ x_2 & y_2 \end{pmatrix} = x_1 y_2 - x_2 y_1.$$

Show that $\det(\mathbf{x}, \mathbf{y})$ equals the (oriented) area of the parallelogram generated by \mathbf{x} and \mathbf{y} .

Remark 38. (1) Hint: Consider Figure B.3. Consider the perpendicular from the vertex of \mathbf{y} to the vector \mathbf{x} and compute its length h in terms of $|\mathbf{y}|$ and the angle θ . Next show that the parallelogram has an area $|\mathbf{x}| \cdot h$. A computation with some trigonometry will lead to the answer. In fact, at some point you may well want to apply the formula $\sin(\beta - \alpha) = \sin \beta \cos \alpha - \cos \beta \sin \alpha$.

- (2) What happens when you interchange \mathbf{x} and \mathbf{y} ? This is what the term “oriented” refers to.
- (3) Can you see why for any linear map A and any real number κ we have $\det(\kappa A) = \kappa^2 \det(A)$?

B.4.2 Basis invariance of the determinant

Show that the determinant of a linear map is invariant under basis transformations.

B.4.3 The trace of a linear map

Given a linear map

$$A = \begin{pmatrix} a_{11} & a_{12} \\ a_{21} & a_{22} \end{pmatrix},$$

the trace $\text{Tr } A$ then is defined as

$$\text{Tr } A = a_{11} + a_{22}.$$

Show that $\text{Tr } A$ also is basis invariant.

B.4.4 The characteristic polynomial

For A as in the previous exercise, show that

$$\det(A - \lambda \text{Id}) = \lambda^2 - (\text{Tr } A) \lambda + \det A.$$

Note that this means that the entire characteristic polynomial is invariant with respect to changes of basis. Can you see why?

B.4.5 The Cayley-Hamilton Theorem

For A as in the previous exercise, show that the linear map A satisfies its own characteristic polynomial, namely that

$$A^2 - (\text{Tr } A) A + \det A = 0,$$

where $A^2 = AA$, is the matrix product of A with itself.

This theorem holds generally for $n \times n$ -matrices. One of its consequences is that we can write the n -th power A^n as a linear combination of lower order powers. In the example above:

$$A^2 = \text{Tr } A A - \det A.$$

B.4.6 One more Hookian problem

This exercise is from Bottema [31]. Its solution needs the theory of this appendix.

In Euclidean 3-space, you are given three lines ℓ_i ($i=1,2,3$) which are all passing through the point 0. The angle between any of the two

lines is α ($0 < \alpha < \pi/2$). Three particles P_i of unit mass move along the lines ℓ_i , respectively. Any two particles P_i, P_j ($i \neq j$) attract each other by the force $k^2 \overline{P_i P_j}$, where $k > 0$ is a positive constant and $\overline{P_i P_j}$ denotes the distance between P_i and P_j . Determine the general motion of the three particles.

Appendix C

The Foucault problem

Jean Bernard Léon Foucault (1819-1868) was a French physicist who is known for his demonstration of the *Foucault pendulum*, a device demonstrating the rotation of the Earth. The Foucault Pendulum was first exhibited in 1851 at the World's Fair in Paris. The device is a spherical pendulum, like we already met in the introduction of Chapter 3, so where the pendulum mass can move over a sphere, mounted on the rotating Earth. The motion of the pendulum is affected by the Earth in several ways. First and for all there is gravity, that at the scale of the pendulum is reflected in the constant gravitational field with downward acceleration g . But there is at least one more force to take into account, that we shall briefly discuss in the Scholium, below.

C.1 The Foucault pendulum



Fig. C.1. The Foucault pendulum [163]

rotation of the Earth.

The idea is to let the pendulum move in a vertical plane and examine how this plane moves when the Earth rotates beneath it. To make this more clear, let us imagine that the pendulum is mounted on the North Pole. Then in the span of 24 hours the Earth makes a full rotation beneath it. An observer on Earth that keeps track of the vertical plane of oscillation, then would observe a full turn of the plane: since the Earth rotates eastward, the pendulum should rotate westward. Indeed, from the point of view of the pendulum, the vertical plane does not change its position with respect to the “fixed” stars. But to the Earthly observer the plane changes continuously. A success of this experiment would confirm the diurnal

Remark 39. The vertical plane of the Foucault pendulum, when positioned on the equator, would not rotate at all. Can you explain why

and can you also find the amount of rotation in 24 hours as a function of the latitude?

C.1.1 The spherical pendulum

To understand what is going on we need to look more closely at the spherical pendulum in its own right. In particular we have to move from cartesian to spherical coordinates, see Figure C.2, and make use of the concept of *Taylor series*. At the linear level we first meet small oscillations. If we include the quadratic terms we shall then encounter the so-called *spherical precession*, a nonlinear effect that will turn out to substantially complicate the Foucault experiment.

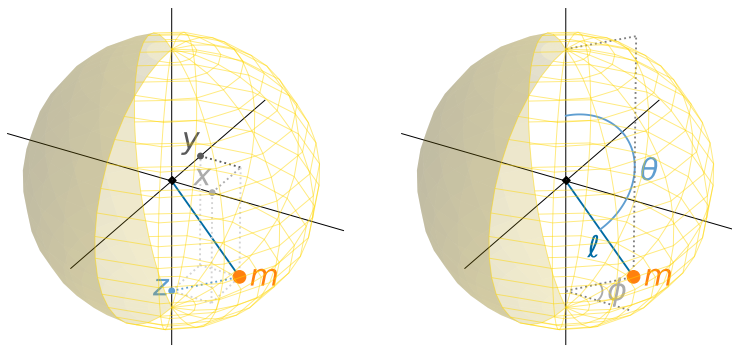


Figure C.2. Configuration of a spherical pendulum in cartesian (left) and spherical (right) coordinates

Our investigation starts with the dynamics of the spherical pendulum near its south pole equilibrium. We take a cartesian coordinate system (x, y, z) , where the center of the sphere is at the origin and the z -axis is vertical (pointing upward), see Figure C.2. Passing to spherical coordinates

$$z = r \cos \theta \quad (\text{C.1})$$

$$x = r \sin \theta \cos \varphi$$

$$y = r \sin \theta \sin \varphi,$$

the lower equilibrium occurs at the south pole $(x, y, z) = (0, 0, -\ell)$, corresponding to $r = \ell$ and $\theta = \pi$.

The evolution $(x(t), y(t), z(t))$ in cartesian coordinates of the spherical pendulum can be rewritten as an evolution in spherical coordinates $(r(t), \theta(t), \varphi(t))$. Differentiating both sides of the above equations (C.1) with respect to time, and applying the Chain Rule, then leads to

$$\begin{aligned}\dot{z} &= \dot{r} \cos \theta - r \sin \theta \dot{\theta} \\ \dot{x} &= \dot{r} \sin \theta \cos \varphi + r \cos \theta \cos \varphi \dot{\theta} - r \sin \theta \sin \varphi \dot{\varphi} \\ \dot{y} &= \dot{r} \sin \theta \sin \varphi + r \cos \theta \sin \varphi \dot{\theta} + r \sin \theta \cos \varphi \dot{\varphi}.\end{aligned}$$

Therefore, in analogy with the derivation of the pendulum in the main corpus of the book, the kinetic and potential energy are given by

$$\begin{aligned}T &= \tfrac{1}{2}m(\dot{x}^2 + \dot{y}^2 + \dot{z}^2) = \tfrac{1}{2}m\ell^2\dot{\theta}^2 + \tfrac{1}{2}m\ell^2 \sin^2 \theta \dot{\varphi}^2 \\ \text{and } U &= mgz = mgl \cos \theta,\end{aligned}$$

where g is the gravitational acceleration. We now turn to adapted cartesian coordinates that parametrize the southern hemisphere and approximate the system near the south pole's equilibrium. To this end, we define coordinates (ξ, η) from the polar coordinates φ and $\varrho = \pi - \theta$ by $\xi = \varrho \cos \varphi, \eta = \varrho \sin \varphi$. These just serve to simplify the equations, since they take the value $(0, 0)$ at the equilibrium point at the south pole. Note that so the rotational symmetry of the problem is preserved.

Computational intermezzo. A few computations are in order.

(1) A first useful formula turns out to be

$$\dot{\xi}^2 + \dot{\eta}^2 = \dot{\varrho}^2 + \varrho^2 \dot{\varphi}^2. \tag{C.2}$$

To prove this we take derivatives

$$\dot{\xi} = \dot{\varrho} \cos \varphi - \varrho \sin \varphi \dot{\varphi} \quad \text{and} \quad \dot{\eta} = \dot{\varrho} \sin \varphi + \varrho \cos \varphi \dot{\varphi},$$

after which squaring and summing the two equations gives the desired result.

In the same spirit, we have

$$\dot{\varphi} = \frac{\dot{\eta}\xi - \dot{\xi}\eta}{\xi^2 + \eta^2} \quad (\text{C.3})$$

which directly follows from deriving the identity $\varphi = \arctan \frac{\eta}{\xi}$.

- (2) In the approximation at the lower equilibrium we need the first terms of the Taylor expansions for sine and cosine:

$$\begin{aligned} \sin \varrho &= \varrho - \frac{1}{6}\varrho^3 + O(\varrho^5) \\ \cos \varrho &= 1 - \frac{1}{2}\varrho^2 + \frac{1}{24}\varrho^4 + O(\varrho^6). \end{aligned} \quad (\text{C.4})$$

This is a way to get a good approximation of a function around the equilibrium. In general, let us consider a function $f : \mathbb{R} \rightarrow \mathbb{R}$ that is sufficiently often differentiable, say at least $(n+1)$ times. Near any point x_0 we can approximate f by a so-called *Taylor polynomial* of degree n as follows:

$$\begin{aligned} f(x) &= f(x_0) + f'(x_0)(x - x_0) + \frac{f''(x_0)}{2!}(x - x_0)^2 \\ &\quad + \cdots + \frac{f^{(n)}(x_0)}{n!}(x - x_0)^n, \end{aligned}$$

and the error can be shown to be small of the order $\mathcal{O}(|x-x_0|^{n+1})$. This means that the error decreases rapidly when one is nearer to the point x_0 . See [4] for more details, or any other book on calculus.

C.1.2 Small oscillations

We first approximate to second order at the south pole using (C.4):

$$\sin \varrho \approx \varrho \quad \text{and} \quad \cos \varrho \approx 1 - \frac{1}{2}\varrho^2$$

from which we get approximately

$$T = \frac{1}{2}m\ell^2(\dot{\varrho}^2 + \varrho^2\dot{\varphi}^2) \quad \text{and} \quad U = -mg\ell(1 - \frac{1}{2}\varrho^2) \equiv \frac{1}{2}mg\ell\varrho^2,$$

where we also used that $\cos \theta = -\cos \varrho$. By formula (C.2) we find

$$T = \frac{1}{2}m\ell^2(\dot{\xi}^2 + \dot{\eta}^2) \quad \text{and} \quad U = \frac{1}{2}mg\ell(\xi^2 + \eta^2),$$

which, again by (B.1), corresponds to the linear system

$$\begin{aligned}\ddot{\xi} &= -\frac{g}{\ell}\xi \\ \ddot{\eta} &= -\frac{g}{\ell}\eta\end{aligned}$$

of two uncoupled harmonic oscillators, in this case with equal frequencies $\omega = \sqrt{g/\ell}$. Referring to Remark 23 we conclude that the small oscillations consist of all possible Lissajous ellipses with the origin as center.

Remark 40. Notice that we don't need the machinery of Section B.2. Can you identify the matrices A and B here?

C.1.3 Spherical precession

Using one more term in the Taylor expansions (C.4)

$$\sin \varrho \approx \varrho - \frac{1}{6}\varrho^3 \quad \text{and} \quad \cos \varrho \approx 1 - \frac{1}{2}\varrho^2 + \frac{1}{24}\varrho^4$$

gives approximately

$$\begin{aligned}T &= \frac{1}{2}m\ell^2 (\dot{\varrho}^2 + (\varrho - \frac{1}{6}\varrho^3)^2\dot{\varphi}^2) \\ U &= -mg\ell \cos \varrho \equiv \frac{1}{2}mg\ell(\varrho^2 - \frac{1}{12}\varrho^4).\end{aligned}$$

Simplifying further and neglecting terms of order ϱ^6 we get

$$\begin{aligned}T &= \frac{1}{2}m\ell^2 (\dot{\varrho}^2 + (\varrho^2 - \frac{1}{3}\varrho^4)\dot{\varphi}^2) \\ &= \frac{1}{2}m\ell^2(\varrho^2 + \varrho^2\dot{\varphi}^2) + \frac{1}{6}\varrho^4\dot{\varphi}^2 \\ U &= -mg\ell \cos \varrho \equiv \frac{1}{2}mg\ell\varrho^2 - \frac{1}{6}mg\ell\varrho^4,\end{aligned}\tag{C.5}$$

where we added the fourth-order terms to the former approximation. The fourth-order part of the kinetic energy T reads

$$\frac{1}{6}\varrho^4\dot{\varphi}^2 = \frac{1}{6}(\dot{\eta}\xi - \dot{\xi}\eta)^2,$$

where we use formula (C.3). This term corresponds to a slow motion in the φ -direction, in other words, a rotation (= precession) of the system, that roughly deforms any Lissajous ellipse into a rosette, see Figure C.3 and C.4. Again compare Remark 23. This holds at least when the ellipse does not degenerate to a straight line, in which case we would have $\dot{\varphi} \equiv 0$.

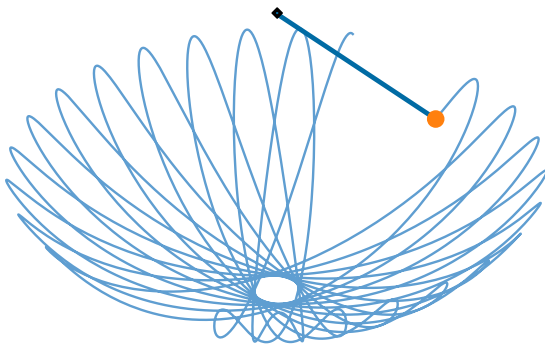


Figure C.3. A trajectory of the Foucault pendulum clearly showing a spherical precession

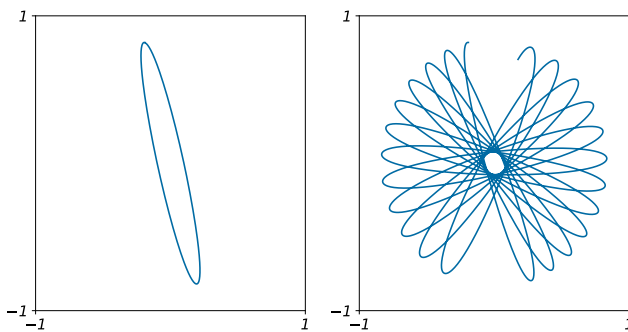


Figure C.4. Left: Lissajous ellipse for the linearization of a pendulum with the same initial condition as the trajectory in Figure C.3 projected on the (x, y) -plane; Right: the trajectory of Figure C.3 projected on the (x, y) -plane

C.2 Scholium

The spherical precession complicates the Foucault experiment, since practically it is impossible to restrict the pendulum motion to one vertical plane. In terms of the Lissajous figures, the ellipses, however narrow, do not completely degenerate to a straight line. This means that the rotation of the pendulum 'plane' may just as well be affected by the precession as by the rotation of the earth. This is probably the case with many of the Foucault pendulums – they do actually exist! – all over the world.

A solution for this problem is to damp out the transversal motion $\dot{\phi}$ at the maximum of its swings. The physics Nobel laureate Heike Kamerlingh Onnes doctorated in 1879 at Groningen University with the thesis *Nieuwe Bewijzen voor de Aardweteling der Aarde* [106] under the supervision of the mathematical physicist Rudolf Adriaan Mees. In his dissertation, Kamerlingh Onnes designs an ingenious construction, where a ring is mounted on the device that performs the damping: the first functioning Foucault pendulum. For background information also see [52].

Remark 41. (1) Until now, when considering the spherical pendulum in its own right, the detected spherical precession already casts serious doubt on the Foucault experiment.

As announced in the beginning of this appendix, the motion of the pendulum mass is also affected by another force that arises from the fact that the Earth provides a rotating frame of reference: the *Coriolis force*. This is a force with curious consequences. For example, it is responsible for the Buys Ballot Law asserting that winds on the Northern hemisphere are deflected to the right. The reason is that the eastwardly rotating Earth moves underneath the winds. The same happens to the pendulum mass! Can you see how this goes on the southern hemisphere?

Taking this Coriolis effect mathematically into account lies beyond the scope of our book, but Kamerlingh Onnes in his thesis [106] performed this considerable task, accompanied by a very careful experimental setup, thereby confirming the relevance of Foucault's experiment.

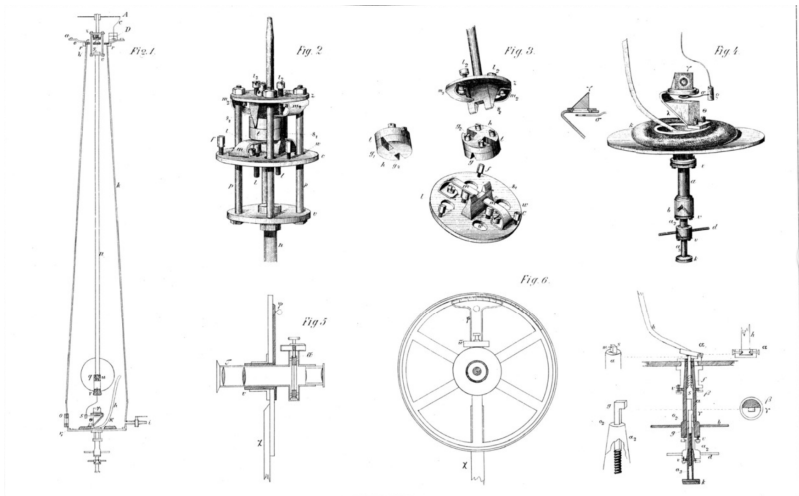
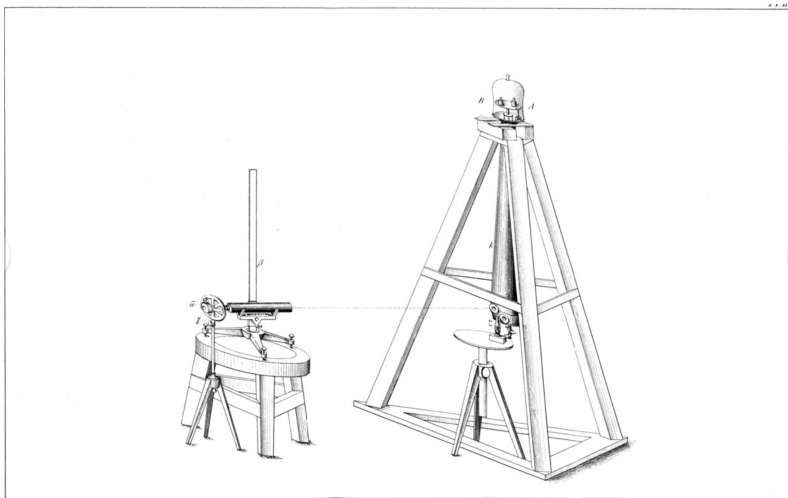


Figure C.5. Two drawings from Kamerlingh Onnes's thesis [106]

An interesting explanation of Kamerlingh Onnes's Foucault pendulum and its proper mathematical understanding can be found in [150].

- (2) When speaking about the Earth providing a rotating frame of reference, the sophisticated reader may well wonder what is the effect of the *centrifugal force*. For this we have to know that both the magnitude and the direction of the gravitational acceleration changes with the position on Earth. Both effects have to do with the shape of the Earth as a somewhat flattened sphere, which makes the distance to the Earth center increase nearer to the equator. This is why the centrifugal force increases when approaching the equator, which makes the effective gravitational acceleration g decrease: the same mass has a lesser weight close to the equator than at the poles.

Another (more minor) consequence of the shape of the Earth is that also the direction of the gravitational field is subject to change: it is deflected to the south on the northern hemisphere and to the north on the southern hemisphere.

- (3) One may well wonder what happens when more terms in the Taylor expansions are included. When expanding the kinetic and potential energy T and U in powers of ϱ we found (C.5) up to and including order 4. The next terms in the expansion are of order 6 which means that their effect is far smaller when $\varrho \downarrow 0$.

To fix thoughts, only think of what would happen for $\varrho = \frac{1}{2}$: indeed, in that case $\varrho^2 = \frac{1}{4}$, $\varrho^4 = \frac{1}{16}$ and $\varrho^6 = \frac{1}{64}$.

In fact introduction of order 6 (or higher order) terms in the expansion will only slightly alter the precession effect, but will not substantially change the qualitative picture as described above.

Appendix D

Chaos in periodically forced oscillators

In Section 2.4.2, when discussing non-linear modeling, we briefly encountered the term “chaotic”. In this appendix we would like to go deeper into the concept of *chaos* as a phenomenon in periodically forced nonlinear oscillators. This appendix largely takes the point of view of [45], as this also is included in [53].

In general, chaos can be characterized by a lack of predictability in the evolution of the system. When studying the long-term dynamics in phase space we often also meet fractal geometry, in particular in the form of Cantor sets [71, 137]. Below, we will go into more details about this.

For a better understanding of what is going on, we start with a small detour around the iteration of maps. Systems of differential equations describe dynamical systems with continuous time, whereas the iteration of maps concerns dynamical systems with discrete time. In the latter context, one may think for example at the size of a population as it changes at some fixed time interval, say per day or year. As we will see, in the time-periodic case, there is a natural way to pass from continuous to discrete time via the *stroboscopic map*, which will be a helpful tool to observe and clarify chaotic phenomena. A general reference to chaotic systems is [53] which also contains an extensive bibliography.

Chaotic dynamics turns out to occur in abundantly many branches of science. One iconic example is the onset of turbulence in fluid or gas flows, which was related to chaos by D. Ruelle (1935-) and F. Takens (1941-2010) in their mind-blowing paper *On the nature of turbulence* [148]. This paper coined the term “strange attractor”. Roughly speaking an attractor of a dynamical system is a set that “attracts” nearby evolutions. Examples are attracting equilibrium points, circles or tori (a torus is a mathematical doughnut). “Strange” attractors are more complicated than that. In the following we shall meet several examples. The overarching idea is that chaotic evolutions move erratically over strange attractors.

Since the 1970’s chaos theory has spread over almost all occurrences of nonlinear systems in physics, biology, economics, meteorology, etc., and we shall also meet forms of chaos in Appendix E.

D.1 The Hénon attractor

In this section we introduce the Hénon map and its attractor, see [92]. The mathematics here becomes partly *experimental*, in the sense that numerically obtained information will get a partially conjectural mathematical interpretation.

We introduce two maps that are iconic for the development of *chaos theory* from the 1960s on: the Logistic map and the Hénon map. These systems are given by low-degree polynomials, but the mathematics involved in their understanding is very tedious. For an accessible introduction to this matter we refer to Devaney [64].

D.1.1 Iterating a map

Given a map

$$F : M \rightarrow M$$

we consider the iterates

$$x_0, x_1, x_2, \dots \quad \text{where} \quad x_{n+1} = F(x_n)$$

for any $x_0 \in M$ and for all $n \in \mathbb{N}$. In the general setting, M is a topological space and F is a continuous map, see Engelking [71]. In many applications the topological space is just Euclidean space, a circle, or, more generally, a manifold. But M may also be a Cantor set.

Here $n \in \mathbb{N}$ or $n \in \mathbb{Z}$, depending on whether F is invertible or not, stands for the discrete time. A subset

$$\{x_0, x_1, x_2, \dots\} \subseteq M$$

is called an orbit of F . The interest is in the long-term behavior of orbits, in particular, on which subset of M they accumulate as $n \rightarrow \infty$.

The Logistic map. As a first example we briefly touch on the family of *Logistic* maps

$$\mathfrak{L}_\mu : \mathbb{R} \rightarrow \mathbb{R}, \quad x \mapsto \mu x(1 - x). \tag{D.1}$$

Iterates

$$x_0, x_1, x_2, \dots, \quad \text{with} \quad x_{n+1} = \mathfrak{L}_\mu(x_n),$$

are being used to model population dynamics, in particular of the fruit fly (*drosophila melanogaster*). This map is an endomorphism, i.e. non-invertible. Despite the innocent-looking form of \mathcal{L}_μ , books have been written on the properties and the dynamics of unimodal maps like (D.1). Here we will limit ourselves to a very basic and superficial discussion, and refer the reader to the references [53, 64, 162] for further details.

Remark 42. There exist two versions of the Logistic family: next to (D.1) we also have

$$x \mapsto 1 - ax^2.$$

The latter can be derived from the former by scaling x from $[0, 1]$ to $[-1, 1]$ and by reparametrizing

$$\mu \in [0, 4] \xleftarrow{a = \frac{1}{4}\mu(\mu-2)} a \in [0, 2]$$

In the present context, the basic question concerns the long-term dynamics of the logistic map. That is, for a fixed parameter value μ , what is the behaviour of x_n as $n \rightarrow \infty$?

A numerical experiment. To fix thoughts we perform the following numerical experiment. We take any initial point x_0 and plot the iterates x_{800}, \dots, x_{1000} for various values of the parameter μ between 0 and 4. Note that in this way we neglect an initial transient segment of iterates and so can get an idea where the iterates of $\mathcal{L}_\mu(x_0)$ settle down to, or, in other words, where they are *attracted* to.

In Figure D.1 you can see the result of this experiment. For values of μ between 0 and 3.0 we can see that the dynamics settles down in a stable equilibrium point. However at $\mu = 3.0$ it suddenly bifurcates (branches): the dynamics jumps between two different values, we have an orbit of period 2. When μ increases further such a period doubling happens more and more often, until at some value it seems that there is an infinity of periodic orbits. For even larger values of μ we get into a chaotic regime, where the dynamics becomes erratic, corresponding to the longer term unpredictability of the dynamics, which at the end of this appendix will be related to randomness. The chaotic regime is interspersed by windows where the behavior is periodic and

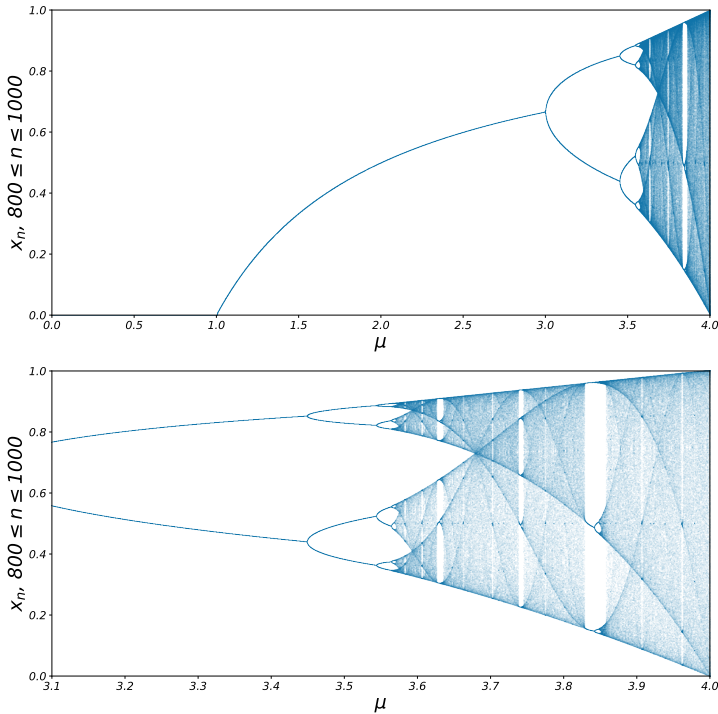


Figure D.1. Bifurcation diagram for the Logistic map or $\mu \in [0, 4]$ (top) and close to the chaotic region for $\mu \in [3.1, 4]$ (bottom).

hence predictable. The scenario and the diagram described here are attributed to Feigenbaum, see below for more details. It turns out to be amazingly difficult to give a solid mathematical explanation for all of this, compare with the above references.

The take-home message of this brief example is that plotting the evolution of discrete maps can tell us a lot about their dynamical properties. We will exploit this in the rest of this appendix to describe the nature of certain dynamical attractors.

The Hénon map. The *Hénon* family of planar maps, defined as

$$\mathfrak{H}_{a,b} : \mathbb{R}^2 \rightarrow \mathbb{R}^2, \quad (x, y) \mapsto (1 - ax^2 + y, bx),$$

is a diffeomorphism and the inverse map again is polynomial. Observe that for $b = 0$ the line $y = 0$ is invariant in the sense that

$$\mathfrak{H}_{a,0} : (x, 0) \mapsto (1 - ax^2, 0)$$

Remark 43. From Remark 42 we see that $\mathfrak{H}_{a,0}$ exactly corresponds to the second version of the Logistic family. Many mathematical results for the Hénon family are derived from what is known of the Logistic family by a perturbation analysis for small values of $|b|$.

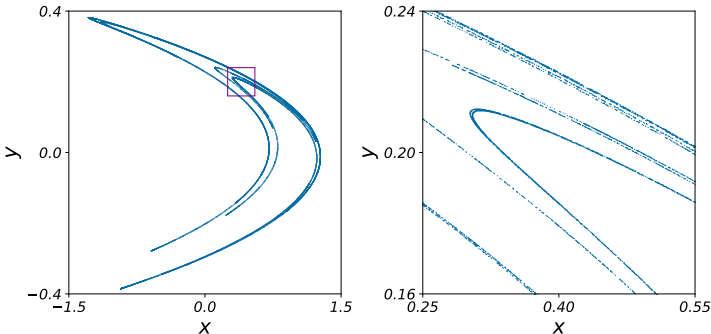


Figure D.2. The attractor of the Hénon map and a magnification by a factor of 10

In another numerical experiment we can observe that for the parameter values $a = 1.4$ and $b = 0.3$ all initial positions (x_0, y_0) have orbits

$$(x_0, y_0), (x_1, y_1), (x_2, y_2) \dots, \quad \text{with} \quad x_{n+1}, y_{n+1} = \mathfrak{H}_{a,b}(x_n, y_n),$$

that for $n \rightarrow \infty$ tend to the *Hénon attractor* $\mathcal{H} \subseteq \mathbb{R}^2$ as depicted in Figure D.2 (left), where we also showed a magnification (right). The set \mathcal{H} locally has a lot of self-similarity, as it roughly looks like a curve in one direction and a Cantor set in the other. For a definition of Cantor set, see below.

The attractor \mathcal{H} is invariant under the dynamics of $\mathfrak{H}_{1.4,0.3}$ and the iteration looks quite erratic, which again corresponds to the longer term unpredictability of the dynamics and hence to chaos. And in

fact the Hénon attractor usually is called a strange attractor. Again see below for a certain comparison with randomness.

A first topological digression. A brief topological digression is in order now. A *Cantor set* is a compact set that is both *perfect* and *totally disconnected*. Perfect means that there are no isolated points and totally disconnected that each point of the set has arbitrarily small neighborhoods with empty boundary. The great Dutch mathematician L.E.J. Brouwer has proved that such sets are all *homeomorphic*, that is, they can be continuously deformed into each other. For more background on this, see [71, 137]. One might say that Cantor sets are very small in the topological sense. In Appendix D we shall meet a Cantor set as a subset of \mathbb{R} , the complement of which is open and dense.

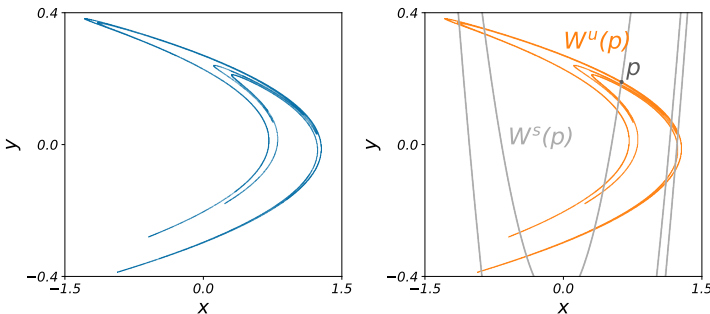


Figure D.3. Left: The Hénon attractor, compare Figure D.2. Right: pieces of the stable and unstable manifolds $W^s(p)$ and $W^u(p)$ of the saddle point $p = (.63, .19)$ of the Hénon map. See the text for an explanation. Note the strong resemblance between the attractor and $W^u(p)$.

Cantor sets have a fractal nature, in the sense that their dimension is non-integer, also compare with a discussion in Appendix E. Indeed, for the *box counting dimension* the numerical estimate reads $\dim_{BC} \mathfrak{H} = 1.2$, so \mathfrak{H} definitely is “thicker” than a curve. For general background on fractal sets see [74, 75].

D.1.2 The Benedicks-Carleson Ansatz

The Hénon map, i.e., with $a = 1.4$ and $b = 0.3$, has a fixed point $p = (.63, .19)$, that turns out to be a saddle point, see the plot in the right hand side of Figure D.3. Its linearization (derivative) $D_p \mathfrak{H}_{a,b}$ at p is a 2×2 -matrix with a positive and a negative eigenvalue. The stable and unstable manifolds of p are defined as

$$W^s(p) = \left\{ q \in \mathbb{R}^2 \mid H_{a,b}^j(q) \rightarrow p \quad \text{as } j \rightarrow \infty \right\},$$

$$W^u(p) = \left\{ q \in \mathbb{R}^2 \mid H_{a,b}^{-j}(q) \rightarrow p \quad \text{as } j \rightarrow \infty \right\}.$$

In other words $W^s(p)$ consists of all points q that converge to p as time $j \uparrow +\infty$, whereas for $W^u(p)$ this happens for $j \downarrow -\infty$. The Normally Hyperbolic Invariant Manifold Theorem [101, Theorem 4.1] implies that both $W^s(p)$ and $W^u(p)$ are smooth curves passing through p and at p are tangent to the corresponding eigenspaces of $D_p \mathfrak{H}_{a,b}$. In Figure D.3 (right) we depicted both $W^s(p)$ and $W^u(p)$ for some length and observe a striking similarity between \mathcal{H} and $W^u(p)$.

However, since curves have dimension 1 and $\dim_{BC} \mathfrak{H} = 1.2$, they cannot be equal. The difference between the curve $W^u(p)$ and \mathcal{H} is formed by all the *accumulation points* of $W^u(p)$, so we have to look at the *closure* $\overline{W^u(p)}$ of the unstable manifold $W^u(p)$. Again compare with [4, 71]. And indeed, the general folklore says the following:

Theorem 4 (Benedicks-Carleson Ansatz). $\mathcal{H} = \overline{W^u(p)}$.

This has been a long-standing conjecture that was proven by Benedicks and Carleson [22] for a subset of the (a, b) -parameter plane of positive Lebesgue measure, close to the a -axis. The proof is a complicated perturbation analysis for small values of $|b|$, entirely in the spirit of Remark 43. However, the point $(a, b) = (1.4, 0.3)$ does not belong to this subset ...

In the next section, computer simulations show that the Ansatz of Theorem 4 reaches farther than the Hénon map. Many strange attractors of two-dimensional diffeomorphisms are of the type described above, reason why they are commonly called *Hénon-like strange attractors*. Once we turn to periodically forced nonlinear oscillators we

will find many more examples of such strange attractors. This computer assisted way of reasoning belongs to the area of *experimental mathematics*. But first, we have to establish a useful connection between time-dependent differential equations and maps.

D.2 The stroboscopic map

In Chapter 2 we met oscillatory systems of the general (smooth) form

$$\ddot{x} = f(x, \dot{x}, t), \quad (\text{D.2})$$

for instance both forced and with or without friction and where the time dependence is periodic, e.g., see equations (2.7), (2.11), or (2.12). The latter means that

$$f(x, y, t + T) \equiv f(x, y, t),$$

for a given period $T > 0$.

D.2.1 Determinism again

In Section 1.3 we turned a second order differential equation in x into a system of two first-order differential equations in (x, y) by adding the term

$$y = \dot{x}.$$

We called the (x, y) -plane, phase plane. This is the plane in which the system became deterministic: given any initial point (x_0, y_0) the entire future evolution of the system is completely determined.

However, the case of (D.2) is time-dependent and to obtain again a deterministic system we need to introduce one more variable that represents the time t . This leads to a new autonomous system

$$\begin{aligned} \dot{x} &= y & (\text{D.3}) \\ \dot{y} &= f(x, y, z) \\ \dot{z} &= 1. \end{aligned}$$

As an example consider the *swing*, where

$$f(x, \dot{x}, t) = -c\dot{x} - (a + \varepsilon \cos t) \sin x$$

and, thus, with an equation of motion

$$\ddot{x} + (a + \varepsilon f(t)) \sin x = 0 \quad \text{with} \quad f(t + 2\pi) \equiv f(t). \quad (\text{D.4})$$

This leads to the following special case of (D.3)

$$\dot{x} = y \quad (\text{D.5})$$

$$\dot{y} = -cy - (a + \varepsilon \cos z) \sin x$$

$$\dot{z} = 1.$$

With this, we have obtained determinism in the three-dimensional phase space with coordinates x, y, z : since the system of differential equations is of first order and autonomous, for any initial point (x_0, y_0, z_0) the entire future evolution is completely determined.

In the former case of Section 1.3, when dealing with an autonomous planar system, a planar phase portrait gives a quite clear idea of the dynamics. But in the present three-dimensional autonomous case, the three-dimensional phase space is filled by a collection of integral curves forming a kind of spaghetti tangle that in general does not offer too much transparency.

D.2.2 The stroboscopic phase portrait

Fortunately, the time-periodicity helps us to obtain another quite informative two-dimensional picture by constructing a planar map. This is the so-called *stroboscopic map*, that takes a snapshot of the (x, y) -plane at instants $z = 0, T, 2T, \dots$, recalling that $z = t$, see Figure D.4.

Consider the integral curve starting at the point $(x, y, 0)$ and follow this till it hits the vertical plane $z = T$. The intersection point is called $(P(x, y), T)$. This defines a map

$$P : \mathbb{R}^2 \rightarrow \mathbb{R}^2.$$

We list a few properties of the map P , without proof, that follow from the Existence and Uniqueness Theorem for solutions of ordinary differential equations [100].

Proposition 6. (1) *The map P is a diffeomorphism;*

(2) *Extending the integral curve from $(x, y, 0)$ to $(P(x, y), T)$ to the section $z = 2T$ gives the point $(P^2(x, y), 2T)$.*

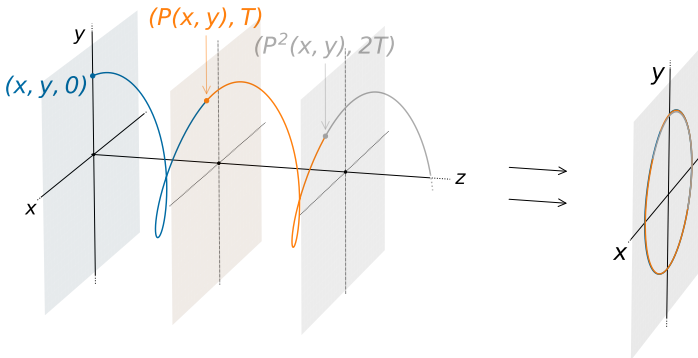


Figure D.4. A solution of (D.5) in the (x, y, z) space with snapshots taken at time instants $t = 0, T, 2T$

The former of these two properties can be easily seen by considering the evolution in negative time, thereby constructing the inverse P^{-1} . The latter property holds for all sections $z = nT$ ($n \in \mathbb{Z}$) and the corresponding iterates P^n of the map P . This means that by plotting orbits

$$\dots, (x_{-1}, y_{-1}), (x_0, y_0), (x_1, y_1), (x_2, y_2), \dots \quad \text{with} \\ (x_{n+1}, y_{n+1}) = P(x_n, y_n)$$

in the (x, y) -plane, we can get a good idea of the dynamics of the system corresponding to (D.2). We here speak of a *stroboscopic phase portrait*.

A fixed point of P corresponds to a periodic solution of the system of differential equations. Similarly for a periodic orbit of P . Note that in the example of the swing (D.5) the origin $(x, y) = (0, 0)$ always is a fixed point.

Other sets that are invariant under iteration of P are also of interest. Another numerical experiment performed on the damped swing system (D.5), i.e., with $c > 0$, leads to Figure D.5 (left), which surely looks like a strange attractor!

Remark 44. The stroboscopic map in the present context also is called *return map*. This can be explained as follows. Since the system (D.5)

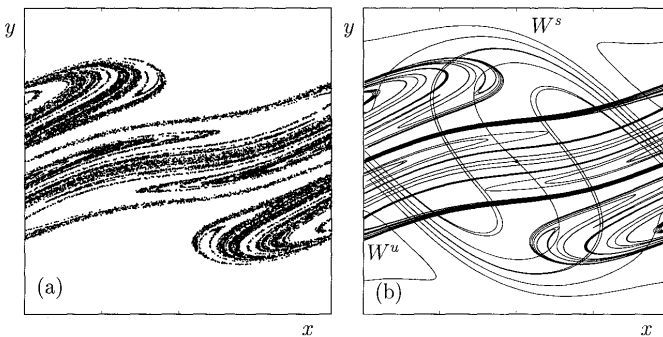


Figure D.5. Strange attractor for a damped driven swing (left) and the stable and unstable manifolds of the saddle point $(0, 0)$ (right) [45, p. 48].

is periodic in the z -direction, we can identify all the sections $z = nT$ ($n \in \mathbb{Z}$) with each other. So we can change the geometry of the phase space from \mathbb{R}^3 to $\mathbb{R}^2 \times \mathbb{S}^1$, where \mathbb{S}^1 denotes the unit circle. For any $p \in \mathbb{S}^1$, the stroboscopic map then becomes a map from a section $\mathbb{R}^2 \times \{p\} \subseteq \mathbb{R}^2 \times \mathbb{S}^1$ to itself, so indeed, as a return map. Fortunately, return maps are very suitable for iteration.

In the setting of periodically forced oscillators, given the flow of the equations of motion, we can construct the stroboscopic map using the time periodicity to find the right point on the trajectory. Outside the world of time periodicity it is possible to define a slightly more general concept, where the sampling is instead dictated by space: in this case we use a subset Σ of the space that is transversal to the flow, and then sample the trajectory at the point where it intersects with Σ . The corresponding map is called *Poincaré map* and is a useful tool to study stability and regularity of dynamical systems. In this more general case, however, obtaining the return points can be harder than in the time periodic case.

D.2.3 Hénon-like strange attractors

Indeed, the attractor in the left hand side of Figure D.5 locally shows a great similarity with the Hénon attractor \mathcal{H} : in one direction we distinguish a curve and, transverse to this, some kind of Cantor set.

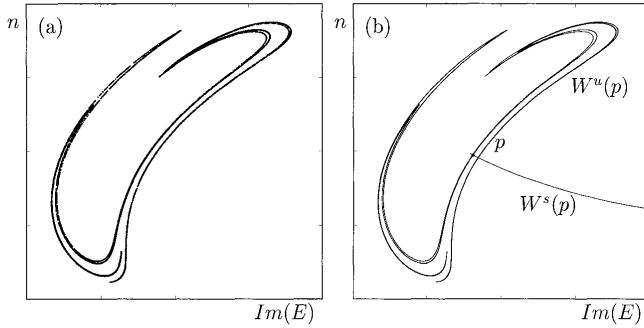


Figure D.6. Strange attractor appearing in the equation modeling an optically injected semiconductor laser (left) and the stable and unstable manifolds of the saddle point (right) [45, p. 50].

Moreover, the origin $(x, y) = (0, 0)$ is a saddle point and, when plotting the stable and unstable manifolds, see the right hand side of Figure D.5, we observe the same phenomenon as before: namely the attractor strongly resembles the unstable manifold and again we are tempted to see the Benedicks-Carleson Ansatz confirmed.

Another example occurs in the context of an optically injected semiconductor laser [45, 175], where the same Ansatz seems to apply, see Figure D.6.

In these and many other examples we find *Hénon-like strange attractors* in the context of periodically forced oscillators with damping, so where the Benedicks-Carleson Ansatz (Theorem 4) seems to work very well.

D.3 Scholium

Please notice the careful formulations used here. According to Wikipedia an Ansatz is nothing but

an educated guess or an additional assumption made to help solve a problem, and which may later be verified to be part of the solution by its results.

And, indeed, the statements are still far from being a mathematical theorem, compare our remarks at the end of Section D.1.2 on the validity of the result in Benedicks-Carleson [22].

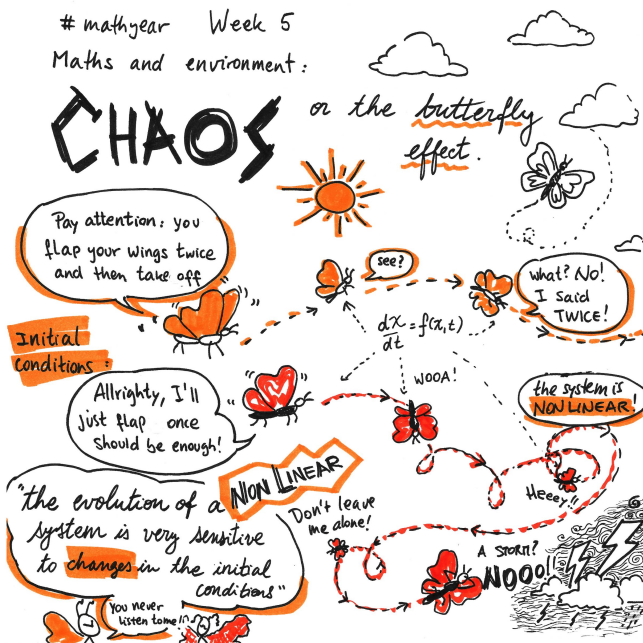


Figure D.7. Chaos and the butterfly effect, courtesy of Constanza Rojas-Molina. If you feel creative, consider contributing to the #mathyear challenge.

The understanding of chaotic dynamics is an ongoing and difficult research program; the difficulty shows already from the fact that such simple models have such complicated dynamics. Interestingly the impetus behind the idea of chaos came largely from outside mathematics. We list a few pioneers. The physicist M.J. Feigenbaum (1944-2019) [76], who performed computer experiments on the Logistic family of maps to obtain the diagram of Figure D.1 and, related to this, quite a number of interesting conjectures that had a large mathematical follow-up. The biologist R.M. May (1936-2020) [121, 122].

who studied the fruit fly *drosophila melanogaster* in terms of one-dimensional maps related to the Logistic family. The astronomer M. Hénon (1931-2013) [92], who developed the attractor named after him. Another propagator of these ideas is the mathematical physicist Sir Michael Berry (1941-) [25], among other things interested in semi-classical physics, in particular in quantum chaos. For more historical remarks also compare [53].

D.3.1 Towards an understanding of chaos

The chaotic iterates on the strange attractors we met so far are erratic, which is related to the long-term unpredictability of the motion. We now shall relate this unpredictability in a certain way to randomness.

D.3.1.1 Ergodicity

This kind of thinking can be formalized in applications of probability theory on dynamical systems; the ensuing theory is called *ergodic theory*. Note that here we returned to the general setting of Section D.1.1. The main aim is the study of the long-term behavior of orbits of maps or flows. Here, for simplicity, we shall restrict ourselves to a map $F : M \rightarrow M$. Moreover, we assume that

- (1) the space M satisfies some general assumptions that we shall not detail here, but that hold for all the spaces occurring in general dynamical systems theory;
- (2) we can define a probability measure μ on M , that is, roughly speaking, a mapping from “reasonable” subsets $A \subseteq M \mapsto \mu(A) \in [0, 1]$. Here we call “reasonable” any subset for which $\mu(A)$ is defined;
- (3) the measure μ is invariant under the map $F : M \rightarrow M$, in the following sense: for any “reasonable” set $A \subseteq M$, it holds that $\mu(F^{-1}(A)) = \mu(A)$.

It is common to use the following measure in this context [53, Section 6.5]. For $x \in M$ let $x, F(x), F^2(x), \dots$ be the orbit generated from x , then for any “reasonable” subset $A \subseteq M$ we define

$$\mu(A) = \lim_{n \rightarrow \infty} \frac{\#\{j \mid 0 \leq j \leq n \text{ and } F^j(x) \in A\}}{n}, \quad (\text{D.6})$$

where $\#$ denotes the cardinality. The measure μ assigns to A the average fraction of points of the orbit $\{F^j(x)\}_{j=0}^\infty$ that are in A . If this measure is well-defined it is called the *measure of relative frequencies* of the sequence $\{F^j(x)\}_{j=0}^\infty$. Often we speak loosely of *physical measure*. From the definition (D.6) it directly follows that μ is F -invariant. The attractor then is the support of the measure μ .

Remark 45. In many cases the periodic points of F densely fill this attractor. When this happens, the support of the measure is just a finite set. Yet for almost all values of x we obtain the same (strange) attractor.

An important property is that the measure μ is *ergodic* in the sense that for any continuous function $\psi : M \rightarrow \mathbb{R}$,

$$\lim_{n \rightarrow \infty} \frac{1}{n} \sum_{j=0}^{n-1} \psi(F^j(x)) = \int_M \psi d\mu,$$

which roughly means that the orbit $\{F^j(x)\}_{j=0}^\infty$ is well-spread over the attractor.

And indeed, a widely used definition that the orbit $\{F^j(x)\}_{j=0}^\infty$ is chaotic just boils down to this ergodicity. When the μ -measure of the underlying attractor is finite, we can scale μ to a probability measure, and one may well be tempted to see each iterate $F^j(x)$, $j \in \mathbb{N}$ as a sample from this. Of course the successive samples cannot be stochastically independent, however, for generic values of x the iterates $F^j(x)$, $j = 0, 1, \dots, N$ become more independent for larger N . There is a lot of mathematics hidden in here, and often we don't get much further than numerically supported conjectures. For classical references see Arnold & Avez [10], Eckmann and Ruelle [67], Mañé [119] or Viana and Oliveira [171].

One question is how to express the amount of chaoticity of a given orbit. Quite a few indicators and quantifications of this have been developed and reported in the literature. In terms of ergodic theory, it is common to use various forms of *entropy*. Other related indicators are the *dispersion exponent* [53, Chapter 2], and the *Lyapunov exponents* [139], where the latter compares a given orbit with nearby ones.

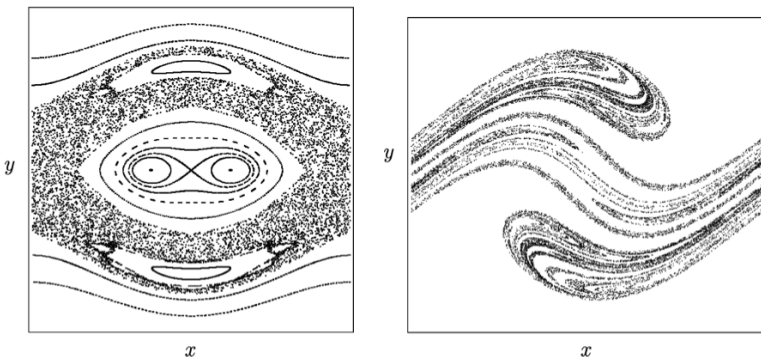


Figure D.8. Stroboscopic phase portraits of the swing without damping, i.e., with $c = 0$ (left), and with positive damping $c > 0$ (right) [53, p. vi]; compare with Figure D.5.

Remark 46. (1) We like to mention that from the *Takens Reconstruction Theory* [53, Section 6.4], [167, Section 4] it follows that there remains a clear difference between a chaotic deterministic signal and a purely random signal.

(2) To explore some of the many ramifications of the theory, the interested reader may also consult Einsiedler and Ward [68], that winks towards old and new connections with number theory.

D.3.2 Chaotic dynamics without damping

All of this works more or less for the strange attractors found in the dissipative situations, i.e., with damping.

Let us briefly discuss the case without damping, the conservative case. By Liouville Theorem [5, Section 15] the stroboscopic map P is always area-preserving. In other words, the Lebesgue measure is invariant under P . In terms of the above the Lebesgue measure in this case also is the physical measure. To fix thoughts, in Figure D.8 (left) the stroboscopic phase portrait is being shown of the system (D.5) with damping $c = 0$. In this portrait we detect

- (1) A couple of periodic points. For instance, the “pupils of the eyes” correspond to a period 2 orbit.
- (2) A couple of invariant closed curves.
- (3) A few clouds of points, where each cloud consists of one single orbit.

We shall return to the invariant closed curves in Appendix E, but the present interest is in a cloud, which replaces the strange attractor in the dissipative case. Indeed, the motion inside the cloud seems to be just as erratic as in the attractors. The question then is what ergodic theory has to say here.

The long-standing Arnold conjecture reported in [10], claims that the cloud(s) depicted in Figure D.8 (left) densely fill a set of positive Lebesgue measure where this measure is ergodic for the stroboscopic map P . As far as the authors know this conjecture has only been confirmed in a few exceptional cases, compare Bäcker [19], or Chernov and Markarian [58] which focuses on the theory of chaotic billiards. For more or less generic cases as studied in the present book, the Arnold conjecture still stands ... Mutatis mutandis, the considerations of the previous subsection also apply here.

Remark 47. In the present context billiards are played with only one ball that moves in straight lines on a table and bounces “at equal angles” at the boundary. The entire motion is assumed frictionless, so it can go on forever.

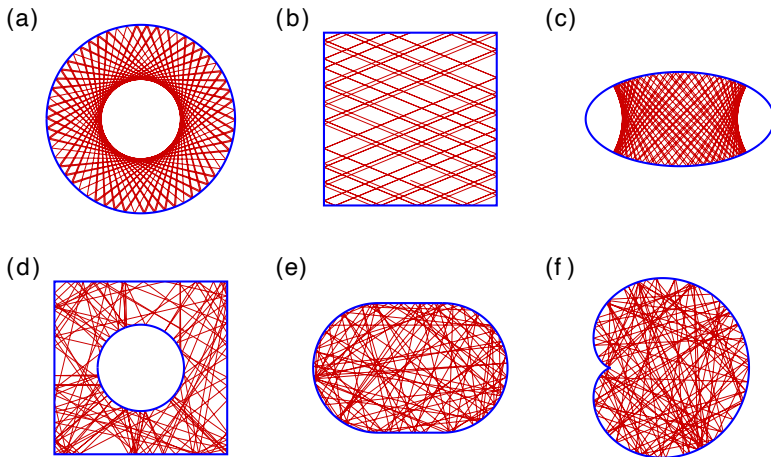


Figure D.9. We show 100 successive reflections of one orbit on different billiards. Note the contrast between the regular dynamics in the (a) circle, (b) square and (c) ellipse billiard and the chaotic dynamics for the (d) Sinai billiard, (e) stadium billiard and (f) cardioid billiard. Figure from [19]

Appendix E

More on resonance

We already encountered the phenomenon of resonance in periodically forced oscillators in Chapter 2, in particular in the Sections 2.3.2, 2.4 and 2.4.1. We will now study the somewhat more general setting of systems depending on parameters. The resonance phenomenon then appears as the interaction of oscillating subsystems, where the frequencies have a rational relation and where a motion occurs that is compatible with this relation. One of the leading examples concerns Huygens' weakly coupled clocks that are (almost) identical. This is a $1 : 1$ resonance and the compatible motion is that both clocks tend to synchronize [102]. Forced oscillators will also come up again for discussion.

One of our interests is the organization of the parameter space in relation to resonances: in the examples this will give rise to so-called resonance *tongues*. For parameter values inside the tongues the actual resonance occurs, but in between the tongues several things may happen that are interesting from both the topological and measure theoretical points of view, see Oxtoby [137]. In fact, we shall encounter here *fractal sets* in the sense of Mandelbrot, see Section E.3.4. In the ensuing nonlinear dynamics we again meet with the phenomenon called *quasi-* or *multiperiodicity* as already illustrated in Example 1 of Section 2.4.2. Chaos may also emerge, as we already saw in Section 2.4.2 and in Appendix D.

The appendix concludes with a discussion on celestial resonances, in particular on orbital and spin-orbit resonances.

Some phenomenology. In Section 2.3.2 we discussed a few occurrences of $1:1$ -resonances, like the exact tuning of the radio frequency on the incoming signal. Another example is the resonance in the earth-moon system, where the rotation of the moon about its axis occurs with the same period as its revolution around the earth: reason why on earth we always see the same face of the moon. This is a so-called spin-orbit resonance and it can be explained by the tidal force the earth exerts on the moon. For more details see below.

An example of a $1 : 2$ -resonance is the motion of the Botafumeiro in the cathedral of Santiago de Compostela. This is a large incense container suspended on a long rope mounted over a pulley high up in the cathedral and that is kept swinging by a couple of men pulling the



Figure E.1. Botafumeiro in Santiago de Compostela

rope to and from over the pulley. The Botafumeiro is pulled up each time that it is near its lowest point, which means that the pulling frequency is twice as high as that of the pendulum: the system is in a $1 : 2$ -resonance. Another example of the $1 : 2$ -resonance, already mentioned in Section 2.4.1, is the rolling and even capsizing of ships that go astern on an increasing wind.

Indeed, the lower equilibrium solution then has become unstable, as also shown in Figure 2.16. The strong effect of this is related to the occurrence of resonance peaks as depicted in Figure 2.15.

On the other hand in Section 2.5.4 we met an example where the inverted pendulum is stabilized by oscillating the point of suspension. For a more mathematical treatment we refer to Arnold [5, Section 25E]. We like to note that Arnold claims that circus artists use this stabilizing effect for balancing acts.

For the inverted pendulum we need to consider the upside down equilibrium which is usually unstable, but that can become stable by the $1:2$ -resonance. In fact we then meet parametric resonance again. For background on the interesting dynamical phenomenology we refer to [26, 39, 47]. The stabilization of the inverted pendulum was first described by A. Stephenson in 1908. However, it was only in 1951 that its behaviour was properly explained by the Nobel laureate Pyotr

Kapitza [105]. That is also why the inverted pendulum is often called Kapitza's pendulum.

On methodology. The mathematical program for understanding phenomena like the above is to provide models in terms of dynamical systems depending on parameters and to study the emerging dynamics. The dynamics, as we mentioned, can vary from periodic to quasi- or multiperiodic and even chaotic. Varying the parameters, the type of dynamics can change, giving rise to bifurcations (or phase transitions) between those various types of dynamics. Apart from the examples mentioned above, the theories presented in this appendix are being applied widely in the sciences, in contexts varying from climate change to biological systems.

E.1 Huygens' clocks

Our leading example concerns the following experiment described by Huygens [102], see Figure E.2. A beam is mounted not too rigidly on two chairs and two almost identical pendulum clocks are suspended on the beam. Huygens observed that the clocks tend to synchronize and the two pendulums tend to swing in anti-phase. Following [34], we are going to give a mathematical description that explains this as a form of averaged synchronization.

E.2 Arnold resonance tongues and fractal geometry

In Huygens' experiment, each pendulum consists of a point mass that moves on a circle. Since we have two pendulums we are dealing with two circles, say with angles (φ, ψ) , which together parametrize a two-dimensional torus: the product of the two circles.

So the dynamics consists of integral curves on this torus, see Figure E.3. Let us assume that a Poincaré map is defined from some “vertical” circle of the form $\psi = \text{constant}$ to itself. In terms of Appendix D we may well speak of a return map. Such a map may well

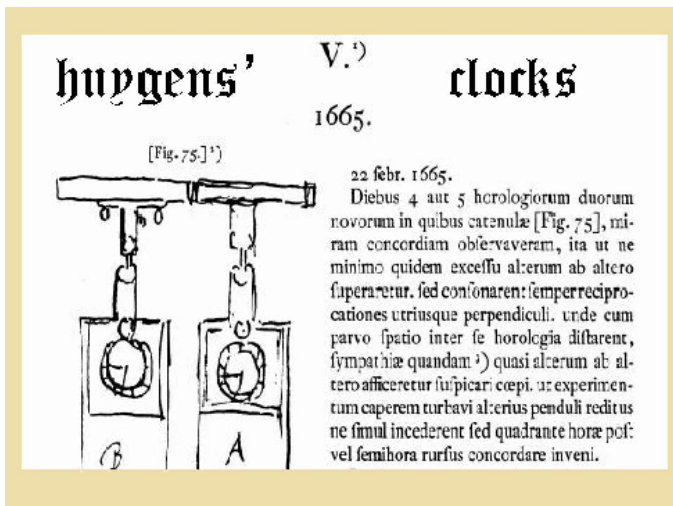


Figure E.2. Huygens' weakly coupled pendulum clocks [102]

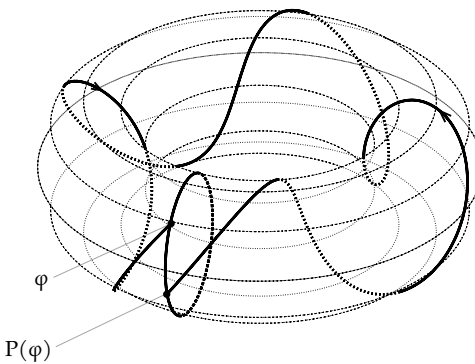


Figure E.3. Poincaré map maps the circle to itself [53]

take the following form,

$$P : \mathbb{S}^1 \rightarrow \mathbb{S}^1 \quad (\text{E.1})$$

$$\varphi \mapsto \varphi + 2\pi\alpha + \varepsilon f(\varphi),$$

and its iterations, as in Appendix D, would give us a good idea of the long-term dynamics. In general, we speak of resonance whenever this dynamics is periodic. Our investigation of Huygens' clocks has led us to the theory of circle maps. We now first need some properties of such maps.

Note that meanwhile, we have abandoned the context of Huygens' clocks; the study of dynamical systems consisting of iterations of maps like (E.1) has a far wider interest. For details see [6, 53, 64]. We shall come back to Huygens at the end of this section.

E.3 A theoretical digression into circle maps

An important tool is the *rotation number* as introduced by Poincaré. Part of the content of this section is also due to the work of Arnaud Denjoy in the 1930s and Andrej Kolmogorov two decades later in the 1950s.

E.3.1 Denjoy Theory

A tutorial introduction to Denjoy Theory can be found in Devaney [64, Ch. 1.14].

Let us start with an orientation preserving homeomorphism

$$F : \mathbb{S}^1 \rightarrow \mathbb{S}^1$$

and consider a lift

$$\tilde{F} : \mathbb{R} \rightarrow \mathbb{R}$$

defined by the property

$$\Pi \circ \tilde{F} = F \circ \Pi$$

where $\Pi : \mathbb{R} \rightarrow \mathbb{S}^1$ is the projection

$$x \in \mathbb{R} \mapsto \varphi = e^{2\pi i x} \in \mathbb{S}^1 \subseteq \mathbb{C},$$

Here we consider $\mathbb{S}^1 \cong \mathbb{R}/2\pi\mathbb{Z}$, which we identify to a subset of the complex plane \mathbb{C} whenever convenient. Note that the lift is not unique, but only defined modulo $2\pi\mathbb{Z}$.

We define the *rotation number* of F by

$$\varrho(F) = \frac{1}{2\pi} \lim_{n \rightarrow \infty} \frac{\tilde{F}^n(x)}{n},$$

which can be shown to be independent of the point x [64]. Moreover, since the lift \tilde{F} is not unique, we take the rotation number modulo \mathbb{Z} . The rotation number measures the average rotation of F . It turns out that the important distinction is whether or not the value of ϱ is rational. We now list some properties of this quantity.

Proposition 7. (1) *Let F and G be orientation preserving circle homeomorphisms, i.e., continuous maps with continuous inverses, and assume that they are topologically conjugate, i.e., there exists an homeomorphism $H : \mathbb{S}^1 \rightarrow \mathbb{S}^1$ such that*

$$G \circ H = H \circ F. \quad (\text{E.2})$$

Then $\varrho(F) = \varrho(G)$.

- (2) *$\varrho(F) \in \mathbb{Q}$ if and only if F has a periodic orbit.*
- (3) *Assuming that the map F is sufficiently smooth (say of class C^2), then the fact that $\varrho(F)$ is irrational implies that F is topologically conjugate to a rigid rotation.*

We give some comments on Proposition 7. Equation (E.2) means that the following diagram commutes.

$$\begin{array}{ccc} \mathbb{S}^1 & \xrightarrow{F} & \mathbb{S}^1 \\ H \downarrow & & \downarrow H \\ \mathbb{S}^1 & \xrightarrow{G} & \mathbb{S}^1 \end{array}$$

Loosely speaking it means that up to the continuous transformation H (say, a change of variables) the maps F and G are the same. A transformation like H is often referred to as a *conjugacy*.

The first statement then says that if such a conjugacy exists, then the rotation numbers of F and G are equal. In other words, the rotation number is a topological invariant. The second statement, together with the first, implies that the periodic orbits of F are in correspondence with the given rotation number. The third item is known as the *Denjoy Theorem* [133]. It says that for sufficiently smooth F there is a *topological conjugacy* with the rigid rotation

$$\mathfrak{R}_{2\pi\varrho(F)} : \varphi \mapsto \varphi + 2\pi\varrho(F).$$

Recall from the first statement of the proposition that two circle-maps are topologically conjugate if there exists a homeomorphism that transforms one into the other.

By the way, in general

$$\varrho(\mathfrak{R}_{2\pi\alpha}) = \alpha .$$

Moreover, the fact that $\alpha \notin \mathbb{Q}$ implies that every single orbit of $\mathfrak{R}_{2\pi\alpha}$ densely fills the circle, see [53, Lemma 2.4]. The latter property is preserved by the topological conjugacy.

The dynamics of such an irrational rotation often is referred to as *quasiperiodic* or *multiperiodic*. When returning to the context of dynamics on the 2-torus this means that in average rotations in the φ and ψ direction are no rational multiples of each other, or more compactly, not rationally related.

Remark 48. In the Denjoy Theorem (Proposition 7, third item) regularity is essential in the following sense. There exists a C^1 -diffeomorphism of the circle with an irrational rotation number, that is *not* conjugate to a rigid rotation [64, Chapter 1.14]. For further details also see [133]. This map is called the *Denjoy counterexample*; all of this contributed to motivating the follow-up mentioned before and that is in part presented in the upcoming sections.

We continue sketching some further background theory.

E.3.2 Kolmogorov-Arnold-Moser (KAM)

Kolmogorov extended the Denjoy Theory greatly into what today is known as Kolmogorov-Arnold-Moser Theory. The combination of these theories forms a cornerstone of the discipline of dynamical systems. The heritage of Denjoy and Kolmogorov has a vast follow-up that runs till the present day and that includes many applications in mathematical physics and celestial mechanics. In the present context, we only lightly touch on this rich material, for general background referring to [12, 33, 43, 44, 49, 96, 165, 179]. More or less tutorial introductions to KAM Theory can be found in [53, Chapters 2 and 5], also see [44, Chapter 6], [108, Chapter 15.4], [113] and [141].

KAM Theory. Consider irrational numbers that are badly approximated by rational numbers in the sense that *Diophantine conditions*

$$\left| \alpha - \frac{p}{q} \right| \geq \frac{\gamma}{q^\tau} \quad (\text{E.3})$$

hold for given constants $\gamma > 0, \tau > 2$ and for all rationals p/q .

We name this set $\mathfrak{D}_{\tau,\gamma}$. As a closed set, by the Cantor-Bendixson Theorem [90], this is the union of a perfect and a discrete set. Since the rational numbers are in its complement, $\mathfrak{D}_{\tau,\gamma}$ is totally disconnected and hence the perfect set is a Cantor set. As we saw in our first topological digression of Section D.1.1, the definition of a Cantor set is a purely topological matter. However, measure theoretically we have the following.

Proposition 8. *The intersection $\mathfrak{D}_{\tau,\gamma}$ with any closed interval has positive measure that tends to full measure as $\gamma \downarrow 0$.*

Proof. For simplicity consider the closed interval $[0, 1]$. We shall prove that the measure of the complement $[0, 1] \setminus \mathfrak{D}_{\tau,\gamma}$ tends to zero as $\gamma \downarrow 0$.

Indeed, for a fixed integer q consider the rational numbers $\frac{p}{q} \in [0, 1]$ for $p = 0, 1, \dots, q-1$. The Diophantine condition requires us to delete the open interval

$$\left(\frac{p}{q} - \gamma q^{-\tau}, \frac{p}{q} + \gamma q^{-\tau} \right)$$

from $[0, 1]$. Each of these intervals has length $2\gamma q^{-\tau}$. Since there are q values of p , the measure (length) of the union of deleted intervals is less than or equal to $2\gamma q^{-\tau+1}$. Taking the sum over all integers $q \leq 1$ then gives

$$\text{measure}([0, 1] \setminus \mathfrak{D}_{\tau,\gamma}) \leq 2\gamma \sum_{q \leq 1} q^{-\tau+1} = \mathcal{O}(\gamma)$$

as $\gamma \downarrow 0$, where we use that $\tau > 2$.

Compare [53, Section 5.2.2], for more background we refer to [71, 137]. \square

In the case that $\alpha \in \mathfrak{D}_{\tau,\gamma}$, the conjugacy with the rigid rotation $\mathfrak{R}_{2\pi\alpha}$ is smooth! This result is typical for the *Kolmogorov-Arnold-Moser Theory* [53, Chapters 2 and 5].

Remark 49. (1) KAM Theory deals with the so-called problem of *small denominators*, when looking for the conjugation H of Proposition 7 in terms of Fourier series. Small denominators are central in dynamical systems, also in higher dimensions. Applications can be found, among many other areas, in celestial mechanics and, more generally, in mathematical physics, see the above references. We will discuss some of these in the rest of this Appendix.

- (2) In the related context of linearizing quadratic polynomials on \mathbb{C} with linear part $e^{2\pi i\alpha}$, Jean-Christophe Yoccoz (1957-2016) was awarded a *Fields medal* in 1994. He proved that the so-called Bruno condition on α is necessary and sufficient for linearization. The Bruno condition is an extension of (E.3) in terms of continued fractions [178, 180].

The Fields Medal is the analog of the Nobel Prize for mathematics and Yoccoz was the first Fields medalist in the field of dynamical systems.

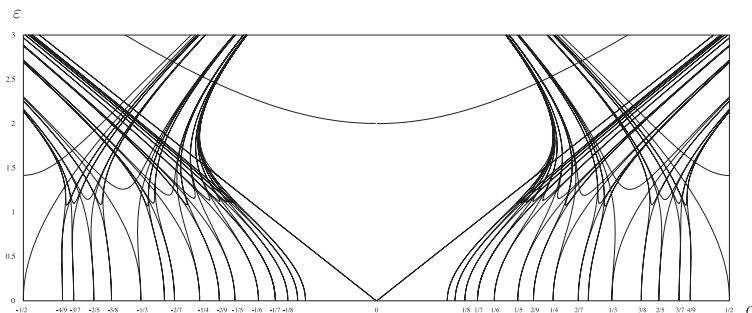


Figure E.4. Arnold resonance tongues in the (α, ε) -plane [34]

E.3.3 The Arnold family of circle maps

The simplest non-trivial case of a parametrized circle map is the following:

$$\begin{aligned} \mathfrak{A}_{\alpha,\varepsilon} : \mathbb{S}^1 &\rightarrow \mathbb{S}^1 \\ \varphi &\mapsto \varphi + 2\pi\alpha + \varepsilon \sin \varphi, \end{aligned} \tag{E.4}$$

the so-called *Arnold family* of circle maps [5]. This example already contains many interesting properties that can help to understand Huygens' experiment somewhat better.

Without a detailed proof we present Figure E.4, that contains an array of resonance tongues, the *Arnold (resonance) tongues*, that forms a catalogue of the dynamics of the family $\mathfrak{A}_{\alpha,\varepsilon}$ in the (α, ε) -plane. In fact from each point $(\alpha, \varepsilon) = (p/q, 0)$ a resonance tongue emanates in which for the rotation number $\varrho(\mathfrak{A}_{\alpha,\varepsilon})$ we have

$$\varrho(\mathfrak{A}_{\alpha,\varepsilon}) \equiv \frac{p}{q}$$

and for parameter values inside there are periodic orbits of exactly that rotation type, in other words in $p : q$ -resonance. In particular, within the $1 : 1$ *main* tongue emanating from $(\alpha, \varepsilon) = (0, 0)$ there are fixed points.

Such arrays of tongues occur frequently in science. For an example in chronobiology we refer to [21].

On computing the tongues. To fix thoughts we compute the main tongue of the Arnold family $\mathfrak{A}_{\alpha,\varepsilon}$. So we are looking for fixed points

$$\mathfrak{A}_{\alpha,\varepsilon}(\varphi) = \varphi,$$

i.e.,

$$\varphi + 2\pi\alpha + \varepsilon \sin \varphi = \varphi,$$

which leads to

$$\sin \varphi = -\frac{2\pi\alpha}{\varepsilon}.$$

This equation has solutions in φ for all parameter values

$$2\pi|\alpha| \leq \varepsilon,$$

which exactly determines the main tongue. On the circle you can find two fixed points, one attracting and one repelling, that annihilate each

other at the boundaries $2\pi\alpha = \varepsilon$ in a saddle-node bifurcation [64, Chapter 1.12]. Note that the main tongue has boundaries that meet with a nonzero angle at the tip $(\alpha, \varepsilon) = (0, 0)$.

The higher-order tongues have been computed numerically, but much is known of the asymptotics at the tongue tips $(\alpha, \varepsilon) = (p/q, 0)$. The tongue boundaries here are tangent of order $O(|q|)$, see [51] for more details.

The global picture. Another property of the rotation number is that it is a continuous function of the parameters (α, ε) . Thus, since $\varrho(\mathfrak{A}_{\alpha,0}) = \alpha$, for sufficiently small ε_0 fixed, the rotation number $\varrho(\mathfrak{A}_{\alpha,\varepsilon_0})$ is continuous and non-decreasing as a function of α . Moreover, it is constant for any rational value. The graph of this function, depicted in Figure E.5, is referred to as a *Devil's staircase*.

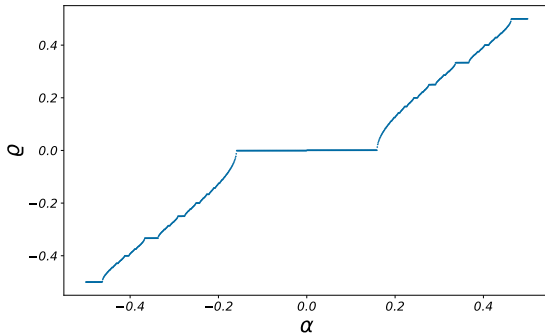


Figure E.5. Devil's staircase: graph of $\alpha \mapsto \varrho(\mathfrak{A}_{\alpha,\varepsilon_0})$ for small $\varepsilon_0 > 0$ [34]; at rational values the graph is horizontal on plateaux corresponding to the resonance tongues. The points where the function is not constant forms a *fractal set* in the sense of Mandelbrot, see Section E.3.4. This set has a positive Lebesgue measure; see the main text for further explanatory remarks.

E.3.4 A second digression on topology and measure theory

We conclude this section on circle maps with another discussion on the topological- and measure-theoretic properties of the Arnold family, in particular on Figure E.4.

Again consider a horizontal line in the (α, ε) -plane at height $\varepsilon_0 > 0$, chosen sufficiently small. We observe the following.

- (1) The intersection of the line $\varepsilon = \varepsilon_0$ with the union of resonance tongues forms an open and dense set.

According to the Denjoy Theorem (Proposition 7, item 3), its complement is the set of parameter values with quasiperiodic dynamics. It follows that this is a totally disconnected closed set, that contains Diophantine sets $\mathfrak{D}_{\tau, \gamma}$, as described above in relation to KAM Theory. By Proposition 8, for sufficiently small γ , this set is of positive Lebesgue measure. Next, we choose the constant γ as a suitable function of ε that tends to 0 with ε . This implies that

$$\text{measure } \mathfrak{D}_{\tau, \gamma(\varepsilon)}$$

tends to full measure as $\varepsilon \downarrow 0$. For additional details we refer to the above references, to the first topological digression in Appendix D and for general background to [71, 137].

- (2) According to Mandelbrot [118], we speak of a *fractal set* when its *Hausdorff dimension* is larger than its *topological dimension* [71, 90, 137]. Without going into all definitions we just mention the following: The fact that the set of parameter values with quasiperiodic dynamics has positive measure implies that the Hausdorff dimension equals 1 while the fact that it is totally disconnected implies that the topological dimension equals 0. Granted the details, this shows that the parameter points with quasiperiodic dynamics form a fractal set.

Finally, we mention that the Arnold family \mathfrak{A} in many respects is already generic, in the sense that most of the above properties also hold for circle maps where the periodic term $f(\varphi) = \sin \varphi$ in (E.1) is replaced by an arbitrary trigonometric polynomial or even a general

smooth periodic function. The only difference with what has been described here is the order of contact that the boundaries of a given tongue may have, compare with [51].

E.3.5 Back to Huygens' clocks

We now return to the torus-circle model for Huygens' weakly coupled pendulum clocks. Generically the periodic term in the corresponding Poincaré map (E.1) has a main tongue as described above, so where the tongue boundaries meet with a positive angle at $(\alpha, \varepsilon) = (0, 0)$; in fact all tongues open up a bit. Since the pendulum clocks are almost identical, the corresponding (α, ε) must be in this main tongue, which implies synchronization on average.

We like to note the universal nature of the above approach. To find sharper forms of synchronization, i.e., where the pendulums move in phase or anti-phase, we must take into account also the dynamics of the beam. We here refer to, e.g., [23, 142].

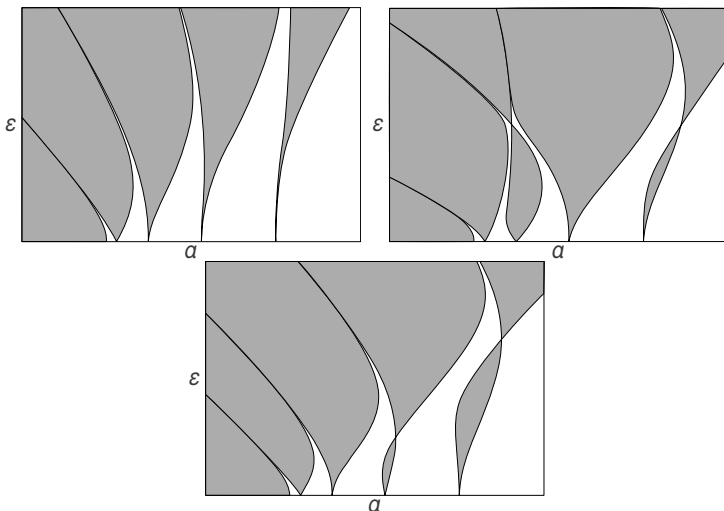


Figure E.6. Tongues in the Mathieu equation [124] (upper left), a modified Mathieu equation [50] (upper right) and Square Hill equation [46] (below)

E.4 Parametric resonance: Mathieu's equation and the like

In Section 2.4.1 we already got acquainted with parametric resonance. Instead of (2.11) we here, as in Appendix D, use the swing form (D.4)

$$\ddot{x} + (a + \varepsilon f(t)) \sin x = 0 \quad \text{with} \quad f(t + 2\pi) \equiv f(t). \quad (\text{E.5})$$

We also use the system form (D.3)

$$\begin{aligned}\dot{x} &= y \\ \dot{y} &= -(a + \varepsilon f(z)) \sin x \\ \dot{z} &= 1.\end{aligned}$$

and the ensuing stroboscopic map. For f we distinguish the following alternatives

$$\begin{aligned}f_\varepsilon(t) &= \cos t + \varepsilon \cos(2t) \\ f(t) &= \operatorname{sign}(\cos t).\end{aligned}$$

In the sequel, we shall also use the linearized version of (E.5)

$$\ddot{x} + (a + \varepsilon f(t))x = 0, \quad (\text{E.6})$$

The case of $f = f_0$ is the classical Mathieu equation, see [124]. The case f_ε for $\varepsilon > 0$ is the modified Mathieu equation, see [50], and the other case is known as Square Hill equation [46].

E.4.1 The stability diagram

We consider the trivial periodic solution $x \equiv 0 \equiv \dot{x}$ and its stability. In terms of the stroboscopic map, this amounts to whether the corresponding fixed point $(x, y) = (0, 0)$ is an elliptic point or a saddle point, something that can be read off from the derivative $D_{(0,0)}P$. In turn, this derivative is completely determined by the linearized, Mathieu-like equation (E.6) that for $\varepsilon = 0$ turns into

$$\ddot{x} + ax = 0.$$

The system form then is

$$\begin{pmatrix} \dot{x} \\ \dot{y} \end{pmatrix} = \begin{pmatrix} 0 & 1 \\ -a & 0 \end{pmatrix} \begin{pmatrix} x \\ y \end{pmatrix}$$

The eigenvalues are $\pm i\sqrt{a}$ and therefore

$D_{(0,0)}P$ has eigenvalues $e^{\pm i\sqrt{a}}$.

For $a > 0$ these are always elliptic (i.e., imaginary) but for

$$a = \frac{1}{4}k^2, \quad k = 0, 1, 2, \dots$$

they equal ± 1 . In the (a, ε) -plane the points $(a, \varepsilon) = (\frac{1}{4}k^2, 0)$, $k = 0, 1, 2, \dots$ turn out to be tips of resonance tongues in which the eigenvalues are real, which means that the fixed point $(x, y) = (0, 0)$ is a saddle point and is therefore unstable. Bifurcations (so-called subharmonic bifurcations) then take place at the corresponding tongue boundaries. For instance the tongue with $k = 1$ when the eigenvalues of $D_{(0,0)}P$ are close to -1 , this bifurcation is a period doubling and we speak of a $1 : 2$ -resonance. For more details see below. In Figure E.6 we displayed three diagrams with tongues in the (a, ε) -plane for different choices of f .

Remark 50. (1) In two of the three stability diagrams tongues occur with intersections in their boundary curves. It turns out that the corresponding patterns are universally arranged by so-called \mathbb{A}_{2k-1} -singularities, see [46, 50], [11, Chapter 15] for details.

(2) Note that the $1 : 2$ -resonance near the tongue tip with $k = 1$ resembles the Botafumeiro motion as described in the introduction to this appendix.

E.4.2 The nonlinear dynamics

In this section we focus on the $1 : 2$ -resonance tongue emanating from $(a, \varepsilon) = (\frac{1}{4}, 0)$ and the corresponding dynamics. As said before the ensuing bifurcation is a period doubling.

One way to get information on the nonlinear dynamics of (E.5) is to consider its system form.

$$\begin{aligned}\dot{x} &= y \\ \dot{y} &= -(a + \varepsilon f(z)) \sin x \\ \dot{z} &= 1,\end{aligned}\tag{E.7}$$

compare (D.5), and by a repeated averaging procedure arrive at a planar vector field defined on an appropriate covering space. This procedure largely follows Takens [166]. The stroboscopic map then

is approximated to arbitrarily high order by the time 1 map of this *Takens vector field* T , composed with the reflection $-\text{Id}$. The vector field T also is invariant under $-\text{Id}$. For details see [54]. The Takens vector field is sometimes called *interpolating*, for a phase portrait see Figure E.7.

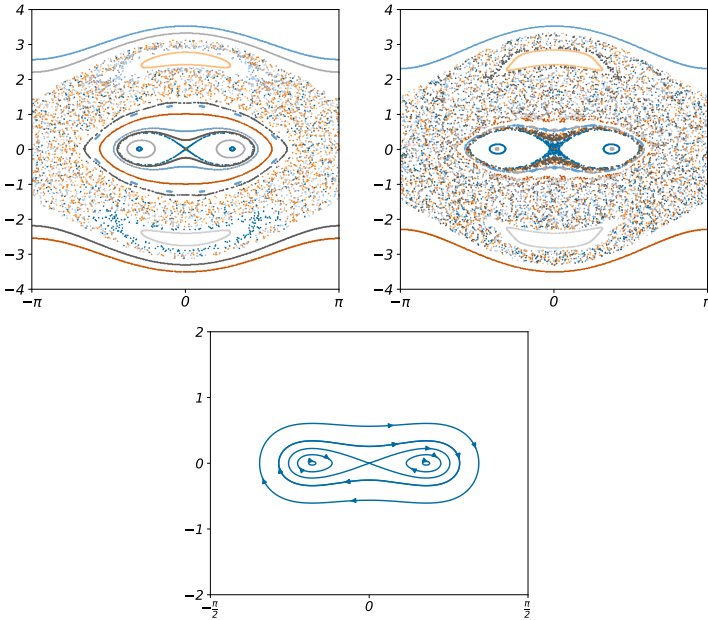


Figure E.7. Stroboscopic phase portraits near $1 : 2$ -resonance in the case of Mathieu forcing; top left $\varepsilon = 0.25$, top right $\varepsilon = .40$. Compare Figure D.5. Bottom: approximating Takens vector field T

We shall not go into the details here, but just comment on the numerically obtained stroboscopic phase portraits in Figure E.7.

We can still more or less recognize the underlying vector field T . The parameters (α, ε) are inside the tongue so the central fixed point, corresponding to the trivial periodic solution $x = 0 = y$, is a saddle point. The vector field T has a figure-8 homoclinic loop, enclosing two equilibria. However, by the flipping for the stroboscopic map this

is a periodic orbit of period 2 and a 4π -periodic solution of the system (E.7). In fact, all equilibria of the vector field T occur in pairs that form period 2 orbits. Moreover

- (1) There exist (pairs of) families of invariant circles, that are densely filled by quasiperiodic dynamics. This is in agreement with the KAM Theory described in Section E.3.
- (2) As is to be generically expected all homo- and heteroclinic connections of the Takens vector field turn into a *tangle*, with its abundance of Smale horseshoes [53, Chapter 4]. In simulations we don't see the tangle, but just orbits that seem to densely fill up large areas. In Appendix D, particularly in Section D.3.1, we discussed this type of conservative chaos. As spelled out there, the long-standing Arnold conjecture is that the Lebesgue measure is ergodic for the stroboscopic map at hand [10].

E.5 Scholium

This appendix concludes with a number of examples where several kinds of resonance play a role. In the first example, the forcing is quasiperiodic and we touch on the corresponding Mathieu equation being the spectral equation of a Schrödinger operator.

The second example deals with celestial resonances, a phenomenon that turns out to occur often in the solar system. Here we distinguish between sheer orbital resonances and spin-orbit resonances.

E.5.1 Quasiperiodic Mathieu versus Schrödinger

In this section we consider a quasiperiodic analogue of the Mathieu equation, given by

$$\ddot{x} + (a + \varepsilon f(t))x = 0 \quad (\text{E.8})$$

with $f(t) = F(\omega_1 t, \omega_2 t, \dots, \omega_n t)$ for a sufficiently smooth (or real analytic) map $F : \mathbb{T}^n \rightarrow \mathbb{R}$.

This equation can be largely treated in the same way as (E.6) [42], where we assume ω to be quasiperiodic. It turns out that the geometry per tongue is as before, but globally we find the same fractal geometry as in the case of the Arnold family (E.4), see Figure E.4.

E.5.1.1 Schrödinger operators

The connection between dynamical systems, including KAM Theory, and spectral theory runs deep and is the subject of ongoing research in mathematical physics. Here we shall not go into the details of quantum chaos and semiclassical analysis and restrict ourselves to some relevant aspects.

The equation (E.8) is of special interest since it is the spectral equation of the one-dimensional Schrödinger operator

$$(H_\varepsilon x)(t) = -\ddot{x}(t) - \varepsilon f(t)x(t)$$

for $x = x(t) \in L^2(\mathbb{R})$, with quasiperiodic potential εf . Here $L^2(\mathbb{R})$ is the space of Lebesgue measurable functions $x = x(t)$ such that $\int_{\mathbb{R}} |x(t)|^2 dt < \infty$.

This operator is widely being studied, among others by Dinaburg and Sinai [66], by Moser and Pöschel, Eliasson, and by Broer, Puig and Simó [48, 69, 126], where tools from both KAM- and singularity theory are being used. The lettering however is mostly chosen differently: the time t is replaced by a spatial variable x , and the potential $\varepsilon f(t)$ by $V(x)$ or $U(x)$.

From gaps to tongues. Usually ε is not taken into account as a parameter and, in the above terms, one is just dealing with a fixed, (sufficiently) small $\varepsilon_0 > 0$. The intersection with the tongues then correspond to spectral gaps. In [48] a rotation number ϱ is introduced that, as before, is a continuous function of the parameters a and ε . In Figure E.8 a graph is depicted which shows another Devil's staircase. Here one speaks of a *Cantor spectrum*.

Moser and Pöschel [126] state that generically the gaps do not close. However, the results of [48] show that the addition of the parameter ε leads to a generic gap-closing theory where the pattern again is governed by the singularities \mathbb{A}_{2k-1} [11].

From continuous to discrete. Next we consider a discrete Schrödinger operator, also known as *almost Mathieu operator*,

$$(H_{\lambda,\alpha,\theta}x)_n = x_{n+1} + x_{n-1} + 2\lambda \cos(2\pi\alpha n - \theta)x_n \quad (\text{E.9})$$

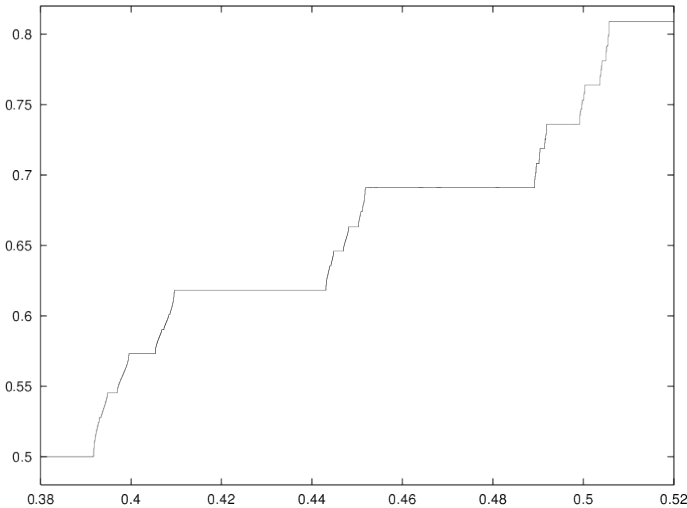


Figure E.8. Another Devil's staircase [48], where we take $n = 2$, $\omega_1 = 1$ and $\omega_2 = \frac{1}{2}(\sqrt{5} - 1)$, for $\varepsilon = \varepsilon_0$ sufficiently small. The description in the caption of Figure E.5 largely applies also here.

where $\lambda, \alpha, \theta \in \mathbb{R}$ are real parameters and

$$u = (\dots, x_{-2}, x_{-1}, x_0, x_1, x_2, \dots) \in \ell^2(\mathbb{Z}),$$

where $\ell^2(\mathbb{Z})$ is the space of square-summable doubly infinite sequences, i.e., with $\sum_{n \in \mathbb{Z}} |x_n|^2 < \infty$.

The spectrum turns out to be independent of θ but varies wildly with respect to the other parameters. Here we will not go into the effect of λ on the spectral type but just focus on the remaining parameter α . When the value of $\alpha = p/q \in \mathbb{Q}$ is rational, the spectrum of $H_{\lambda, p/q, \theta}$ is given by the union of q intervals possibly touching at endpoints, see Figure E.9. This follows from Floquet theory, which we have met in disguise in the previous discussion of the Hill and Mathieu equation. When α is irrational, we again see a Cantor spectrum for all $\lambda \neq 0$ and therefore with Devil's staircases.

Remark 51. The latter statement,

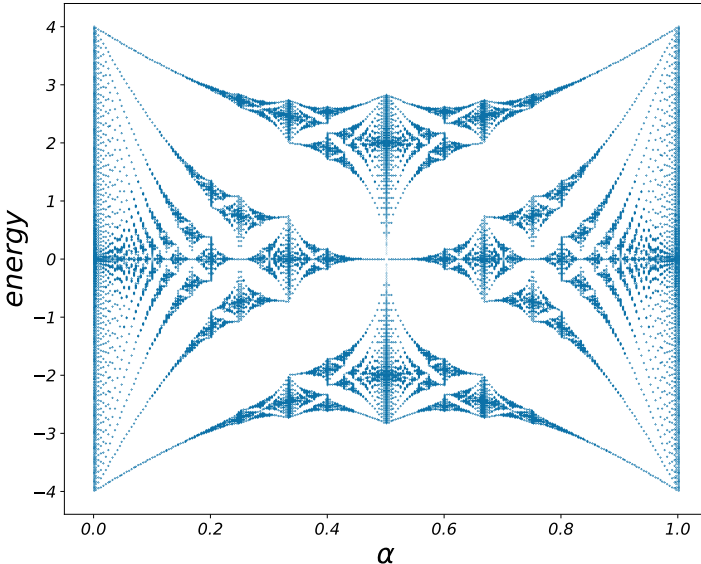


Figure E.9. Hofstadter's butterfly [99] is the fractal obtained by plotting the spectrum of the operators $H_{1,\alpha,\theta}$ for the rational values $\alpha \in \mathbb{Q} \cap [0, 1]$. It describes the spectral properties of non-interacting electrons in a two-dimensional lattice under the influence of a perpendicular magnetic field.

for irrational α the spectrum of the almost Mathieu operator (E.9) is a Cantor set,

is commonly referred to as *the Ten Martini problem*. This name came from Barry Simon in 1981, after Marc Kac had offered a prize for its solution [154, Problem 4]. The conjecture was proven 24 years later, in 2005, by Artur Avila and Svetlana Jitomirskaya, see [15, 16, 110].

The almost Mathieu operator arises in the context of the Integral Quantum Hall Effect [177] at the center stage of the 1985 Nobel Prize in physics in [135]. And it brings us to the verge of many recent mathematical advances, contributing to the award of a 2014 Fields Medal to Avila [78].

Abundance of Cantor sets and Devil's staircases. Referring to the Figures E.5 and E.8, to Smale horseshoes, tangle and the like [53], and also to the general discussion on KAM Theory in Section E.3, it should be no longer a surprise that Cantor sets and Devil's staircases appear widely in dynamical systems and various other theories within mathematical physics. Here it is noteworthy that the Cantor sets sometimes have positive measure and sometimes measure zero.

Remark 52. (1) In the literature on theoretical solid-state physics, field theory and statistical mechanics, one stumbles over these gadgets [79]. For instance, it turns out [110] that models like the almost Mathieu operators presented here are also at the roots of the so-called Fractional Quantum Hall Effect [18, 80] (see also Figure E.10), a phenomenon the discovery of which led to a Nobel Prize in physics in 1998 [81].

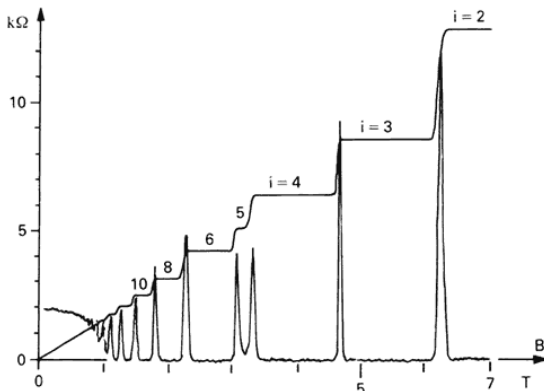


Figure E.10. The Hall resistance varies stepwise with changes in the magnetic field B . The lower peaked curve represents the Ohmic resistance, which disappears at each step [81]. Note that this figure relates to the case of rational α and therefore does not correspond to a Devil's staircase. Perhaps, however, that you can still see the ghost of such a staircase ...

- (2) We also like to point out that the mathematics used in the history of the Ten Martini problem and many of the proofs of partial results that appeared over the years heavily rest on applications of KAM Theory, e.g. [14, 66, 70, 95, 153].

E.5.2 Celestial resonance

When looking at the night sky we may see a lot of rotations and oscillations, especially when studying the heavenly bodies within our solar system. These motions form the main subject of celestial mechanics. And although the dimensions of the phase spaces are much higher than in the present book, the mechanical principles remain the same: one works mainly within the Newtonian theory, now and again applying a relativistic correction.

A taste of resonance. The solar system exhibits many resonances. We distinguish between two types of these: orbital and spin-orbit resonances.

An example of the former resonance is given by the inner three Galilean moons of Jupiter: Io, Europa and Ganymedes. These trace their almost circular orbits in an orbital $1 : 2 : 4$ resonance. This means that Europa has a period of revolution that is twice that of Io and similarly that Ganymedes takes twice as long as Europa to revolve. This resonance was conjectured by Laplace [109] and an appropriate periodic solutions were provided by Willem de Sitter [155, 156]; for later references on quasiperiodic librations of the latter see [40, 41, 55].

An example of a spin-orbit resonance is given by the motion of the moon around the earth. Since the moon always shows us the same face, its revolution around the earth and the rotation (spin) around its own axis must be equal (at least on average). We speak of a $1 : 1$ spin-orbit resonance. Other examples are the Galilean moon Io with respect to the planet Jupiter, and Enceladus and Rhea both with respect to Saturn. Similarly Mercury is in a $3 : 2$ spin-orbit around the sun: it rotates twice about its axis against two revolutions around the sun [57].

One main physical explanation is given by the tidal effects that the celestial bodies exert on each other and that by friction slow down

the rotation about their axes. Indeed, to give an idea consider the tidal waves caused by the moon (and sun) on the Earth, that are clearly visible in the oceans. However, also Earth's surface itself, at the equator, in each wave is lifted for about 40 cm. In this way the earth has *captured* the moon into this 1 : 1 spin-orbit resonance, but in the very long run the earth itself will also be captured by the moon. Then days and months will have become equally long and the pair will move around in the solar system as a rigid body. By the same mechanism Pluto and his companion Charon have already captured each other in this mutual embrace. For an overview see [34].

An adiabatic Ansatz. The general philosophy is that by the tidal effects the rotations decrease in an *adiabatic* way, being captured in a resonance now and again [94]. As a caricature think of the Arnold tongues in Figure E.4, where the parameter α is moving adiabatically towards 0. The system then passes through many resonances, where the higher-order ones are barely observed, finally ending up being captured in the lowest possible, ‘synchronizing’ 1 : 1 resonance.

When considering orbital resonances with more satellites, validity of Kepler's third law may well lead to a final 1 : 2 : 4 resonance capture [40, 41] ...

A spin-orbit model. To further explain the capture in a spin-orbit resonance, we introduce a mathematical model [86, 56] to describe the spinning motion of a satellite around a central heavy body.

The simplest form of the model assumes that a triaxial satellite is orbiting a larger, heavier body on a Keplerian ellipse. Furthermore, we also assume that its spin-axis is perpendicular to the orbital plane and that it coincides with the smallest axis of the satellite. The equation of motion that describes the rotation of such a satellite around its spin-axis ends up being a particular damped forced oscillator, ruled by two parameters: the asphericity of the satellite and the elliptic eccentricity of the orbit.

It was one of the great achievements of Newton to recognize the central role of the *linear momentum* in his *Philosophiae Naturalis Principia Mathematica* [132]. This linear momentum, for a body

of mass m that moves with velocity \dot{x} , reads

$$p = m\dot{x}. \quad (\text{E.10})$$

Newton's famous second law (1.1), then gets the form

$$F = \dot{p}. \quad (\text{E.11})$$

It is to be noted that usually these notions go in vectorial form.

Similar equations exist for rotating motion. Assuming that the body moves along an angle θ with an angular velocity $\dot{\theta}$, then we can replace the expression (E.10) by

$$L = I\dot{\theta},$$

the *angular momentum*. Here I is the *moment of inertia* of the spinning body [84], with respect to the (instantaneous) axis of rotation. Just like the mass m of an object can be understood as the physical property that resists to its velocity \dot{x} , so can the moment of inertia I be understood as the property that resists to its rotational velocity $\dot{\theta}$. The role of the force F is now taken over by the *torque* N and equation (E.11) for this case reads

$$N = \dot{L}.$$

Since I also depends on t we here get

$$\dot{L} = \dot{I}\dot{\theta} + I\ddot{\theta}$$

and so the equation of motion of the spin-orbit motion reads

$$N(\theta, t) = \dot{I}\dot{\theta} + I\ddot{\theta}. \quad (\text{E.12})$$

It turns out that it is a realistic assumption that I has the format

$$I(t) = \tilde{I} + \varepsilon \cos(\Omega t),$$

so with average \tilde{I} that varies periodically with some frequency Ω . Moreover the torque $N = N(\theta, \dot{\theta}, t)$ that accounts for the revolution of the satellite around the heavy body, is also assumed to be periodic in t . Damping is included as well in the model, to express tidal friction. As in the models of Chapter 2 and Appendix D, the small

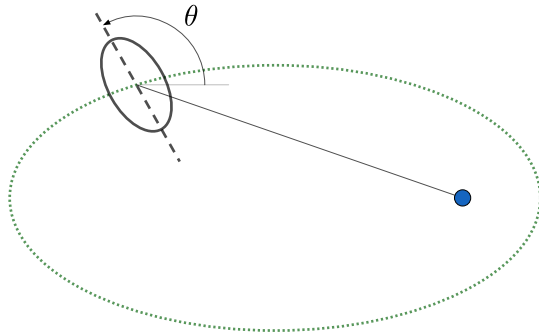


Figure E.11. Schematic representation of the spin-orbit model

damping is dealt with in a perturbative way. Thus we can rewrite the equation of motion (E.12) in the familiar form

$$\ddot{\theta} + \frac{dI}{dt} \frac{\dot{\theta}}{I} - \frac{N(\theta, \dot{\theta}, t)}{I} = 0, \quad (\text{E.13})$$

assuming that $I \neq 0$. As in Appendix D, we can plot stroboscopic phase portraits to get an idea of the dynamics of (E.13), for examples see Figures E.12 and E.13.

Resonance capture. Compared to the general philosophy of Ansatz E.5.2, the spin-orbit model gives a more realistic view and more detailed idea of a specific resonance capture, especially in Figure E.13. Nevertheless, the time scale in Figure E.13 also here indicates an adiabatic process. For details we refer to [82, 83, 94, 144].

Given the perturbative nature of damping in (E.13), the evolution of the damped system for a long time remains close to an orbit of the undamped system. In Figure E.13 we can witness a ‘chaotic’ orbit being captured over a long time span into a $1 : 1$ resonance: after some time the satellite effectively is in synchrony with the revolution around the planet, with only remarkably small deviations.

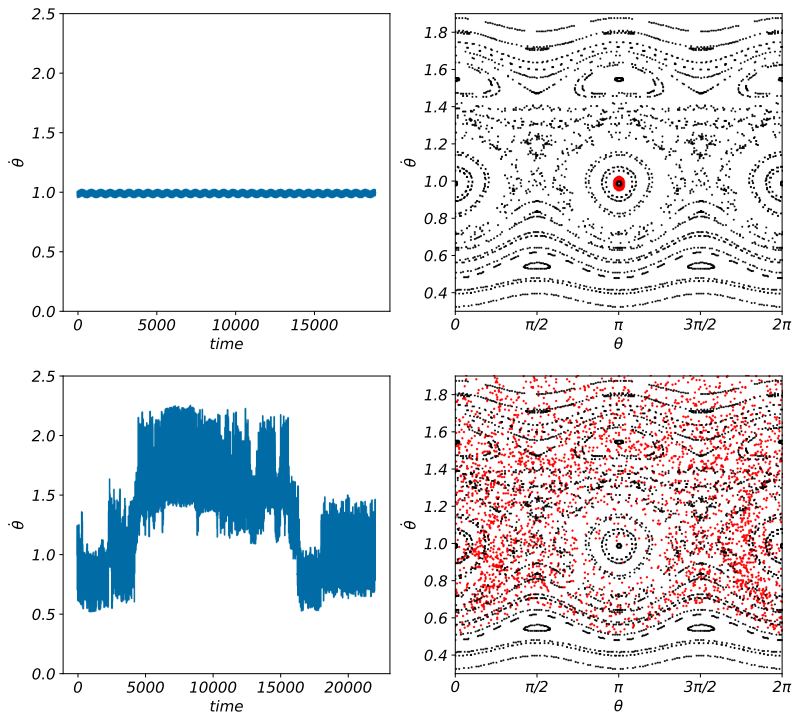


Figure E.12. The left-hand panels present the time-evolution of $\dot{\theta}$ for the spin-orbit model (E.12) in the non-resonant case $\Omega = \sqrt{2}$ for $\varepsilon = 0.01$ (top) and $\varepsilon = 0.2$ (bottom). The right-hand panels show the stroboscopic phase portraits of the damped model (red or gray dots) as compared to the undamped model with $\varepsilon = 0$ (black dots) [32].

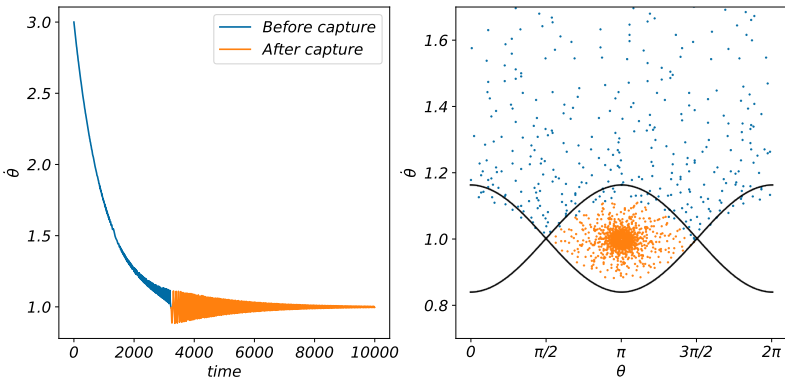


Figure E.13. The evolution of $\dot{\theta}$ for the spin-orbit model (E.13) in the case of capture in the synchronous 1 : 1 resonance (left); The stroboscopic phase portrait on the right clearly confirms this resonance capture [32].

We note that the present model has two frequencies which makes it harder to analyze, also compare Section E.5.1. Indeed, a full understanding of this phenomenon is still the subject of scientific debate [127, 128, 129]. Considering the spin-orbit resonances in our solar system, it remains quite unclear why certain 'non-synchronizing' resonances, like the 2 : 3 spin-orbit resonance of Mercury, are so prevalent. Nevertheless, a careful analysis of the spin-orbit problem of the Earth-Moon system [56] indicates that the system may well be in the middle of a narrow tongue close to the frequency 1, which again confirms the adiabatic philosophy of Ansatz E.5.2.

Remark 53. Considering the dissipative stroboscopic phase portraits of Figure E.12, one may well ask whether there is chaos in the sense of Appendix D. For recent research in this direction see [62, 63]. On the other hand, the graphics also suggests the possibility of infinitely many sinks in the sense of Newhouse [130, 131], also compare with [138].

E.5.3 A final exercise on Kepler's third law

In this exercise we determine Kepler's third law from mathematical principles under Newtonian gravitation, also using Newton's second law

$$\mathbf{F} = m \mathbf{a} \quad (\text{E.14})$$

compare with [132]. For simplicity, we restrict to uniform circular motions.

In the plane consider two point masses M (the sun) and m (a planet). Let x and y be cartesian coordinates and set

$$\mathbf{r}(t) = \begin{pmatrix} x(t) \\ y(t) \end{pmatrix}.$$

The sun is positioned at the origin and the planet moves in a uniform circular orbit

$$\mathbf{r}(t) = R \begin{pmatrix} \cos\left(\frac{2\pi}{T}t\right) \\ \sin\left(\frac{2\pi}{T}t\right) \end{pmatrix}, \quad (\text{E.15})$$

so with radius R and period of revolution T .

- (1) Under the assumption of a Newtonian inverse square central force

$$\mathbf{F} = -\frac{k M m}{r^2} \mathbf{e}_r, \quad (\text{E.16})$$

where \mathbf{e}_r is the unit vector in the radial direction, show that

$$T = \text{cst. } R^{3/2},$$

and determine the constant. This result is known as Kepler's third law or also as Kepler's 3/2 law.

- (2) What changes in the above when Newton's inverse square law is replaced by

$$\mathbf{F} = -\frac{k M m}{r^\kappa} \mathbf{e}_r \quad (\text{E.17})$$

for a constant $\kappa \neq 0$?

Remark 54. (1) For completeness we also briefly discuss Kepler's first two laws for planetary motion. The first is that the planet travels along an ellipse with the sun in one of its focal points. The second law says that in equal times the radius \mathbf{r} of the planet sweeps out

equal areas. Note that the motion (E.15) surely is in agreement with these two laws.

By the way, in Arnold [5, Section 7], it is shown that Kepler's second law holds for any central force field (E.17).

- (2) From the above exercise it follows that the inverse square attraction law is equivalent to Kepler's third law. Until the early 1680's Newton (and some of his contemporaries) understood that the sun attracts each planet according to the inverse square law, but there was no mention yet of mutual interaction between the planets or of universal gravitation.

Then Newton proposes the following crucial experiment: he asks the First Astronomer Royal John Flamsteed to check Kepler's third law on the four Galilean moons of Jupiter, which happen to follow almost circular orbits. After an affirmative answer, Newton concludes that Jupiter also attracts its moons with the inverse square law and only then he dares to postulate the law of universal gravitation. See Westfall [174].

Newton immediately realized that this was the end of all these beautiful Keplerian ellipses, since these were perturbed by their mutual gravitational interactions. This may well have given him severe headaches but it also marked the onset of ages of perturbation theory.

Appendix F

Solutions of selected exercises

F.1 Exercises from Section 1.6

F.1.1 Exercise 1.6.1: The vertical spring

- (1) Since m is at rest, the sum of the gravitational force $-mg$ and the spring force $-kx$ should be equal to 0. This means that $-mg - kx = 0$, and therefore that the position is $x = -mg/k$.
- (2) Newton's law gives

$$m\ddot{x} = -kx - mg.$$

We can use the change of variables $s(t) = x(t) + \frac{mg}{k}$, which shifts the rest position to 0, to get to the following equation of motion

$$m\ddot{s} = -ks.$$

- (3) We already know the solutions of this equation of motion, namely

$$s(t) = A \cos\left(\sqrt{\frac{k}{m}}t\right) + B \sin\left(\sqrt{\frac{k}{m}}t\right).$$

For x therefore we find the solutions

$$x(t) = -\frac{mg}{k} + A \cos\left(\sqrt{\frac{k}{m}}t\right) + B \sin\left(\sqrt{\frac{k}{m}}t\right).$$

F.1.2 Exercise 1.6.2: The horizontal pendulum

Since there are no forces in the direction of the motion, the equation of motion is

$$\ell\ddot{x} = 0 \quad \text{or} \quad \ddot{x} = 0.$$

The corresponding solutions are of the form $x(t) = At + B$, where $A = \frac{dx}{dt}(0)$ and $B = x(0)$.

Since the potential energy in this example is identically zero, the energy here is $H(x, y) = \frac{1}{2}\ell^2y^2$, and so the integral curves are horizontal lines, while all points on the x axis are singular. This horizontal pendulum can be considered as the limit of an ordinary vertical pendulum when we let the gravity g go to zero. Furthermore, as $E \rightarrow \infty$ (E being the value of the energy), there is increasingly less difference between the solutions of the equation of motion of the horizontal and the vertical pendulum.

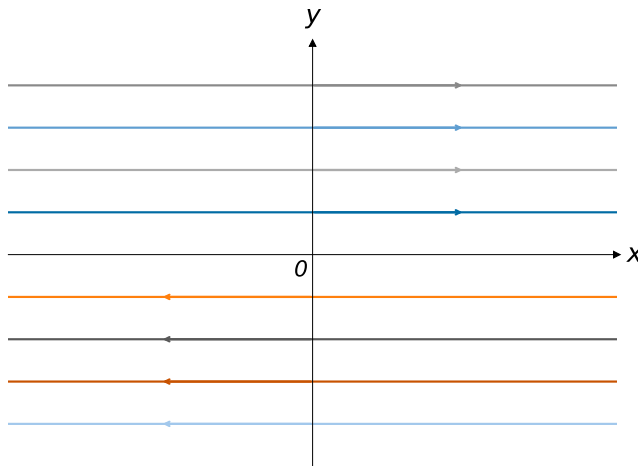


Figure F.1. Phase portrait of the horizontal pendulum

F.1.3 Exercise 1.6.3: Symmetries of the line element field

In the direction (ξ, η) defined at (x, y) we have

$$-F(x)\xi + y\eta = 0,$$

and therefore

$$-F(x)\xi + (-y)(-\eta) = 0.$$

It follows that the line element field is symmetrical under the reflection on the x -axis.

Let now the direction in $(x, 0)$ be given by (ξ, η) . Then, by the above discussion (ξ, η) and $(\xi, -\eta)$ correspond to the same direction and therefore $\xi = 0$ or $\eta = 0$. From the formula for the line element field it follows that at a point $(x, 0)$ for which $F(x) \neq 0$, the direction is vertical (i.e., in the y direction), while at a point $(x, 0)$ for which $F(x) = 0$, we have a singularity.

When the map $x \mapsto y(x)$ defines an integral curve, by the symmetry, $x \mapsto -y(x)$ also defines an integral curve. The “motions” associated with these integral curves are each other’s “inverse” in the sense that the latter in x can be obtained by performing the former backward in x . The integral curve and its mirror image may or may

not be equal, as you can see in Figure F.2. (What does the potential $V(x)$ look like?)

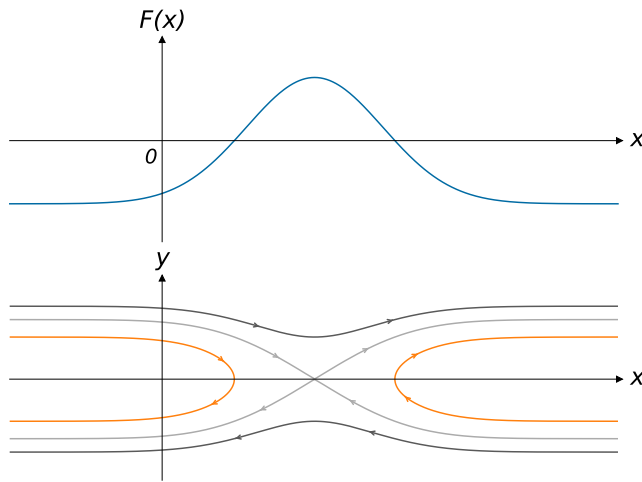


Figure F.2. Integral curves for a given force $F = F(x)$

F.1.4 Exercise 1.6.4: Ellipses and time rescalings on the spring

The equation of motion is $\ddot{x} = -kx$, the potential energy is $V(x) = \frac{1}{2}kx^2$ and the total energy is $H(x, y) = \frac{1}{2}y^2 + \frac{1}{2}kx^2$, where $y = \dot{x}$.

- (1) The energy level for some energy E is described by the equation $\frac{1}{2}y^2 + \frac{1}{2}x^2 = E$. Curves described by such an equation are called *ellipses* (see Figure F.3).
- (2) Substituting $y = z\sqrt{k}$ in the equation for the energy level with value E gives $\frac{1}{2}kx^2 + \frac{1}{2}kz^2 = E$: the equation of a circle.
- (3) For $\tau = \sqrt{k}t$ the chain rule gives that $\frac{dx}{d\tau} = \frac{1}{\sqrt{k}}\frac{dx}{dt}$ and thus $\frac{d^2x}{d\tau^2} = \frac{1}{k}\frac{d^2x}{dt^2} = -x$. That is, the transformation $z = \frac{1}{\sqrt{k}}y$ has the same effect as the time rescaling $z = \frac{dx}{d\tau}$.

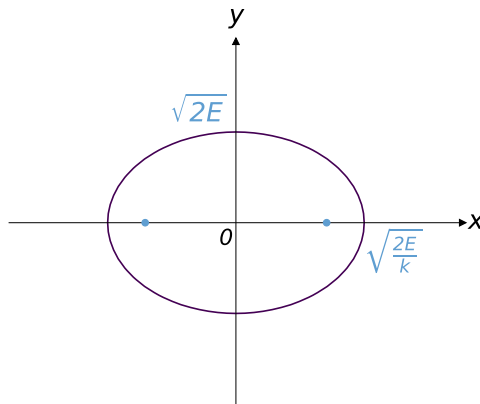


Figure F.3. Elliptic integral curve

F.1.5 Exercise 1.6.5: Energies and amplitudes

An oscillation with energy E occurs between x_{\min} and x_{\max} ; since at maximum deviation the velocity and therefore the kinetic energy vanishes, these values of x satisfy $V(x) = E$. Therefore, the amplitude is $\frac{1}{2}(x_{\max} - x_{\min})$.

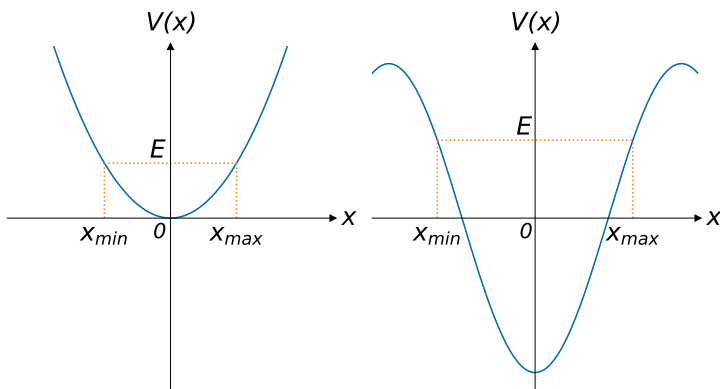


Figure F.4. Oscillations bounds for the two potentials in Exercise 1.6.5

In the first case, we get $x_{\max} = -x_{\min} = \sqrt{\frac{2E}{k}}$ and this is the amplitude. Similarly for the second potential we find the amplitude

$$\arccos\left(\frac{-\ell E}{g}\right),$$

where $-\frac{g}{\ell} \leq E < \frac{g}{\ell}$. For the other values of E there is no oscillation.

F.1.6 Exercise 1.6.6: Phase portraits

The integral curves are of the form $y(x) = \pm\sqrt{2E - V(x)}$. So for solutions above the x axis local maxima and local minima of V correspond to local minima, resp. maxima, of the function $x \mapsto y(x)$ that defines the integral curve. Moreover, the local maxima and minima of V correspond to singularities of the line element field on the x -axis. The configuration of integral curves in such configurations depends on whether there is a local maximum or local minimum, see Figure F.5.

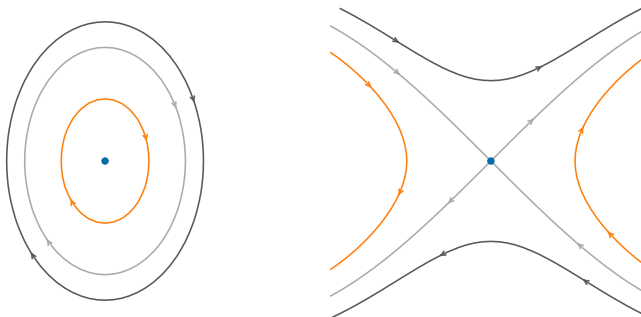


Figure F.5. Left: integral curves around a local minimum of V , this singularity is called a *center*; Right: integral curves around a local maximum of V , this singularity is called a *saddle point*

Horizontal asymptotes correspond to a separation between integral curves that go to infinity and bounded integral curves.

In Figure F.6 we drew the phase portraits associated with the potentials in Figure 1.19.

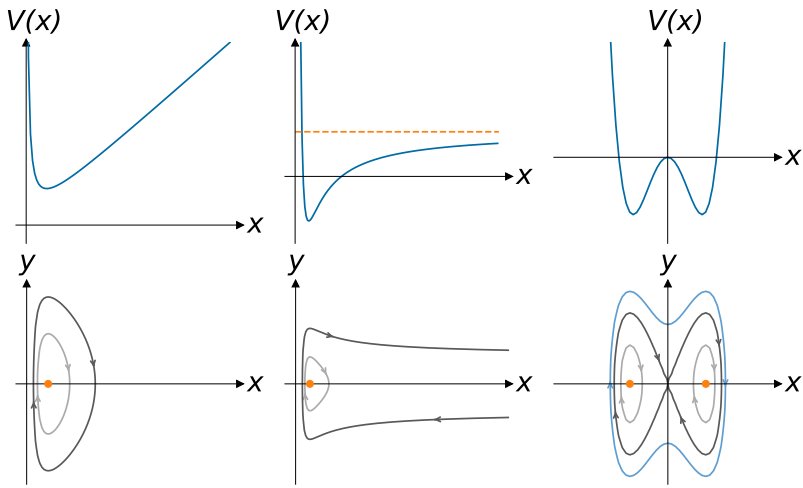


Figure F.6. Phase portraits for the potentials in Exercise 1.6.6

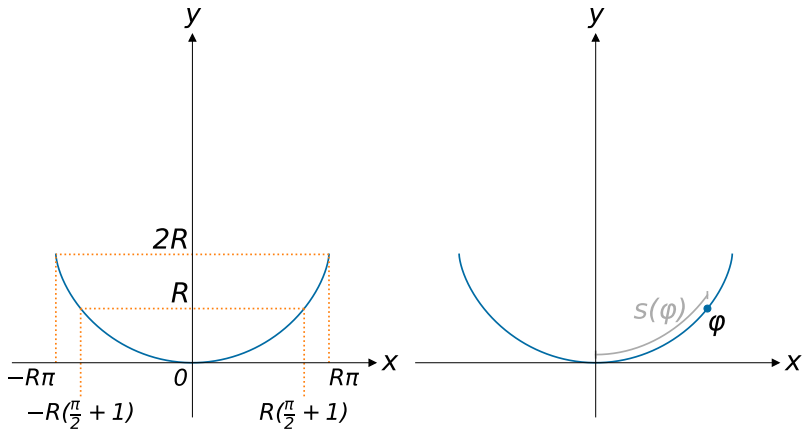


Figure F.7. Cycloid and its arclength

F.1.7 Exercise 1.6.7: The cycloid

- (1) Let (x, y, φ) be the variables as indicated in Exercise 1.6.7 and the figure therein. The parametrization of the center of the wheel then is given by $x(\varphi) = -R\varphi$, $y(\varphi) = R$. The vector from the center of the wheel to the valve is $(-R\sin\varphi, -R\cos\varphi)$, which leads to the following parametrization of the valve:

$$x(\varphi) = -R(\varphi + \sin\varphi), \quad y(\varphi) = R(1 - \cos\varphi).$$

- (2) The figure is symmetric with respect to the y -axis, see Figure F.7 (just replace φ with $-\varphi$). At a point with horizontal tangent line we get $\frac{dy}{d\varphi} = 0$ or $R\sin\varphi = 0$. Such points, therefore, occur for $\varphi = k\pi$ or $x = Rk\phi$. Similarly we can determine points with a vertical tangent line and so obtain the points $x = (2k+1)R\pi$, $y = 2R$. Finally, at $\varphi = (k+1/2)\pi$ we have $y(\varphi) = R$.

NB: in the points $x = (2k+1)R\pi$, $y = 2R$, there is both a vertical and a horizontal tangent. The curve has a *cusp* there.

- (3) We indicate the position of the bead (or marble) with the distance, measured along the cycloid, from the bead to the lowest point of the curve. Since the position of the bead is $(-R(\varphi + \sin\varphi), R(1 - \cos\varphi))$, from the previous discussion we obtain

$$s(\varphi) = 2\sqrt{2}R\sqrt{1 - \cos\varphi} = 4R\sin\left(\frac{1}{2}\varphi\right),$$

which can be interpreted as an arclength ‘with sign’; so the variable s can serve as a new coordinate.

- (4) The proof is part of the above item.

F.1.8 Exercise 1.6.8: Huygens’ isochronous and tautochronous curve

The potential energy here is the height in the y coordinates, thus $V(s(\varphi)) = R(1 - \cos\varphi) = \frac{s(\varphi)^2}{8R}$. This means that the potential energy associated to this exercise reads $V(s) = \frac{1}{8R}s^2$. Therefore the motion is harmonic. This proves the isochronicity of the motion. For the tautochronicity we observe that dropping the bead from a certain height amounts to one-quarter of an oscillation.

Note that if we are working with the potential energy, we have to use “real distances” to indicate the position, see also in Section 1.4.1, when defining

$$V(x) = - \int_0^x F(s) \, ds.$$

F.1.9 Exercise 1.6.9: Period and area

We don’t present a rigorous proof here, but rather an argument based on working with “infinitesimal quantities” such as dE , dx , etc.

We aim to show that the area of the region between $H(x, y) = E$ and $H(x, y) = E + dE$ is equal to $P(E) dE$, see Figure 1.20. Indeed, if we denote the enclosed areas by $A(E)$ and $A(E + dE)$ then this would mean that

$$A(E + dE) - A(E) = P(E) dE,$$

which would prove our point.

We know that $H(x, y) = \frac{1}{2}y^2 + V(x)$. This means that the intersections of the line with equation $x = x_0$ with the energy levels E and $E + dE$ (above the x -axis) have y -coordinates

$$y_0 = \sqrt{E - V(x_0)} \quad \text{and} \quad \sqrt{2(E + dE - V(x_0))}.$$

Since dE is supposed to be a small quantity, we can rewrite the latter expression as

$$\begin{aligned} y_0 + \frac{dy_0}{dE} dE &= y_0 + \frac{dE}{\sqrt{2(E - V(x_0))}} \\ &= y_0 + \frac{dE}{y_0}. \end{aligned}$$

The distance between these two points is therefore equal to dE divided by the velocity y_0 . This, indeed, means that the shaded area in Figure 1.20 must be equal to $dE \times dt$, where dt is the time the oscillator needs to travel from x_0 to $x_0 + dx$. We can now integrate this and find the following expression for the area between the energy levels for E and $E + dE$

$$\left(2 \int_{x_{\min}}^{x_{\max}} \frac{1}{y_0(x_0)} dx_0 \right) dE.$$

We already know that the expression in brackets denotes the period.

F.1.10 Exercise 1.6.10: Elliptic integrals

Using the substitution $z = \cos x$ gives $dz = -\sin x \, dx$ and

$$dx = -\frac{1}{\sin x} \, dz = -\frac{1}{\sqrt{1-z^2}} \, dz.$$

Note that since $\sin x = \pm\sqrt{1-\cos^2 x}$, we here made a small omission ... We then obtain

$$\int \frac{dx}{\sqrt{2\cos x + C}} = -\int \frac{dz}{\sqrt{1-z^2}\sqrt{C+2z}} = -\int \frac{dz}{\sqrt{C+2x-cz^2-2z^3}}.$$

This final equation has the desired shape.

For the length of the ellipse, we start with $(ds)^2 = (dx)^2 + (dy)^2$ so

$$ds = \sqrt{1 + \left(\frac{dy}{dx}\right)^2}.$$

To compute $\frac{dy}{dx}$ we write y as a function of x and then differentiate. Recalling that an ellipse is the solution set of $\frac{x^2}{a^2} + \frac{y^2}{b^2} = 1$, we have $y^2 = b^2(1-x^2/a^2)$ or $y = b\sqrt{1-x^2/a^2}$. Therefore, we get $\frac{dy}{dx} = -\frac{bx}{a\sqrt{a^2-x^2}}$, and

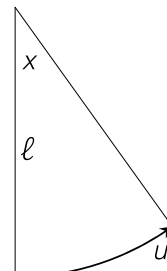
$$\begin{aligned} ds &= \sqrt{1 + \frac{b^2x^2}{a^4 - a^2x^2}} \, dx \\ &= \sqrt{\frac{a^4 - a^2x^2 + b^2x^2}{a^4 - a^2x^2}} \, dx \\ &= \frac{a^4 - a^2x^2 + b^2x^2}{\sqrt{(a^4 - a^2x^2 + b^2x^2)(a^4 - a^2x^2)}} \, dx, \end{aligned}$$

so that now $\int ds$ indeed takes the desired form.

F.1.11 Exercise 1.6.11: The potential energy of the pendulum

Let us indicate our new variable, the *arclength*, by u . Then we have $u = \ell x$. The equation of motion then is given by

$$\frac{d^2}{dt^2}(\ell x) = -g \sin x,$$



which can be rewritten as

$$\ddot{u} = -g \sin \frac{u}{\ell} = F(u).$$

If we use this to compute the potential energy, we find

$$\begin{aligned} V(u) &= - \int_0^u F(s) ds \\ &= \int_0^u g \sin \frac{s}{\ell} ds \\ &= -\ell g \cos \frac{s}{\ell} \Big|_{s=0}^{s=u} \\ &= g\ell(1 - \cos \frac{u}{\ell}). \end{aligned}$$

If you instead calculate the potential energy using the formula

$$\frac{d^2x}{dt^2} = -g \sin x = F(x),$$

you get $V(x) = \frac{g}{\ell}(1 - \cos x)$ which is wrong. Nevertheless, you can find the correct equation of motion in this way . . .

F.2 Exercises from Section 2.6

F.2.1 Exercise 2.6.1: Negative damping

With the help of the chain rule we get

$$\begin{aligned} \frac{dx}{d\tau} &= \frac{dx}{dt} \frac{dt}{d\tau} = -\frac{dx}{dt}, \\ \frac{d^2x}{d\tau^2} &= \frac{d}{dt} \left(\frac{dx}{d\tau} \right) \frac{dt}{d\tau} = \frac{d^2x}{dt^2}. \end{aligned}$$

So, the equation

$$\frac{d^2x}{dt^2} = -\frac{dV}{dx} - c \frac{dx}{dt} \quad (\text{F.1})$$

transforms to

$$\frac{d^2x}{d\tau^2} = -\frac{dV}{dx} + c \frac{dx}{d\tau}.$$

Indeed we see that the transformation $\tau = -t$ reverses the sign of the friction term. If we know the phase portrait of an oscillator, or even for the solutions of a general equation of the form (F.1), then,

after applying the change of variable $\tau = -t$, we can get the phase portrait after transformation as follows:

- We flip the image around the x -axis (after all $\frac{dx}{d\tau} = -\frac{dx}{dt}$);
- We reverse the directions of the arrows (after all, the arrows indicate the direction of the time).

It may be clear now, that with negative damping the energy will increase. Here you can also see that when there is no friction, the transformation $\tau = -t$ does not change the equation (compare this with Exercise 1.6.1).

F.2.2 Exercise 2.6.2: Tossing a fair coin

We first give the phase portrait of the frictionless equation that we find by determining the level curves of $H(x, y) = \frac{1}{2}y^2 + V(x)$. There are three types of oscillations.

- (1) Oscillations where the x -variable is always positive (for small energies these are very close to the point $x = 1$);
- (2) Oscillations where the x -variable is always negative;
- (3) Oscillations where x changes sign twice in each period. For this kind of oscillation, the amplitude is greater than $\sqrt{2}$. These regions of oscillation are separated from each other by a “figure 8” consisting of one saddle point $(x, y) = (0, 0)$ and two solutions which converge to $(x, y) = (0, 0)$ both as $t \rightarrow +\infty$ and as $t \rightarrow -\infty$.

As a result of adding friction, the motion continuously loses energy. If we assume that the friction is low, we will get approximately the phase portrait on the right-hand side of Figure F.8. In this case we have only shown the solutions that reach the saddle point as $t \rightarrow +\infty$ or $t \rightarrow -\infty$. All other solutions will converge to $x = 1$ or $x = -1$ as $t \rightarrow \infty$.

If we denote by L the part of the phase plane where the solutions converge to $x = -1$ and by R the part where the solutions go to $x = 1$, then we can see that L and R have “the same shape”: by reflection in the x -axis, L is mapped to R en vice versa. If we choose

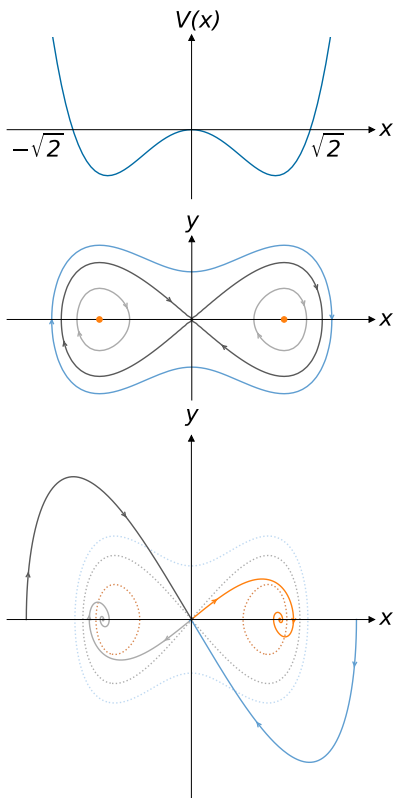


Figure F.8. Top: graph of the potential $V(x)$. Middle: phase portrait of frictionless system from Exercise 2.6.2; Bottom: phase portrait after introducing friction. The frictionless phase portrait is shown in transparency for comparison.

a “random point” in the phase plane, then the probability that the corresponding solution goes to $x = -1$ (heads) is just as large as the one that it goes to $x = 1$ (tails); the probability of the solution going to the saddle point is zero. (Why?)

F.2.3 Exercise 2.6.3: A “controlled” oscillator

The integral curves are composed of semicircles. In the positive half-plane ($y > 0$) these are semicircles with center $(x, y) = (-a, 0)$, and in the negative half-plane semicircles with center $(x, y) = (a, 0)$. For $y = \dot{x} = 0$ our equation is actually not defined. Outside the interval from $x = -a$ to $x = a$ on the x -axis, we can continue the solutions continuously, but not in this interval. The displacement of the center

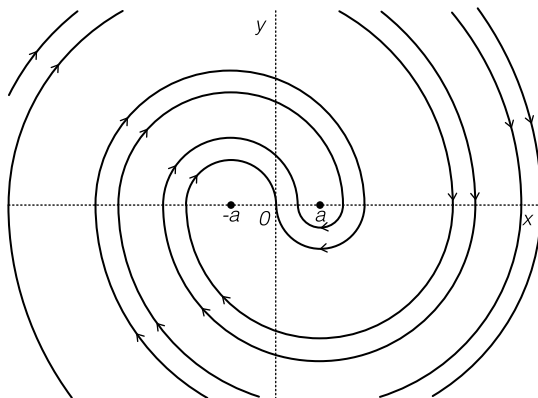


Figure F.9. A controlled oscillator

of a harmonic oscillator can be described in terms of the application of a constant external force. We can therefore also interpret our equations of motion as a harmonic oscillator (with center zero) on which an extra force of size a acts in a direction that is always opposite to the motion. This means that the extra force behaves like dry friction.

F.2.4 Exercise 2.6.4: A damped oscillator with forcing

- (1) We compute the energy as the integral of the product of force and speed. The desired amount of energy then is

$$\begin{aligned} \int_0^{\frac{2\pi}{\Omega}} F \frac{dx}{dt} dt &= \int_0^{\frac{2\pi}{\Omega}} AB\Omega \sin(\Omega t) \cos(\Omega t + \phi) dt \\ &= AB\Omega \int_0^{\frac{2\pi}{\Omega}} \sin(\Omega t) (\cos(\Omega t) \cos(\phi) - \sin(\Omega t) \sin(\phi)) dt \\ &= -AB\pi \sin \phi. \end{aligned}$$

- (2) By the same reasoning we now find

$$\begin{aligned} \int_0^{\frac{2\pi}{\Omega}} c \left(\frac{dx}{dt} \right)^2 dt &= cB^2\Omega^2 \int_0^{\frac{2\pi}{\Omega}} \cos^2(\Omega t + \phi) dt \\ &= cB^2\Omega\pi. \end{aligned}$$

- (3) Since the motion is periodic, the energy absorbed and the energy delivered must be equal per period. Using the above results we find

$$-A \sin \phi = cB\Omega. \quad (\text{F.2})$$

Since A, B, c, Ω are all positive, necessarily $\sin \phi < 0$.

- (4) Since here the mass equals 1, the force must be equal to the acceleration, which is $= B\Omega^2$. This, in turn, must be equal to the sum of the oscillating force $-B$ and the external force $A \sin(\frac{1}{2}\pi - \phi)$. Therefore

$$-B\Omega^2 = -B + A \sin(\frac{1}{2}\pi - \phi) = -B + A \cos \phi,$$

which implies

$$A \cos \phi = B(a - \Omega^2). \quad (\text{F.3})$$

- (5) The ratio of (F.2) and (F.3) gives

$$\tan \phi = \frac{c\Omega}{1 - \Omega^2}.$$

Using the identity

$$\sin \phi = -\sqrt{\frac{\tan^2(\phi)}{1 + \tan^2(\phi)}},$$

where the minus sign follows from the third item above, we obtain

$$\sin \phi = -c\Omega \sqrt{\frac{1}{c\Omega^2 + (1 - \Omega^2)^2}}.$$

The latter, replaced in (F.2) gives

$$B = \frac{A}{\sqrt{c\Omega^2 + (1 - \Omega^2)^2}}.$$

F.2.5 Exercice 2.6.5: The Van der Pol-Liénard differential equation

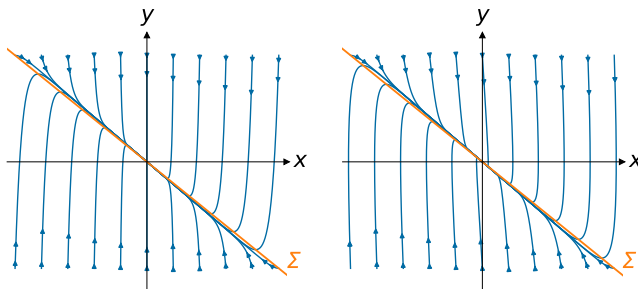


Figure F.10. Exercice 2.6.5

Left: phase portrait of the second and third case; Right: phase portrait of the fourth case

- (a) See Figure 2.20;
- (b) See the left-hand side related to Figure F.10;
- (c) See the left-hand side related to Figure F.10 (this is no mistake, they are effectively the same);
- (d) See the right-hand side related to Figure F.10;
- (e) See Figure F.11. In this case, if the solution approaches P or Q , there will be another (short) time interval in which the rapid motion of the second equation dominates. This is

due to the fact that the solution can no longer follow Σ : for example near P the solution must move to the right ($y > 0$) and thus will have to move away from Σ .

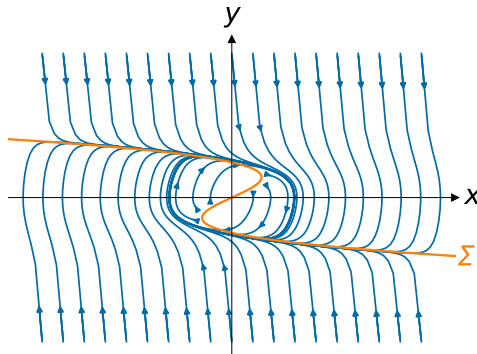


Figure F.11. Exercise 2.6.5, last case

For $\mu \geq 0$, the phase portrait of

$$\dot{x} = y, \quad \epsilon \dot{y} = -(x + \mu y + y^3)$$

is not essentially different from the right-hand side of Figure F.10: all the solutions eventually will go to the origin. For $\mu < 0$, on the other hand, we get a phase portrait similar to Figure F.11.

It can be shown that for $\mu < 0$ our equation has a periodic solution, i.e., a solution $(x(t), y(t))$ such that there is certain period $T > 0$ for which $x(t+T) = x(t)$ and $y(t+T) = y(t)$ for all $t \in \mathbb{R}$. Moreover, all solutions will approach this periodic solution, with the only exception of $x(t) = 0 = y(t)$. As μ approaches 0, the periodic solution, as a figure in the phase plane, becomes smaller and approaches the origin. See also Section 3.4.3.

F.3 Exercise from Chapter 3: On Hooke's n -body problem

Solution of Part 1. The solution consists of two steps.

The Steiner ellipse.: Let Z be the center of mass of $A_1A_2A_3$. Then the Steiner ellipse S of $A_1A_2A_3$ exactly is the ellipse passing through the vertices A_1, A_2 and A_3 , that has Z as its center. Moreover, the areas of the sectors A_1ZA_2, A_2ZA_3 and A_3ZA_1 of S are equal.

Proof. The assertion is obviously true for an equilateral triangle, in which case the Steiner ellipse is the circumscribed circle. Now there exists an affine transformation F from the equilateral triangle to $A_1A_2A_3$ and this transformation has the following properties:

- (1) F preserves the center of mass;
- (2) F preserves the parallelism of straight lines and hence maps the circumscribed circle to S ;
- (3) F maps equal areas to equal areas.

The latter follows since F multiplies all areas by a fixed constant (a Jacobian determinant). From this the assertion follows. \square

Equation of motion.: Let \mathbf{r} denote the position of P with respect to Z . Then its equation of motion is

$$\ddot{\mathbf{r}} = -3k\mathbf{r}.$$

Proof. Let \mathbf{a}_i denote the position vector of A_i with respect to Z ($i = 1, 2, 3$). Then $\mathbf{F}_i = k(\mathbf{a}_i - \mathbf{r})$ and therefore for the total force F we have

$$\mathbf{F} = \mathbf{F}_1 + \mathbf{F}_2 + \mathbf{F}_3 = -3k\mathbf{r} + k(\mathbf{a}_1 + \mathbf{a}_2 + \mathbf{a}_3) = -3k\mathbf{r}.$$

From this the assertion follows by Newton's second law. \square

From the latter assertion, it directly follows that the possible motions of P are all Lissajous ellipses with center Z . One of these is the Steiner ellipse S . It also follows that the motion of P takes place in a central force field where Kepler's second law holds true: equal areas are swept out at equal times. In view of the former assertion this solves the problem.

Solution of Part 2.

Let particle A_i have the three-dimensional position \mathbf{x}_i . Then the equations of motion read

$$m_i \ddot{\mathbf{x}}_i = \sum_{j=1}^n k^2 m_i m_j (\mathbf{x}_j - \mathbf{x}_i), \quad (i = 1, 2, \dots, n).$$

Let

$$\mathbf{z} = \frac{1}{M} \sum_{j=1}^n m_j \mathbf{x}_j$$

be the center of mass, where $M = \sum_{j=1}^n m_j$. It then follows that

$$\ddot{\mathbf{x}}_i = k^2 M \mathbf{z} - k^2 M \dot{\mathbf{x}}_i.$$

Summation yields that $M \ddot{\mathbf{z}} = 0$, i.e., the center of mass moves uniformly. The relative motion of the particle A_i ($i = 1, 2, \dots, n$) with respect to \mathbf{z} moreover is given by

$$\ddot{\mathbf{x}}_i + k^2 M \mathbf{x}_i = 0 \quad (i = 1, 2, \dots, n),$$

which describes a system of three decoupled harmonic motions. This leads to 3-dimensional Lissajous figures. We shall now argue why this still is a planar Lissajous ellipse.

Indeed, the projection in all three coordinate directions form 2-dimensional Lissajous figures. Since all frequencies are equal, the latter are just planar Lissajous ellipses. But then the 3-dimensional Lissajous figure also is an ellipse moving in a plane that is generic with respect to the coordinate directions. Thus each particle A_i moves in a plane along a Lissajous ellipse with center \mathbf{z} and period $T = 2\pi/k\sqrt{M}$.

F.4 Exercise from Appendix B: One more Hookian problem

For $i = 1, 2, 3$ let x_i denote the position of P_i on ℓ_i , measured from O , and with all x_i of the same sign in the same ‘half’ of the cone. We write $\mathbf{x} = (x_1, x_2, x_3)^T$ as a vector. This is a linear problem with kinetic energy T and potential energy U , which read

$$T = \frac{1}{2}(\dot{x}_1^2 + \dot{x}_2^2 + \dot{x}_3^2)$$

and

$$\begin{aligned} U &= \frac{1}{2}k^2 \left(\overline{P_1 P_2}^2 + \overline{P_2 P_3}^2 + \overline{P_3 P_1}^2 \right) \\ &= \frac{1}{2}k^2(x_1^2 + x_2^2 + x_3^2 - x_1 x_2 \cos \alpha - x_2 x_3 \cos \alpha - x_3 x_1 \cos \alpha). \end{aligned}$$

So in the format $T = \frac{1}{2}\langle A\dot{\mathbf{x}}, \dot{\mathbf{x}} \rangle$ and $U = \frac{1}{2}\langle B\mathbf{x}, \mathbf{x} \rangle$ we have $A = \text{Id}$, while

$$B = k^2 \begin{pmatrix} 2 & -\cos \alpha & -\cos \alpha \\ -\cos \alpha & 2 & -\cos \alpha \\ -\cos \alpha & -\cos \alpha & 2 \end{pmatrix}$$

Direct computation yields that B has a single eigenvalue $\omega_1^2 = 2k^2(1 - \cos \alpha)$ and a double eigenvalue $\omega_2^2 = 2k^2(1 + \cos \alpha)$. The corresponding eigenspaces are the diagonal

$$\left[\begin{pmatrix} 1 \\ 1 \\ 1 \end{pmatrix} \right]_{\mathbb{R}},$$

where $[-]$ takes the linear span, and its orthogonal complement, which is the plane given by the equation $x_1 + x_2 + x_3 = 0$. The corresponding characteristic oscillations are as follows.

- (1) The three particles oscillate in an equilateral triangle perpendicular to the diagonal with characteristic frequency

$$\omega_1 = k\sqrt{2}\sqrt{1 - \cos \alpha};$$

- (2) The vector \mathbf{x} oscillates in the plane $x_1 + x_2 + x_3 = 0$ in Lissajous ellipses, with characteristic frequency

$$\omega_2 = k\sqrt{2}\sqrt{1 + \cos \alpha}.$$

F.5 Exercise from Appendix E: On Kepler's third law

Given the uniform circular motion with period T and radius R , the velocity is

$$\mathbf{v}(t) = \begin{pmatrix} \dot{x}(t) \\ \dot{y}(t) \end{pmatrix} = R \begin{pmatrix} -\frac{2\pi}{T} \sin\left(\frac{2\pi}{T}t\right) \\ \frac{2\pi}{T} \cos\left(\frac{2\pi}{T}t\right) \end{pmatrix}$$

and the (centripetal) acceleration

$$\mathbf{a}(t) = \begin{pmatrix} \ddot{x}(t) \\ \ddot{y}(t) \end{pmatrix} = R \begin{pmatrix} -\left(\frac{2\pi}{T}\right)^2 \cos\left(\frac{2\pi}{T}t\right) \\ -\left(\frac{2\pi}{T}\right)^2 \sin\left(\frac{2\pi}{T}t\right) \end{pmatrix} = -R \left(\frac{2\pi}{T}\right)^2 \mathbf{e}_r.$$

Combining (E.14) and (E.16) now gives

$$m\mathbf{a} = -mR \left(\frac{2\pi}{T}\right)^2 \mathbf{e}_r = -\frac{kMm}{R^2} \mathbf{e}_r$$

and so

$$T^2 = \frac{4\pi^2}{kM} R^3,$$

which amounts to Kepler's third law for this case of circular motion. The answer in the case when the central force has size $-kMm/R^\kappa$ reads

$$T^2 = \frac{4\pi^2}{kM} R^{\kappa+1}.$$

By the way, the case where $\kappa = -1$ corresponds exactly to Hooke's universe of an exercise in Section 3.5, where the motion is isochronous. For a neat connection between the Hookian and the Newtonian ellipse see Arnold [8, Appendix 1].

Bibliography

- [1] J.M. Aarts, *Christiaan Huygens: Het Slingeruurwerk. Een studie.* Epsilon Uitgaven **80** 2015
- [2] H. Aldersey-Williams. *Dutch Light. Christiaan Huygens and the Making of Science in Europe.* Pan Macmillan 2021
- [3] C. Andriesse, *Titan kan niet slapen, biografie van Christiaan Huygens.* Olympus Pockets 2007
- [4] T.M. Apostol, *Calculus, Vol. 1: One-Variable Calculus, with an Introduction to Linear Algebra.* Second edition. John Wiley 1967
- [5] V.I. Arnold, *Mathematical Methods of Classical Mechanics. Second edition.* GTM **60** Springer 1989
- [6] V.I. Arnold, *Geometrical Methods in the Theory of Ordinary Differential Equations.* Springer 1983
- [7] V.I. Arnold, *Catastrophe theory* (Third edition). Springer-Verlag 1992
- [8] V.I. Arnold, *Huygens & Barrow, Newton & Hooke.* Birkhäuser 1990
- [9] V.I. Arnold, *Mathematical Understanding of Nature: Essays on Amazing Physical Phenomena and Their Understanding by Mathematicians.* AMS 2014
- [10] V.I. Arnold and A. Avez, *Problèmes Ergodiques de la Mécanique Classique.* Gauthier-Villars 1967; *Ergodic Problems of Classical Mechanics.* Addison-Wesley 1989

- [11] V.I. Arnold, S.M. Gusein-Zade and A.N. Varchenko, *Singularities of Differentiable Maps Volume 1: Classification of Critical Points, Caustics and Wave Fronts*. Modern Birkhäuser Classics, Birkhäuser 1985
- [12] V.I. Arnold, V.V. Kozlov and A.I. Neishtadt, Mathematical Aspects of Classical and Celestial Mechanics. In: V.I. Arnol'd (ed.) *Dynamical Systems III*. Encyclopædia of Mathematical Sciences **3** Springer 1988
- [13] N.H. Asmar, *Partial Differential Equation with Fourier Series and Boundary Value Problems*. Second Edition. Pearson 2000
- [14] A. Avila, B. Fayad and R. Krikorian, A KAM scheme for $SL(2\mathbb{R})$ cocycles with Liouvillean frequencies. *Geom. Funct. Anal.* Vol. 21 (2011) 1001-1019
- [15] A. Avila and S. Jitomirskaya. *Solving the Ten Martini Problem*. In: J. Asch, A. Joye (eds.), Mathematical Physics of Quantum Mechanics. Lecture Notes in Physics, vol 690. Springer 2006
- [16] A. Avila and S. Jitomirskaya. *The Ten Martini problem*. *Ann. Math.* (2) **170**(1) 303-342 (2009)
- [17] S. Axler, *Linear Algebra Done Right*. Fourth Edition. Springer 2023
- [18] P. Bak and R. Bruinsma, *One-Dimensional Ising Model and the Complete Devil's Staircase*. *Phys. Rev. Lett.* **49** (1982) 249
- [19] Arnd Bäcker, *Eigenfunctions in chaotic quantum systems*. Habilitations thesis. TU Dresden (2007) <https://nbn-resolving.org/urn:nbn:de:bsz:14-ds-1213275874643-50420>
- [20] Nate Barlow, What happens when a raindrop hits a puddle? *The Conversation*. May 10, 2019. <https://theconversation.com/what-happens-when-a-raindrop-hits-a-puddle-115984>
- [21] D.G.M. Beersma, H.W. Broer, K. Efstathiou, K.A. Gargar and I. Hoveijn, Pacer cell response to periodic Zeitgebers. *Physica D: Nonlinear Phenomena* **240**(19) (2011) 1516-1527

- [22] M. Benedicks and L. Carleson, The dynamics of the Hénon map. *Ann. Math.* **133** (1991) 73-169
- [23] M. Bennett, M.F. Schatz, H. Rockwood and K. Wiesenfeld, Huygens' clocks. *Proc. R. Soc. Lond. A* **458** (2002) 563-579
- [24] J. Bernoulli, *Opera Johannis Bernoullii* (G. Cramer ed.; 4 vols), Genève 1742
- [25] M. Berry, Quantum physics on the edge of chaos. *New Scientist* 19 November 1987
- [26] J.A. Blackburn, H.J.T. Smith and N.Groenbech-Jensen, Stability and Hopf bifurcations in an inverted pendulum. *American Journal of Physics* **60** (10) (1992) 903–908.
- [27] D. Borthwick, *Spectral Theory – Basic concepts and applications*. Graduate Texts in Mathematics, vol. 284. Springer (2020)
- [28] H.M. Bos, Huygens, Christiaan (Also Huyghens, Christian). *Complete Dictionary of Scientific Biography* Encyclopedia.com 2012
- [29] O. Bottema, Problem 673, *Nieuw Archief voor Wiskunde* **2** **1** (1983)
- [30] O. Bottema, Problem 683, *Nieuw Archief voor Wiskunde* **3** **1** (1983)
- [31] O. Bottema, Problem 701, *Nieuw Archief voor Wiskunde* **2** **2** (1984)
- [32] A. Bravetti, M. Seri, M. Vermeeren, F. Zadra, Numerical integration in Celestial Mechanics: a case for contact geometry *Celestial Mechanics and Dynamical Astronomy* **132** (2020)
- [33] H.W. Broer, KAM theory: The legacy of Kolmogorov's 1954 paper. *Bulletin of the American Mathematical Society* **41**(4) (2004) 507-521
- [34] H.W. Broer, Resonance and fractal geometry. *Acta Applicandae Mathematicae* **120** DOI 10.1007/s10440-012-9670-x (2012) 61-86

- [35] H.W. Broer, *Hemelverschijnselen Nabij de Horizon*. Epsilon Uitgaven **77** 2013
- [36] H.W. Broer, Bernoulli's light ray solution of the brachistochrone problem through Hamilton's eyes. *Int. J. Bifurcations Chaos* **24**:1440009, 2014
- [37] H.W. Broer, *Near the Horizon: an Invitation to Geometric Optics*. The Carus Mathematical Monographs **33** MAA 2016
- [38] H.W. Broer, J. Epema and M. Kuipers, *Oscillaties: trillingen en slingerbewegingen vanuit wiskundig oogpunt*. Internal Publication Rijksuniversiteit Groningen 1987
- [39] H.W. Broer, I. Hoveijn, M. van Noort, C. Simó and G. Vegter, The parametrically forced pendulum: a case study in $1\frac{1}{2}$ degree of freedom. *Journ. Dynamics and Differential Equations* **16**(4) (2004) 897-947
- [40] H.W. Broer and H. Hanßmann, On Jupiter and his Galilean satellites: librations of De Sitter's periodic motions. *Indag Math NS* **27**(5) (2016) 1305-1337
- [41] H.W. Broer and H. Hanßmann, A Galilean dance: 1:2:4 resonant periodic motions and their librations of Jupiter and his Galilean moons. *DCDS-S* **13**(4) (2020) 1043-1059
- [42] H.W. Broer, H. Hanßmann, Á. Jorba, J. Villanueva and F.O.O. Wagener, Normal-internal resonances in quasi-periodically forced oscillators: a conservative approach. *Nonlinearity* **16** (2003) 1751-1791
- [43] H.W. Broer, H. Hanßmann and F.O.O. Wagener, *Quasi-periodic bifurcation theory. The geometry of KAM*. Springer Verlag, in preparation
- [44] H.W. Broer, G.B. Huitema and M.B. Sevryuk, *Quasi-periodic tori in families of dynamical systems: order amidst chaos*. Springer LNM **1645** (1996) (195 p)

- [45] H.W. Broer and B. Krauskopf, Chaos in periodically driven systems. In: B. Krauskopf and D. Lenstra (eds.), *Fundamental Issues of Nonlinear Laser Dynamics*. Amer. Inst. Phys. (2000) 31-53
- [46] H.W. Broer and M. Levi, Geometrical aspects of stability theory for Hill's equations. *Archive Rat. Mech. An.* **131** (1995) 225-240
- [47] H.W. Broer, M. van Noort and C. Simó, Existence and measure of invariant tori in Hamiltonian one-and-a-half degree of freedom systems. In: F. Dumortier, H.W. Broer, J. Mawhin, A. Vanderbauwhede and S.M. Verduyn Lunel (eds.), *Equadiff 2003, Proceedings International Conference on Differential Equations Hasselt 2003*. World Scientific, Singapore, 2005, 595-600. ISBN 981 256 169 2
- [48] H.W. Broer, J. Puig and C. Simó, Resonance tongues and instability pockets in the quasi-periodic Hill-Schrödinger equation. *Commun. Math. Phys.* **241** (2003) 467-503
- [49] H.W. Broer and M.B. Sevryuk, KAM Theory: Quasi-periodicity in Dynamical Systems. In H.W. Broer, B. Hasselblatt and F. Takens (Eds.), *Handbook of Dynamical Systems* **3** North-Holland Ch. 6, 2010
- [50] H.W. Broer and C. Simó, Resonance tongues in Hill's equations: a geometric approach. *Journ. Diff. Eqns.* **166** (2000) 290-327
- [51] H.W. Broer, C. Simó and J.C. Tatjer, Towards global models near homoclinic tangencies of dissipative diffeomorphisms. *Nonlinearity* **11** (1998) 667-770
- [52] H.W. Broer and H.S.V. de Snoo, Mathematische Fysica in Groningen I: Van Mees tot Zernike. *Nederlands Tijdschrift voor Natuurkunde* to appear
- [53] H.W. Broer and F. Takens, *Dynamical Systems and Chaos*. Epsilon Uitgaven **64** 2009; Appl. Math Sc. **172** Springer 2011
- [54] H.W. Broer and G. Vegter, Bifurcational aspects of parametric resonance. *Dynamics Reported, New Series* **1** (1992) 1-51

- [55] H.W. Broer and Lei ZHAO, De Sitter's theory of Galilean satellites and the related quasi-periodic orbits. *Celest. Mech. Dyn. Astr.* **127** (2017) 95-119
- [56] A. Celletti, Analysis of resonances in the spin-orbit problem in celestial mechanics: The synchronous resonance, Part I *J. Appl. Math. Phys. (ZAMP)* **41**, 174; Part II: *ZAMP* **41**, 453 (1990)
- [57] A. Correia and J. Laskar, Mercury's capture into 3/2 spin-orbit resonance as a result of its chaotic dynamics. *Nature* **429** (2004) 848-850
- [58] N. Chernov, R. Markarian, *Chaotic billiards*. Mathematical Surveys and Monographs, vol. **127**. AMS 2006
- [59] G. Cornelissen and N. Peyerimhoff, *Twisted isospectrality, homological wideness, and isometry*. SpringerBriefs in Mathematics (2023) XVI+111 pp.
- [60] I. De Blasi, S. Terracini, Refraction periodic trajectories in central mass galaxies, *Nonlinear analysis*, **218** 112766 (2021)
- [61] I. De Blasi, S. Terracini, On some Refraction Billiards, *arXiv preprint*, arXiv:2108.11159 (2021)
- [62] A. Celletti and L. Chierchia Measures of basins of attraction in spin-orbit dynamics. *Celest Mech Dyn Astr* (2008) 101:159-170 DOI 10.1007/s10569-008-9142-9
- [63] A. Celletti and L. Chierchia Quasi-Periodic Attractors in Celestial Mechanics *Arch. Rational Mech. Anal.* **191** (2009) 311-345 (DOI) 10.1007/s00205-008-0141-5
- [64] R.L. Devaney, *An Introduction to Chaotic Dynamical Systems* Second Edition. Addison Wesley 1989
- [65] F.J. Dijksterhuis, *Lenses and waves: Christiaan Huygens and the Mathematical Science of Optics in the Seventeenth Century*. Springer 2004

- [66] E.I. Dinaburg and Ya.G. Sinai, The one-dimensional Schrödinger equation with quasiperiodic potential. *Funktional. Anal. i Prilozhen.* **9**(4) (1975) 8-21
- [67] J.P. Eckann and D. Ruelle, Ergodic theory of chaos and strange attractors. *Reviews of Modern Physics.* **57**(3) (1985) 617-656
- [68] M. Einsiedler, T. Ward, *Ergodic Theory with a view towards Number Theory.* GTM **259** Springer 2011
- [69] L.H. Eliasson, Floquet solutions for the one-dimensional quasi-periodic Schrödinger equation. *Commun. Math. Phys.* **146** (1992) 447-482
- [70] L.H. Eliasson, Discrete one-dimensional quasi-periodic Schrödinger operators with pure point spectrum, *Acta Math.* **179** (1997) 153-196
- [71] R. Engelking, *General Topology.* - Revised and Completed Ed. Helderman 1989
- [72] Euclid, *The thirteen books of the Elements.* Three volumes translations and commentary by T.L. Heath. Dover 1956
- [73] L. Euler, *Leonhardi Euleri Opera Omnia.* 72 vols. Bern 1911-1975
- [74] K.J. Falconer, *The Geometry of Fractal Sets.* Cambridge University Press 1985
- [75] K.J. Falconer, *The Fractal Geometry.* Wiley 1990
- [76] M.J. Feigenbaum, Universal behavior in nonlinear systems. *Physica D: Nonlinear Phenomena.* **7** (1-3) (1983) 16-39
- [77] R.P. Feynman, R.B. Leighton and M. Sands, *The Feynman Lectures on Physics* Vols. **1**, **2** and **3**. Addison-Wesley 1963, 1964 and 1965
- [78] Press release: Fields Medal 2014, Arthur Avila.
https://www.mathunion.org/fileadmin/IMU/Prizes/Fields/2014/news_release_avila2.pdf Accessed on Fri. 10 Jun 2022.

- [79] G. Gallavotti, G. Gentile and V. Mastropietro, Field theory and KAM theory. *MPEJ* **1** 1995
- [80] A. Di Gioacchino, M. Gherardi, L.G. Molinari, P. Rotondo. *Jack on a Devil's Staircase*. In: P. Bortignon, G. Lodato, E. Meroni, M. Paris, L. Perini, A. Vicini (eds.) Toward a Science Campus in Milan. CDIP 2017. Springer 2018
- [81] Press release: Nobel Prize in Physics 1998.
<https://www.nobelprize.org/prizes/physics/1998/press-release/> Accessed on Fri. 10 Jun 2022.
- [82] I. Gkolias, C. Efthymiopoulos, A. Celletti, G. Puacacco, Hamiltonian formulation of the spin-orbit model with time-varying non-conservative forces *Commun Nonlinear Sci Numer Simulat* **51** (2017) 23–38
- [83] I. Gkolias, C. Efthymiopoulos, A. Celletti, G. Puacacco, Accurate modelling of the low-order secondary resonances in the spin-orbit problem *Commun Nonlinear Sci Numer Simulat* **77** (2019) 181–202
- [84] H. Goldstein, *Classical Mechanics*. Addison-Wesley 1950 (second edition 1980)
- [85] H.H. Goldstine, *A History of the Calculus of Variations from the 17th through the 19th Century*. Studies in the History of Mathematics and Physical Sciences **5** Springer 1980
- [86] P. Goldreich, S. Peale, Spin-orbit coupling in the solar system. *The Astronomical Journal* **71** (1966)
- [87] C. Gordon, D. Webb, S. Wolpert, Isospectral plane domains and surfaces via Riemannian orbifolds *Inventiones Mathematicae* **110**(1) (1992) 1–22
- [88] R.W. Hall and J. Krešimir, The Mathematics of Musical Instruments. *The American Mathematical Monthly* 108 (2001) 347–357
- [89] K.P. Hart, De Cycloïde. *Pythagoras* **39**(4) 2000
- [90] F. Hausdorff, *Set Theory*. Second Edition. Chelsea 1962

- [91] H. Helmholtz. Theorie der Luftschwingungen in Röhren mit offenen Enden *J. reine angew. Math.* 57 (1860) 1-72
- [92] M. Hénon, A two-dimensional mapping with a strange attractor. *Commun. Math. Phys.* **50** (1976) 69-77
- [93] M. Hendriks, *Introduction to Physical Hydrology*. Oxford University Press 2010
- [94] J. Henrard, Capture into resonance: An extension of the use of adiabatic invariants. *Celestial Mechanics* **27** (1982) 3-22
- [95] M. Herman, Une méthode pour minorer les exposants de Lyapounov et quelques exemples montrant le caractère local d'un théorème d'Arnold et de Moser sur le tore de dimension 2, *Comment. Math. Helv.* 58:3 (1983) 453-502
- [96] M. Herman, Sur la conjugaison différentiable des difféomorphismes du cercle à des rotations. *Publ. Math. IHES* **49** (1979) 5-234
- [97] A. L. Hodgkin and A. F. Huxley, A quantitative description of membrane current and its application to conduction and excitation in nerve. *J. Physiol.* **117** (1952) 500-544
- [98] R.A. Horn, C.R. Johnson, *Matrix analysis*. Second edition. Cambridge University Press 2013
- [99] D.R. Hofstadter. Energy levels and wavefunctions of Bloch electrons in rational and irrational magnetic fields. *Physical Review B* **14** 6 (1976)
- [100] M.W. Hirsch, S. Smale and R.L. Devaney, *Differential Equations, Dynamical Systems, and an Introduction to Chaos*. Academic Press 2004; 2013
- [101] M.W. Hirsch, C.C. Pugh and M. Shub, *Invariant Manifolds*. Lecture Notes in Mathematics **583** 1977
- [102] Chr. Huygens, *Horologium Oscillatorium*. Œuvres Complètes de Christiaan Huygens publiées par la Société Hollandaise des Sciences **16**, Martinus Nijhoff, The Hague 1929 Vol. **5** 241-262; Vol. **17** 156-189

- [103] J. Israel, *The Dutch Republic: Its Rise, Greatness, and Fall, 1477-1806*. Oxford University Press 1995
- [104] M. Kac, Can One Hear the Shape of a Drum? *American Mathematical Monthly*. **73** 4, part 2 (1966) 1–23
- [105] P.L. Kapitza, Dynamic stability of a pendulum when its point of suspension vibrates. *Soviet Phys. JETP.* **21** (1951) 588–597
- [106] H. Kamerlingh Onnes, *Nieuwe Bewijzen voor de Aswenteling der Aarde*. Proefschrift Universiteit Groningen 1879
- [107] D.E. Kirk, *Optimal Control Theory: an Introduction*. Dover 2004
- [108] A. Knauf, *Mathematical Physics: Classical Mechanics*. Unitext **109** Springer 2018
- [109] P.S. de Laplace, *Traité de Mécanique Céleste, Œuvres Complètes*. Tome **4** (1799), 1-501
- [110] Y. Last, Spectral Theory of Sturm-Liouville Operators on Infinite Intervals: A Review of Recent Developments. In: W.O. Amrein, A.M. Hinz, D.P. Pearson (eds) *Sturm-Liouville Theory*. Birkhäuser 2005
- [111] G.W. Leibniz, *Nova methodus pro maximis et minimis. Acta Eruditorum* 1684; In: D.J. Struik, *A Source Book in Mathematics 1200-1800*. Harvard University Press 1969 271-281
- [112] M. Levi, F.C. Hoppensteadt and W.L. Miranker, Dynamics of the Josephson junction. *Quarterly of Applied Mathematics* **36**(2) (1978) 167-198, Brown University
- [113] R. de la Llave, A tutorial on KAM Theory. In A. Katok et al. (Eds.), *Proceedings of Symposia in Pure Mathematics* **69** Amer. Math. Soc. (2001) 175-292
- [114] H. Levine, and J. Schwinger. On the radiation of sound from an unflanged circular pipe. *Phys. Rev.* **73** (1948) 383–406
- [115] T.Y. Li and J.A. Yorke, Period three implies chaos. *American Mathematical Monthly* **82** (1975) 985-992

- [116] H.A. Lorentz, Alte und Neue Frage der Physik. *Wolfskehl lectures Göttingen*, 24–29 october 1910, transcribed by Max Born, in: H.A. Lorentz, *Collected Papers* (P. Zeeman and A.D. Fokker, eds), ‘s-Gravenhage: Nijhoff, 1935–1939, vol. 7, pp. 236–237
- [117] J.A. van Maanen, *Een Complexe Groothed, leven en werk van Johann Bernoulli*, 1667–1748. Epsilon Uitgaven **34** 1995
- [118] B.B. Mandelbrot, *The Fractal Geometry of Nature*. Freeman 1977
- [119] R. Mañé, *Ergodic Theory and Differentiable Dynamics*. Ergebnisse der Mathematik und ihrer Grenzgebiete 3. Folge Band **8** Springer 1987
- [120] J. Martin, The Helen of Geometry. *The College Mathematical Journal* **41** (2010) 17-28
- [121] R.M. May, Simple mathematical models with very complicated dynamics. *Nature* **261** (1976) 459-466
- [122] R.M. May, Biological populations obeying difference equations: Stable points, stable cycles, and chaos. *J. Theor. Biol.* **51** (1975) 511-524
- [123] H.C. Mayer and R. Krechetnikov, Walking with coffee: Why does it spill? *Phys. Rev. E* **85** (2012) 046117
- [124] J. Meixner and F.W. Schäfke, *Mathieusche Funktionen und Sphäroidfunktionen*. Die Grundlehren der Mathematischen Wissenschaften in Einzeldarstellungen, Band **LXX1**, Springer 1954
- [125] M.G.J. Minnaert, *De Natuurkunde van 't Vrije Veld* delen **1**, **2** en **3**, Vijfde Editie, ThiemeMeulenhoff 1996; *The Nature of Light and Colour in the Open Air*, Dover 1954 (first edition 1937-40)
- [126] J. Moser and J. Pöschel, An extension of a result by Dinaburg and Sinai on quasi-periodic potentials. *Comment. Math. Helvetici* **59** (1984) 39-85

- [127] M. Misquero and R. Ortega, Some Rigorous Results on the 1 : 1 Resonance of the Spin-Orbit Problem. *SIAM J. Appl. Dyn. Syst.* **19**(4) (2020) 2233-2267
- [128] A. Neishtadt, Averaging, passage through resonances, and capture into resonance in two-frequency systems. *Russ. Math. Surv.* **69**(5) (2014) 771
- [129] A. Neishtadt and A. Okunev, Averaging and passage through resonances in two-frequency systems near separatrices. ArXiv preprint arXiv:2108.08540v2
- [130] S.E. Newhouse, Diffeomorphisms with infinitely many sinks. *Topology* **13** (1974) 9-18
- [131] S.E. Newhouse, The abundance of wild hyperbolic sets and non-smooth stable sets for diffeomorphisms. *Publ. Math. I.H.E.S.* **50** (1979) 101-151
- [132] I. Newton, *Philosophiae Naturalis Principia Mathematica*. Translated by I. Bernard Cohen and Anne Whitman as *Isaac Newton, The Principia – Mathematical Principles of Natural Philosophy*. University of California Press 1999 (first edition 1687)
- [133] Z. Nitecki, *Differentiable Dynamics, An introduction to the Orbit Structure of Diffeomorphisms*. The M.I.T. PRESS, Cambridge Massachusetts, and London, England 1971
- [134] E. Noether, Invariante Variationsprobleme. *Nachrichten der Königlichen Gesellschaft der Wissenschaften zu Göttingen, Math-phys. Klasse* (1918) 235-257
- [135] Press release: Nobel Prize in Physics 1985.
<https://www.nobelprize.org/prizes/physics/1985/press-release/> Accessed on Fri. 10 Jun 2022.
- [136] P.J. Olver, *Introduction to Partial Differential Equations*. Springer 2014
- [137] J. Oxtoby, *Measure and Category*. Springer 1971

- [138] J. Palis and F. Takens, *Hyperbolicity & sensitive chaotic dynamics and homoclinic bifurcations*. Cambridge studies in advanced mathematics **35** 1993
- [139] Y.B. Pesin, (1977). Characteristic Lyapunov Exponents and Smooth Ergodic Theory. *Russian Math. Surveys.* **32**(4) (1977) 55-114.
- [140] J.P. Philips, Brachistochrone, Tautochrone, Cycloid – Apple of Discord. *The Mathematics Teacher* **60**(5) (1967) 506-508
- [141] J. Pöschel, KAM à la R. *Regular Chaotic Dynamics* **16** (2011) 17-23
- [142] A. Pogromsky, D. Rijlaarsdam and H. Nijmeijer, Experimental Huygens synchronization of oscillators. In: M. Thiel, J. Kurths, M.C. Romano, A. Moura and G. Károlyi, *Nonlinear Dynamics and Chaos: Advances and Perspectives*. Springer Complexity (2010) 195-210
- [143] T. Poston and I. Stewart, *Catastrophe Theory and its Applications*. Pitman 1978
- [144] Alice C. Quillen, Reducing the probability of capture into resonance, *Monthly Notices of the Royal Astronomical Society* **365**, 4 (2006) 1367-1382
- [145] A. Robinson, *Nonstandard Analysis*. Princeton Landmarks in Mathematics 1966
- [146] David E. Rowe, *Emmy Noether - Mathematician Extraordinaire*. Springer, 2021.
- [147] David E. Rowe and Mechthild Koreuber, *Proving It Her Way. Emmy Noether, a Life in Mathematics*. Springer, 2020.
- [148] D. Ruelle and F. Takens, On the nature of turbulence. *Commun. Math. Phys.* **20** (1971) 167-192; **23** (1971) 343-344
- [149] L. Russo and S. Levy. *The Forgotten Revolution: How Science Was Born in 300 BC and Why it Had to Be Reborn*. Springer-Verlag, Berlin, Heidelberg 2004

- [150] E.O. Schulz-DuBois, Foucault Pendulum Experiment by Kamerlingh Onnes and Degenerate Perturbation Theory. *American Journal of Physics* **38**, 173 (1970)
- [151] H. Seifert and W. Threlfal, *Variationsrechnung im Grossen*. Chelsea Publishing Company 1938
- [152] G.F. Simmons, *Differential Equations with Applications and Historical Notes* Third Edition. CRC Press 2017
- [153] B. Simon, Almost Periodic Schrödinger operators: a review. *Adv. in Applied Mathematics* **3** (1982) 463-490
- [154] B. Simon, Schrödinger operators in the twenty-first century. In: *Mathematical Physics 2000* (A. Fokas, A. Grigoryan, T. Kibble, and B. Zegarlinski, eds.), Imp. Coll. Press, London, 2000, 283-288
- [155] W. de Sitter, Outlines of a new mathematical theory of Jupiter's satellites *Ann. Sterrewacht Leiden* **12** (1925) 1-55
- [156] W. de Sitter. Jupiter's Galilean satellites (George Darwin lecture). *Monthly Notices of the Royal Astronomical Society* **91** (1931) 706-738
- [157] D.G. Shafer, The brachistochrone: historical gateway to the calculus of variations. *MATerials MATemàtiques* **5**(14) 2007
- [158] D. Sobel, *Longitude*. Walker 1995; 2005
- [159] M. Spivak, *Calculus on Manifolds*. Benjamin 1965
- [160] I.H. Stamhuis, Christiaan Huygens correspondeert met zijn broer over levensduur. Hoe wetenschappelijke begrippen kunnen ontstaan. In: *De Zeventiende Eeuw*. **12** (1996) 161-170
- [161] L.A. Steen, Highlights in the History of Spectral Theory. *The American Mathematical Monthly*, Vol. 80, No. 4 (1973) 359-381
- [162] Steven H. Strogatz, *Nonlinear Dynamics and Chaos: With Applications to Physics, Biology, Chemistry, and Engineering*, 2n ed. Westview Press, 2015

- [163] C.L. Stong "The Amateur Scientist. How to make a pendulum that will demonstrate the rotation of the earth". *Scientific American* **198**, 115-124 (June 1958)
- [164] H.J. Sussmann and J.C. Willems, 300 years of optimal control from the brachystochrone to the maximum principle. *IEEE Control Systems* (1997) 32-44
- [165] F. Takens, A C^1 counterexample to Moser's twist theorem. *Indag Math* **74** (1971) 379-386
- [166] F. Takens, Forced oscillations and bifurcations. In: Applications of Global Analysis I, *Comm. of the Math. Inst. Rijksuniversiteit Utrecht* 1974; In H.W. Broer, B. Krauskopf and G. Vegter (eds.), *Global Analysis of Dynamical Systems*. IOP (2001) 1-62
- [167] F. Takens, Reconstruction Theory and Nonlinear Time Series Analysis. In H.W. Broer, B. Hasselblatt and F. Takens (Eds.), *Handbook of Dynamical Systems* **3** North-Holland Ch. 7, 2010
- [168] Toonder Studio's, *Kappie en de Meester en De Kraak* 1951
- [169] N. Thistletonwaite and G. Webber, Eds. *The Cambridge Companion to the Organ*. Cambridge University Press 2003
- [170] R. Vermeij, *Christiaan Huygens. De mathematisering van de werkelijkheid*. Veen 2007
- [171] M. Viana and K. Oliveira, *Foundations of Ergodic Theory*. Cambridge University Press 2016
- [172] B.L. van der Waerden, *Erwachende Wissenschaft. Ägyptische, Babylonische und Griechische Mathematik*. Zweite Auflage. Birkhäuser 1966
- [173] H.F. Weinberger. *A First Course in Partial Differential Equations: With Complex Variables and Transform Methods*. Dover Publications 1995
- [174] R. Westfall, *Never at rest: a biography of Isaac Newton*. Cambridge University Press 1983

- [175] S.M. Wieczorek, B. Krauskopf, T.B. Simpson and D. Lenstra, The dynamical complexity of optically injected semiconductor lasers. *Physics Reports* **416**(1-2) (2005) 1-128
- [176] E.A. Whitman, Some historical notes on the cycloid. *The American Mathematical Monthly* **50**(5) (1943) 309-315
- [177] D.R. Yennie, Integral quantum Hall effect for nonspecialists. *Rev. Mod. Phys.* **59**(3) 781-824 (DOI:) 10.1103/RevModPhys.59.781
- [178] J.C. Yoccoz, Conjugaison différentiable des difféomorphismes du cercle dont le nombre de rotation vérifie une condition diophantienne. *Ann. Sci. École Norm. Sup.* (4) **17** (1984) 333-359
- [179] J.C. Yoccoz, Travaux de Herman sur les tores invariants. *Séminaire Bourbaki* **34** (1991-1992) 311-344
- [180] J.C. Yoccoz, Théorème de Siegel, nombres de Bruno et polynômes quadratiques. Petits diviseurs en dimension 1. *Astérisque* **231** (1995) 3-88
- [181] J.G. Yoder, *Unrolling Time. Christiaan Huygens and the Mathematization of Nature*. Cambridge University Press 1988
- [182] E.C. Zeeman, *Catastrophe Theory: Selected Papers 1972-1977*. Addison-Wesley 1977
- [183] S. Zelditch Spectral determination of analytic bi-axisymmetric plane domains *Geometric and Functional Analysis* **10**(3) (2000) 628-677